

The Role of Resveratrol and Sirtuin1 in Skeletal Muscle Under a Nutrient Stress

Hannah Fox Dugdale

A thesis submitted in partial fulfilment of the requirements of
Liverpool John Moores University for the degree of Doctor of
Philosophy

January 2017

Abstract

Dietary restriction (DR) is the only known nutritional manipulation that can increase both lifespan and healthspan in a variety of species. Underlying these increases are improvements in metabolic health and reductions in cancer incidence. Despite these physiological improvements, the regulation of skeletal muscle mass is extremely sensitive to alterations in nutrients [reviewed in (Sharples et al., 2015)] and as such has been reported to reduce regenerative potential and increase atrophy in skeletal muscle cells and myotubes. Interestingly, the activation of Sirtuin1 (SIRT1) has been reported during DR and its reduction abrogates lifespan extension. Importantly, SIRT1 activation via resveratrol treatment has been indicated to be important in the presence of inflammatory stress (TNF- α) (Saini et al., 2012). Resveratrol supplementation has also improved survival and regeneration of skeletal muscle cells as well in muscle cell remodelling following oxidative stress (Bosutti and Degens, 2015). We therefore sought to create an *in-vitro* physiological model of DR by mimicking levels of glucose in the circulation and interstitium *in-vivo* in response to DR (Chapter 3) as well as optimising the activation and inhibition of SIRT1 using resveratrol and SIRT1 inhibitor, EX-527 respectively (Chapter 4). With our ultimate aim to investigate the potential role and mechanisms of the activation/inhibition of SIRT1 in ameliorating the degenerative/atrophic effect of DR in both differentiating myoblasts (Chapter 5) and mature myotubes (Chapter 6). Indeed, in Chapter 3 we present two models of reduced glucose; one reduced (medium/ MED) and the other blocked (LOW) differentiation and myotube hypertrophy. The former represented circulatory glucose blood levels (MED 1.13 g/L or 6.25 mM) and the latter interstitial represented glucose levels (LOW 0.56 g/L or 3.12 mM) of rodents under DR. In Chapter 4 we also suggest that within the *in vitro* muscle cell model, activation/inhibition of SIRT1 phosphorylation (western blot analysis) was thought to be most effective at 10 μ M of resveratrol and 100 nM of EX-527 respectively. In chapter 5, we observed that resveratrol treatment did not improve fusion when

administered to differentiating myoblasts. Resveratrol did however evoke increases in myotube hypertrophy under normal glucose conditions. Importantly resveratrol enabled improved myotube hypertrophy over an acute 24 h period when administered to existing mature myotubes in low glucose environments. If this finding translates to whole organisms and human populations it could provide healthspan improvements via reductions in fragility associated with loss of muscle mass in individuals undergoing dietary restriction. After this 24 h period resveratrol was unable to reduce myotube atrophy and the myotubes continued to atrophy, suggestive of a need for repeated resveratrol treatment to enable continued protection against muscle atrophy under low glucose conditions. SIRT1 activation increased Myogenic regulatory factor 4 (MRF4) gene expression under LOW glucose conditions which was associated with the observed improvements in myotube size at 24 h. Whereas, SIRT1 activation via resveratrol treatment in normal glucose conditions modulated increased gene expression of Myosin heavy chain 7 (MYHC7) coding for the slow isoform while inhibition of SIRT1 (EX-527) lead to reductions in gene expression of MYHC 1, 2 and 4, coding for faster IIx, IIa, IIb isoforms respectively. Perhaps suggesting that elevated SIRT1 was important in the activation of genes coding for slower myosin heavy chain isoforms. Furthermore, while SIRT activation via resveratrol did modulate increases in IGF-I gene expression, it did not appear to modulate energy sensing AMP activated protein kinase (AMPK) vs. growth related Protein 70 S6 Kinase (p70S6K) signalling pathways. However, SIRT1 inhibition increased AMPK activity in both low and normal glucose with corresponding mean reductions in p70S6K in normal glucose conditions. This indicates that perhaps normal SIRT1 activity was required for appropriate AMPK activation, which may therefore prevent the suppression of p70S6K and the corresponding reductions in myotube size observed in SIRT1 inhibitor conditions. Furthermore, during low glucose induced myotube atrophy resveratrol reduced gene expression of the negative regulator of muscle mass, myostatin and protein degradative ubiquitin ligase enzyme, MUSA1. Overall, SIRT1 activation via a single

dose of resveratrol appears to have a role in acutely negating the effect of low glucose induced myotube atrophy and promoting myotube hypertrophy when glucose is readily available.

Acknowledgements

For their wise words of encouragement and understanding during difficult times as much as their academic prowess and willingness to always help. I truly do not believe you could find a more friendly, understanding and knowledgeable supervisory team as Dr. Adam Sharples and Prof. Claire Stewart. To both of you, thank you!

I wish to thank the Physiological Society, the Foundation of Joanna Scott and to the Sidney Perry Foundation, all of whom helped to fund either myself or the work, to all I am extremely grateful.

Finally, to Liverpool John Moores University thank you for welcoming me with open arms and allowing me produce this work with both financial contributions and laboratory facilities.

Author declaration

I declare that while registered as a candidate for the University's research degree, I have not been a registered candidate or enrolled student for another award of the LJMU or other academic or professional institution.

I declare that no material contained in the thesis has been used in any other submission for an academic award.

Dedications

I would like to dedicate this thesis to my father, the loving memory of my mother and my “other” mother.

Firstly to Checka Dugdale, although it hasn't always been plain sailing I am very thankful for everything you have done and do for me and for making my father so happy! To my mother, Sarah-Jane Fox, whose pride I may never truly feel but will always crave, a thought that has driven me to accomplish many dreams; I hope you approve of who I have become. And to my father, John Dugdale, who will always be my hero. I don't know every dad in the world so I can't say he's the best, but he must be on the podium. I am truly thankful for him each and every day and I wouldn't be the person I am today without him!

Abbreviations

ATCC	American type culture collection
BCA	Bicinchoninic acid assay
cDNA	complementary DNA
CK	Creatine kinase
CO ₂	Carbon dioxide
CR	Calorie restriction
D2H2O	Double distilled water
DM	Differentiation media
DMEM	Dulbecco's modified eagle's medium
DMSO	Dimethyl Sulphoxide
DNA	Deoxyribonucleic acid
DR	Dietary restriction
ECL	Enhanced Chemiluminescence
EDTA	Ethylenediaminetetraacetic acid
EX-527	SIRT1 inhibitor, EX-527
FBS	Foetal Bovine Serum
GM	Growth Media
Hi	Heat inactivated
h	Hour (s)
HRP	Horse radish peroxidase
HS	Horse Serum
IGF	Insulin-like growth factor
IGFBP	IGF binding protein
LOW	Low glucose (0.56 g/L or 3.12 mM)
MED	Medium glucose (1.13 g/L or 6.25 mM)
min	Minute(s)
MYHC	Myosin heavy chain
mTOR	Mammalian target of rapamycin
NAD	Nicotinamide adenine dinucleotide
NADH	Nicotinamide adenine dinucleotide reduced form

NBCS	New Born Calf Serum
NOR	Normal glucose (4.5 g/L or 25 mM)
PBS	Phosphate Buffered Saline
PCR	Polymerase Chain Reaction
Pen Strep	Penicillin–Streptomycin solution
q-PCR	Reverse transcription Polymerase Chain Reaction
ROS	Reactive oxygen species
RT	Room temperature
RT-qPCR	Real Time, reverse transcription Polymerase Chain Reaction
SDS-PAGE electrophoresis	Sodium dodecyl sulfate polyacrylamide gel
siRNA	Small interfering RNA
SIRT1	Sirtuin1
SD	Standard Deviation
TEMED	Tetramethylethylenediamine
TMT	Tris/MES Triton
TNF- α	Tumor Necrosis Factor- alpha

Figures

Chapter 2

Figure 2.1. Cell counting using a heamocytometer.....	34
Figure 2.2. Simplified diagram of the Biuret reaction	39
Figure 2.3. Cu ¹⁺ chelating with two molecules of BCA	40
Figure 2.4. 96 Well plate layout of total protein assay	42
Figure 2.5 BCA Standard graph.	43
Figure 2.6. Construction of transfer stack within the Transbot Turbo blotting system	48
Figure 2.7 Three phase separation during RNA isolation	52
Figure 2.8. RNA pellet in supernatant during RNA isolation	53
Figure 2.9. Calculating threshold and delta CT	58

Chapter 3

Figure 3.1. Representative cell images for reconstituted and liquid media ...	69
Figure 3.2. Representative cell images for glucose dose response	70
Figure 3.3. Representative images for LOW, MED and NOR glucose.....	71
Figure 3.4. Graph for myotube number, glucose dose response	72
Figure 3.5. Graph for CK	73
Figure 3.6. Graph for myotube size and diameter	74
Figure 3.7. Graph for gene expression for MyoD, MRF4 and Myogenin.....	77
Figure 3.8. Graph for gene expression for MYHC7 and MYHC2	79
Figure 3.9. Graph for gene expression for MYHC4 and MYHC1	81
Figure 3.10. Graph for gene expression for IGFBP2, ID3 and MUSA1	84
Figure 3.11. Graph for gene expression for SIRT1	87

Chapter 4

Figure 4.1 Graph for SIRT1 protein activity for resveratrol dose response across a time course (15 min, 30 min, 2 h and 24 h).....	97
Figure 4.2 Graph for SIRT1 protein activity for EX-527 30 and 60 μ M at 15 min, 30 min and 2 h.....	98
Figure 4.3 Graph for SIRT1 protein activity for EX-527 100 nM over a time course (15 min, 30 min, 2 h and 24 h).....	100

Chapter 5

Figure 5.1. Representative images for myoblast culture in LOW, MED and NOR alone or supplemented with resveratrol or EX-527	109
---	-----

Figure 5.2. Graph for myotube number in myoblast differentiation	111
Figure 5.3. Graph for CK in myoblast differentiation	115
Figure 5.4. Graph for myotube size and diameter in myoblast differentiation	117
Figure 5.5. Graph for gene expression for Myogenin	119
Figure 5.6. Graph for gene expression for MRF4	120
Figure 5.7. Graph for gene expression for MYHC7	122
Figure 5.8. Graph for gene expression for MYHC2	123
Figure 5.9. Graph for gene expression for MYHC4	125
Figure 5.10. Graph for gene expression for MYHC1	127
Figure 5.11. Graph for gene expression for SIRT1	130

Chapter 6

Figure 6.1. Representative images for myotube culture in LOW and NOR alone or supplemented with resveratrol or EX-527 at 24 h	138
Figure 6.2. Graph for myotube number in myotube cell culture at 24 h	139
Figure 6.3. Graph for myotube diameter in myotube cell culture at 24 h	140
Figure 6.4. Graph for myotube size in myotube cell culture at 24 h	141
Figure 6.5. Graph for gene expression for MYHC7 and IGF-I at 24 h	143
Figure 6.6. Graph for gene expression for MRF4 and MUSA1	145
Figure 6.7 Graph for AMPK protein activity for LOW and NOR alone or supplemented with resveratrol or EX-527 at 15 min	147
Figure 6.8 Graph for AMPK protein activity for LOW and NOR alone or supplemented with resveratrol or EX-527 at 30 min	148
Figure 6.9 Graph for AMPK protein activity for LOW and NOR alone or supplemented with resveratrol or EX-527 at 2 h.....	149
Figure 6.10 Graph for AMPK protein activity for LOW and NOR alone or supplemented with resveratrol or EX-527 at 24 h.....	150
Figure 6.11 Graph for p70S6K protein activity for LOW and NOR alone or supplemented with resveratrol or EX-527 at 15 min	151
Figure 6.12 Graph for p70S6K protein activity for LOW and NOR alone or supplemented with resveratrol or EX-527 at 30 min	152
Figure 6.13 Graph for p70S6K protein activity for LOW and NOR alone or supplemented with resveratrol or EX-527 at 2 h.....	153
Figure 6.14 Graph for p70S6K protein activity for LOW and NOR alone or supplemented with resveratrol or EX-527 at 24 h.....	154

Appendix 1

Figure A1.1. Representative images for myotube culture in LOW, and NOR alone or supplemented with resveratrol or EX-527 at 72 h	195
Figure A1.2. Graph for myotube number in myotube cell culture at 72 h	197
Figure A1.3. Graph for myotube diameter in myotube cell culture at 72 h ...	198
Figure A1.4. Graph for myotube size in myotube cell culture at 72 h	200
Figure A1.5. Graph for gene expression for MRF4 at 72 h	202
Figure A1.6. Graph for gene expression for MYHC7 at 72 h	204
Figure A1.7. Graph for gene expression for MYHC2 at 72 h	205
Figure A1.8. Graph for gene expression for MYHC4 at 72 h	207
Figure A1.9. Graph for gene expression for MYHC1 at 72 h	208
Figure A1.10. Graph for gene expression for IGF-I at 72 h	210
Figure A1.11. Graph for gene expression for IGF-IR at 72 h	212
Figure A1.12. Graph for gene expression for IGF-II at 72 h	213
Figure A1.13. Graph for gene expression for IGF-IIR at 72 h	214
Figure A1.14. Graph for gene expression for IGFBP2 at 72 h	216
Figure A1.15. Graph for gene expression for mTOR at 72 h	217
Figure A1.16. Graph for gene expression for TNF - α at 72 h	219
Figure A1.17. Graph for gene expression for TNFRSF1 β at 72 h	220
Figure A1.18. Graph for gene expression for Myostatin at 72 h	222
Figure A1.19. Graph for gene expression for MuRF1 at 72 h	223
Figure A1.20. Graph for gene expression for Mafbx at 72 h	225
Figure A1.21. Graph for gene expression for MUSA1 at 72 h	226
Figure A1.22. Graph for gene expression for SIRT1 at 72 h	227

Contents

Abstract	2
Acknowledgements	5
Author declaration	6
Dedications.....	7
Abbreviations	8
Contents	13
2. Materials and Methodology	29
2.1 General equipment and specialized software	29
2.1.1 Cell Culture	29
2.1.2 Biochemical Assays	29
2.1.3 Real Time, Reverse Transcription quantitative Polymerase Chain Reaction (RT-qPCR)	29
2.1.4 SDS-Page and Western Ligand Blotting.....	30
2.1.5 Plastic ware.....	30
2.1.6 Cell Culture Reagents	31
2.2. Methodology- Principles and procedures	32
2.2.1. C2C12 Skeletal Myoblasts	32
2.2.2 Cell Culture of C2C12 Skeletal Myoblasts	32
2.2.3. Cell Counting via Trypan Blue Method	33
2.2.4. Cell Cryopreservation and Resurrection.....	35
2.2.5. Dosing Cells	35
2.2.6. Muscle cell morphological measures by microscopy	38
2.2.7. Cell Lysis for total Protein and Creatine Kinase Assays	39
2.2.8. Total Protein Assay	39
2.2.9. Creatine Kinase Assay	43
2.2.10. SDS Page and Immunoblotting	46
2.2.11. RNA Extraction.....	50
2.2.12. PCR	53

3. Determining Physiological Glucose Concentrations <i>in vitro</i>: A Model to investigate the impact of dietary restriction on muscle cell differentiation.....	62
3.1. Introduction.....	62
3.2. Methods.....	64
3.2.1. Cell culture.....	64
3.2.2. Cell dosing.....	65
3.2.3. Morphology.....	66
3.2.4. Total protein content.....	66
3.2.5. Creatine Kinase.....	66
3.2.6. RNA Extraction and analysis.....	66
3.2.7. Primer design.....	67
3.2.8. RT-PCR and analysis.....	67
3.2.9. Statistical analysis.....	68
3.3. Results.....	68
3.3.1. Preliminary morphological analysis to eliminate irrelevant glucose concentrations from further analysis.....	68
.....	70
3.3.2. Morphological and biochemical analysis for differentiation capacity was reduced in LOW and MED glucose conditions.....	70
3.3.3. Impaired expression of the myogenic regulatory factors (MRF) during LOW glucose.....	74
3.3.4. Myosin Heavy Chain (MYHC) expression is impaired under MED and LOW glucose conditions compared to NOR.....	78
3.3.5. LOW and MED glucose do not have an increased atrophic gene expression.....	81
3.3.6. SIRT1 expression increases following LOW glucose conditions.....	85
3.4. Summary.....	88
3.5. Conclusion.....	89
4. The activation of SIRT1 in myoblasts in response to a pharmacological administration of resveratrol and EX-527.....	91
4.1. Introduction.....	91
4.2. Methods.....	93
4.2.1. Cell culture.....	93
4.2.2. Total protein content.....	94
4.2.3. SDS-PAGE and immunoblotting.....	94

4.2.4. Statistical analysis.....	94
4.3. Results.....	95
4.3.1. Initial resveratrol dose response.....	95
4.3.2. Effect of 10 μ M RES on SIRT1 activation.....	95
4.3.2. The Effect of the SIRT1 inhibitor (EX-527) at a concentration of 30 μ M and 60 μ M on SIRT1 activation.....	97
4.3.3. The Effect of the SIRT1 inhibitor (EX-527) at a concentration of 100 nM on SIRT1 activation.....	99
4.4. Summary	100
5. SIRT1 activation and inhibition in myoblasts under reduced glucose conditions.	104
5.1. Introduction.....	104
5.2. Methods.....	105
5.2.1. Cell culture.....	105
5.2.2. Cell dosing.....	105
5.2.3. Morphology.....	106
5.2.4. Total protein content.....	106
5.2.5. Creatine Kinase.....	106
5.2.6. RNA Extraction and analysis.....	107
5.2.7. Primer design.....	107
5.2.8. RT-PCR and analysis.....	107
5.2.9. Statistical analysis.....	108
5.3. Results.....	109
5.3.2. Resveratrol increases creatine kinase activity at 7D in LOW glucose conditions despite no increase in myotube formation and reduces CK activity with SIRT1 inhibition in normal glucose conditions.....	111
5.3.3 Myotube size increased with resveratrol administration in NOR glucose conditions.....	115
5.3.4. MRF's are unaltered following SIRT1 activation via resveratrol administration.....	118
5.3.5. Resveratrol administration increased MYHC7 and MYHC4 gene expression in NOR glucose conditions.....	121
5.3.6. SIRT1 is reduced in all conditions following 7D and GCN5 remains unchanged under most experimental conditions.....	128
5.4. Summary	131
5.4.1. Future directions for chapter 6.....	132

6. Resveratrol reduces acute myotube atrophy with glucose restriction	135
6.1. Introduction.....	135
6.2. Methods	135
6.2.1. Cell culture and treatments.....	135
6.2.2. Statistical analysis.....	136
6.3. Results.....	Error! Bookmark not defined.
6.3.7. Myotube diameter and area were increased in LOW glucose conditions at 24 h after resveratrol supplementation.	138
6.3.8. Resveratrol increased MYHC7 expression in NOR conditions after 24 h but not in LOW glucose conditions.	142
6.3.9. MRF4 increased after 24 h with resveratrol supplementation in LOW glucose	143
6.3.10. No significant changes were present in MUSA1 gene expression following the activation/ inhibition of SIRT1.	144
6.4. Summary	155
7. Discussion.....	158
7.1. Relevant physiological model of glucose restriction.....	158
7.2. Dose response for SIRT1 activation and inhibition	160
7.3. SIRT1 activation and inhibition in restricted and normal glucose conditions.....	161
7.4. Conclusions	169
8. References	172
9. Appendix 1	195
6.3.1. Low glucose reduces myotube number and promotes myotube atrophy.....	195
6.3.2. MRF4 was unchanged with resveratrol or SIRT1 inhibitor	201
6.3.3. MYHC 7 expression is increased with SIRT1 activator resveratrol and MYHC 1,2,4 reduced with SIRT1 inhibitor EX-527 in normal glucose conditions.....	203
6.3.4. Myotube growth/hypertrophy	209
6.3.5. Genes associated with myotube atrophy and protein degradation:.	218
6.3.6. Ubiquitin Ligases: MAFbx, MuRF1 and MUSA1	222

Chapter 1

1. Introduction

1.1. Calorie restriction

The strikingly simple intervention of calorie restriction (CR) originates from the 1935 publication by McCay *et al.* in which reduced energy intake extended both mean and maximum lifespan in rats. Despite its simplicity CR is often mistaken for a minimal or lack of dietary intake known as fasting, when literature actually describes CR as an absence of malnutrition, while maintaining meal frequency, neither of which are present during fasting (Selman, 2014). CR is most accurately described as a 20-50% reduction in caloric energy intake in comparison to *ad libitum* (AL) counterparts (Longo and Mattson, 2014, Fontana and Klein, 2007, Mccay et al., 1935). Replication these initial findings have since been observed in yeast, worms and mice, with similar trends being observed in rhesus monkeys (Fontana *et al.*, 2010, Masoro, 2005, Mattison *et al.*, 2012, Colman *et al.*, 2009, Harper *et al.*, 2006, Weindruch *et al.*, 1986, Kaeberlein *et al.*, 2006, Mccay *et al.*, 1939). Although compelling data suggests that humans display beneficial health improvements under CR conditions, the effect on human lifespan is inconclusive (Roth *et al.*, 2002, Holloszy and Fontana, 2007), partly due to the lack of long term CR studies in humans perhaps due poor adherence/motivation to undertake long term CR.

1.2. Dietary restriction

Alternative investigations into CR involve manipulation of micro and/ or macro nutrients which differ from ad lib counterparts, in addition or independently to an overall changes in energy intake. For the purpose of this thesis the term dietary restriction (DR) will henceforth encompass both the traditional definition of CR and the aforementioned nutritional manipulations (Selman, 2014). Dietary restriction increases longevity (Longo and Mattson, 2014, Fontana and Klein, 2007, Mccay et al., 1935). Before establishing how DR is instrumental in delaying the onset of ageing it is important first to understand the ageing phenotype. Eukaryotic aging

is defined as increasing dysfunction in both tissue and organs as a whole and can be considered both as a chronological and biological process (Hekimi and Guarente, 2003, Tatar *et al.*, 2003, Carter *et al.*, 2007). A plethora of functional changes have been associated with this pathology including a reduction in tissue regenerative capacity, a decrease in endocrine response and increases in oxidative stress (Lightfoot *et al.*, 2014, Carter *et al.*, 2007). Not only does DR reduces mortality via the reduction of these age related changes it also reduces the prevalence of morbidity. Disease risk reductions during DR include, but are not limited to, the prevalence of type II diabetes, hypertension and obesity, as well as a decline in some cancers and cardio-vascular disease (Longo and Mattson, 2014, Lam *et al.*, 2013, Carter *et al.*, 2007). Therefore, regardless of the limited data to suggest that DR improves lifespan in humans, the implementation of DR reduces numerous physiological afflictions often associated with obesity and age and is therefore widely considered to improve healthspan. Skeletal muscle is one such tissue that maybe particularly susceptible to age related changes and DR.

1.3. DR, muscle size regulation and regeneration

During chronic DR, there may be an increased dependence on protein metabolism thus leading to reductions in skeletal muscle mass as a result of reductions in protein synthesis and increases in protein degradation (Ballor *et al.*, 1988, Carter *et al.*, 2007, Fulco *et al.*, 2008). Indeed, pioneering work in 2003 suggested that cells prioritized maintenance/survival over growth during starvation (Inoki *et al.*, 2003). They reported increased AMPK activity and phosphorylated tuberous sclerosis 2 (TSC2) under starvation, TSC2 then inhibited mammalian target of rapamycin (mTOR) and other downstream substrates, including translation initiators and elongators P70S6K, 4EBP-1 and EIF2. This subsequently resulted in reduced cellular growth rates. Despite this, fascinatingly, but perhaps intuitively, the complex nature of skeletal muscle mass regulation has led to inconsistent adaptations following DR. Indeed, short-term DR has actually been shown to increased skeletal muscle stem cell availability and

repair following injury in young and old mice (Cerletti *et al.*, 2012). And DR has been shown to reduce both the loss of total fibres as well as the atrophy of the remaining slow twitch fibres in a long-lived hybrid rat strain (Mckiernan *et al.*, 2004). DR also appears to delay or prevent age-related loss of SkM mass in rats and rhesus monkeys (Phillips and Leeuwenburgh, 2005, Aspnes *et al.*, 1997, Hepple *et al.*, 2008, Mckiernan *et al.*, 2011). These observations may be as a result of alleviating the production of chronically upregulated inflammatory cytokines during DR (Spaulding *et al.*, 1997a). When chronically upregulated, TNF- α regulates inflammatory, apoptotic and protein degradative pathways and is associated with reduced muscle size with age (Bruunsgaard *et al.*, 2003a, Greiwe *et al.*, 2001, Bruunsgaard *et al.*, 2003b, Brüünsgaard and Pedersen, 2003). However, the mediation of these pathways has been shown to be reduced following the attenuation of TNF- α due to the implementation of DR (Spaulding *et al.*, 1997b, Phillips and Leeuwenburgh, 2005). In addition to the reduction of chronic inflammation, DR has also been documented to reduce apoptotic cell death (Cohen, 2004), as well as oxidative and DNA damage, among other factors (Carter *et al.*, 2009).

In humans, chronic DR (by 30% of recommended daily intake) for an average period of 9.6 years, resulted in reduced growth factor expression of insulin-like-growth-factor I (IGF-I) levels. Additionally AKT phosphorylation was reduced by 35 - 50% under DR conditions, consistent with the observed reductions in transcription, an important finding due to the AKT pathways' associated involvement in growth/ protein synthetic signaling. Furthermore, in the same study authors showed the reduction in AKT resulted in an increase in genes associated with protein degradation, including FOXO3a (Mercken *et al.*, 2013). Yet with increased FOXO3a the authors also observed increased genes associated with stress resistance and DNA repair (Mercken *et al.*, 2013) as suggested above (Carter *et al.*, 2009). Therefore, it is worth noting that with DR, this decrease in protein synthetic signaling, increase in protein degradation and shift from growth towards stress resistance, would potentially reduce protein synthesis and

increase degradation over time (Sandri *et al.*, 2004, Edström *et al.*, 2006) It is also worth noting that despite some unintuitive findings with respect to the influence of DR on muscle mass regulation some *in-vivo* studies that investigate the impact of DR on skeletal muscle mass provide muscle mass relative to fat mass or total mass, with DR animals reportedly possessing higher lean mass to fat mass and/ or total mass ratio, therefore perhaps underestimating the influence of DR on lean mass. (Colman *et al.*, 2008, Mckiernan *et al.*, 2011) (Mckiernan *et al.*, 2011). Furthermore, even if muscle mass is maintained during a specific DR regimen, the ability of skeletal muscle to undergo hypertrophy may also be limited. This was observable within combined diet and resistance exercise training studies, where the loss of muscle mass experienced with DR in human cohorts was diminished when undertaken alongside resistance exercise in comparison to DR alone (Larson-Meyer *et al.*, 2006, Ballor *et al.*, 1988, Weiss *et al.*, 2007, Ross *et al.*, 2000, Janssen and Ross, 1999).

As aluded to above, in addition to the reductions in AKT activity (Mercken *et al.*, 2013) a reduction in the insulin/IGF signaling pathway is also present and has been previously associated with increased lifespan and healthspan in model organisms (Clancy *et al.*, 2001, Holzenberger *et al.*, 2003, Barbieri *et al.*, 2003, Tatar *et al.*, 2003, Giannakou and Partridge, 2007, Piper *et al.*, 2008, Selman *et al.*, 2008, Vallejo *et al.*, 2009, Kenyon, 2011, Selman *et al.*, 2011). With ageing however, where considerable muscle loss occurs, there is a paradoxical reduction of approximately 33% in circulating IGF-I (Benbassat *et al.*, 1997) and a 45% decline in SkM-derived IGF-I mRNA in older (70 ± 0.3 years) vs. younger (20 ± 0.2 years) human males (Léger *et al.*, 2008). These observations indicate that although DR may reduce IGF-I to evoke improvements in lifespan and healthspan, reduced IGF-I is associated with reductions in muscle mass with age. Indeed, this is demonstrated in insulin receptor substrate 1 (IRS1) knockout mice (required for intracellular signalling following successful IGF-I/IGFI receptor binding), where despite having increased lifespan, have reduced body weight and fat mass compared to age-

matched controls (Pete *et al.*, 1999, Selman *et al.*, 2008) and importantly have reduced gastrocnemius skeletal muscle weight that is proportionately greater than the decrease seen in total body weight (Pete *et al.*, 1999).

DR therefore may be a successful intervention at improving lifespan and healthspan and evidence suggests in animal models that DR does not affect muscle mass possibly due to a reduction in inflammation. Contradictory evidence suggests however that DR evokes a reduction in IGF-I and related signalling associated that is also observed with muscle loss in older age. Finally, the loss of cellular differentiation capabilities in myoblasts have been observed in low glucose conditions (Elkalaf *et al.*, 2013, Khodabukus and Baar, 2014). Fulco *et al.* (2008) suggested that increased activation of Sirtuin 1 (SIRT1) was responsible for the observed impaired differentiation in low glucose conditions. Fulco *et al.* (2008) further suggests that this mediated via activation of the energy dependent, AMPK pathway, in which the expression of downstream genes such as FOXO, atrogin1/ MAFbx and MuRF1 associated with protein degradation are up regulated (Nakashima and Yakabe, 2007) an observation discussed later in this introduction under section 1.6, however suggests that further SIRT1 activation may be important under DR in skeletal muscle cells.

1.5. SIRT1 and DR

Indeed, Sirtuin 1 (silent information regulator/ SIRT1) is a nicotinamide adenine dinucleotide (NAD⁺) dependant class III histone deacetylase, the closest homologue of all seven mammalian Sirtuins to the yeast Sir2 enzyme (Boily, 2008, Inoue *et al.*, 2007). Both SIRT1 and Sir2 are activated via an increase in the NAD⁺: NADH ratio (Canto and Auwerx, 2008, Bk, 2006). This reliance on nutrient sensing has led to extensive research on the involvement of Sir2 in yeast and more recently SIRT1 in mammalian longevity experienced during DR (Baur *et al.*, 2012, Brenmoehl and Hoeflich, 2013, Gurd *et al.*, 2011, Mercken *et al.*, 2014a). Sir2 overexpression improves lifespan in budding yeast and similar trends

have been recorded regarding SIRT1 in mammalian models (Kaeberlein *et al.*, 1999, Herranz *et al.*, 2010).

The effect SIRT1 has on lifespan is demonstrated by Boily (2008), in which the maximal survival of SIRT1 null mice is 24 months compared to approximately 32 months in similar wild type counterparts (Harper *et al.*, 2006). This suggests that adequate SIRT1 is required for normal lifespan. Furthermore, this reduced lifespan is further exacerbated by the employment of DR in these mice (Boily, 2008). These findings are indicative of SIRT1 knockout mice being unable to adapt to reduced calorie intake, thus highlighting the importance of SIRT in longevity during DR. Also, administration of the SIRT1 activator, STR2104 in murine populations has resulted in lifespan improvements similar to that observed during DR (Mercken *et al.*, 2014b). Additionally, the use of an alternate SIRT1 activator, resveratrol has also shown improvements in age related diseases and ultimately lifespan in mice, albeit the most prominent research suggests this phenomenon is more likely to occur on a background of a high fat diet (Baur *et al.*, 2006, Pearson *et al.*, 2008, Barger, 2008). Short-term resveratrol supplementation in humans also elicits similar metabolic and inflammatory adaptations as those observed during DR (Timmers *et al.*, 2011). Unfortunately, there are inconsistencies in the literature regarding overexpression of SIRT1 not always leading to lifespan improvements, however in these instances where longevity is not experienced, age-related disease prevalence appears to decline similarly to DR (Mercken *et al.*, 2014b, Herranz *et al.*, 2010), suggesting an important role in healthspan. Overall, it is evident that SIRT1 plays a significant role in both the life and health span experienced during DR.

1.6. SIRT1 and skeletal muscle mass

Although there is limited data regarding the effect of SIRT1 on skeletal muscle mass *per se*, its role in metabolism has been studied more extensively. Overexpression of SIRT1 in murine models has led to improved glucose uptake in skeletal muscle. In addition, the age-

associated accumulation of nuclear foci of DNA damage proteins have been shown to be suppressed in comparison to wild type (WT) counterparts. Both these outcomes suggest a slowing in metabolic damage (Herranz et al., 2010). Bordone *et al.* (2007) implemented a transgenic mouse model (overexpresses SIRT1) and observed an increase in metabolic activity via increased oxygen and food consumption relative to body weight compared to their controls. SIRT1 may consequently play an important role in increasing metabolic activity, possibly preventing accretion of metabolic damage and ultimately inducing a reduction in overall pathological incidence. In some tissues, overexpression of SIRT1, despite no further improvements in lifespan, reduces pathological incidence such as eye infections and abnormal growths by 13% (Mercken et al., 2014a).

There is also now emerging evidence that SIRT1 could also be involved in muscle mass regulation under stressful environments (see below). Overexpression of SIRT1 via the administration of SRT2014, during the employment of a 2 week hind-limb unloading protocol, has reportedly maintained skeletal muscle mass compared with unsupplemented controls, in addition to increasing rodent lifespan (Mercken et al., 2014b). Despite this, it has been observed that aged mice had a blunted hypertrophic response following synergistic ablation with a lower satellite cell content }and not as large an increases in in type II fibres vs. young adult mice (Ballak *et al.*, 2015). However, resveratrol did not rescue the blunted hypertrophic response and actually even reduced, rather than increased, the number of satellite cells in the hypertrophied muscles. These findings indicate that SIRT1 may play an important role in stressful environments such as disuse and disease, yet perhaps not in basal ageing and warrants further investigation.

1.6 Role of SIRT1 and DR in skeletal muscle cells *in vitro*:

Adult skeletal muscle fiber number is set in-utero and adult fibers are post-mitotic (incapable of cellular division) (Buckingham *et al.*, 2003).. Despite

these phenomena, adult skeletal muscle is highly adaptable, readily responding environmental cues. Much of this adaptability (growth and repair) is achieved via resident adult stem cells, termed satellite or muscle precursor cells that have mitotic potential (Once activated these cells are termed myoblasts) (Brown and Stickland, 1993, Rudnicki *et al.*, 2008, Charge and Rudnicki, 2004).

Despite the sparse literature involving the role of SIRT1 in whole skeletal muscle maintenance, *in vitro* studies involving mouse skeletal muscle satellite cells, primary myoblasts and myoblast cell lines have also begun to be conducted. As previously discussed, the loss of differentiation capabilities in myoblasts, have been observed in low glucose (DR) (Elkalaf *et al.*, 2013, Khodabukus and Baar, 2014). Also, as discussed above, Fulco *et al.* (2008) suggested that increased SIRT1 activity was responsible for impaired differentiation, mediated via activation of the energy dependent, AMPK pathway, in which the expression of downstream genes such as FOXO, atrogin1/ MAFbx and MuRF1 associated with atrophy are up regulated (Nakashima and Yakabe, 2007).

Contrary to this finding research by our group were first to demonstrate (Saini *et al.*, 2012), with replication by Wang *et al.* (2014), a survival and regenerative effect of SIRT1 on myoblast differentiation when the SIRT1 activator, resveratrol is administered together with an inflammatory cytokine known to induce an inhibition of myoblast differentiation, TNF- α (Saini *et al.*, 2012). This is important given that TNF- α increases chronically in both the circulation and skeletal muscle tissue of elderly humans, and correlates with loss of muscle function, morbidity and mortality (Greive *et al.*, 2001) (Greive *et al.*, 2001, Bruunsgaard and Pedersen, 2003, Bruunsgaard *et al.*, 2003a, Bruunsgaard *et al.*, 2003c), Saini *et al.* (2012) observed an increase in SIRT1 mRNA associated with TNF- α induced cell death, which was further exacerbated through SIRT1 inhibition by siRNA. However, death was rescued through SIRT1 activation via resveratrol. These findings imply that SIRT1 is important in

cell survival. Furthermore, TNF- α induced reductions in differentiation were restored with SIRT1 activation via resveratrol administration also an indication that SIRT1 may actually be important in maintaining myoblast differentiation in stressful catabolic environments (Saini et al., 2012). Furthermore, resveratrol has been shown to improve myoblast migration (albeit not differentiation) in the presence of oxidative stress via hydrogen peroxide (Bosutti and Degens, 2016). Overall suggesting that SIRT1 activation via resveratrol administration may mediate survival, remodelling and differentiation in muscle cells.

1.7. Summary

Despite the dramatic improvements in health observed under dietary restricted environments the chronic reduction in caloric intake may lead to impaired growth related signaling causing a potential breakdown in muscle protein over time. The activation of SIRT1 via resveratrol treatment in the presence of inflammatory and oxidative stress, has been previously shown to protect myoblasts from a loss of myotube formation and improve muscle cell remodelling, therefore the activation of SIRT1 under the alternate stress of DR may provide a similar protective effect.

1.8 Aim

The overall aim of this thesis was to determine whether the supplementation of resveratrol via activation of SIRT1 was able to ameliorate the potential losses in myoblast differentiation and myotube hypertrophy observed under DR conditions.

1.9 Thesis Overview

Following this introduction, we first documented the methodology used to carry our aims in the following four data chapters, this information can be found in **Chapter 2**. A physiological model of glucose restriction *in vitro* was then established in **Chapter 3**. Glucose concentrations that mimic both the circulating/ interstitial levels in rodents following DR were assessed for skeletal muscle cells differentiation capacity via

morphological (myotube number, diameter, area) and biochemical analysis (CK activity). In addition gene expression analysis was also performed for fundamental genes related to myogenesis, the differentiation program, myotube maturation and protein degradation (MyoD, MRF4, Myogenin, MYHC 1, 2, 4 and 7, IGFBP2, ID3, MUSA1 and SIRT1). In **Chapter 4** the most appropriate doses of SIRT1 activator resveratrol and inhibitor (EX-527) was determined as to evoke increased/ decreased SIRT1 activity via western blot analysis, respectively. Both **Chapter 5 and 6** utilised the findings from both chapter 3 and 4 and carried out glucose restriction in the presence of the SIRT1 activator and inhibitor. **Chapter 5** addressed the role of altering SIRT1 activity in differentiating myoblasts under glucose restriction via morphological, biochemical and gene expression analysis (as in chapter 3) to determine whether SIRT1 had a role in ameliorating the effect of low glucose on myoblast regeneration capacity. Finally, data from chapter 5 led us to believe SIRT1 activation may play a role in later myotube hypertrophy and therefore in **Chapter 6** we addressed the role of SIRT1 activation/ suppression in fully differentiated formed myotubes. This was carried out through extensive morphological analysis and gene expression of important genes identified above in this introduction and those associated with late differentiation and myotube maturation (MRF4, MYHC1, 2, 4 and 7) myotube hypertrophy (IGF-I, IGF-IR, IGF-II, IGF-IIR, IGFBP2, mTOR) and myotube atrophy (TNF- α , myostatin, MuRF, MAFbx, MUSA1, FOXO1, 3, NF-kB, p53). Furthermore, we assessed protein activity of energy sensing (AMPK) vs. growth cellular signalling (P70S6K) identified in this introduction above to be important in DR in muscle cells Fulco et al. (2008) and other cell types (Inoki et al., 2003). Finally, **Chapter 7** provides the final discussion and conclusions that can be drawn from the work, as well potential future directions.

Chapter 2

2. Materials and Methodology

2.1 General equipment and specialized software

2.1.1 Cell Culture

All cell culture experiments were performed in a certified class II cabinet (BioULTRA, Telstar, Terrassa, Spain). All liquid handling was performed using a portable pipet aid (Drummond, PA, USA) and waste liquid was vacuum pump aspirated (Capex 8c, Charles Austen pump Ltd. U.K.). The cells were incubated in a CO₂ incubator (CB 150, Binder, Germany), maintained at 37°C and 5% CO₂.

2.1.2 Biochemical Assays

A CLARIOstar® plate reader (BMG Labtech, Germany) was used for both total protein and CK at 540-590 nm and 340 nm respectively. The BCA protein assay kit was purchased from ThermoScientific (IL, USA) and the DiscretPak™ Creatinine kinase Reagent kit from Catachem (CT, USA).

2.1.3 Real Time, Reverse Transcription quantitative Polymerase Chain Reaction (RT-qPCR)

A Spectrophotometer (Nanodrop 2000, ThermoScientific, IL, USA) was used at absorbency ratios of 260/ 280 nm and 260/ 230 nm to measure quantity and quality of each RNA isolation. Samples were prepared for PCR using an automated pipetting system (QIAgility, Qiagen, Venlo, Netherlands). The prepared samples were then placed in a qPCR cycler (Rotor-gene Q®, Qiagen, Venlo, Netherlands). Reagents, reaction tubes and pipette tips used for q-PCR (Syber green, RT master mix and RNA free water) were all supplied by Qiagen (Venlo, Netherlands).

2.1.4 SDS-Page and Western Ligand Blotting

Mini Protean® Tetra stands with clamp kit (Bio-Rad Laboratories, Inc. CA, USA) were used for gel casting, a Powerpac™ Basic Power Supply used for electrophoresis and Trans-blot® Turbo™ Blotting system (Bio-Rad Laboratories, Inc. CA, USA) for transfer from gel to nitrocellulose membrane. Protein detection was carried out using Pierce™ Fast Western Kit, Supersignal West Pico, Rabbit (ThermoFisher scientific, MA, USA) and enhanced chemiluminescence (ECL) detections were performed using the Chemidoc™ MP system (Bio-Rad Laboratories, Inc. CA, USA).

2.1.5 Plastic ware

Plasticware used during cell culture procedures were acquired from Falcon™ (ThermoFisher scientific, MA, USA), this included; 75 cm² Straight neck cell culture flask and 6 well plate cell culture plate. Biochemical assays used Falcon™ (ThermoFisher scientific, MA, USA) 96 Well plates. Cryotubes® used for cryopreservation were purchased from Nunc® (Sigma-Aldrich, MO, USA). Differentiation media was filtered using Stericup® Filter units (0.2 µm) and collected into receiver flask produced by Merck Millipore (Darmstadt, Germany). Filtering of media components was performed using 0.2 µm syringe filters originally produced by Corning™ (MA, USA) and purchased from ThermoFisher scientific (MA, USA). Preparation of liquid for cell dosing and Biochemical assays was performed in either a 5, 10 and 25 ml Falcon™ tube (ThermoFisher scientific, MA, USA). Extraction of samples from cell culture was aided using Fisherbrand™ cell scrapers (ThermoFisher scientific, MA, USA) and the sample was collected into tubes originally produced by Eppendorf (Hamburg, Germany) of either 2, 1.5 or 0.5 ml. During RNA extraction and isolation Applied Biosystems™ 1.5 ml RNA free tubes were used, purchased from ThermoFisher scientific (MA, USA). Reaction tubes for q-PCR were purchased from Qiagen (Crawley, UK). Pipette tips used for cell culture, biochemistry and western blotting as well as filter tips for RNA

isolations were purchased from Fisherbrand™ (Thermofisher scientific, MA, USA).

2.1.6 Cell Culture Reagents

The purchase of sterile cell culture reagents is listed below: Dulbecco's modified eagle's medium (DMEM) from Sigma-Aldrich (MO, USA). Heat inactivated (hi) New Born Calf Serum (NBCS), hi Foetal bovine serum (FBS) and hi horse serum (HS) were originally produced by Gibco™ (Paisley, UK) and purchased from Sigma-Aldrich (MO, USA). Powdered DMEM with no glucose was also purchased from Sigma-Aldrich (MO, USA), the reconstitution of which was performed using Hyclone™ water, cell culture grade (endotoxin free) purchased from Thermofisher scientific (MA, USA). L-Glutamine 200 mM, Penicillin-Streptomycin solution 5000 U/ml (Pen-strep), Trypsin EDTA (0.05%) and phenol red were produced by Gibco™ (Paisley, UK) and purchased from Thermofisher scientific (MA, USA). These items were purchased unsterile and were filtered using the above mentioned syringe filters. Porcine gelatine was reconstituted using 1 g in 500 ml of D₂O. Phosphate buffered saline (PBS) was reconstituted using 1 tablet per 100 ml of D₂O. Both gelatine type A (from porcine skin (cat no. G2500-100G) and PBS were purchased from Sigma-Aldrich (MO, USA). The distilled water was produced using a Milli-Q® direct 8 purification system from (Merck Millipore, Darmstadt, Germany). These reagents were reconstituted in glassware bottles. These were then autoclaved. Items that were bought in large quantities e.g. Pen-strep and Trypsin were aliquoted into smaller volumes ready for use, this reduced the number of freeze thaw cycles.

2.2. Methodology- Principles and procedures

2.2.1. C2C12 Skeletal Myoblasts

The C2C12 cell line were used in both the cell and myotube studies (Blau, 1993). These cells were purchased from the American type culture collection (ATCC). Once these cells arrive they are categorized as P0, the first passage is subsequently known as P1. Each additional passage increases the P number by 1. C2C12 and C2 myoblasts undergo spontaneous differentiation into myotubes on serum withdrawal, and do not require growth factor addition to stimulate the process (Blau, 1993, Tollefsen *et al.*, 1989).

2.2.2 Cell Culture of C2C12 Skeletal Myoblasts

T75 flasks were prepared using 8 ml of 0.2% gelatine left at room temperature for 10 min and then incubated at 37 °C for 10 min. The excess gelatine was removed and 14 ml of Growth Media (DM) (DMEM, 10% hiFBS, 10% hiNCS, 1 % pen-strep) was added. Cryovials were brought up from liquid nitrogen containing 1-2 ml of cell solution consisting of 1-2 ml of growth media (GM) suspending 1×10^6 cells per ml. The cells were then thawed at 37 °C, 1 ml cell solution was added to one pre-prepared T75 and incubated at 37 °C and 5% CO₂ for 72 hr.

Following the 72 h incubation, cells were visually assessed in order to ensure confluency. Once achieved the GM was aspirated and the cells were washed twice using 8 ml of Phosphate Buffered Saline (PBS). Pre-warmed Trypsin (1 ml per T75) was then applied for 5 min at 37 °C. Once cells were no longer adhered to the dish (assessed by looking at the cells under an Olympus CKX31 inverted microscope (Olympus Corporation, Japan) the Trypsin was neutralized by adding 4-8 ml of GM. The solution containing Trypsin, cells and GM was then removed into a 50 ml tube and homogenized gently using a 19G needle BD Microlance 3, (Becton,

Dickinson and Company, UK) to reduce cell clumps thus increasing the accuracy of the cell count (section 2.2.3).

Prior to use, 6-well plates were pre-treated with 1 ml, 0.2% porcine gelatine per well and incubated for 10 min at room temperature (RT) and 10 min in a humidified incubator at 37°C with 5% CO₂. The excess gelatine was aspirated and cells were seeded at 8×10^4 cells per ml in 2 ml of GM per well, these were then incubated until 80% confluency. High serum (20%) GM was removed and the cells were washed once with 2 ml PBS, 2 ml of low serum Differentiation Media (DMEM, 2% horse serum, 1% pen-strep) was then added to each well. It is during this change in DM that the cells were treated in various conditions specific to individual chapters detailed below (**Section 2.2.5.**).

2.2.3. Cell Counting via Trypan Blue Method

The Trypan blue method of cell counting was originally devised to determine cell viability of the cell population by differentiating between trypan incorporated (blue non-vivable) and non-coloured (viable) cells. Here the Trypan blue dye infiltrates perforated cells, a characteristic of the impaired membrane integrity of non-viable cells, thus making them appear blue under a microscope where cell death occurs. A haemocytometer was used for manual counting; this consists of a thick glass microscope slide with two chambers. Each chamber can contain a total of 10 µl of liquid. (Fig.2.1).

Fig. 2.1. The original, unedited image was obtained from www.microbehunter.com/the-hemocytometer-counting-chamber. Viable cells and dead cells are represented by grey and blue dots respectively. The red lines indicate a magnification of the area.

Preparation of the cell solution consisted of a 1:1 dilution, produced using a 50 μ l Trypan blue solution 0.4% (Thermofisher scientific, MA, USA) and 50 μ l cell solution, once removed from a confluent T75. The solution was applied in 10 μ l to both chambers of the Bright-line™ haemocytometer (Sigma-Aldrich, MO, USA) and the coverslip was placed over the chambers. After leaving the solution to settle for 1-2 min the haemocytometer was placed under a CKX31 inverted microscope (Olympus Corporation, Tokyo, Japan) at a 10 x magnification. Each chamber was divided into 4 segments; A-D, the viable cells were counted in all of the segments and an average was calculated across all 4 segments in both chambers. If one cell was situated across the single line edge then it was not counted, if it was across the multiple lines (closest to the centre) then these were counted (Fig.2.1).

To obtain the number of cells per ml the average cell number was multiplied by 2. This is because the cell solution was diluted 1:1 with the Trypan blue. As each grid section in which the average cell count was obtained has a volume of 0.1 mm^3 it must therefore contain $0.1 \text{ } \mu\text{l}$ of solution. The value obtained above (following the x 2 multiplication) was therefore multiplied by 10^4 to obtain the number of cells ml^{-1} . The same cell solution was used across both chambers as a duplicate and an average of these was also taken to ensure accurate cell numbers were obtained.

2.2.4. Cell Cryopreservation and Resurrection

Cells at densities above or below 1×10^6 cells/ml were diluted in GM or centrifuged (5 minutes at 2500 rcf) and resuspended in GM respectively to provide a concentration of 1×10^6 cells/ml. To prevent the formation of ice crystals cells were treated with 10% Dimethyl sulfoxide (DMSO). The treated solution was then aliquoted into labelled cryotubes (Sigma-Aldrich, MO, USA) and stored in a Mr Frosty™ Freezing container (Thermofisher scientific, MA, USA) at -80°C for 24 h. The cryotubes were then moved into a labelled holder and stored in liquid nitrogen until required for future experimentation.

2.2.5. Dosing Cells

2.2.5.1. Reconstitution of powdered cell culture media

The powdered DMEM (Sigma, Cat no D5030) was reconstituted according to manufacturers instructions (8.3 g/L of DMEM) supplemented with 0.58 g/L L-Glutamine, 3.70 g/L Sodium Bicarbonate, 0.11 g/L, Sodium Pyruvate, 0.02 g/L, Phenol red and either 0 g/L or 4.5 g/L (25 mM) D-Glucose in HyPure™ Molecular grade water (Hyclone, Thermofisher scientific, MA, USA). This was to ensure the composition matched the more generally used liquid DMEM.

2.2.5.2 Procedure for Dosing Cells at various glucose concentrations

Media of varying glucose concentrations are implemented in Chapters 3, 5 and 6. To obtain the different concentrations of glucose containing media powdered glucose (4.5 g/L) media was diluted using powdered glucose free media (0 g/L) detailed above, by creating the following concentrations; 24.90, 18.75, 12.50, 6.24, 3.12, 0.00 mM.

2.2.5.3. Reconstitution of Resveratrol

Resveratrol, cat no. 554325 (Calbiochem, USA) was purchased in from Merck Millipore, (Darmstadt, Germany) in powder form and was reconstituted using 1 ml DMSO per 25 mg (25 mg/ml). Once reconstituted the resveratrol was frozen at -20°C. Concentrations of 5, 10 and 15 µM where used in Chapter 4. Chapter 5 used 10 µM only.

2.2.5.4. Reconstitution of SIRT1 inhibitor

SIRT1 inhibitor, EX-527 (Merck Millipore, Darmstadt, Germany) was reconstituted using 500 µl DMSO per 5 mg (concentration of 10 mg/ml). Once reconstituted aliquots of 15 and 10 µl were stored at -20°C for up to 6 months. Concentrations of 30 µM and 60 µM and 100 and 200 nM were used on C2C12 cells in the dose response study (Chapter 4) and 100 nM was carried forward for use in the co-incubation studies (Chapter 5 and 6). Molarity calculations for each compound were first carried out based on the equation in Equation 2.1. The dilution equation, Equation 2.2, could then be used depending on the amount of media needed for the specific experiment.

Equation 2.1. Resveratrol and SIRT inhibitor (EX-527) molarity calculation

Molarity x Volume (L) = Amount of powder (g) / Molecular weight (kD)

$$\text{Molarity} = \frac{\text{Amount of powder (g)} / \text{Molecular weight (kD)}}{\text{Volume (L)}}$$

Resveratrol:

$$\text{Molarity} = \frac{0.025 \text{ g} / 228.2 \text{ MW}}{0.001 \text{ L}}$$

$$\text{Molarity} = 0.109 \text{ M}$$

SIRT1 inhibitor:

$$M = \frac{(0.005 \text{ g} / 248.7 \text{ MW})}{0.001 \text{ L}}$$

$$M = 0.0201 \text{ M}$$

Equation 2.2 Resveratrol and SIRT1 inhibitor dilution

$$M_1 \times V_1 = M_2 \times V_2$$

$$V_1 = \frac{M_2 \times V_2}{M_1}$$

e.g. Resveratrol (10 μM) in 50 ml of media:

$$V_1 = \frac{0.000010 \text{ M} \times 50000 \mu\text{l} (50 \text{ ml})}{0.109 \text{ M}}$$

$$V_1 = 4.59 \mu\text{l} \text{ in } 50 \text{ ml of media}$$

e.g. SIRT1 inhibitor (100 nM) in 50 ml of media:

$$V = \frac{0.0000001 \text{ M} \times 50000 \mu\text{l}}{0.0201}$$

$$V = 0.248 \mu\text{l} \text{ in } 50 \text{ ml of media}$$

2.2.6. Muscle cell morphological measures by microscopy

2.2.6.1. Principle

The assessment of myotube number using microscopy is a morphological measure of the myoblasts differentiating and forming myotubes. Myotube diameter and area can be used to assess if myotubes have increased in size (i.e. undergone hypertrophy or decreased (undergone atrophy)).

2.2.6.2. Procedure

Following media aspiration and 2× PBS washes (1 ml/well), cells were fixed by adding 1 ml methanol/ acetone (1:1) to 1 ml PBS per well in a drop-wise manner and incubated for 10 min at room temperature. Following aspiration, 2 ml methanol and acetone (1:1) were added to each well and incubated for a further 10 min. Finally, PBS (2 ml/well) was added after removal of the methanol and acetone solution and plates were stored at 4 °C until further analyses. This fixing process allowed nuclei to become discernible under light microscopy alone, without the need for additional nuclear staining. A total of 6 fields per well in duplicate, thus 12 per experimental condition for each time point were captured with a cell imaging system at x10 magnification on a microscope (DM6000 FS, Leica, Germany). Automated mark and find setting on the microscope allowed 6 images per well to be taken in the same position in each well automatically, with the 6 locations chosen equally spread around the well. Images were analysed using Image J (Java) software (National Institutes of Health, USA). Morphology was assessed by determination of myotube number of myotubes per view, diameter and area. A myotube was defined as containing 3+ nuclei encapsulated within cellular structures, so to avoid counting of single cells undergoing mitosis. Myotube diameter (μm) was determined by measuring the diameter of 3 equidistant points on each myotube (left end, middle, right end) and determining the mean of the 3 values as previously described (Trendelenburg *et al.*, 2009, Deane *et al.*, 2013, Hughes *et al.*, 2016). Myotube area (μm^2) was determined by carefully tracing around myotube structures using Image J software and

converting pixel length to the known distance in μm taken from the scale bar on each image produced on each image automatically by the microscope.

2.2.7. Cell Lysis for total Protein and Creatine Kinase Assays

Following the intended incubation time for cells under various conditions (see specific detail in each chapter) cells were washed once using 2 ml PBS per well and PBS aspirated. The cell lysis buffer: Tris/ MES Triton (TMT; 50 mM Tris-MES, pH 7.8, 1% Triton X-100). A volume of 300 μl TMT was applied to each well of a 6 well plate and was then left at room temperature for 5 min to allow lysis to take place. The cells were scraped and the solution was collected into a 1.5 ml eppendorf tube and vortexed. Tubes were labelled with experiment name and number, time point and condition. These samples were kept at -80°C until further analysis was performed.

2.2.8. Total Protein Assay

2.2.8.1. Principle

Total protein measurements were carried out using the Bicinchoninic acid (BCA) assay, originally devised by Smith *et al.* (1985). This colorimetric detection, similar to the previously popular Lowery method, implements the biuret reaction which states that Cu^{2+} is reduced to Cu^{1+} in the presence of protein under alkaline conditions (Fig 2.2.).

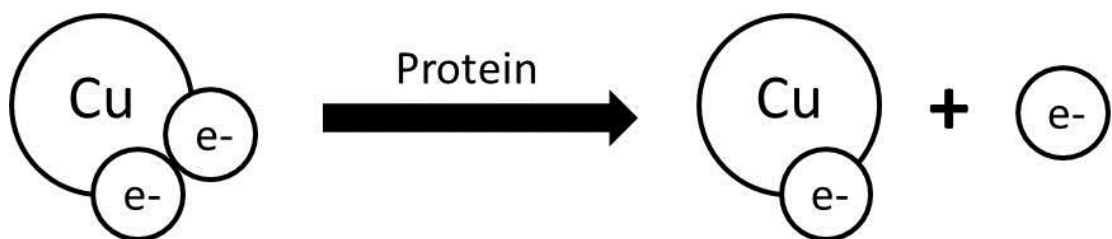


Fig. 2.2. Simplified diagram of the Biuret reaction.

The sensitivity of the biuret reaction alone is approximately 100 times less accurate than the additional BCA step. This addition allows one atom of Cu^{1+} produced during the biuret reaction to chelate with two molecules of

BCA (Fig. 2.3.). Following a 30 min incubation at 37°C, this reaction creates a purple colour when protein is present. This colour is proportional to the number of peptide bonds utilized during the reaction. Following the colour analysis at a wavelength of 540-590 nm, linear response curves of known standards were produced with an $r^2 > 0.95$ (Fig. 2.5.).

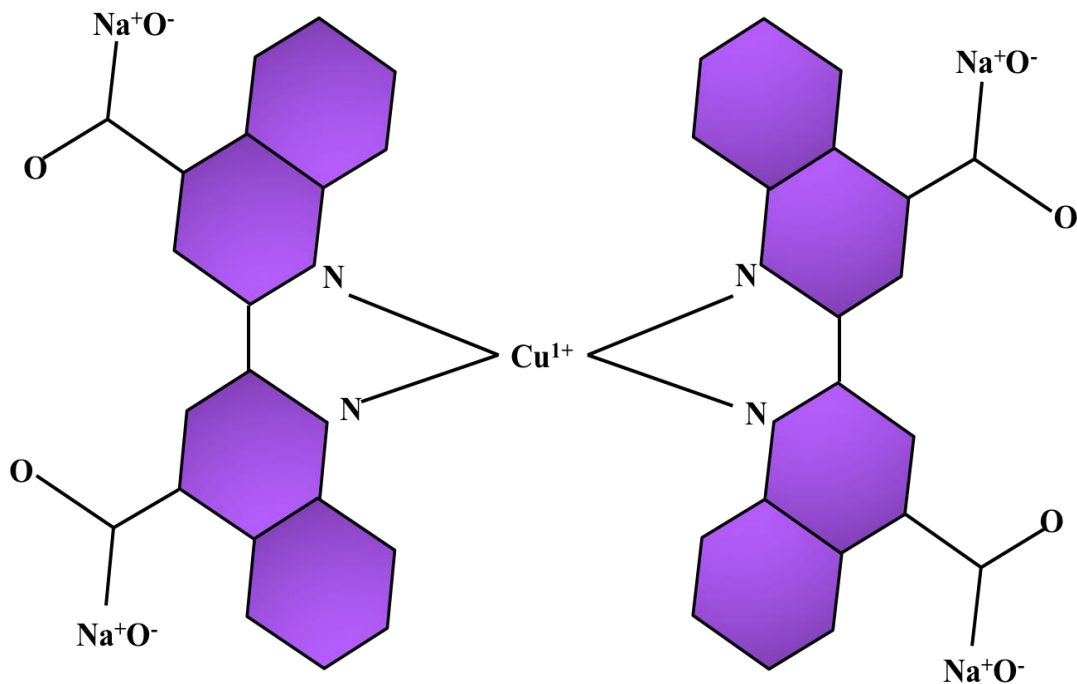


Fig. 2.3. One molecule of Cu^{1+} produced from the Biuret reaction chelating with two molecules of BCA.

2.2.8.2. Procedure

Ultimately this protocol will consist of comparing the obtained samples to a known set of standards. These standards were produced in house using the same TMT used for lysis of the experimental samples. Here 4 mg/ml of bovine serum albumin (BSA) was serially diluted to produce eight standards: 4.00, 2.00, 1.00, 0.50, 0.25, 0.13, 0.06 and 0.00 mg/ml. These standards along with an additional blank (0.00 mg/ml standard) were then pipetted (in duplicate) into the first 18 wells in a non-UV, 96 wellplate. Each standard and the blank were then pipetted in a volume of 10 μl per well in duplicate. The experimental samples were pipetted into the remaining wells in duplicate using the same volume of 10 μl as the standards (Fig 2.4.)

Both reagents needed for the BCA assay were purchased from Pierce (IL, USA). Reagent A consisted of sodium carbonate, sodium bicarbonate, bichoninic acid and sodium tartrate in 0.1 M of sodium hydroxide and reagent B consisted of 4% cupric sulphate. To calculate the amount of reagent A required in total, the number of standards and samples in duplicate were multiplied by 200 μ l (the volume of reconstituted reagent A required per well). The calculation for working reagent in a full plate would therefore be: $96 \times 200 \mu\text{l} = 19,200 \mu\text{l}$ or 19.2 ml. Then reagent B was mixed with Reagent A (19.2ml) in a 1:50 ratio to produce the reaction solution e.g. $19,200 \mu\text{l reagent A} / 50 = 384 \mu\text{l}$ of reagent B.

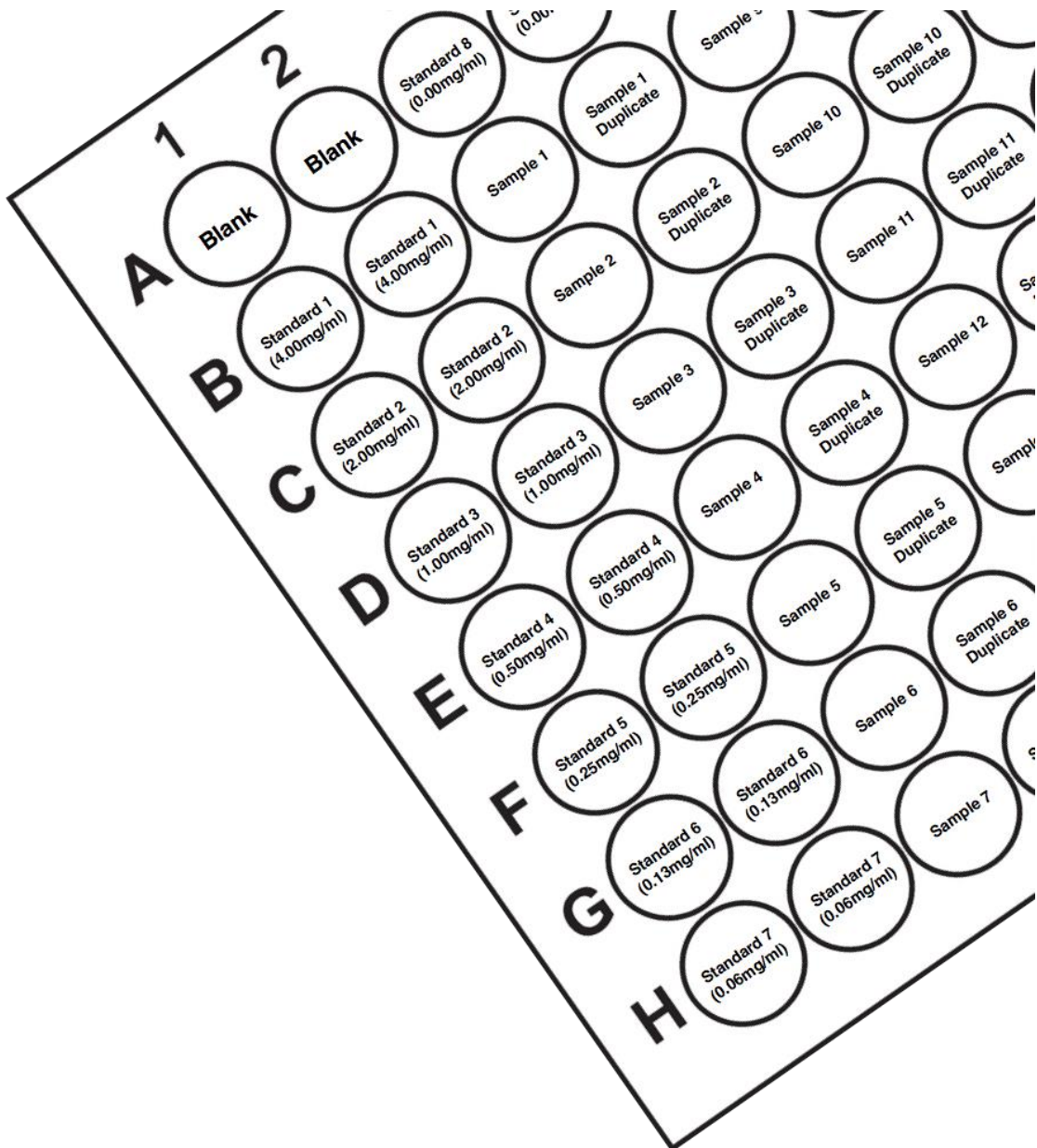


Fig. 2.4. Total Protein assay, 96 Well Plate layout. Depiction of the position of the standards, samples and their accompanying duplicates.

2.2.8.3. Analysis

The plate was incubated for 30 min at 37°C following the above preparation of the samples. After this time the plate was inserted into a CLARIOstar® plate reader (BMG Labtech, Germany) and absorbance was measured at 540-590 nm. Background was removed through blank correction (0.00 mg.ml⁻¹ and reagent). Absorbance of the BSA standards were plotted against their known concentrations thus creating a standard

curve. (Fig 2.5.). Sample concentrations were then derived through comparison to this curve.

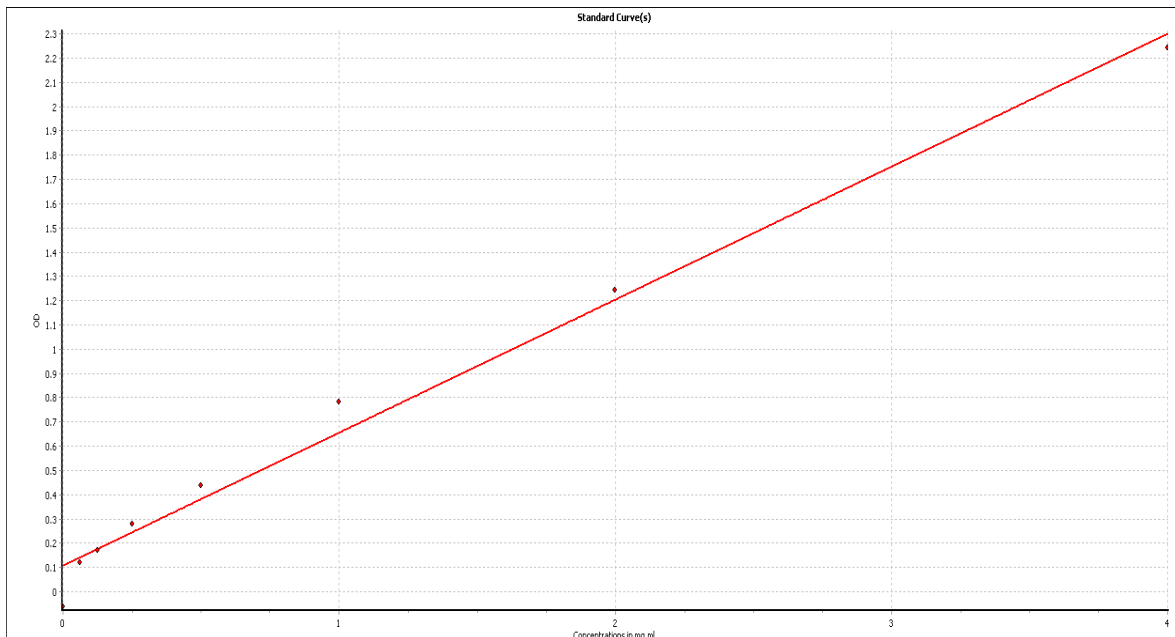


Fig.2.5. BCA standard graph produced for the sample values to be obtain following comparison. r value = 0.99 and $r^2 = 0.98$.

2.2.9. Creatine Kinase Assay

2.2.9.1. Principle

Creatine Kinase (CK) *in vitro* is used to mark the withdrawal from the cell cycle when myoblasts are fusing/differentiating. Where CK activity increases are detectable 3 h after induction of differentiation and serum withdrawal and 6 h before fusion occurs, where at 48 h of differentiation/fusion CK can be over 400 fold higher in myoblasts (Chamberlain *et al.*, 1985). Furthermore, CK gene expression is a transcriptional target of MyoD the muscle-specific protein that is able to induce myogenesis (Lassar *et al.*, 1989) and therefore investigating its biochemical activity at the protein level can help to indicate increased/decreased differentiation/fusion between experimental conditions and together with myotube morphology (myotube number,

diameter, area and gene expression of myoD/myogenin) enables a complete picture of changes in differentiation in myoblasts.

2.2.9.2. Procedure

Cells were lysed according to the above protein procedure (Section 2.2.6). As described above, the samples were kept at -80°C until further analysis was carried out. Samples were thawed at room temperature and vortexed. A TMT blank was pipetted into the first two wells of 96 well UV plate in a volume of 10 µl. Each sample was then pipetted in duplicate into the remaining wells at the same volume as the blank.

In order for each reaction to take place a working reagent was created. These reagents included two reagents purchased in a specific CK kit from Catachem, Inc. (Connecticut, NE, USA). According to manufacturers instructions these were combined as follows: 5 ml of liquid from bottle A with 0.118 g of powder from bottle B. The amount of reagent required was calculated according to the following equation. Reagent from bottle A (µl) = Reagent needed for each reaction per well (200 µl) x number of wells in use.

Because 0.118 g bottle B was required per 5 ml of bottle A, the amount of powder required per ml was calculated as follows: $0.118 \div 5 = 0.0236$ g. This is summarised in the equation below (Equation 2.3.). Once thoroughly mixed the working reagent were poured into a mixing trough and 200 µl working reagent was added to each well (except the blanks) using a multichannel pipette.

Amount of Reagent of Bottle A (µl) = 200 µl x number of samples in duplicate

Amount of powder from Bottle B (g) = Amount of Reagent of Bottle A (µl) x 0.0236

Therefore the calculation for working reagent in a full plate would read:

$$\text{Amount of reagent from Bottle A (}\mu\text{l)} = 200 \mu\text{l} \times 96$$

$$\begin{aligned}
 &= 19,200 \mu\text{l (or 19.2 ml)} \\
 \text{Amount of powder from Bottle B (g)} &= 18.8 \text{ ml} \times 0.0236 \text{ g} \\
 &= 0.45312 \text{ g}
 \end{aligned}$$

Equation 2.3. Calculation to determine quantities of reagents A and B needed for the CK assay.

2.2.9.3. Analysis

The 96 well plate was inserted into a CLARIOstar® plate reader (BMG Labtech, Germany) and readings were taken every minute for 15 minutes allowing a linear enzymatic relationship to be observed to carry out further analysis. The absorbance level of every sample in the plate per minute was read at 340 nm. A change in absorbance over time was used to calculate CK activity, Equation 2.4. was applied to the change in absorbance values. This was normalised to total protein content established using the BCA protein assay protocol above (Section 2.2.8).

$$\Delta A \cdot \text{min}^{-1} = (\text{Final A} - \text{Initial A}) \div (\text{Final Reading Time} - \text{Initial Reading time (min)})$$

CK activity was then determined using the following calculation:

$$\text{CK (U.l}^{-1}\text{)} = (\Delta A \cdot \text{min}^{-1} \times \text{TV} \times 1000) \div (6.22 \times \text{SV})$$

Where:

$\Delta A \cdot \text{min}^{-1}$	=	Change in absorbance per minute at 340 nm
TV	=	Total volume (ml)
1000	=	Conversion of units per ml to units per litre.
6.22	=	Millimolar absorptivity of NADH at 340nm
SV	=	Sample volume (ml)

Therefore, using 10 μl of sample and 200 μl of reagent the following equation applies:

$$\text{CK (U.l}^{-1}\text{)} = (\Delta A \cdot \text{min}^{-1} \times 0.21 \times 1000) \div (6.22 \times 0.01)$$

Equation 2.4. Calculation of CK activity

2.2.10. SDS Page and Immunoblotting

2.2.10.1. Principle

Separation of proteins according to their molecular weight (kilo Daltons (kDa)) is performed using discontinuous sodium dodecyl sulphate polyacrylamide gel electrophoresis (SDS-PAGE) (Laemmli, 1970). Bis-Acrylamide at different concentrations allows for the polymerisation of the gel by forming cross-links between the acrylamide polymers and the differentiation of the protein of interest by size e.g. 7% bis-acrylamide gels for a protein of high molecular weight versus 12% gel for proteins of low molecular weight. The process of polymerisation is catalysed by mixing ammonium per sulphate (APS) and N, N, N', N'-Tetramethylethylenediamine (TEMED) and two stacking gels are generated for each SDS page: i) the resolving gel (10%) which separates the protein by size and ii) the stacking gel (5%) which enables large volume of dilute sample to be loaded into lanes and thus align at the gel interface, prior to separation occurring in the resolving gel.

2.2.10.2. Procedure

The procedure consists of: Sample preparation, SDS-page Gel production, Electrophoresis, Transfer of proteins to nitrocellulose membranes, Immunoblotting and Enhanced chemiluminescence (ECL).

2.2.10.3. Sample Preparation

Cell lysis buffer (10 mM TrisHCL, 5 mM EDTA, 50 mM Sodium Chloride, 30 mM Sodium Pyrophosphate, 50 mM Sodium Fluoride, 100 µM Sodium Orthovanadate, 1 mM PMSF and 1% Triton X-100.) was supplemented with commercial protease and cOmplete™, Mini, EDTA-free Protease Inhibitor Cocktail (Roche, Switzerland). Following analysis of total protein via BCA assay as above (2.2.7) 30 µg of protein was reconstituted in a 5th volume of the loading buffer (5 x Laemmli buffer, made up of: 3 ml 1M TRIS-HCl (pH 6.8.), 1 g Sodium dodecyl sulphate, 5 ml glycerol and 1 ml

DH₂O, 25 mg Bromophenol blue).

2.2.10.4. SDS-Page Gel production

The SDS-Polyacrylamide (SDS-Page) gels were cast in a Mini-PROTEAN® Tetra cell casting stand (Bio-Rad Laboratories, Inc. CA, USA). Glass plates were aligned and clipped into place with gaskets below sealing the opening. A 10% resolving gel solution (4 ml 30% acrylamide 1% BIS solution, 3.4 ml d₂H₂O, 2.5 ml 1.5M Tris Base, 100 µl 10 % SDS, 50 µl 10% APS and 5 µl TEMED) was syringed between the plates. A layer of butanol was then syringed across the top of the resolving solution. Once removed this created a straight line on the resolving gel. Following a 30 min incubation the butanol was removed and a 5% stacking gel solution (1.7 ml 30% acrylamide 1% BIS solution, 5.7 ml D₂H₂O, 2.5 ml 0.5M Tris Base, 100 µl 10% SDS, 50 µl 10% APS and 10 µl TEMED) was applied, again using a syringe. A comb was carefully inserted at this point to prevent any bubbles forming in the gel. The comb selected was dependant on the number of samples, this ranged between 10 and 15 wells.

2.2.10.5. Electrophoresis

The prepared gels where removed from their casting stand and inserted into a Mini- PROTEAN® Tetra vertical electrophoresis cell (Bio-Rad Laboratories, Inc. CA, USA.). These gels were run at 200 V until the bromophenol blue dye line reached the bottom of the gel (approximately 1 h). The gels were closely monitored to ensure the sample did not run off the bottom of the gel. In addition these gels were also monitored to ensure the Amps did not exceed 3 A as this causes overheating of the gels.

2.2.10.6. Transfer

Following fractionation of the protein based on molecular weight, the protein was transferred onto a nitrocellulose membrane. Originally described by Towbin *et al.* (1979) the polyacrylamide gel was stacked against nitrocellulose paper and scotch-brite pads. The scotch brite pads

where replaced with extra thick filter paper for these experiments (Fig 2.6). The construction of the gel stack was carried out within semi-dry Trans-blot® Turbo™ Blotting system (Bio-Rad Laboratories, Inc. CA, USA) cassette. This stack began with the extra thick filter paper (Bio-Rad Laboratories, Inc. CA, USA.), which had been pre-soaked in transfer buffer (20 ml 10 x Tris Glycine, 40 ml methanol and 140 ml DH₂O) followed by a nitrocellulose membrane, the SDS-Page gel and a final sheet of pre-soaked filter paper. Care was taken to remove bubbles using a roller. The cassette lid was firmly and evenly pressed against the sandwiched gel and locked into place. The transfer protocol was run at 200 V for 30 min. The gel was then disposed of and the nitrocellulose membrane was either used in the immunoblotting stage (see below) or stored in plastic wrap at 4 °C until needed.

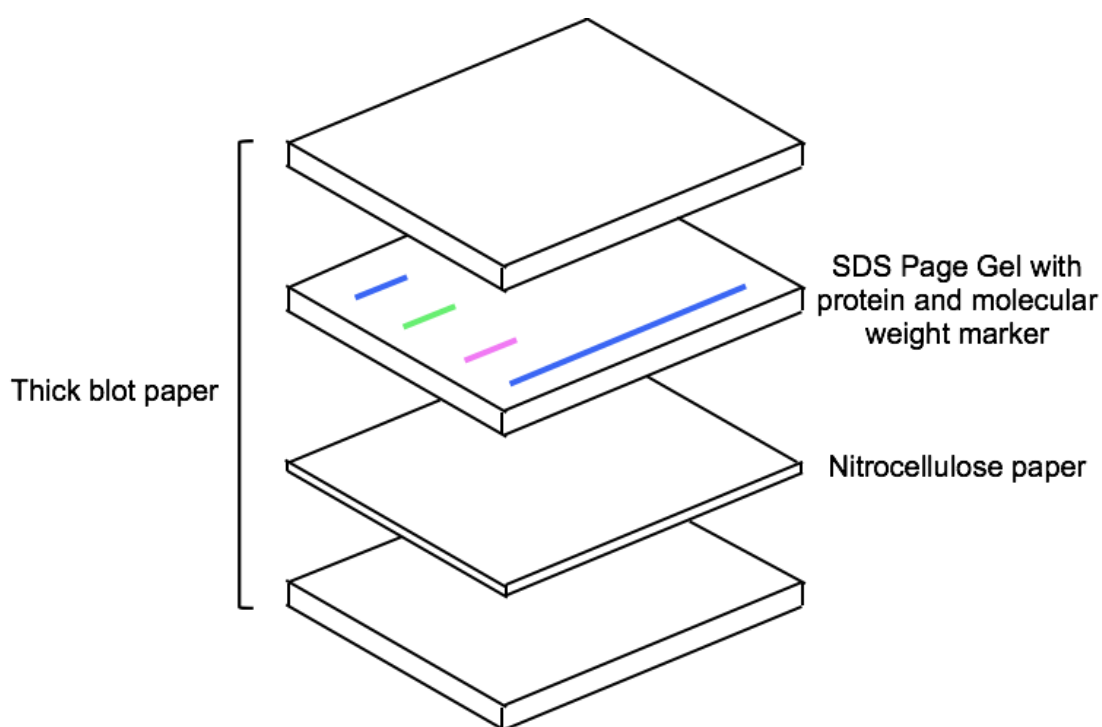


Figure 2.6. Construction of transfer stack located within the cassette of the Trans-blot® Turbo™ Blotting system (Bio-Rad Laboratories, Inc. CA, USA). The specific order is required to perform accurate transfer of protein from SDS page gel to nitrocellulose membrane.

2.2.10.7. Immunoblotting

The nitrocellulose membrane was prepared for detection using a Pierce™ Fast Western Kit, Supersignal West Pico (Rabbit) (Thermofisher scientific, MA, USA). The membranes were incubated using the wash buffer provided in these kits for 10 min, during all incubations caution was taken to ensure the membrane were covered. Following the wash buffer (which includes an unspecified blocking agent) the membrane was incubated in a primary antibody, the manufacturer, catalogue number and concentration of primary antibodies (all of which were raised in a rabbit) used in the data chapters are available in Table 2.1. The membrane was then washed twice for 5 min using TBS-Tween at 0.1% (TBS-T) (100 ml TBS, 900 ml DH₂O, 1 ml Tween-20) followed by the secondary rabbit antibody, raised in mouse, provided in the fast western kit. Finally, the wash buffer from the Pierce™ Fast Western Kit was used again for 2 x 5 min washes before ECL detection (see details below).

Table 2.1. Dilution factors and product information for Primary antibodies used during immunoblotting. All antibodies were raised in rabbits. All antibodies were purchased from Cell Signalling Technology® (MA, USA) except the one marked * which was purchased from Merck Millipore (Darmstadt, Germany).

Antibody	Catalogue Number	Dilution Factor
Phosphorylated AMPK	#2535S	1:1000
Total AMPK	#2532	1:1000
Phosphorylated P70S6K	#9205S	1:1000
Total P70S6K	#9202	1:1000
Phosphorylated SIRT1	#2314L	1:2000
Total SIRT1	#07-131 *	1:2000
GAPDH	#5174	1:4000

2.2.10.8. ECL detection

The Peirce™ fast western blot kit (Thermofisher scientific, MA, USA) also provided the enhanced chemiluminescence (ECL) detection reagents, these were used in a 1:1 dilution and incubated over the membrane for 5 min. The membrane was then placed in the Chemidoc™ MP System (Bio-Rad Laboratories, Inc. CA, USA.) where the band images were detected by densitometry in which the first image was taken at 5 sec and intervals of 30.5 sec thereafter until either the bands were overexposed, appearing red in colour or a maximum of 46 images had been taken (25 min in total).

2.2.10.9. Analysis

Following imaging, the band volumes were detected using Image lab™ (Bio-Rad Laboratories, Inc. CA, USA.). The bands for the phosphorylated protein were normalised to its own total protein counterpart before determining changes between experimental groups. Glyceraldehyde 3-phosphate dehydrogenase (GAPDH) was detected on all membranes prior to further detection. To establish whether loading of protein was comparable, we determined the volume values for GAPDH, following determination that no change was present independent of loading when glucose concentration is changed. If GAPDH was significantly different following t-test, the samples were also relativized to the GAPDH before continuing with further analysis.

2.2.11. RNA Extraction

2.2.11.1. Principle

The role of mRNA is to act as a chemical messenger to carry the genetic information from specific genes contained within the DNA to the protein factory, the ribosome, in order to produce functional proteins. As a result, there is usually an association between an increase in mRNA leading to an increase in a particular protein. The production of mRNA is also more rapid than changes in protein abundance due to the time it takes for proteins to be translated. Therefore, by assessing mRNA we are therefore able to assess important temporal changes following experimental

manipulation that provide information for potential alterations at the protein level. Furthermore, due to past literature characterising strong association between the alterations in gene expression with subsequent alterations in morphology or function (e.g. myogenin gene expression and myoblast differentiation), gene expression can be an important tool to establish the underlying molecular mechanisms to muscle cell adaptation. Prior to analysis of mRNA expression, extraction of RNA is required using the method below.

2.2.11.2. Procedure

RNA isolation was performed using the TRIzol method, as previously described by Simms *et al.* (1993). At specific time points, following relevant cell incubations current media was aspirated and the cells were washed once with 1ml PBS, which was then aspirated prior to the administration of 250 µl TRI Reagent® per well of a 6 well plate (Sigma-Aldrich, MO, USA). TRIzol was left at room temperature for 5 min and cells were scraped using Fisherbrand™ cell scrapers (Thermo Fisher Scientific, MA, USA). Wells containing the same sample conditions were pooled and collected into a 1.5 ml RNAfree tube and stored at -80 °C until RNA isolation was performed.

Samples were thawed at room temperature and vortexed thoroughly. Once fully defrosted 0.2 ml of chloroform was added per 1ml TRI Reagent®. Samples were then mixed via shaking vigorously and centrifuged for 15 min at 12,000 x g and 4 °C, with all tube hinges facing upwards. During centrifugation, separation of the solutions occurs, in which the colourless, aqueous phase resides on the top (containing the RNA), the white interphase (where the DNA and protein reside) and finally the red, phenol-chloroform phase (cell debris) residing on the bottom (Fig. 2.7.). The aqueous phase was carefully removed to avoid contamination with DNA from the milky interphase and collected into a new 1.5 ml RNA free tubes. Precipitation of RNA was performed via the addition of 0.5 ml of isopropanol, per ml of TRI Reagent® initially used. The samples were

vortexed and left at room temperature for 10 min and then centrifuged at 12,000 x g for 10 min at 4°C.

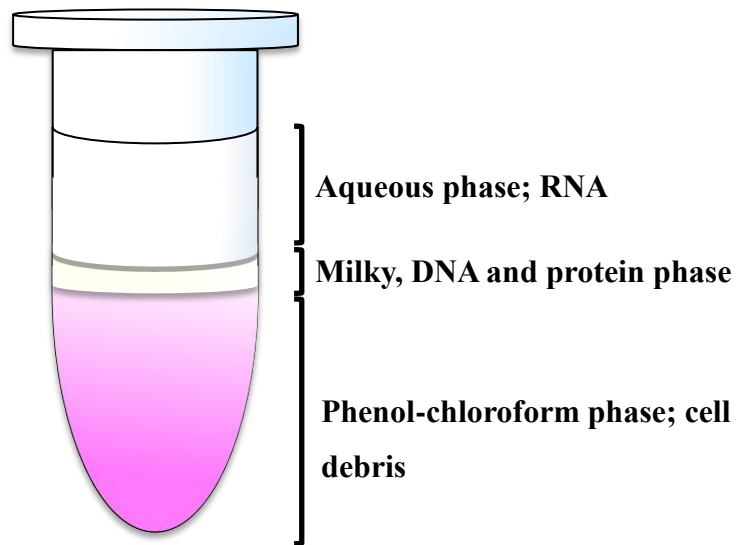


Fig.2.7. Graphic representation depicting the three phases present following addition of chloroform and the first centrifugation of the RNA isolation protocol.

The centrifugation produced an RNA pellet at the bottom of the tube (Fig. 2.8.), for which the surrounding supernatant was removed. A wash of 1 ml of 75% molecular grade ethanol was added to the pellet, gentle shaking then removed the pellet from the side of the tube and the sample was centrifuged at 7500 x g for 8 min at 4°C. Ethanol was removed and allowed to air dry and then dissolved in 30 µl RNA storage solution (Ambion®, Thermo Fisher Scientific, MA, USA).

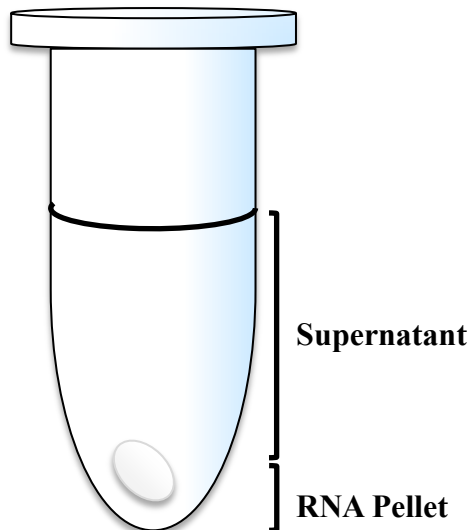


Fig.2.8. Graphic representation depicting the RNA pellet in the supernatant following addition of isopropanol and centrifugation.

2.2.11.3. RNA quantification

RNA purity and concentration was assessed using 1 μ l of sample on a NanoDrop 2000c, UV-Vis (Ultraviolet–visible spectroscopy) spectrophotometer (Thermo Fisher Scientific, MA, USA) using ODs (Optical Density) of 260 and 280 nm. A ratio of these OD values was calculated for each sample with 1.8-2.2 being accepted as high RNA quality and were carried forward for reverse transcription and PCR amplification.

2.2.12. PCR

2.2.12.1. Principle

Real-time Polymerase chain reaction analysed the extracted mRNA by first converting it to a double strand of complementary DNA (cDNA) using reverse transcriptase. This cDNA then undergoes a series of approx. 40-45 cycles of heating and cooling to allow denaturation of the cDNA, annealing of gene specific primers and extension of the new cDNA products using free nucleotides and the enzyme DNA polymerase. This process produces a doubling of the template cDNA at each cycle, with a fluorescent dye (e.g. SYBR green) incorporated into every double

stranded product. Therefore, as the product begins to accumulate above background levels, this allows quantification of the cDNA at the end of each cycle.

2.2.12.2. Sample Preparation

First, samples were all diluted to 7.3 ng/μl using RNA free water. This normalisation allowed the same amount of starting RNA to be present in all samples. The samples were added to the PCR reaction in a volume of 9.5 μl, making a total concentration per reaction 70 ng per reaction/sample. Sample reactions were produced in optically clear strip tubes (Qiagen, Crawly, UK). The components of the aforementioned reactions consisted of:

- 10 μl of 2x Quantifast SYBR green (Qiagen, Crawly, UK),
- 0.2 μl Quantifast RT Mix (Qiagen, Crawly, UK),
- 0.15 μl of both a forward and reverse primer (Sigma-Aldrich, MO, USA) of a specific stock/starting concentration of 100 μM.

This process was carried out using a QIAGility automated pipetting system (Qiagen, Crawly, UK).

2.2.12.3. PCR cycles

One step RT-q-PCR (reverse transcription, quantitative PCR) was performed using a Rotorgene 3000 (Qiagen, Crawly, UK) and consisted of: 10 min at 50°C (reverse transcription, cDNA production), 5 min at 95°C (transcription inactivation and initial denaturation), followed by 10 sec at 95°C (denaturation), and 30 sec at 60°C (annealing and extension) for 40 cycles. Melt curve analysis (Fig.2.9.) was performed as a final stage to identify non-specific amplifications and/or primer-dimer issues. Following initial characterisation and redesigning of primers where melt curves produced multiple peaks, all of the genes using the primers in table 2.2. produced a single melt curve peak suggestive of amplification of one single product. Average Efficiency of PCR reaction per sample (e.g. 100% is perfect doubling at every cycle) was determined by the software. All efficiencies for the primers of genes listed in table 2.2 were within 10% of

each other and therefore satisfied the MIQE guidelines (Lassar et al., 1989) for relative gene expression analysis (described below under section 2.2.12.5.) where efficiency particular of the gene of interest and the calibrator gene should be within 10% of each other.

2.2.12.4. Primer design

Primers (Table 2.2.) were identified using a genome browser at www.genome.ucsc.edu or PubMed Gene (<https://www.ncbi.nlm.nih.gov/gene/>) and designed using web-based OligoPerfect™ Designer (Invitrogen, Life Technologies, Pasiley, U.K) or Primer Blast (<https://www.ncbi.nlm.nih.gov/tools/primer-blast/>). Primers were purchased from Sigma-Genosys (Suffolk, UK) without the requirement of further purification. Sequence homology searches against the Genbank database ensured specificity to ensure the primers only matched the sequence and therefore gene that they were designed for. Where possible, the primers were ideally designed to yield products spanning exon-exon boundaries to prevent any non-specific amplification of genomic DNA. Three or more GC bases in the last 5 bases at the 3' end of the primer were avoided as stronger bonding of G and C bases can cause nonspecific amplification. Searches for secondary structure or inter/intra- molecular interactions (hairpins, self-dimer and cross-dimer) within the primer were also performed which would potentially lead too poor or no yield of the product. All primers designed were between 17 and 24 bp and amplified a product of between 76-353 bp (Table 2.2.). GC content ranged between 38% and 60% (Table 2.2.).

Table 2.2. Real qPCR primer sequences

IGF-I mature and MGF were not designed by use and were taken from (Yang *et al.*, 1996)

Target Gene	Primer Sequence (5'-3')	Reference number	Amplicon length (bp)	GC%
MyoD	F: CATTCCAACCCACAGAAC	NM_010866.2	125	50.00
	R: GGCGATAGAAGCTCCATA			50.00
MRF4	F: GGCTCTCCTTTGTATCCAGGG	NM_008657	194	57.20
	R: CGATCTGTGGGGGCAGATTT			55.00
Myogenin	F: CCAACTGAGATTGTCTGTC	NM_031189.2	173	47.37
	R: GGTGTTAGCCTTATGTGAAT			40.00
MYHC1	F: CGGTCGAAGTTGCATCCCTA	NM_030679.1	145	55.00
	R: TTCTGAGCCTCGATTCGCTC			55.00
MYHC2	F: GCGAAGAGTAAGGCTGTCCC	NM_001039545.2	76	60.00
	R: GGCGCATGACCAAAGGTTTC			55.00
MYHC4	F: AGGAGGCTGAGGAACAATCC	NM_010855.3	192	55.00
	R: TTCTCCTGTCACCTCTCAACA			47.62
MYHC7	F: TGTGCTACCCAGCTCCAAG	NM_080728.2	77	57.89
	R: CTGCTTCCACCTAAAGGGCTG			57.14
ID3	F: AGCGTGTCATAGACTACATCCTC	NM_008321	135	47.82
	R: TCCTCTTGCCTTGGAGATCAC			47.82
MUSA1	F: CCTTGAGGCTCCCGGCAAAT	NM_001168297	189	60.00
	R: ACTGCTCCACAAACCAATGGA			47.70
SIRT1	F: ACAATTCCTCCACCTGAG	NM_001159589.2	124	50.00
	R: GTAACCTCACAGCATCTTCAA			38.10
Myostatin	F: TACTCCAGAATAGAAGCCATAA	NM_010834.3	194	36.36
	R: GTAGCGTGATAATCGTCATC			45.00
IGF-I	F: GCTTGCTCACCTTACCAGC	NM_001111276.1	280	55.00
	R: TTGGGCATGTCAGTGTGG			55.56
IGF-IR	F: TGCGGTGTCCAATAACTAC	NM_010513.2	110	47.40
	R: TGTTGATGGTGGTCTTCTC			47.40
IGF-II	F: GTACAATATCTGGCCCGCCC	NM_010514.3	198	60.00
	R: GTATGCAAACCGAACAGCGG			55.00
IGF-IIR	F: GGAACCTCTGAATTTGTAAC	NM_010515.2	181	38.00
	R: CTACCAGATAGCCACCATT			47.00
IGFBP2	F: AGTGCCATCTCTTCTACAA	NM_008342.3	197	42.20
	R: GCTCAGTGTGGTCTCTT			50.00

IGF-IEa	F:GCTTGCTCACCTTTACCAGC	NM_010512.4	300	55.00
	R:AATGTACTTCCTTCTGGGTCT			50.00
MGF	F: GCTTGCTCACCTTTACCAGC	NM_184052.3	353	55.00
	R:AAATGTACTTCCTTTCTCTC			38.10
mTOR	F: CACTCCACTATCCTGTTACCT	NM_020009.2	190	47.62
	R: GAGATCCTTGGCACACCT			55.56
MuRf1	CCAAGGAGAATAGCCACCAG	NM_001039048.2	84	55.00
	R: CGCTCTTCTTCTCGTCCAG			58.00
MafBx	F: GTCGCAGCCAAGAAGAGAA	NM_026346.3	156	53.00
	R: CGAGAAGTCCAGTCTGTTGAA			47.00
FoxO1	F: AGTGGATGGTGAAGAGCGTG	NM_019739.3	96	55.00
	R: GAAGGGACAGATTGTGGCGA			55.00
FoxO3	F: CGGACAAACGGCTCACTTT	NM_019740.2	272	52.63
	R: TCGGCTCTTGGTGTACTTG			52.63
TNF- α	F: TCAACAACACTCAGAAACAC	NM_001278601.1	130	38.10
	R: AGAACTCAGGAATGGACAT			42.11
TNFRS1b	F: GTTGCTCTGTTATAGGATGGT	NM_011610.3	113	42.00
	R: TGCTGTCTGCTGTCTACT			52.94
NF κ B	F: ACACGAGGCTACAACCTCTGC	NM_008689	164	60.00
	R: GGTACCCCCAGAGACCTCAT			55.00
RPII β (a.k.a: pol2rb)	F:GGTCAGAAGGGAACCTTGTGGTAT	NM_153798.2	197	47.82
	R:GCATCATTAATGGAGTAGCGTC			43.47

2.2.12.5. Analysis

Using RotorgeneQ 3000 software (Qiagen, Manchester, UK) a threshold line was positioned manually where there was an exponential rise in fluorescence above background levels on the lower third of the exponential increase (Bustin *et al.*, 2009) (Fig. 2.9.).

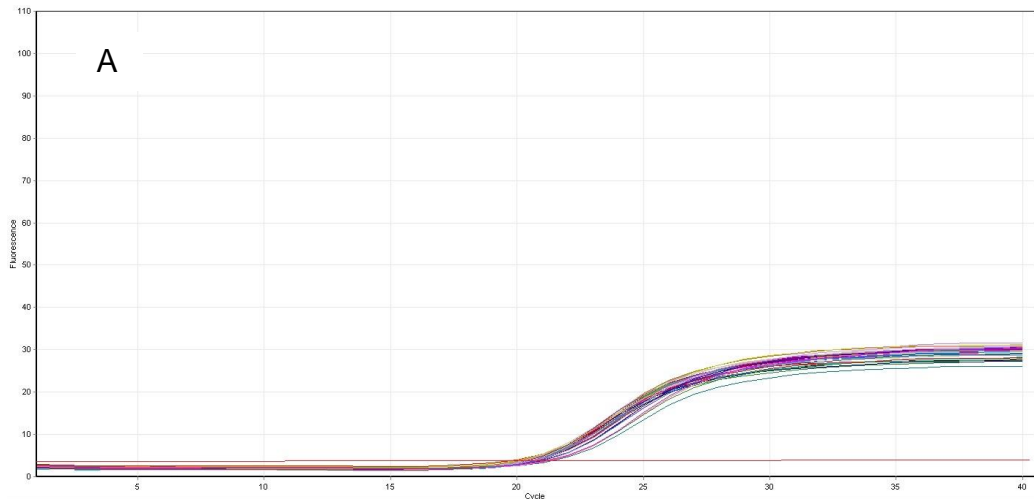


Figure 2.9. A) Displays the output and threshold applied to actual data output. B) Shows an enlarged example of RT-PCR fluorescence (relative fluorescent units) at incrementing cycles of an experimental sample (exp) and a control sample. The threshold is positioned on the lower third of the exponential rise in fluorescence on the y axis above background levels of fluorescence vs. cycle number axis (x axis) and the threshold cycle (Ct) is calculated by reading of the cycle number on the x axis. Imaged acquired from http://www.bio-rad.com/webroot/web/pdf/lsr/literature/Bulletin_5990.pdf

From this, the C_T values (defined as the cycle at which the samples fluorescence trace crosses the threshold line) for all genes were compiled in table format imported into Excel to perform a relative analysis. Here a spreadsheet was formulated to apply the Delta Delta C_T ($\Delta\Delta C_T$) equation

(Equation 2.5. otherwise known as the Livak Method (Schmittgen and Livak, 2008))

Equation 2.5. Delta Delta C_T ($\Delta\Delta C_T$) equation otherwise known as the Livak Method (Schmittgen and Livak, 2008).

Equation 1: $\Delta C_T = \text{Mean } C_T \text{ (Target gene, test e.g. MyoD)} - \text{Mean } C_T \text{ (Reference gene, test e.g. GAPDH)}$

Equation 2: $\Delta C_T = \text{Mean } C_T \text{ (Target gene, calibrator)} - \text{Mean } C_T \text{ (Reference gene, calibrator)}$

Equation 3: $\Delta\Delta C_T = \Delta C_T \text{ of Equation 1} - \Delta C_T \text{ of Equation 2}$

Equation 4: $2^{-\Delta\Delta C_T}$ (gives a normalised expression ratio)

Where:

$\text{Mean } C_T \text{ (Target gene, test)}$ = The average C_T value (sample and duplicate) of targeted gene (e.g. myoD) in the experimental condition e.g. RNA isolated from C₂C₁₂ after 72 h in DM.

$\text{Mean } C_T \text{ Reference gene, test}$ = The average C_T value (sample and duplicate) of reference housekeeping gene (e.g. RPII β /polr2b) in the experimental condition e.g. RNA isolated from C₂C₁₂ cells after 72 h in DM.

$\text{Mean } C_T \text{ (Target gene, calibrator)}$ = The average C_T value (sample and duplicate) of targeted gene (e.g. myoD) in the calibrator condition e.g. RNA isolated from C₂C₁₂ cells after 0 h in DM (0 h being the calibrator condition in all of the experiments in this thesis).

$\text{Mean } C_T \text{ (Reference gene, calibrator)}$ = The average C_T value (sample and duplicate) of reference housekeeping gene (e.g. RPII β) in the calibrator condition e.g. RNA isolated from C₂C₁₂ cells after 0 h in DM.

For Example:

Equation 1: $\Delta C_T = 22.18_{\text{(myoD, 72 hrs DM)}} - 20.69_{\text{(RPII } \beta, 72 \text{ hrs DM)}}$

then:

Equation 2: $\Delta C_T = 26.86_{\text{(myoD, 0 hrs DM)}} - 20.49_{\text{(RPII } \beta, 0 \text{ hrs DM)}}$

Equation 3: $\Delta\Delta C_T = \Delta C_T \text{ of Equation 1 (1.49)} - \Delta C_T \text{ of Equation 2 (6.37)}$

Equation 4: $2^{-(-4.88)}$ (gives a normalised expression ratio of 29.45)

Therefore, in this example (which is hypothetical data and corresponds to no true analysis) the expression ratio of MyoD between C₂C₁₂ cells that have placed in DM for 0 h and 72 h is 29:1. Therefore, in this hypothetical example MyoD is highly expressed (29 fold higher) after 72 h in C₂C₁₂ cells compared with the 0 h time point, and after being normalised to the housekeeping gene of RPII β .

Chapter 3

3. Determining Physiological Glucose Concentrations *in vitro*: A Model to investigate the impact of dietary restriction on muscle cell differentiation.

3.1. Introduction

Dietary restriction administered *in vivo* is calculated as a reduction in calories and/ or macronutrients in comparison to control *ad libitum* (AL) counterparts. Mimicking this model in culture however is more problematic. Firstly the assessment of calories consumed requires a more complex assessment *in vitro* than *in vivo*. Secondly, the current glucose concentration implemented in both rodent (Sharples *et al.*, 2011, Stitt *et al.*, 2004, Dimchev *et al.*, 2013, Hao *et al.*, 2011, Staiger *et al.*, 2004, Hao *et al.*, 2006) and human culture (Steitz *et al.*, 2001, Clempus *et al.*, 2007) is 24.9 mM or 4.5 g/L (NOR), which is much higher than has been detected physiologically. Despite this the concentration will therefore be carried forward as a reference control, allowing comparison with the existing literature and future glucose manipulation studies, however a more physiologically relevant dose needs to be established that mimics dietary restriction.

Various studies have compared changes in glucose concentration in both rodent and human studies, both determining a drop in serum/ blood glucose concentration during DR. Murine models have reported 30 – 40% reductions in glucose both acutely over a 3 week period from 2.79 to 1.63 g/L (15.5 to 9.1 mM) (Mahoney *et al.*, 2006) and chronically over a 20 month period from 1.5 to 1 g/L (8.3 to 5.6 mM) (Cartee *et al.*, 1994). Walford *et al.* (1992) suggested a 30% calorie

reduction decreased human serum levels from 0.92 g/L to 0.74 g/L (5.1 to 4.1 mM) over 6 months. Whereas an average of 6.9 years calorie restriction in humans compared to western diet counterparts displayed a 12.6% reduction in fasted glucose concentration (0.95 vs. 0.83 g/L and 5.2 vs. 4.6 mM) (Fontana *et al.*, 2006).

Although this data is indicative of the systemic effect of decreased calorie intake will have on the body it is not necessarily the concentration that skeletal muscle is exposed to due to the change in concentration from the blood and interstitial space. Glucose values in the muscle interstitium have been reported to be 30% lower than those found in the blood of both rodents (Aussedat *et al.*, 2000) and humans (Maggs *et al.*, 1995). To our knowledge, muscle interstitium values have unfortunately, not yet been reported during chronic DR, therefore using the above information we may only produce an approximation, as follows. The previously reported values for blood glucose during DR consisted of approximately 0.74 g/L (4.1 mM) in humans (Walford *et al.*, 1992) and 1 g/L (5.6 mM) in murine models (Cartee *et al.*, 1994). Therefore applying the aforementioned 30% reduction to represent the differences between interstitium and blood would estimate DR interstitium at nearly 0.5 and 0.7 g/L (2.8 and 3.9 mM) for humans and rat respectively.

Fulco *et al.* (2008) initially assessed the effect of glucose deprivation on muscle *in vitro*, whose findings of reduced muscle differentiation was confirmed later by Elkalaf *et al.* (2013) and Khodabukus and Baar (2015). None of these studies reported the rationale behind the glucose concentration administered, which varied from 1 g/L (5.6 mM) (Elkalaf *et al.*, 2013, Khodabukus and Baar, 2015) to 0.1 g/L (0.6 mM) (Fulco *et al.*, 2008). The former appears to be similar to the previously reported fasted blood glucose level and the latter is much lower than the predicted value for the interstitium during DR. Ideally we would aim to implement a physiologically relevant glucose concentration found in the interstitium, however, when undertaking studies in proliferating muscle cells the

viability of these cells must also be taken into account. Consequently, prior to carrying out any studies utilizing glucose concentrations in conjunction with other variables we will implement various percentage reductions in glucose concentration from the NOR, 4.5 g/L (25 mM) due to its widespread use in the literature (despite its lack of physiological relevance) in a dose response manor and assess the impact of these varying doses on growth and differentiation of muscle cells. These doses are as follows: 4.50 g/L (NOR), 3.38 g/L, 2.25 g/L, 1.13 g/L (MED), 0.56 g/L (LOW) or 0.00 g/L (25.00 mM (NOR), 18.75 mM, 12.50 mM, 6.25 mM (MED), 3.12 mM (LOW) or 0.00 mM) where LOW, MED and NOR are closest to glucose levels expected during DR in the interstitium, circulation and in 'normal' basal myoblast media respectively.

We aimed initially to assess the impact on muscle cell differentiation via morphological analysis of myotube number, diameter and area and non-subjective biochemical analysis (CK activity). Additionally molecular analysis of gene expression (mRNA) was performed to determine changes in genes that have been extensively characterised to be highly correlated with fusion/differentiation (IGF-1, myoD, myogenin, ID3 and IGFBP2), myotube maturation (MRF4, MYHC1 (IIX), 2 (IIA), 4 (IIB) and 7 (slow type I) and protein degradation (MUSA1) and survival (SIRT1).

3.2. Methods

3.2.1. Cell culture

C2C12 murine myoblasts (Blau *et al.*, 1985) at passage 12 were incubated in separate T75 flasks in a humidified, 37°C with 5% CO₂ in Growth media (GM) containing: Dulbecco's Modified Eagle Serum (DMEM) (D6429-6, Sigma-Aldrich, UK), 1% Penicillin Streptomycin (Pen Strep), 10% New born calf serum (NBCS) and 10% Fetal Bovine Serum (FBS) until 80% confluency was attained.

Experiments were initiated by removing GM (as described in the general methods, chapter 2, section 2.2.2), washing once with phosphate buffered saline (PBS) followed by the addition of differentiation media (DM). Two media forms were implemented for use in control DM conditions, 1) liquid, commercially available and ready to use with a 4.5 g/L glucose concentration (D6429, Sigma-Aldrich, UK) supplement with 2% horse serum (HS) and 1% PenStrep (PS) to allow a control that would be comparable to existing literature and 2) a powdered form (D5030, Sigma-Aldrich, UK). The chosen powdered DMEM was reconstituted according to manufacturer's instructions (8.3 g/L of DMEM) supplemented with 0.5840 g/L L-Glutamine; 3.7000 g/L Sodium Bicarbonate; 0.1100 g/L, Sodium Pyruvate; 0.0159 g/L Phenol red and either 0 g/L or 4.5 g/L D-Glucose in order for the composition to match that of the more generally used liquid DMEM. This media was also supplemented with 2% HS and 1% PS. The powdered DM supplemented with glucose was comparable to the liquid DMEM in section 3.3.1, thus making this DMEM a relevant control as well as being used to produce the dosing conditions described below under section 3.2.2. The reduction in serum content, causing the C2C12 myoblasts to undergo spontaneous differentiation without requiring the addition of growth factors to initiate the process (Blau et al., 1985). Cells were seeded following trypsinization of the adherent cells, counts were performed using haemocytometer in the presence of Trypan Blue dye as described in general methods (section 2.2.3).

3.2.2. Cell dosing

6Well plates were pre-treated with 0.2% porcine gelatine for 10 min at room temperature (RT) and 10 min in a humidified incubator at 37°C with 5% CO₂. The excess gelatine was aspirated and cells were seeded at 8 X 10⁴ cells/ml in 2 ml of GM, and incubated until 80% confluence. Cells were washed in PBS and transferred into 2 ml of DM at 37°C with 5% CO₂ for up to 7 days (7D). Time point zero was defined as an incubation of 30 min after transfer to DM and is denoted as 0 hours (0 h). To assess the effect of glucose restriction on myoblasts the cells were incubated in

reconstituted powdered media as described above with either: 4.50 g/L, 3.38 g/L, 2.25 g/L, 1.13 g/L, 0.56 g/L or 0.00 g/L or 25.00 mM, 18.75 mM, 12.50 mM, 6.25 mM, 3.12 mM, 0.00 mM of glucose respectively. All experiments were carried out as N = 3, each N consisting of a different cell set brought out of liquid nitrogen at the same time.

3.2.3. Morphology

Myotube parameters including; number, diameter and size were assessed using a live imaging light microscope (AF600 modular system, Leica, Germany) cell imaging system at x10 magnification at time points; 0, 48 and 72 hours and 7 days. Experiments were replicated three times (N=3), each experiment consisted of each time point and experimental condition being performed in duplicate with 6 images taken per well providing a total of 12 images per condition per timepoint. Analysis was performed on the images acquired at 72 h and 7D using ImageJ software (NIH, USA) (See general methods chapter 2, section 2.2.6.)

3.2.4. Total protein content

Protein was measured using BCA™ (Pierce, Rockford, IL) according to instructions and detected using CLARIOstar® plate reader (BMG labtech, Germany) at a wavelength of 540-590 nm to quantify total protein concentrations prior to relative comparison of CK samples (See general methods chapter 2, section 2.2.8.).

3.2.5. Creatine Kinase

Assessment of creatine kinase activity was measured using an assay kit (Catachem, Inc, Connecticut, NE) according to manufactures instructions and detected using a CLARIOstar® plate reader (BMG labtech, Germany) at a wave length of 340 nm. See general methods chapter 2, section 2.2.9.

3.2.6. RNA Extraction and analysis

RNA extraction was performed using the TRIzol method (See method chapter 2, section 2.2.11.), following the manufactures instructions

(Invitrogen, Life technologies, Carlsbad, CA). RNA purity and concentration was assessed using 1 μ l of sample on a NanoDrop 2000c, UV-Vis (Ultraviolet–visible spectroscopy) spectrophotometer (Thermo Fisher Scientific, MA, USA) using ODs of 260 and 280 nm. A ratio of these OD value was calculated for each sample with all samples possessing 260/280 ratios of between 1.8-2.2 and therefore accepted as high RNA quality.

3.2.7. Primer design

Identification of target sequences were carried out via Gene (<http://www.ncbi.nlm.nih.gov/gene>). Primers (Chapter 2, section 2.2.12.4 table 2.2.) were designed using Primer-Blast (<http://www.ncbi.nlm.nih.gov/tools/primer-blast/>). Primer details can be found under 2.2.12.4.

3.2.8. RT-PCR and analysis

RT-PCR was carried out using Quantifast SYBR green RT-PCR kit (Qiagen, Manchester, UK) on a Rotor-Gene® (Qiagen, Manchester, UK) supported by Rotor-Gene® Q Software, version 2.1.0.9 (Qiagen, Manchester, UK). The RT-PCR cycles consisted of; 48°C, 30 min (reverse transcription/ synthesis of cDNA), 95°C, 10 min (transcriptase inactivation and initial denaturation) followed by 40 cycles at 95°C, 15 sec (denaturation), 60°C, 1 min (annealing and extension in 1 step). Disassociation melt-curve analysis was performed to reveal and exclude non-specific amplification and primer dimer issues. All gene products yielded a single melt peak/temperature suggesting one product was amplified. Relative gene expression analysis was carried out using $\Delta\Delta C_t$ equation, otherwise known as the Livak method (Schmittgen and Livak, 2008), to establish normalised expression ratios, where the relative expression is calculated as $2^{-\Delta\Delta C_t}$ and C_t represents the threshold cycle. RPII β was extremely stable between experimental conditions (mean C_t 15.62 \pm 0.11) and therefore used as the housekeeping gene in all RT-PCR assays and the pooled mean used in the $\Delta\Delta C_t$ calculations. All RT-PCR

figures are presented as a relative gene expression in comparison to the 0 h cell incubated in “Normal” glucose (4.5g/L or 25 mM). This sample was used as a calibrator condition in the subsequent equations in order to compare expression values across glucose concentrations.

3.2.9. Statistical analysis

All data was performed using three separate cell populations thus performed N=3. Analysis was then carried out using Minitab® 17 (Minitab Ltd, Coventry U.K). Outliers were removed using Grubbs outlier test. All data was parametric, assessed using the Anderson-Darling test for normality. General linear models were carried out for morphological data CK (3 x 3, time (48, 72 h and 7D) x glucose concentration (NOR, MED and LOW) and gene expression (3 x 3, time (0, 72 h and 7D) x glucose concentration (NOR, MED and LOW). Post hoc tests were performed using Bonferroni, Tukey and Fisher. The results produced through the Bonferroni tests are reported throughout the results as this test is more stringent. Use of Tukey and Fisher is stated within the text if no significance was observed using Bonferroni.

3.3. Results

3.3.1. Preliminary morphological analysis to eliminate irrelevant glucose concentrations from further analysis

Two 25.00 mM concentrations were implemented and appeared to produce similar results regardless of DMEM used (reconstituted powder vs. commercially bought liquid) (Fig. 3.1.). Therefore, as the glucose dose response media was created using the reconstituted powder DM and there was no morphological difference between this media and the liquid form the reconstituted (powdered) DMEM was used as the control condition (NOR) for all subsequent studies (Fig. 3.2.). Glucose dose response (25.00, 18.75, 12.50, 6.25, 3.12, 0.00 mM) initially investigated morphological analysis only, as some of the lowest concentrations we expected to have few viable cells.

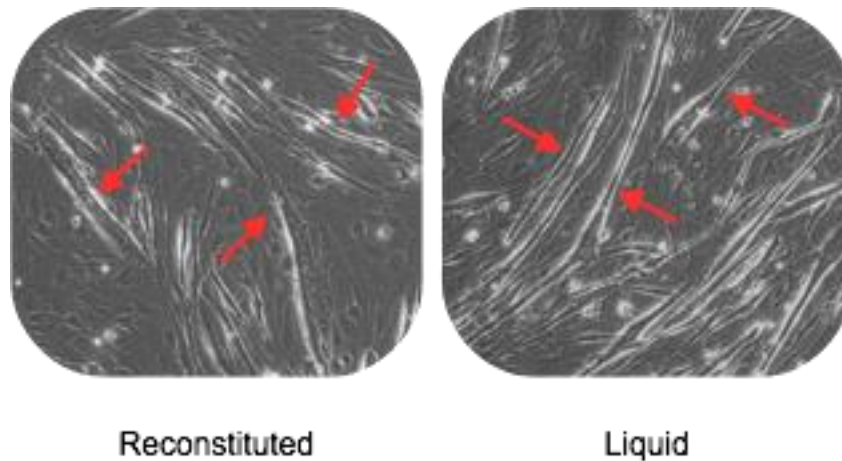


Fig 3.1. Images displaying similar number and size of myotubes within two different types of DMEM. Two 25 mM glucose conditions, the first created using a powered DMEM and supplementing with glucose, this is denoted as “reconstituted”. The second created using a commercially available DMEM denoted as “liquid”.

Following 72 h in 0 mM glucose it was determined that the majority of cells had died and were no longer adherent to the plate (Figure 3.2. top left image). As such, this concentration could not be utilized as a suitable model for DR in myoblasts and was therefore not carried forward for further investigation. A morphological reduction in differentiation was present in the 3.12 mM glucose concentration. This concentration was similar to the glucose levels observed in interstitial concentrations during DR and was therefore carried forward for further morphological, biochemical and molecular analysis below. The apparent morphology between the remaining concentrations (6.25, 12.50, 18.75 mM) did not appear to differ appreciably between conditions. However, as the 6.25 mM (MED) concentration was also the most reflective of serum concentrations of glucose in fasted (but not dietary restricted) rodents this dose was also carried forward. It should be noted that morphological images only (Fig. 3.2) were conducted for this wide range of dosing in order to initially narrow the focus to more relevant dosing conditions. Based on these initial observations further analysis degrading myotube number, diameter and size, as well as CK activity and transcriptional response was performed on doses of 25 mM (NOR), 6.25 mM (MED) similar to fasted serum levels and 3.12 mM (LOW), similar to predicted interstitial concentration during DR.

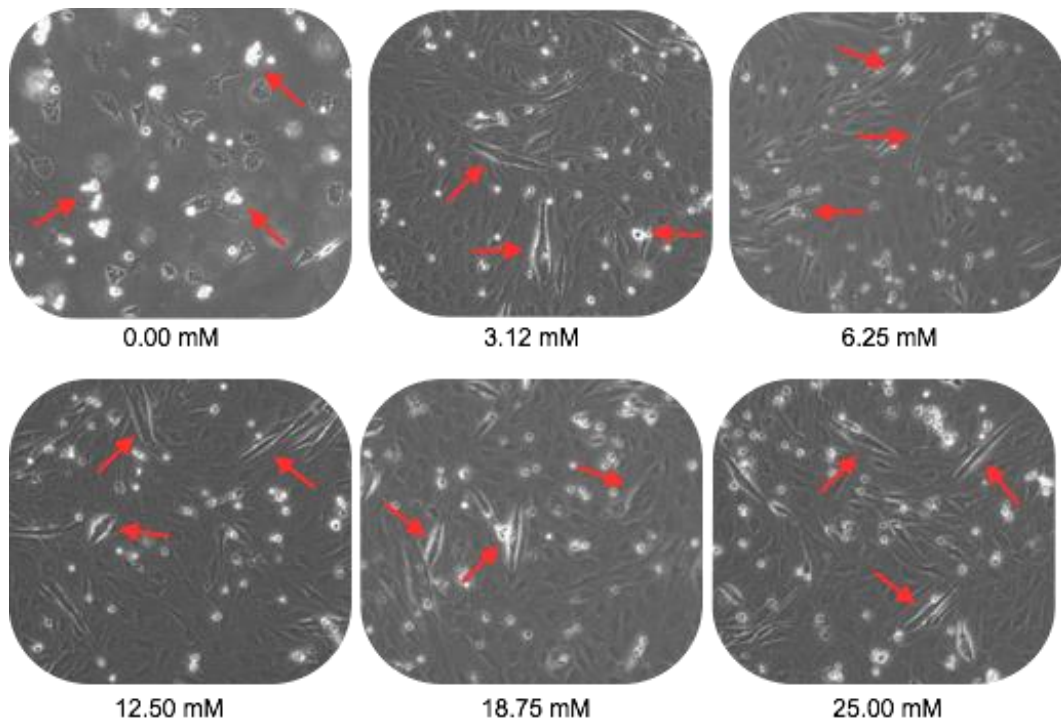


Fig 3.2. Initial dose response for glucose concentrations following 72 h. Doses include the readily used 25.00 mM (NOR) and a serial dilution of 18.25 mM, 12.50 mM, 6.25 mM (MED), 3.13 mM (LOW) and 0.00 mM. The 25.00 mM is the control glucose condition this condition contained larger and more plentiful myotubes than the glucose restricted conditions. Compared to the control condition both 0.00 and 3.12 mM displays an increase in cell death, whereas 6.25 mM displayed a reduction in myotube differentiation, observed via reduced number of myotubes. Glucose conditions 12.50 and 18.75 mM appeared unchanged in comparison to the control

3.3.2. Morphological and biochemical analysis for differentiation capacity was reduced in LOW and MED glucose conditions.

Following a brief time course experiment (data not shown) we determined that myotube formation was slightly delayed in the cell population used in comparison to other groups utilizing C2C12 cell lines. As a result there were a limited number of myotubes present at the 72 h time point and a much greater number was present following 7D within the NOR condition. The end time point was therefore extended to 7D for future studies allowing late differentiation and myotube maturation to take place. We investigated differentiation via myotube imaging (Fig. 3.3.), this allowed

analysis of myotube number and these results were confirmed with a biochemical assay for CK (marker of differentiation). Finally, myotube hypertrophy was analysed via measurement of myotube area and diameter.

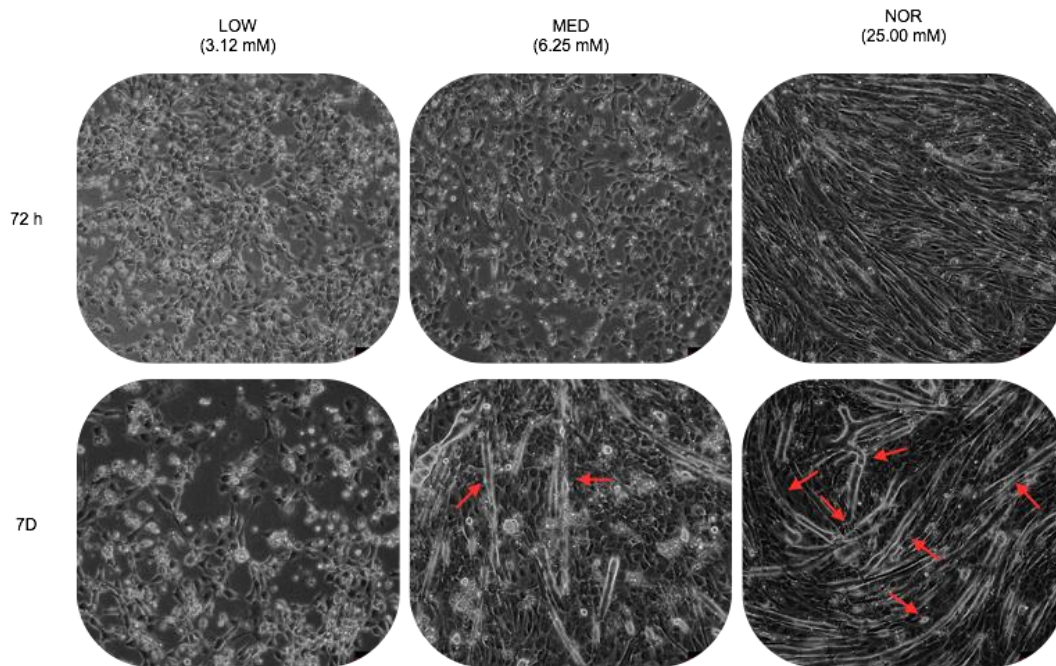


Fig 3.3. 10X magnification images of: 25.00 mM (NOR), 6.25 (MED) and 3.12 (LOW) glucose concentrations. Images taken following 72 h and 7D. No myotubes have been formed following 72 h in any condition. After 7D there are no myotubes formed in LOW glucose conditions and there is a large amount of cell death. In MED and NOR conditions myotubes have formed (only counted as a myotube when 3 or more nuclei were present) however there are a much greater number and area in NOR compared to MED.

No myotubes were formed in either the MED or LOW glucose conditions following 72 h as such no further morphological analysis was carried out. Following 7D myotubes had formed in MED and NOR conditions however the number was greatly diminished in MED glucose conditions following in comparison to the NOR glucose condition (NOR vs. MED: 21.72 ± 1.22 vs. 1.44 ± 0.30 , $p < 0.001$). Again no myotubes were observed in the LOW glucose condition (Fig 3.4.) As a result following ANOVA analysis there was a significant main effect for glucose condition ($F_{(2,105)} = 281.33$, $p < 0.001$).

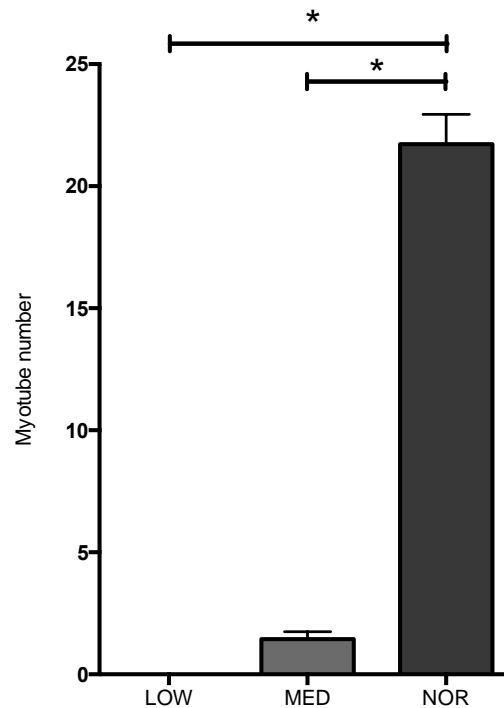


Fig 3.4. Myotube number is dramatically reduced at 7D in cells undergoing MED glucose restriction with no observable myotubes in LOW glucose conditions. Data was displayed as mean and SD values of following experimentation to three cell populations (n =3). Significant difference ($p < 0.05$) is denoted using a *.

To confirm morphological analysis of myotube number, CK activity a biochemical marker of fusion/ differentiation and early myotube formation was assessed (Fig 3.5.). Following an ANOVA test there was an interaction for CK activity between time and glucose dosing ($F_{(4,99)} = 2.43$, $p = 0.053$) and as predicted there was also a significant main effect for glucose alone ($F_{(2,99)} = 49.23$, $p < 0.001$). Post hoc tests revealed that the NOR glucose conditions exhibited higher CK activity than both the MED and LOW conditions at both 72 h (NOR: 208.20 ± 84.00 vs. MED: 86.20 ± 68.90 , $p < 0.001$ vs. LOW: vs. 37.21 ± 26.03 mU.mg.ml^{-1} , $p < 0.001$) and at 7D (NOR vs. MED vs. LOW: 281.50 ± 101.50 vs. 84.03 ± 32.63 vs. 40.50 ± 29.90 mU.mg.ml^{-1} , $p < 0.001$, respectively, Fig 3.5). NOR was also significantly higher at 48 h than the LOW glucose condition (130 ± 104 vs. 46 ± 13 mU.mg.ml^{-1} , $p = 0.042$ (tukey)) with a definite trend towards significance between NOR and MED (130 ± 104 vs. 79 ± 21 mU.mg.ml^{-1} , $p = 0.055$ (fisher)). Although not significant it is worth noting MED glucose

showed a trend towards an increased CK expression when compared to LOW at 72 h (86.20 ± 68.90 vs. 37.21 ± 26.03 , mU.mg.ml^{-1} , $p = 0.061$ (fisher)) and 7D (84.03 ± 32.63 vs. 40.50 ± 29.90 mU.mg.ml^{-1} , $p = 0.096$ (fisher)).

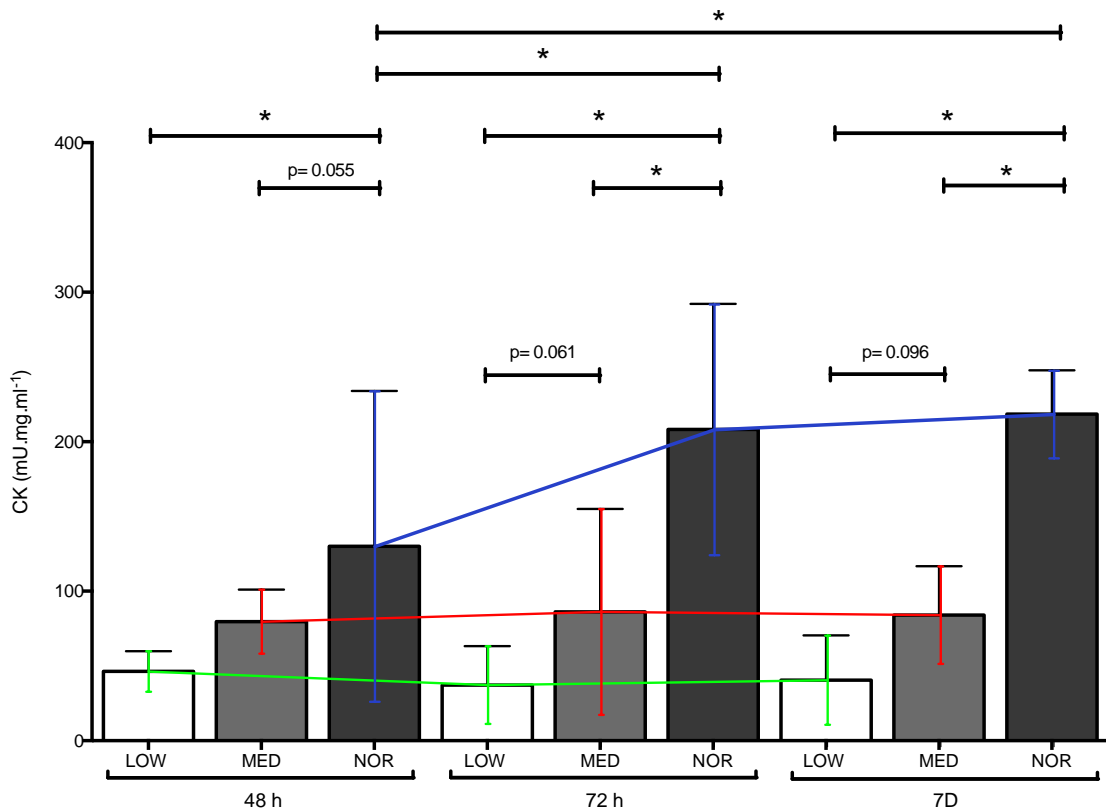


Fig 3.5. CK is relativized to total protein. The NOR dose indicates differentiation is occurring more rapidly between 48 h and 7D compared with MED and LOW glucose conditions. There is also significantly higher CK activity in NOR vs. MED and LOW conditions at 72 h and 7D and between NOR and LOW at 48 h. Significant differences ($p < 0.05$) are denoted using a *. If approaching significance p value is stated.

No myotubes were formed following 7D in the LOW condition therefore measurement of myotube size and diameter was only carried out on the MED and NOR conditions (Fig. 3.6.). The total size of the myotubes was established via measurements of myotube area. There was a significant reduction in size of myotubes between NOR and MED conditions (NOR vs. MED: 7395 ± 4544 vs. 4805 ± 2732 μM^2 , $p < 0.001$). Myotube diameter however displayed no significant difference between NOR and MED

conditions (NOR vs. MED: 15.55 ± 5.14 vs. 16.80 ± 6.51 μM , $p = 0.103$). Overall there was a significant reduction in number and size of myotubes in MED glucose conditions compared with NOR. Additionally myotube formation was completely inhibited under LOW conditions.

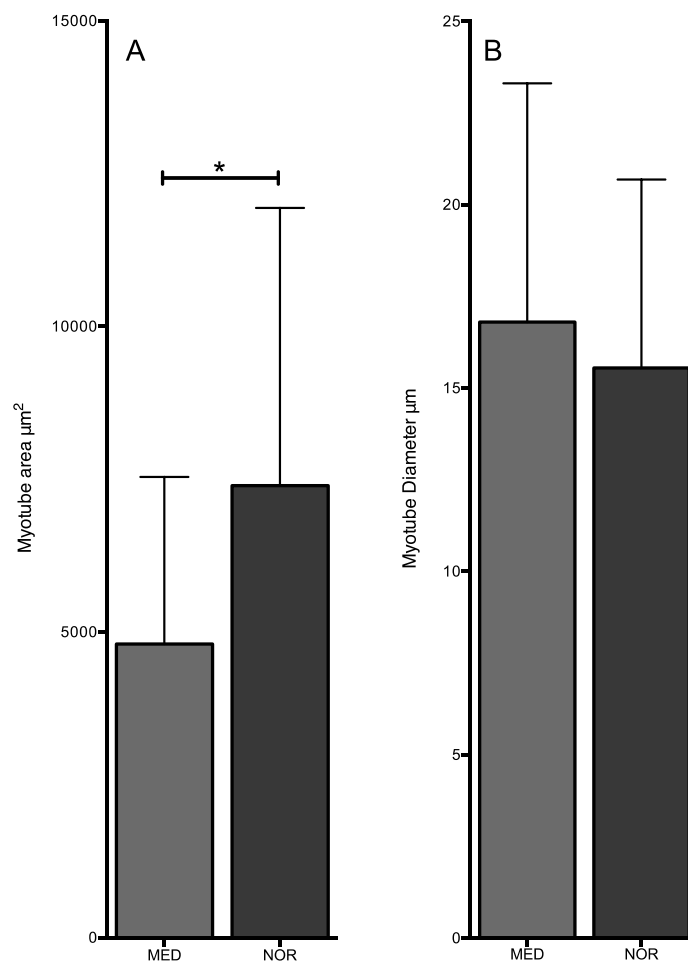


Fig 3.6. Graphs depicting myotube size (A) and myotube diameter (B). As described above there are no myotubes observed under LOW conditions and as such there are no measurements to report and therefore this glucose concentration was removed from analysis. There are no significant difference present between MED and NOR glucose for diameter, Myotube size is significantly higher in the MED condition than in the NOR. Significant difference ($p < 0.05$) is denoted using a *.

3.3.3. Impaired expression of the myogenic regulatory factors (MRF) during LOW glucose.

Myogenic regulatory factors (MRF's) are involved in the lineage commitment of myoblasts, myoblast fusion and differentiation as well as

the maintenance of differentiation. MyoD underpins myoblast determination and the onset of fusion (Buckingham et al., 2003, Cooper et al., 1999), whereas myogenin regulates formation and executes the differentiation program (Berkes and Tapscott, 2005) Analysis of MyoD gene expression suggested a significant main effect for time ($F_{(2,17)} = 4.64$, $p = 0.025$). No change in MyoD expression was observed over time for NOR glucose (0 h vs. 72 h: 0.98 ± 0.53 vs. 0.70 ± 0.21 , $p = 0.480$, 0 h vs. 7D: 0.98 ± 0.53 vs. 0.90 ± 0.66 , $p = 0.836$, 72 h vs. 7D: 0.70 ± 0.21 vs. 0.90 ± 0.66 , $p = 0.600$). Compared to 0 h, LOW glucose displayed a reduced MyoD expression at 72h, (0 h vs. LOW: 0.98 ± 0.53 vs. 0.08 ± 0.03 , $p = 0.020$) and 7D (0 h vs. LOW: 0.98 ± 0.53 vs. 0.22 ± 0.04 , $p = 0.044$) whereas MED did not (0 h vs. 72 h MED: 0.98 ± 0.53 vs. 0.38 ± 0.46 , $p = 0.107$, 0 h vs. 7D MED: 0.98 ± 0.53 vs. 0.37 ± 0.20 , $p = 0.100$). There is no significant difference at 72 h between NOR and both MED and LOW (NOR vs. LOW: 0.70 ± 0.21 vs. 0.08 ± 0.03 , $p = 0.135$, NOR vs. MED: 0.70 ± 0.21 vs. 0.38 ± 0.46 , $p = 0.435$). There is also no significant difference between MED and NOR following 7D (NOR vs. MED: 0.90 ± 0.66 vs. 0.37 ± 0.20 , $p = 0.145$), however for LOW in comparison to NOR there is a trend towards a decrease in MyoD expression under LOW conditions (NOR vs. LOW: 0.90 ± 0.66 vs. 0.22 ± 0.04 , $p = 0.066$) This data suggests that LOW may have a reduced capacity to produce myotubes, a previously documented in the morphological data (Fig 3.7,A).

MRF4 (*myf6*) activates differentiation so an early time point should see an increase in MRF4. There are no interactional or main effects for MRF4 (Fig 3.7,B). Despite the lack of significance across all time points and conditions the data was reduced on average between certain experimental conditions. The high stringency in our chosen post hoc tests led us to implement these to determine the pairwise comparisons. Following these post hoc tests there was a significant increase in gene expression in MED glucose at 72 h in comparison to both LOW and NOR (MED vs. LOW: 3.66 ± 4.76 vs. 0.09 ± 0.06 , $p = 0.022$, MED vs. NOR: 3.66 ± 4.76 vs. 0.10

± 0.01 , $p = 0.038$). These findings suggest there is a difference between LOW and MED and these concentrations are not simply replicas.

Myogenin promotes terminal differentiation and as such is observed in late differentiation. There was also no significant interaction or main effect present for myogenin (Fig 3.7,C), as with MRF4 despite this lack of significance we chose to assess the pair wise comparisons using post hoc tests due to their stringency. There is no significant difference between 0 h and NOR at 72h (0 h vs. NOR: 1.88 ± 1.31 vs. 5.62 ± 4.12 , $p = 0.069$) which is indicative of the late activation of myogenin required for differentiation to take place. There is however a significant increase in myogenin expression at NOR 7D in comparison to 0 h (NOR vs. 0 h: 10.61 ± 4.81 vs. 1.88 ± 1.31 , $p = 0.010$). Although there is no difference between LOW and MED concentrations at 72 h (LOW vs. MED: 1.48 ± 1.53 vs. 1.60 ± 1.51 , $p = 1.00$) there is a reduction in expression under MED conditions from NOR (MED vs. NOR: 1.60 ± 1.51 vs. 5.62 ± 4.12 , $p = 0.053$ (fisher)) as well as a significant reduction under LOW conditions (LOW vs. NOR: 1.48 ± 1.53 vs. 5.62 ± 4.12 , $p = 0.047$ (fisher)). Additionally there is a significant reduction in LOW and MED compared to NOR at 7D (LOW vs. NOR: 0.68 ± 0.76 vs. 10.61 ± 4.81 , $p = 0.002$, MED vs. NOR: 4.52 ± 0.55 vs. 10.61 ± 4.81 , $p = 0.006$ (fisher)). Additionally there is a trend between LOW and MED (LOW vs. MED: 0.68 ± 0.76 vs. 4.52 ± 0.55 , $p = 0.064$ (fisher)), which suggests that LOW may reduce myogenin expression to a greater extent. This suggests that terminal differentiation is inhibited in both glucose-restricted conditions but more severely under LOW conditions.

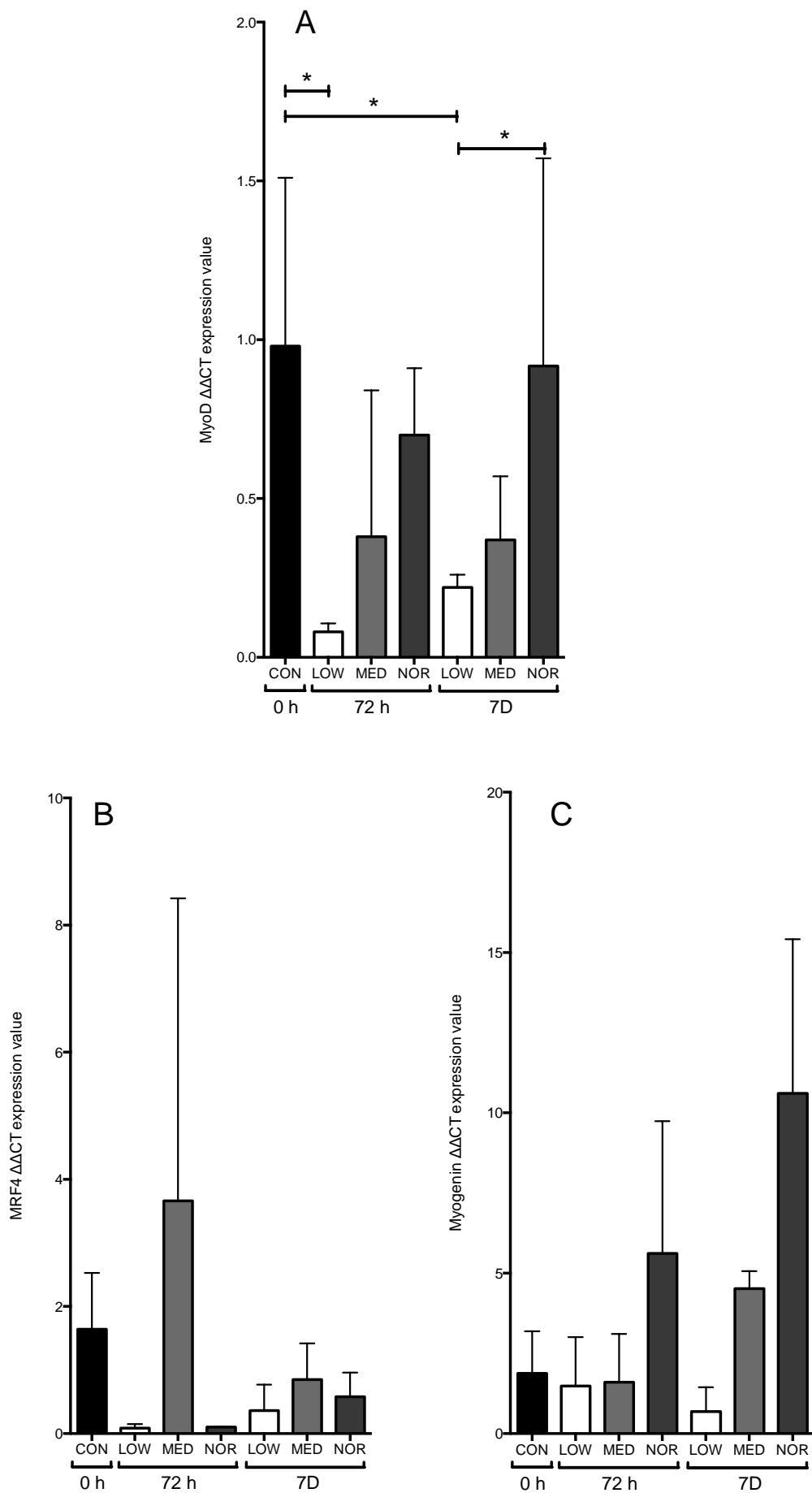


Fig 3.7. Graphs depicting means and SD's for gene expression for: MyoD (A), MRF4 (B) and Myogenin (C). LOW glucose is reduced compared to NOR or MED in at least one time point for all MRF's studied. Significant difference ($p < 0.05$) is denoted using a *. If approaching significance p value is stated.

3.3.4. Myosin Heavy Chain (MYHC) expression is impaired under MED and LOW glucose conditions compared to NOR.

Slow twitch fibres (MYHC7) have been observed to increase expression earlier during maturation whereas fast twitch fibres; MYHC: 1 (IIx), 2 (IIa) and 4 (IIb) tend to increase gene expression as myotubes become even more mature (Brown *et al.*, 2012). No main or interactional effects are present for MYHC7. As with MRF4 and myogenin previously discussed, despite no significant main effect or interaction we still obtained pairwise comparisons using post hoc tests due to their stringency. These post hoc tests revealed an early increase in MYHC7 in the NOR glucose condition at 72 h compared to 0 h, (NOR vs. 0 h: 5.54 ± 2.40 vs. 1.46 ± 1.23 , $p = 0.027$ (fisher)). We also see a significant difference between the 0 h baseline and NOR glucose at 7D (0 h vs. NOR: 1.46 ± 1.23 vs. 5.46 ± 4.94 , $p = 0.030$ (fisher)). More importantly, we observed a main effect for glucose ($F_{(2,18)} = 6.57$, $p = 0.007$). This is readily observable at 7D where a significant difference is present between NOR and both the LOW (NOR vs. LOW: 5.46 ± 4.94 vs. 0.61 ± 0.27 , $p = 0.011$ (fisher)) and MED (NOR vs. MED: 5.46 ± 4.94 vs. 1.23 ± 0.87 , $p = 0.023$ (fisher)) conditions (Fig. 3.8, A). MYHC2 also displays no significant difference across time points or glucose concentrations in addition to no significant pairwise comparisons (data not reported, see figure 3.8, B).

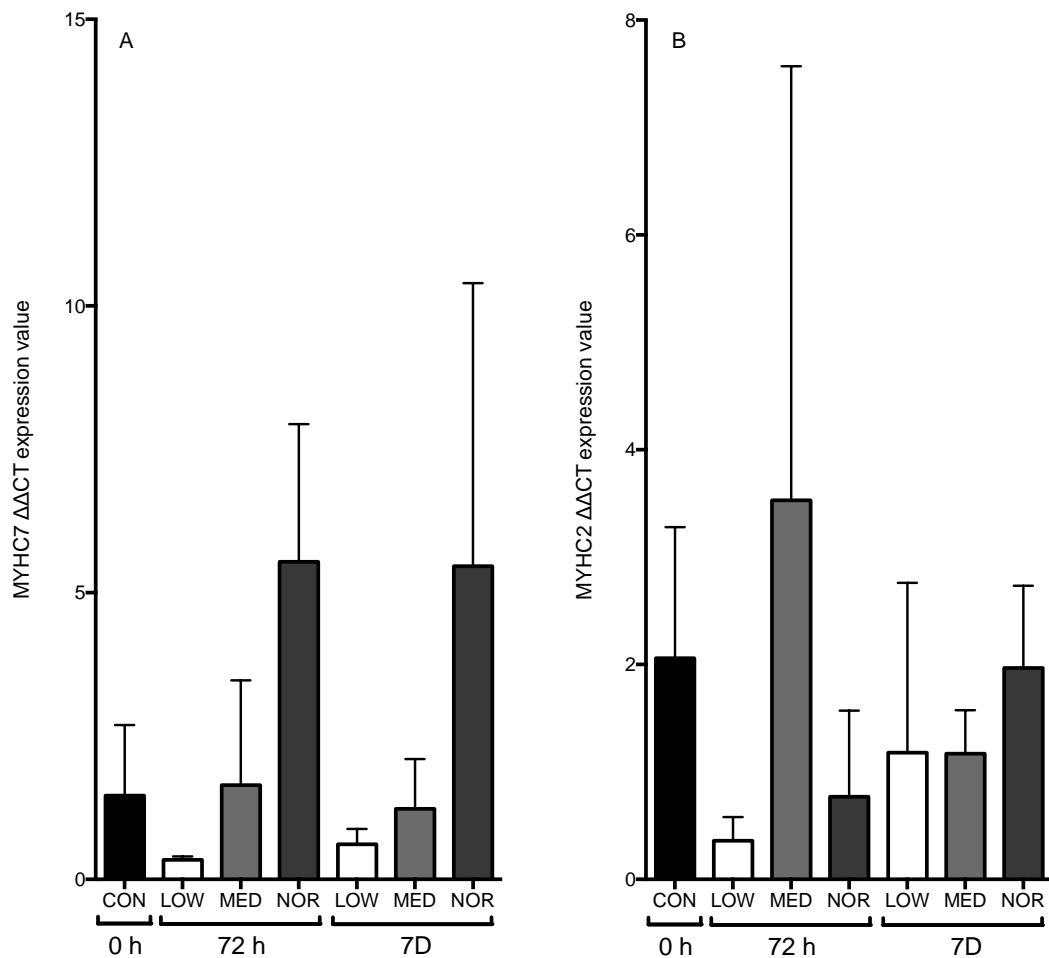


Fig. 3.8. Graphs depicting means and SD's for gene expression for: A) MYHC7 B) MYHC2. MYHC7 is effected by restricted glucose whereas MYHC2 is not. Significant difference ($p < 0.05$) is denoted using a * . If approaching significance p value is stated.

MYHC4 displays a significant main effect for glucose ($F_{(2,18)} = 6.57$, $p = 0.007$), evidenced by the large increase under NOR conditions between 0 h to 7D (0 h vs. NOR: 1.38 ± 1.19 vs. 10.04 ± 10.30 , $p = 0.016$). There was no significance over time in the MED condition overtime (0 h vs. MED: 1.38 ± 1.19 vs. 2.30 ± 1.53 , $p = 1.000$). Importantly there was a significant difference in MYHC4 between NOR and both MED and LOW glucose conditions at 7D (NOR vs. MED: 10.04 ± 10.30 vs. 2.30 ± 1.53 , $p = 0.028$ (fisher), NOR vs. LOW: 10.04 ± 10.30 vs. 0.91 ± 0.06 , $p = 0.012$ (fisher)) (Fig. 3.9, A).

Finally, for MYHC1, a significant main effects for glucose ($F_{(2,17)} = 4.48$, $p = 0.027$) and time ($F_{(2,17)} = 3.78$, $p = 0.044$) as well as a significant interaction between the two ($F_{(4,17)} = 2.95$, $p = 0.051$), was observed for MYHC1 (Fig. 3.9, B). Post hoc tests elucidated a significant increase in MYHC1 gene expression between NOR at 7D and 0 h (NOR vs. 0 h: 386.00 ± 333.00 vs. 1.13 ± 0.77 , $p = 0.028$). A significant difference was also present at 7D between NOR and LOW (NOR vs. LOW: 386.00 ± 333.00 vs. 3.37 ± 1.71 , $p = 0.029$). With fisher comparisons observing a significant difference between NOR and MED (NOR vs. MED: 386.00 ± 333.00 vs. 31.70 ± 40.90 , $p = 0.002$). These findings are similar to both MYHC4 and 7. Overall lowering glucose availability clearly affected early differentiation (MyoD) and myotube formation (myogenin) in line with the reduced myotube number and CK activity. This is in addition to impaired myotube maturation and hypertrophy demonstrated by a reduction in myotube size and gene expression of MYHC 1,4 and 7.

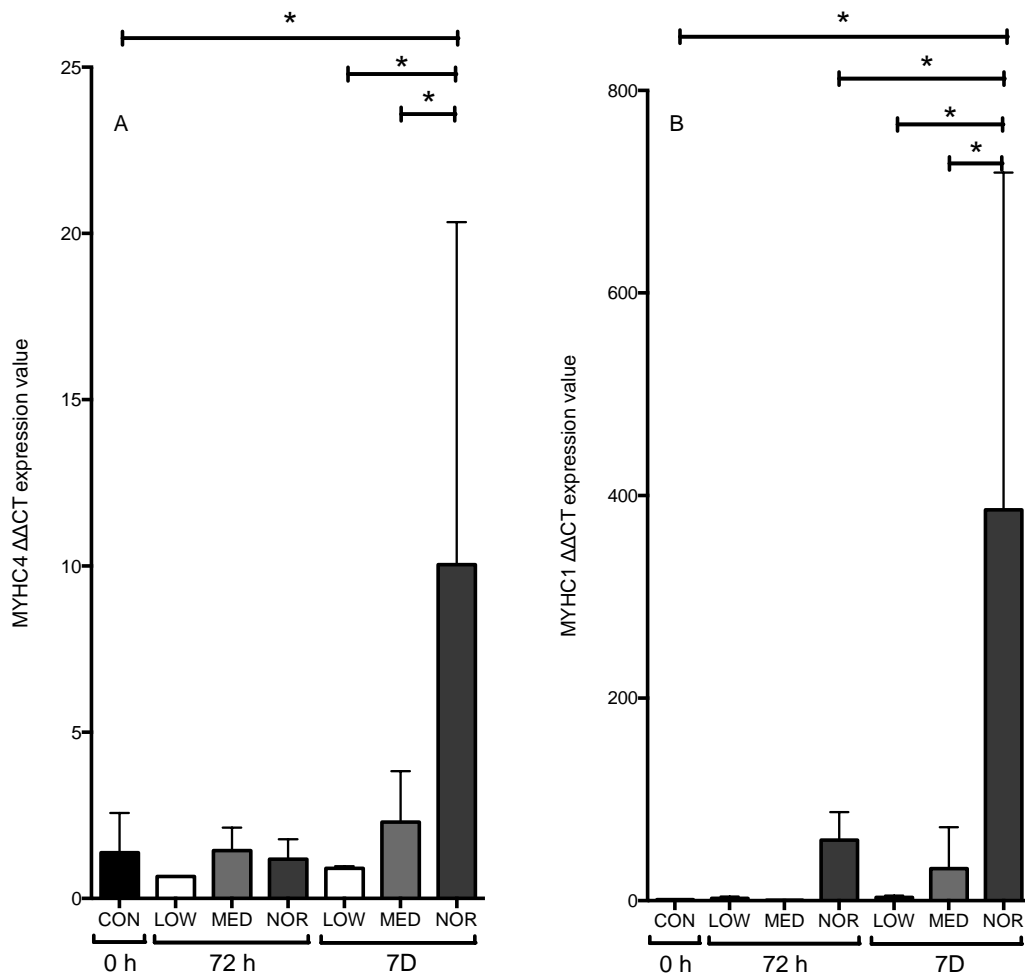


Fig. 3.9. Graphs depicting means and SD's for gene expression for: A) MYHC4 B) MYHC1. Both MYHC4 and 1 display an increase in NOR at 7D compared to 0 h. Additionally there is a significant increase in expression for both MYHC4 and 1 between NOR and both MED and LOW. Significant difference ($p < 0.05$) is denoted using a *. If approaching significance p value is stated.

3.3.5. LOW and MED glucose do not have an increased atrophic gene expression.

Work from our lab has previously documented a reduction in Insulin like growth factor binding protein 2 (IGFBP2) expression across the differentiation timecourse, when expression increased differentiation reduced (Fig 3.10, A) (Sharples *et al.*, 2013a). There was a significant main effect for time for IGFBP2 in these experiments ($F_{(2,17)} = 15.29$, $p < 0.001$). Fisher posthoc tests then confirmed a significant reduction in IGFBP2 expression between the 0 h baseline compared to NOR, MED

and LOW for both 72h (0 h vs. NOR: 1.25 ± 0.82 vs. 0.38 ± 0.31 , $p < 0.046$, 0 h vs. MED: 1.25 ± 0.82 vs. 0.04 ± 0.02 , $p = 0.017$, 0 h vs. LOW: 1.25 ± 0.82 vs. 0.02 ± 0.01 , $p = 0.008$) and 7D (0 h vs. NOR: 1.25 ± 0.82 vs. 0.07 ± 0.06 , $p = 0.012$, 0 h vs. MED: 1.25 ± 0.82 vs. 0.09 ± 0.05 , $p = 0.013$, 0 h vs. LOW: 1.25 ± 0.82 vs. 0.02 ± 0.01 , $p = 0.008$). This surprisingly suggests that all conditions are reducing IGFBP2 across the differentiation timecourse as a decrease over the timecourse has been previously correlated with improved differentiation (Sharples et al., 2013a).

As inhibitor DNA binding protein 3 (ID3) inhibits differentiation. A significant reduction in ID3 is needed following proliferation in order to allow myotube formation to take place (Jen *et al.*, 1992). By measuring ID3 we aimed to establish whether the reduction in MRFs, particularly MyoD, was driven by an increase in ID3 (Chen *et al.*, 1997). There is a main effect for time present for ID3 expression ($F_{(2,17)} = 9.21$, $p = 0.002$ (fisher)). As expected this was due to the reduced expression in comparison to the 0 h for LOW and NOR at both 72 h (0 h vs. LOW: 1.11 ± 0.63 vs. 0.04 ± 0.01 , $p = 0.022$, 0 h vs. NOR: 1.11 ± 0.63 vs. 0.32 ± 0.10 , $p = 0.055$ (all fisher comparisons)) and 7D (0 h vs. LOW: 1.11 ± 0.63 vs. 0.12 ± 0.08 , $p = 0.022$, 0 h vs. NOR: 1.11 ± 0.63 vs. 0.28 ± 0.05 , $p = 0.043$ (all fisher comparisons)) signifying the end of proliferation (Fig 3.10, B). There was no difference between 72 h and 7D (NOR, 72 h vs. 7D: 0.32 ± 0.10 vs. 0.28 ± 0.05 , LOW, 72 h vs. 7D: 0.04 ± 0.01 vs. 0.15 ± 0.13 , $p > 0.05$). Nor was there a significant difference between glucose concentrations at either 72 h (NOR vs. MED: 0.32 ± 0.10 vs. 0.46 ± 0.68 , vs. LOW: 0.04 ± 0.01 , MED vs. LOW: 0.46 ± 0.68 vs. 0.04 ± 0.01 , $p > 0.05$) or 7D (NOR vs. MED: 0.28 ± 0.05 vs. 0.44 ± 0.41 , vs. LOW: 0.15 ± 0.13 , $p = 0.736$, MED vs. LOW: 0.44 ± 0.41 vs. 0.15 ± 0.13 , $p > 0.05$).

Muscle ubiquitin ligase of SCF complex in atrophy-1 (MUSA1) is a Forkhead box O (FoxO) dependant ubiquitin ligase with a role in the tagging of proteins to undergo ubiquitination (Bodine and Baehr, 2014). An

increase in MUSA1 expression has been documented in muscle atrophy, particularly denervation (Bodine and Baehr, 2014) and fasting under the regulation of FoxO3 (Milan *et al.*, 2015). Throughout the time course none of the glucose concentrations differed significantly from the 0 h (0 h: 1.35 ± 0.81 vs. LOW, 72 h: 0.84 ± 0.01 , vs. LOW, 7D: 1.54 ± 1.05 , , vs. MED, 72 h: 1.35 ± 0.81 vs. 0.63 ± 0.43 , vs. MED, 7D: 1.35 ± 0.81 vs. 0.45 ± 0.25 vs. NOR, 72 h: 1.41 v 1.39 , vs. NOR, 7D: 0.83 ± 0.54 , $p > 0.05$). There was also no significant difference present between glucose restriction and NOR conditions at 72 h (NOR vs. MED: 1.41 v 1.39 vs. 0.63 ± 0.43 , NOR vs. LOW: 1.41 v 1.39 vs. 0.84 ± 0.01 , All $p > 0.05$) or 7D (NOR vs. MED: 0.83 ± 0.54 vs. 0.45 ± 0.25 , NOR vs. LOW: 0.83 ± 0.54 vs. 1.54 ± 1.05 , All $p > 0.05$) (Fig 3.10, C). This data taken alone suggests that under glucose reduction there is no increase in atrophic gene expression, this is in direct conflict with the morphological and biochemical data. The reduction in myotube formation observed here may therefore be due to a reduction in hypertrophic gene expression only or MUSA1 is playing a different role in differentiating muscle cells than the previous observations in mature muscle fibres *in-vivo*, described above (Milan *et al.*, 2015).

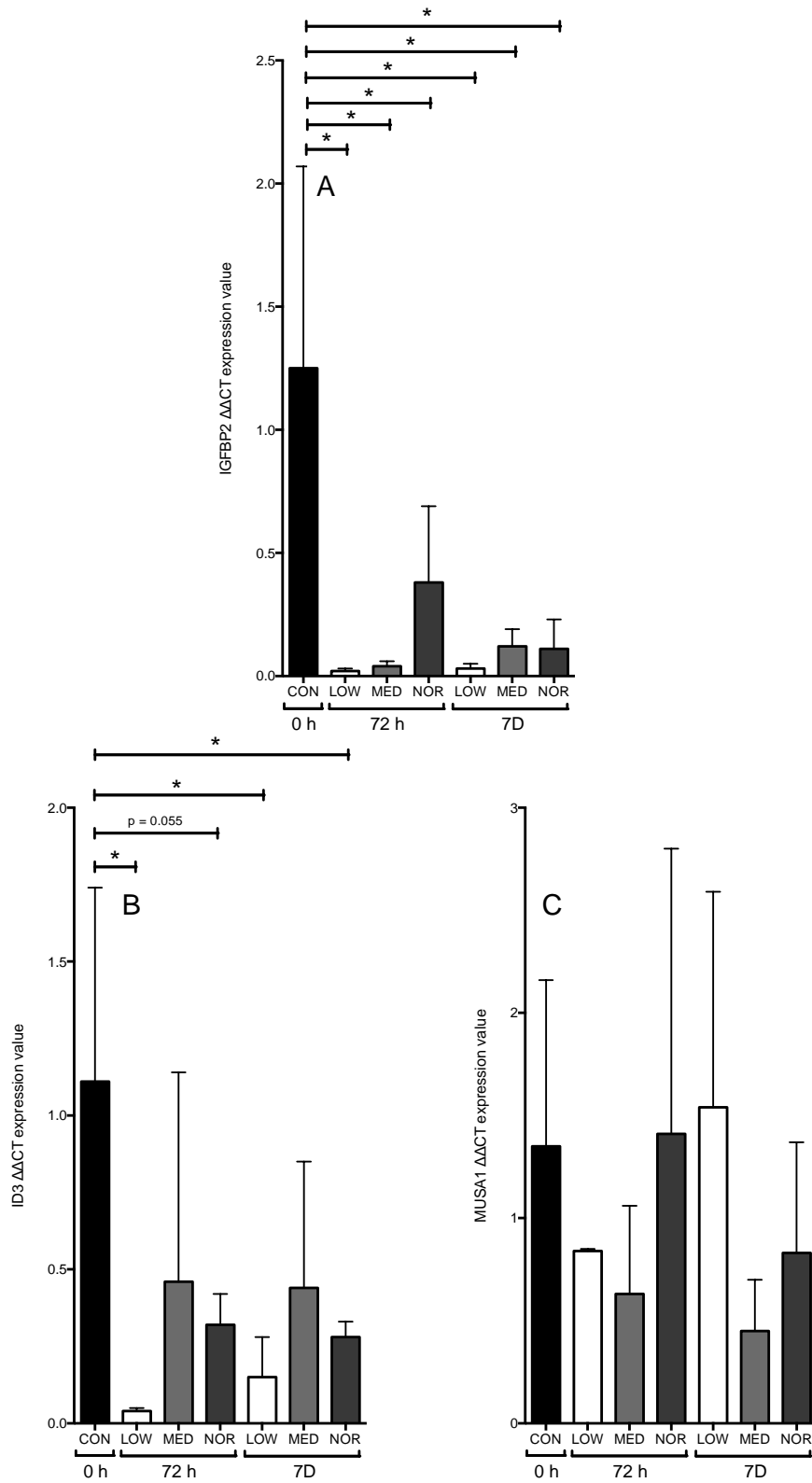


Fig. 3.10. Graphs depicting means and SD's for gene expression for: A) IGFBP2 B) ID3 and MUSA1 C). All experimental conditions are significantly reduced in comparison to 0h. The same is true for LOW and NOR conditions for ID3 gene expression. There are no significant differences present for MUSA1. Significant difference ($p < 0.05$) is denoted using a * . If approaching significance p value is stated.

3.3.6. SIRT1 expression increases following LOW glucose conditions

We have previously observed increases in SIRT1 mRNA expression under the stress induced by the presence of the inflammatory cytokine TNF- α . This increase promoted cell survival in muscle cells as confirmed via SIRT1 siRNA in which further cell death was promoted, Furthermore SIRT1 activation via resveratrol administration aided the maintenance of differentiation under the aforementioned TNF- α condition (Saini et al., 2012). For SIRT1 gene expression we observed significant main effects for glucose ($F_{(2,17)} = 9.62$, $p = 0.002$) and time ($F_{(2,17)} = 6.60$, $p = 0.008$) as well as an interaction between glucose dose and time ($F_{(4,17)} = 5.40$, $p = 0.005$). Interestingly the changes over time for the NOR group consisted of a decrease between 0 h and both 72 h (0 h vs. NOR: 1.41 ± 0.54 vs. 0.55 ± 0.23 , $p = 0.046$ (fisher)) and 7D (0 h vs. NOR: 1.41 ± 0.54 vs. (Fig 3.11). There is however no significant difference for NOR glucose between these time points (72 h vs. 7D: 0.55 ± 0.23 vs. 0.58 ± 0.44 , $p > 0.05$).

The observation above in which the NOR condition is decreased in comparison to the 0 h time point is not detected following 72 h in MED glucose (0h vs. MED, 72 h: 1.41 ± 0.54 vs. 1.27 ± 0.01 , $p > 0.05$). At 72 h there is no significant reduction in SIRT1 present and the expression remained the same as 0 h. A trend similar to the abovementioned reduction in SIRT1 under NOR conditions is instead observed at 7D compared to 0 h (0 h vs. MED, 7D: 1.41 ± 0.54 vs. 0.65 ± 0.25 , $p = 0.075$ (fisher)).

Importantly, initial changes in SIRT1 expression under LOW glucose conditions display an opposing pattern to NOR conditions (Fig 3.11). A large significant increase in SIRT1 expression is observed under LOW conditions following 72 h in comparison to 0 h (0h vs. LOW: 1.41 ± 0.54 vs. 2.97 ± 0.84 , $p = 0.038$). LOW glucose causes a significantly larger expression of SIRT1 than both MED and NOR following 72 h (LOW vs. MED: 2.97 ± 0.84 vs. 1.27 ± 0.01 , $p = 0.047$, LOW vs. NOR: 2.97 ± 0.84 vs. 0.55 ± 0.23 , $p < 0.001$). This observation is similar to that previously

documented under an alternative stress, the presence of TNF- α (Saini et al., 2012). After this initial increase, we observed a dramatic significant decrease at 7D (LOW, 72h vs. LOW, 7D: 2.97 ± 0.84 vs. 1.10 ± 0.33 , $p = 0.007$). This decrease brings SIRT1 levels back to a similar level of the 0 h control (0 h vs. LOW, 7D: 1.41 ± 0.54 vs. 1.10 ± 0.33 , $p > 0.05$). At this timepoint there was no longer a significant difference between any of the glucose conditions (LOW vs. MED: 1.10 ± 0.33 vs. 0.65 ± 0.25 , LOW vs. NOR: 1.10 ± 0.33 vs. 0.58 ± 0.44 , MED vs. NOR: 0.65 ± 0.25 vs. 0.58 ± 0.44 , All $p > 0.05$). The complete loss of myotube formation observed during the LOW glucose conditions may therefore be closely related to this initial increase in SIRT1 (Fig 3.11). where the cells are attempting to survive rather than differentiate. Importantly, by activating SIRT1 in LOW glucose conditions, as in TNF- α administration, we may be able to promote maintenance of differentiation under nutrient stress.

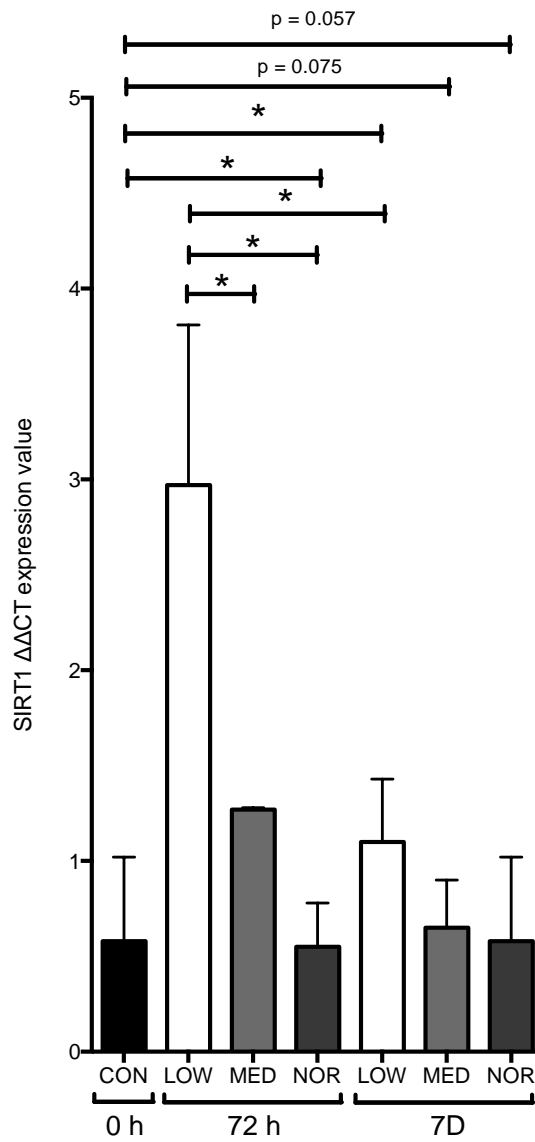


Fig. 3.11. Graphs depicting means and SD's for gene expression for SIRT1. LOW glucose is significantly increased in comparison to NOR and MED following 72 h. Significant difference ($p < 0.05$) is denoted using a *. If approaching significance p value is stated.

3.4. Summary

Following reductions from the normal *in vitro* glucose concentration (NOR) we established that two concentrations were more physiologically relevant than the other possibilities. The morphological and biochemical data determined that there was a reduced ability to differentiate under MED glucose conditions evidenced through the reduction in myotube size. Under LOW conditions no myotubes were formed. This provided us with models of reduced (MED) and impaired (LOW) differentiation which were also physiologically relevant to muscle interstitium levels under regular calorie consumption (MED) and restricted levels (LOW). Gene expression of the MRF's was impaired in both concentrations in comparison to NOR, however the restricted concentrations did not differ from each other in MyoD nor Myogenin. There was, however a significant difference between the two for MRF4 suggesting that the gene expression for these two concentrations are not simply replicas.

MYHC 4 and MYHC 1 expression was reduced in both LOW and MED compared to the NOR glucose condition. As these isoforms are prerequisites to fast and slow twitch fibres respectively it suggests that a change in composition is not present, instead the expression is reduced possibly due to the reduction in both size and number observed under restricted glucose conditions (Fig. 3.4 and 3.6.). NOR glucose had higher expression of MYHC 1, 4 and 7 suggesting that there was no real modification in myotube composition under LOW and MED conditions, instead there was just a reduced expression possibly due to the reduction in myotube size and number. There was no significant difference between any of the glucose concentration in the atrophic gene expression, which is in a direct conflict of the morphological and biochemical data. This may suggest that the reduction in myogenic gene expression drives the reduction in differentiation observed. There was however a reduction in ID3 following in NOR glucose after 0 h which may have given rise to the increase in MyoD observed at the same time points. Although, in

opposition to NOR conditions MyoD was reduced in LOW glucose (Fig 3.5.) there was no significant increase in ID3 (Fig 3.10) which would be indicative of an ID3 mediated increase in MyoD.

As myotube formation was greatest in the NOR condition and there was a reduction observed in SIRT1 it would be most logical to suggest that this reduction may be required for differentiation to take place, especially given that MED glucose conditions display an impaired differentiation and myotube maturation while the reduction in SIRT1 is delayed. Alternatively, based on our groups previous findings, in which an increase in SIRT1 under stress environments is a survival mechanism stress aiding improvements in differentiation (Saini et al., 2012). In this instance this data may be interpreted that under NOR glucose conditions appropriate differentiation is occurring and as such no survival mechanism is required, thus SIRT1 is not increased.

3.5. Conclusion

We can conclude from this data that we have been able to establish a model to investigate the impact of glucose concentration on muscle cell differentiation. The two concentrations we performed in depth morphological, biochemical and gene expression investigations on are models of reduced (MED) and impaired (LOW) differentiation which also provide an *in vitro* representation of both glucose conditions under normo-caloric and restricted levels respectively. Finally, as we observed similar results to those previously documented in the presence of TNF- α , in which SIRT1 is increased under stress. If indeed an increase in SIRT1 under stress environments is a survival mechanism, further activation of SIRT1 than produced by stressed cells may promote successful survival and improvements in myotube differentiation (Saini et al., 2012). Before this can be performed however an optimum SIRT1 activation must first be established.

Chapter 4

4. The activation of SIRT1 in myoblasts in response to a pharmacological administration of resveratrol and EX-527.

4.1. Introduction

The antioxidant resveratrol (RES) has been used widely as a mimetic of dietary restriction (DR) due to its ability to increase cell survival in budding yeast (Howitz *et al.*, 2003) and its purported role in the extension of lifespan in mice consuming high calorie diets (Baur *et al.*, 2006). Found predominately in the skin of red grapes, this polyphenol was originally determined to activate Sir2 in yeast and more recently the Sir2 mammalian homologue SIRT1 (Vinciguerra *et al.*, 2010, Zu *et al.*, 2010). Although most frequently studied in relation to SIRT1 activation RES also increases, which may be responsible for some of the many discrepancies observed within the literature (Gertz *et al.*, 2012). SIRT1 activation via RES administration, can also regulate AMPK activity and mitochondrial function (Price *et al.*, 2012). Calorie restriction has previously been documented to evoke an increase in SIRT1 activity as a potential survival mechanism (Chen *et al.*, 2008) while Fulco *et al.* (2008) suggest that the increase in SIRT1 is the mechanism that instigates the loss in muscle mass under this nutritional stress.

Previous literature has administered RES to assess growth, differentiation and migration in murine skeletal muscle cells (Fröjdö *et al.*, 2011, Kaminski *et al.*, 2012), and has been used to treat parental C2 (Saini *et al.*, 2012) and daughter C2C12 cells (Deane and Sharples *et al.*, Unpublished) It was shown to enable the maintenance of differentiation in the presence of increased inflammation (Saini *et al.*, 2012), with other groups also

suggesting that resveratrol can improve myoblast migration following oxidative stress (Bosutti and Degens, 2015). Therefore, the use of RES to activate SIRT1 in muscle cells may enable us to elucidate the role of SIRT1 activation and the impact of blocked/impaired muscle cell differentiation/myotube hypertrophy under nutrient/glucose restriction (chapter 3) in future chapters (chapter 5 and 6). Although the aforementioned studies used resveratrol, these studies have only characterised the total protein and/or mRNA of SIRT1 (or neither) and have not characterised SIRT1 activity (phosphorylation) in response to resveratrol administration in muscle cells. Therefore we aim to elucidate the changes in SIRT1 activation (phosphorylation) following resveratrol administration in skeletal muscle cells in a dose responsive fashion.

Inhibition of SIRT1 activation will be implemented in order to act as relevant negative control opposing increases in SIRT1 activity in the presence of low glucose conditions later documented in chapters 5 and 6.. SIRT1 inhibition at the gene expression level has been performed in previous studies using siRNA (Rodgers *et al.*, 2005a, Saini *et al.*, 2012). Alternatively, selective SIRT1 inhibitors have also been utilized, EX-527 is one such SIRT1 inhibitor able to reduce SIRT1 activity in a wide variety of cells including; astrocytes (Kauppinen *et al.*, 2013), human embryonic kidney and fibrosarcoma cell lines (Yang *et al.*, 2007). However to the authors' knowledge, there are no studies using EX-527 in myoblasts that assess the impact of this treatment on SIRT1 activation.

This group have previously administered C2C12 cells with concentrations of RES at 30 and 60 μM however these doses compromised cell viability (Deane and Sharples *et al.*, 2015 unpublished). Cell death has also been observed at these doses by other groups in C2C12's (Bosutti and Degens, 2015). We therefore undertook a dose response of resveratrol at 5, 10 and 15 μM and investigate the impact on SIRT1 activation. Additionally recent evidence suggests that 10 μM is beneficial in C2C12 myoblasts remodelling under oxidative stress and as such has potential to be

beneficial under an alternative stress environment (DR) (Bosutti and Degens, 2015). We also aimed to undertake dosing of muscle cells with the SIRT1 inhibitor (EX-527) at both 30 and 60 μ M. We hypothesised that SIRT1 activity would increase and decrease following RES/ EX-527 administration respectively in a dose responsive manner. The ultimate aim was to establish whether activation/inactivation of SIRT1 can ameliorate the nutrient restriction induced block in muscle cell differentiation observed in low glucose (mimicking muscle interstitium glucose during DR) and the reduced differentiation in medium glucose (circulatory glucose during DR) respectively.

4.2. Methods

4.2.1. Cell culture

6Well plates were pre-treated with 0.2% porcine gelatine for 10 min at room temperature (RT) and 10 min in a humidified, 37°C with 5% CO₂. The excess gelatine was aspirated and cells were seeded at 8×10^4 cells/ml in 2 ml of GM per well, these were then incubated until 80% confluence. Cells were washed in PBS and transferred into 2 ml of DM in 37°C with 5% CO₂ for up to 7 days (7D). Time point of extraction was as described in the methods section 2.2.2. i.e. 15 min following administration of the SIRT1 activator/ inhibitor. In order to determine the optimum concentration to increase expression of SIRT1 cells were incubated with either: 5 μ M, 10 μ M or 15 μ M of RES (5RES, 10RES and 15RES respectively). Inhibition of SIRT1 expression was initially assessed via incubation of 30 or 60 μ M and then subsequently lower doses of 100 nM or 200 nM of EX-527. All SIRT1 activation and inhibition experiments for this dose response study were performed in the same reconstituted differentiation media as discussed in chapter 3 at a glucose concentration of 4.5 g/L (NOR condition). Further information of cell culture methods can be found in section 2.2.1 in chapter 2.

4.2.2. Total protein content

Protein was measured using BCA™ (Pierce, Rockford, IL) according to instructions and detected using CLARIOstar® plate reader (BMG labtech, Germany) at a wavelength of 540-590 nm to quantify total protein concentrations prior to relative comparison of CK samples (See general methods chapter 2, section 2.2.8.).

4.2.3. SDS-PAGE and immunoblotting

Full methods can be found in chapter 2, section 2.2.10. Briefly, western blot analysis via SDS-PAGE and immunoblotting was carried out on 10% resolving gels using 30 µg of protein per sample. Semidry transfer was utilized and immunoblotting for total and phosphorylated SIRT1 was carried out using catalogue number 07-131 from Merck Millipore (Darmstadt, Germany) and catalogue number 2314L (Cell Signalling Technology®, MA, USA) respectively. Additionally, GAPDH #5174 (Cell Signalling Technology®, MA, USA) was implemented as a loading control, further information on protocol and the antibody concentrations used factors can be found in chapter 2, section 2.2.10.

4.2.4. Statistical analysis

All data was performed using three separate cell populations thus performed N=3. Analysis was then carried out using Minitab® 17 (Minitab Ltd, Coventry U.K). Outliers were removed using Grubbs outlier test. All data was parametric, assessed using the Anderson-Darling test for normality. General linear models were carried out for the initial RES analysis (4 x 1) for RES concentration (DM, 5, 10, 15 µM) and for the selected time point, this analysis was carried out for timepoints (15 min, 30 min, 2 h and 24 h). Time course analysis for 10 and 15 RES were carried out using a (2 x 4) general linear model for RES concentration (10, 15 µM) and time (15 min, 30 min, 2 h and 24 h). The timecourse, which compared DM to 10 and 15 RES, implemented a general linear model (3 x 4) for RES concentration (DM, 10 and 15 µM) and timepoint (15 min, 30 min, 2 h and 24 h). The SIRT1 inhibitor (EX-527) analysis was performed via a

general linear model (2 x 4) for RES concentration (DM, 100 nM) and timepoint (15 min, 30 min, 2 h and 24 h). Post hoc tests were performed using Fisher, Bonferroni and Tukey. The results produced through the Bonferroni tests are reported throughout results unless otherwise stated.

4.3. Results

4.3.1. Initial resveratrol dose response.

A dose response investigation was implemented to study whether resveratrol (RES) administration could be used to effectively activate SIRT1. Our first objective was to establish the optimal dose of resveratrol in activating SIRT1 via western blot analysis of phosphorylated SIRT1 concomitantly with any changes in total SIRT1 protein levels. Based on our unpublished results that 30 and 60 μ M resveratrol reduces myoblast cell viability, as observed by others (Bosutti and Degens, 2015). We undertook a dose response for resveratrol of 5, 10, 15 μ M. There was an average increase observed for 5, 10 and 15 μ M in comparison to the DM condition following 30 min in which 10RES appeared to possess a higher average activity rate (30 min: 5RES vs. 10RES: 1.27 ± 0.48 vs. 1.34 ± 0.01 , $p > 0.05$, Fig. 4.1.). As this was non-significant to establish whether RES increased over time, therefore we carried out a timecourse analysis over a longer period e.g. 15, 30 mins, 2 h and 24 h. During this analysis we did not carry forward the 5RES as the activation was slightly less favorable than the higher dose of 10 μ M (5Res vs. 10RES: 1.27 ± 0.48 vs. 1.34 ± 0.01 , $p > 0.05$).

4.3.2. Effect of 10 μ M RES on SIRT1 activation

We observed significant increases in SIRT1 activity following 10RES supplementation following 15 min and 24 h with an increase suggested following 30 min (DM 15 min: 1.00 ± 0.00 vs. 10RES 15 min: 16.34 ± 4.26 , $p = 0.021$ vs. 10RES 24 h: 15.65 ± 7.70 , $p = 0.026$, 10RES 2 h: 11.22 ± 5.54 , $p = 0.088$, (all fisher comparisons) Fig. 4.1.). Similarly, 15RES also increased significantly from the 15 min DM at 2 h and 24 h (DM 15 min:

vs. 15RES 24 h: 17.50 ± 10.86 , $p = 0.014$, 15RES 2 h: 13.72 ± 8.51 , $p = 0.047$ (all fisher comparisons) Fig 4.1), 15RES also increased significantly after 30 min but not 15 min (DM 15 min: 1.00 ± 0.00 vs. 15RES 30 min: 13.78 ± 6.41 , $p = 0.046$ (fisher) Fig 4.1.). SIRT1 activity was therefore increased in both 10RES and 15RES. As there was still no observable difference between these two concentrations therefore to save additional reagent costs at higher concentrations the use of the lower concentration 10RES was taken forward. Especially given recent evidence that $10 \mu\text{M}$ is beneficial in C2C12 myoblasts remodelling under oxidative stress (Bosutti and Degens, 2015).

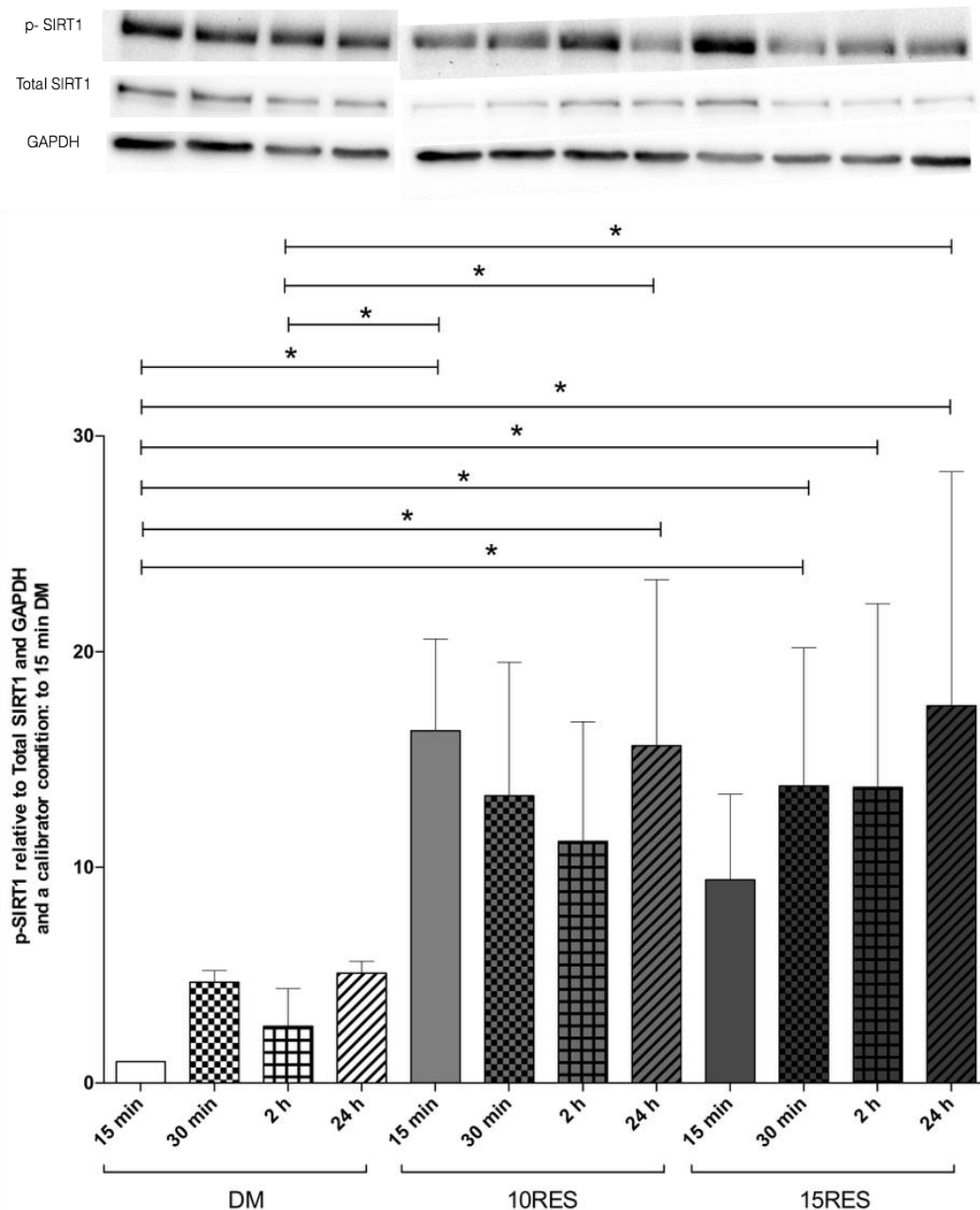


Fig.4.1. Control corrected, Phosphorylated SIRT1 relative to Total SIRT1 across the time course, relative to the loading control, GAPDH. Both 10 and 15RES displayed an increase in SIRT1 in comparison to DM. Significant difference ($p < 0.05$) is denoted using a *.

4.3.2. The Effect of the SIRT1 inhibitor (EX-527) at a concentration of 30 μ M and 60 μ M on SIRT1 activation

We also undertook a dose response study of SIRT1 inhibitor (EX-527). Initially we carried this out using 30 μ M and 60 μ M concentrations as this inhibitor at 30 μ M has been previously shown to inhibit SIRT1 at these

concentrations in C2C12 cells (Price et al., 2012). We however discovered no significant differences in p-SIRT at 15 min, 30 min nor 2 h (All comparisons, $p > 0.05$, Fig.4.2.). Indeed, in some instances there was increased SIRT1 activity with EX-527 administration (Fig. 4.2). A lower doses of 100 nM was consequently carried out, as the lower concentration of 100 nM had been previous shown to inhibit SIRT1 in other non-muscle cell types (Solomon et al., 2006).

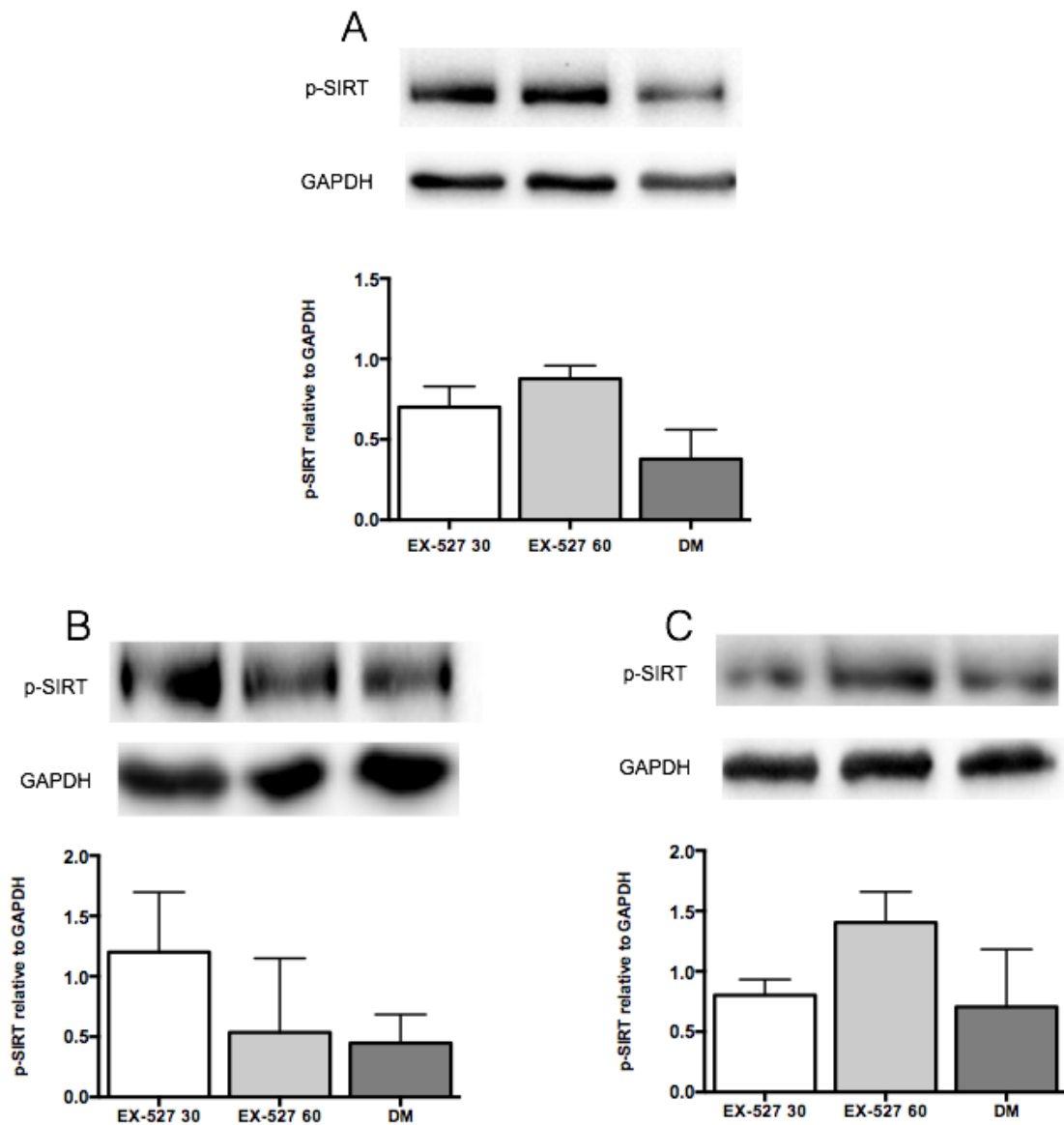


Fig.4.2. Phosphorylated SIRT1 relative to Total SIRT1 at 15 min (A), 30 min (B) and 2 h (C) displayed no significant differences for any experimental conditions.

4.3.3. The Effect of the SIRT1 inhibitor (EX-527) at a concentration of 100 nM on SIRT1 activation

We observed an average decrease of 71% in SIRT1 activity following 24 h in the presence of 100 nM of EX-527 in comparison to the DM control at 15 min, an observation that approached significance (DM 15 min vs. EX-527 24 h: 1.00 ± 0.54 vs. 0.29 ± 0.13 , $p = 0.062$ (fisher), Fig. 4.3.) compared to only a 50% reduction after 24 h in SIRT1 phosphorylation without EX-527 administration (DM 15 min vs. DM 24 h: 1.00 ± 0.54 vs. 0.48 ± 0.34 , $p > 0.05$). This suggested that on average there was a 20% larger reduction in SIRT1 by 24 h with the addition of EX-527 vs. 15 min SIRT1 expression in DM (Fig 4.3.). Additionally, EX-527 at a concentration of 100 nM at 2 and 24 h was also reduced by an average of 20 and 40% respectively in comparison to DM at the same time points although this did not achieve statistical significance (2 h, DM vs. EX-527: 0.48 ± 0.32 vs. 0.40 ± 0.31 , 24 h, DM vs. EX-527: 0.48 ± 0.34 vs. 0.29 ± 0.13 , $p > 0.05$).

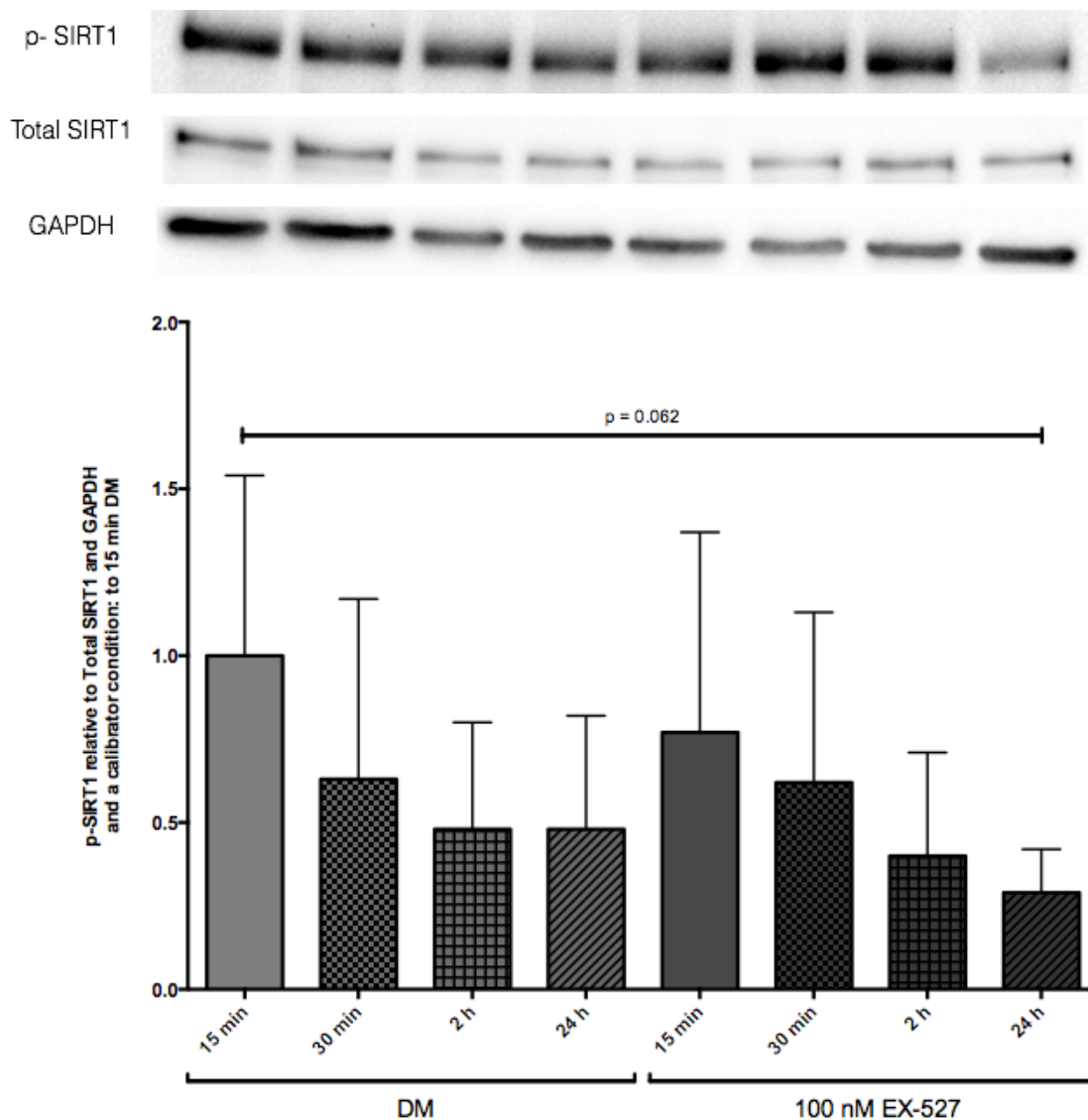


Fig.4.3. Phosphorylated SIRT1 relative to Total SIRT1 across the time course. A larger mean decrease in SIRT1 activity was observed between 15 min DM and 24 h following EX-527 at 100 nM. Significant difference ($p < 0.05$) is denoted using a *. If approaching significance p value is stated.

4.4. Summary

To establish whether SIRT1 activation/inhibition would improve growth and differentiation in muscle cells in glucose restricted environments we needed to establish SIRT1 phosphorylation in the absence or presence of commercially available SIRT1 activator/inhibitor, resveratrol and EX-527 respectively. We observed a significant increase in SIRT1 activity with

both 10 and 15 μ M RES. Activation seemed more consistently elevated over the time course of 15 min, 30 min, 2, and 24 h with 10 μ M RES, with the largest increase in SIRT1 Phosphorylation at 15 min with RES 10 μ M. There was also no significant difference between 10 or 15 μ M of RES. Therefore, these results and in order to save additional reagent costs at higher concentrations the use of the lower concentration 10RES was taken forward to chapter 5 and 6. Especially given recent evidence that 10 μ M is beneficial in C2C12 myoblasts remodelling under oxidative stress (Bosutti and Degens, 2015). Furthermore, it is worth bearing in mind that oral resveratrol treatment is financially expensive and *in-vivo* resveratrol may have poor bioavailability through the gut (Walle *et al.*, 2004), low concentration may only be available to skeletal muscle tissue, subsequently if lower concentrations were able to affect the block/reduced differentiation/ observed in chapter 3 during glucose restriction this would potentially reduce the amount of resveratrol required to pass through the gut and be available to skeletal muscle tissue (Walle *et al.*, 2004).

On average EX-527 reduced SIRT1 across the timecourse to the greatest extent following administration of 100 nM EX527, although this was not to as greater extent as we had previously anticipated. Indeed, initially higher doses of 30 and 60 μ M did not decrease SIRT1 activity and in some instances paradoxically increased SIRT1 activation. There was no explanation as to why these higher doses may increase SIRT1 activation, however doses of 48-100 nM have previously been shown to inhibit SIRT1 by approximately 50% (Solomon *et al.*, 2006, Napper *et al.*, 2005, Zhao *et al.*, 2013). Inhibition in these instances was measured via vitro Fluor de Lys deacetylation assays in embryonic kidney cells to assess SIRT1s deacetylation activity and not phosphorylation (Solomon *et al.*, 2006). Reductions in phosphorylation have been associated with reduced deacetylation activity of SIRT1. Therefore despite the poorer than anticipated reduction in SIRT1 phosphorylation following 100 nM of EX-527 we suggest that the deacetylation may have decreased accordingly or to a greater extent within the C2C12 cells.

In the next chapter the objective was to implement these concentrations of SIRT1 activator/ inhibitor in the presence or absence of low glucose conditions as characterised in the previous chapter (3). This would enable us to determine whether the activation/inhibition of SIRT1 was able to alter the block/reduction of differentiation observed in low/ medium glucose concentrations respectively that mimic circulatory (MED) and interstitial glucose levels (LOW) observed during DR in rodents (observed in chapter 3).

Chapter 5

5. SIRT1 activation and inhibition in myoblasts under reduced glucose conditions.

5.1. Introduction

In chapter 3 we provided evidence for a model of reduced (MED glucose) and blocked (LOW glucose) muscle cell differentiation with glucose concentrations that were physiologically relevant to dietary restricted circulatory blood levels (MED 1.13 g/L or 6.25 mM) and that of the interstitium (LOW 0.56 g/L or 3.12 mM) in rodents. Furthermore, in chapter 3, we also observed increased SIRT1 gene expression where myotube formation was completely blocked in LOW glucose conditions. Because the SIRT1 activator, resveratrol, has been previously observed to improve differentiation, where differentiation was blocked due to TNF- α administration (Saini et al., 2012). We suggested that SIRT1 activation via resveratrol treatment may improve differentiation and myotube maturation in skeletal muscle cells under reduced glucose conditions. Furthermore, in chapter 4 we determined the concentrations of RES and EX-527 for the activation and suppression respectively of SIRT1 activity in myoblasts. Therefore these data from chapter 3 and 4 combined to allow us to determine whether SIRT1 activation or inhibition would affect the loss of differentiation in LOW glucose conditions and the impaired differentiation observed in MED glucose conditions. We aimed to activate or inhibit SIRT1 activity under MED, LOW and NOR glucose conditions in differentiating myoblasts. We hypothesised that SIRT1 activation may ameliorate the blocked and reduced differentiation capacity observed under LOW and MED conditions respectively.

5.2. Methods

5.2.1. Cell culture

C2C12 murine myoblasts (Blau et al., 1985) at passage 12 were incubated in separate T75 flasks in a humidified, 37°C with 5% CO₂ Growth media (GM) containing: Dulbecco's Modified Eagle Serum (DMEM) (D6429-6, Sigma-Aldrich, UK), 1% Penicillin Streptomycin (Pen Strep), 10% New born calf serum (NBCS) and 10% Fetal Bovine Serum (FBS) until 80% confluency was attained.

Experiments were initiated by removing GM (as described in the general methods, chapter 2, section 2.2.2), washing once with phosphate buffered saline (PBS) followed by the addition of powdered differentiation media (DM). The chosen powdered DMEM was reconstituted according to manufactures instructions (8.3 g/L of DMEM) supplemented with 0.5840 g/L L-Glutamine; 3.7000 g/L Sodium Bicarbonate; 0.1100 g/L, Sodium Pyruvate; 0.0159 g/L Phenol red and either 0 g/L or 4.5 g/L D-Glucose in order for the composition to match that of the more generally used liquid DMEM. This media was also supplemented with 2% HS and 1% PS. The powdered DM supplemented with glucose was compared to the liquid DMEM in section 3.3.1, thus making this powdered DMEM a relevant control as well as being used to produce the dosing conditions described below under section 3.2.2. The reduction in serum content, causing the C2C12 myoblasts to undergo spontaneous differentiation without requiring the addition of growth factors to initiate the process (Blau et al., 1985). Cells were seeded following trypsinization of the adherent cells, counts where performed using haemocytometer in the presence of Trypan Blue dye as described in general methods (section 2.2.3).

5.2.2. Cell dosing

6 Well plates where pre-treated with 0.2% porcine gelatine for 10 min at room temperature (RT) and 10 min in a humidified, 37°C with 5% CO₂. The excess gelatine was aspirated and cells were seeded at 8×10^4 cells/ml in 2 ml of GM, these were then incubated until 80% confluence.

Cells were washed in PBS and transferred into 2 ml of DM in 37°C with 5% CO₂ for up to 7 days (7D). Time point zero was defined as an incubation of 30 min after transfer to DM and is denoted as 0 hours (0 h). To assess the effect of SIRT1 manipulation under a glucose restricted environment in myoblasts the cells were incubated in reconstituted powdered media as described above and originally in chapter 2, section 2.2.5.1 with either 25.00 mM (NOR), 6.25 mM (MED), or 3.12 mM (LOW) glucose. Resveratrol and EX-527 were also reconstituted as described in chapter 2, section 2.2.5.1. RES was used at a concentration of 10 µM and EX-527 at 100 nM.

5.2.3. Morphology

Myotube parameters including; number, diameter and size were assessed using a live imaging light microscope (AF600 modular system, Leica, Germany) cell imaging system at x 20 magnification at time points; 0, 72 h and 7D post transfer into DM. Per experiment, each time point and experimental condition was performed in duplicate with 12 images taken per well providing a total of 24 images per condition per timepoint. Experiments were then repeated n = 3. Analysis was performed on the images acquired at 0 h, 72 h and 7D using ImageJ software (NIH, USA) (See general methods chapter 2, section 2.2.6.)

5.2.4. Total protein content

Protein was measured using BCA™ (Pierce, Rockford, IL) according to instructions and detected using CLARIOstar® plate reader (BMG labtech, Germany) at a wavelength of 540-590 nm to quantify total protein concentrations prior to relative comparison of CK samples (See general methods chapter 2, section 2.2.8.).

5.2.5. Creatine Kinase

Assessment of creatine kinase activity was measured using assay kit (Catachem, Inc, Connecticut, NE) according to manufacturer's instructions

and detected using a CLARIOstar® plate reader (BMG labtech, Germany) at a wave length of 340 nm. See general methods chapter 2, section 2.2.9.

5.2.6. RNA Extraction and analysis

RNA extraction was performed using the TRIzol method (See method chapter 2, section 2.2.11.), following the manufactures instructions (Invitrogen, Life technologies, Carlsbad, CA). RNA purity and concentration was assessed using 1µl of sample on a NanoDrop 2000c, UV-Vis (Ultraviolet–visible spectroscopy) spectrophotometer (Thermo Fisher Scientific, MA, USA) using ODs of 260 and 280 nm. A ratio of these OD value was calculated for each sample with all samples possessing 260/280 ratios of between 1.8-2.2 and therefore accepted as high RNA quality.

5.2.7. Primer design

Identification of target sequences were carried out via Gene (<http://www.ncbi.nlm.nih.gov/gene>). Primers (Chapter 2, section 2.2.12.4.-table 2.2) were designed using Primer-Blast (<http://www.ncbi.nlm.nih.gov/tools/primer-blast/>).

5.2.8. RT-PCR and analysis

RT-PCR was carried out using Quantifast SYBR green RT-PCR kit (Qiagen, Manchester, UK) on a Rotor-Gene® (Qiagen, Manchester, UK) supported by Rotor-Gene® Q Software, version 2.1.0.9 (Qiagen, Manchester, UK). The RT-PCR cycles consisted of; 48°C, 30 min (reverse transcription/ synthesis of cDNA), 95°C, 10 min (transcriptase inactivation and initial denaturation) followed by 40 cycles of 95°C, 15 sec (denaturation), 60°C, 1 min (annealing and extension in 1 step). Disassociation melt-curve analysis was performed to reveal and therefore exclude non-specific amplification and primer dimer issues. All out gene products yielding on single melt peak/temperature suggesting one product was amplified. Relative gene expression analysis was carried out using $\Delta\Delta C_t$ equation, otherwise known as the Livak method (Schmittgen and

Livak, 2008), this is to establish normalised expression ratios, where the relative expression is calculated as $2^{-\Delta\Delta C_t}$ and C_t represents the threshold cycle. RPII β was extremely stable between experimental conditions (mean C_t 15.62 \pm 0.11) and therefore used as the housekeeping gene in all RT-PCR assays and the pooled mean used in the $\Delta\Delta C_t$ calculations. All RT-PCR figures are presented as a relative gene expression in comparison to the 0 h cell incubated in “Normal” glucose (4.5g/L or 25 mM). This sample was used as a calibrator condition in the subsequent equations in order to compare expression values across glucose concentrations.

5.2.9. Statistical analysis

All data was performed using three separate cell populations thus performed N=3. Analysis was then carried out using Minitab® 17 (Minitab Ltd, Coventry U.K). Outliers were removed using Grubbs outlier test. All data was parametric, assessed using the Anderson-Darling test for normality. General linear models (3 x 3 x 3) for time (0, 72h, 7D), glucose concentration (LOW, MED, NOR) and SIRT1 activation/inhibition (DM, RES, EX-527) were carried out for morphological analysis of myotube number and CK activity and a general linear model (4 x 3 x 3) for time (0, 24, 72h, 7D), glucose concentration (LOW, MED, NOR) and SIRT1 activation/inhibition (DM, RES, EX-527) gene expression. (Post hoc tests were performed using Bonferroni, Tukey and Fisher). The results produced through the Bonferroni tests are reported throughout results unless otherwise stated.

5.3. Results

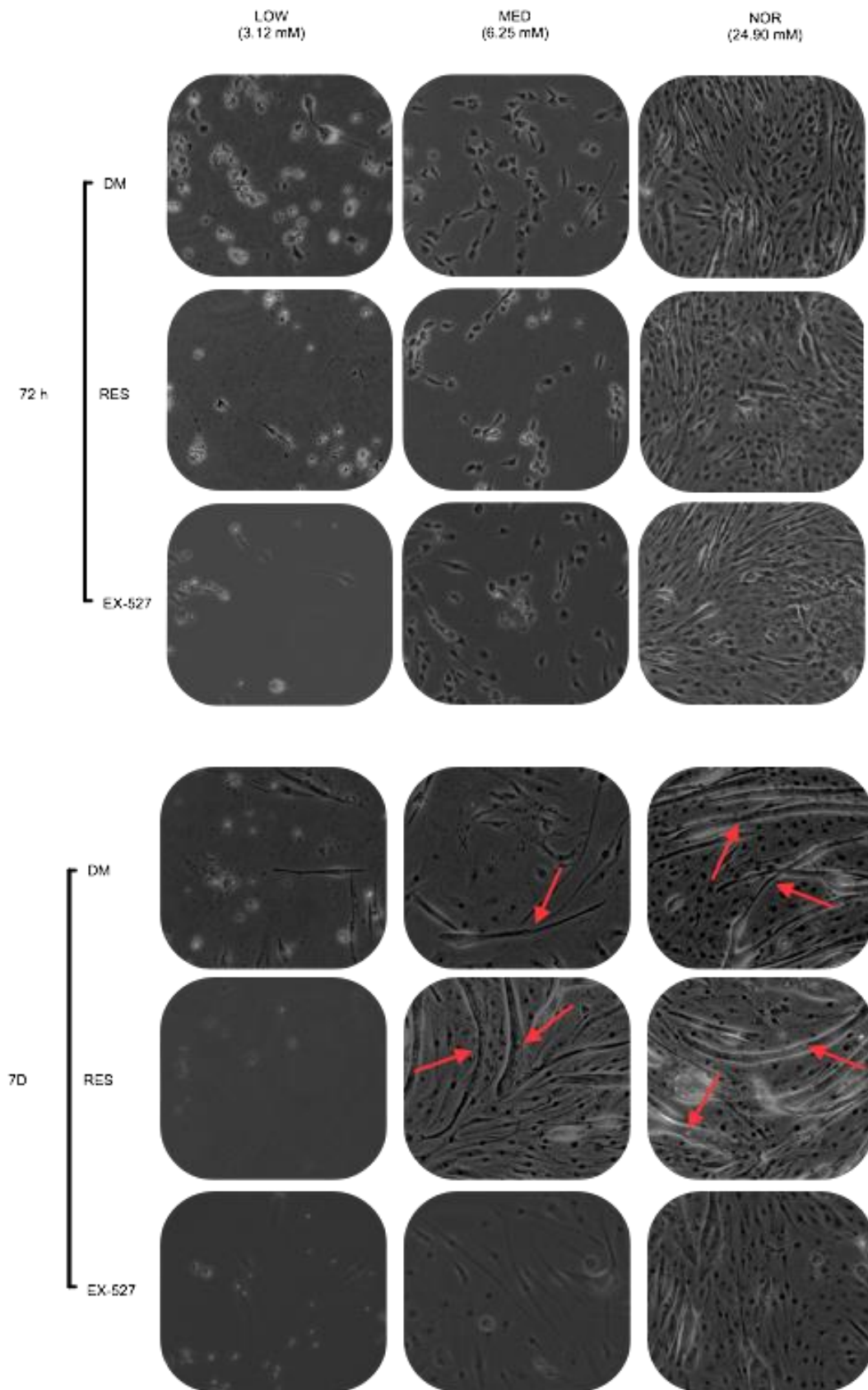


Fig. 5.1. Representative images for 72 h and 7D of myoblast culture in LOW, MED, and NOR glucose alone and with the addition of RES or EX-527.

5.3.1. Effect of EX-527 administration on myotube number under

Myotube number displayed a significant interaction for time, glucose concentration and SIRT1 manipulation ($F_{(8, 868)} = 12.32$, $p < 0.001$), There was also a significant interaction between glucose concentration and SIRT1 ($F_{(4, 868)} = 20.62$, $p < 0.001$), glucose and time ($F_{(4, 868)} = 58.29$, $p < 0.001$). There were significant main effects also present for glucose ($F_{(2, 868)} = 114.82$, $p < 0.001$) and time ($F_{(2, 868)} = 135.41$, $p < 0.005$) but not SIRT1 activation/inhibition alone ($F_{(2, 868)} = 0.87$, $p > 0.05$). As readily observed in Figure 5.1.

In the presence of the SIRT1 inhibitor measurable myotubes were produced in LOW glucose conditions following 7D. This condition was the only LOW glucose condition to produce observable myotubes. Despite this, there was no significant difference between the SIRT1 inhibitor and the LOW glucose alone (LOW EX-527 vs. LOW: 0.03 ± 0.17 vs. 0.00 ± 0.00 , $p > 0.05$, Fig. 5.2.). Therefore SIRT1 activation/inhibition via RES and EX-527 respectively had little or no effect on restoring blocked differentiation observed when no increase was detected in myotube number in LOW glucose conditions at either 72 h or 7D.

At 72 h there was no significance difference in myotube number following administration of RES or EX-527 within either the MED or NOR glucose concentrations. At 7D however, surprisingly under NOR conditions myotube number was significantly reduced when SIRT1 was activated under RES administration (NOR vs. NOR RES: 4.92 ± 3.30 vs. 3.67 ± 2.99 , $p = 0.009$, Fig. 5.2.). SIRT inhibition via EX-527 administration in NOR glucose further reduced myotube number at 7D vs. NOR alone (NOR vs. NOR EX-527: 4.92 ± 3.30 vs. 2.03 ± 2.75 , $p < 0.001$, Fig. 5.2.). Importantly, EX-527 administration in NOR glucose produced the lowest number of myotubes that were also significantly reduced vs. RES in NOR glucose at 7D ($p < 0.001$). In MED glucose concentrations at 7D, there was a non-significant increase in myotube number in the presence of RES (MED RES 0.59 ± 0.33 vs. MED 0.60 ± 0.21 , $p > 0.05$). There was however a

significant increase in myotube number in MED glucose conditions in the presence of EX-527 in comparison to both MED glucose alone and MED glucose in the presence of resveratrol (MED EX-527 vs. MED: 3.04 ± 3.11 vs. 0.13 ± 0.34 , $p < 0.001$ and vs. MED RES: 0.79 ± 1.32 , $p < 0.001$, Fig. 5.2.).

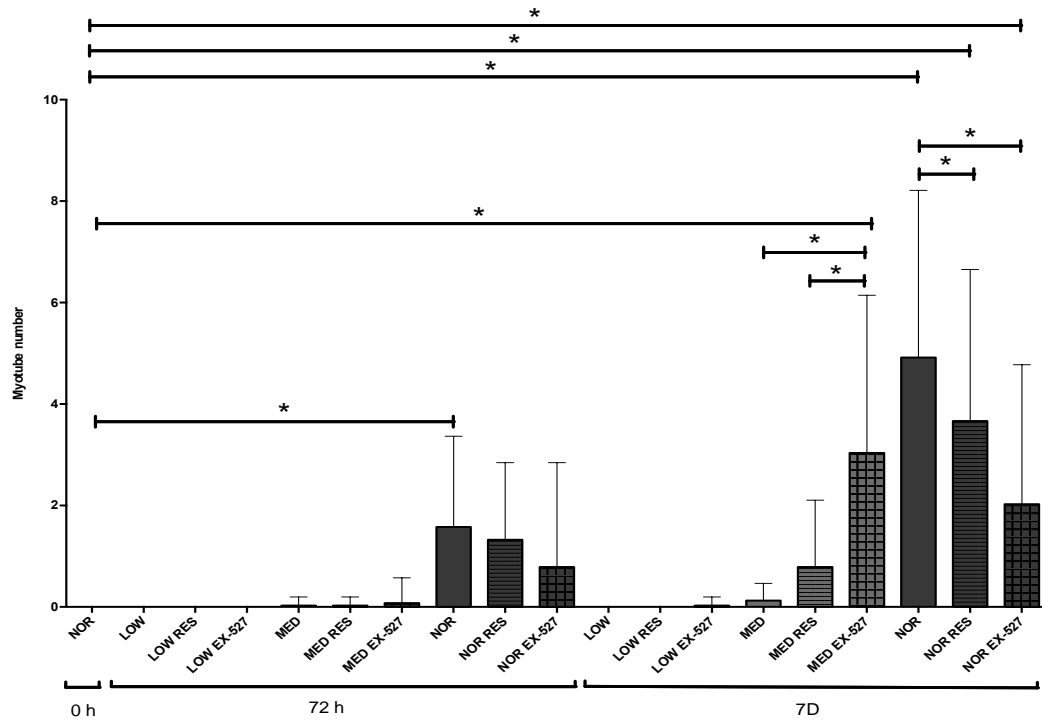


Fig. 5.2. Myotube number is reduced in cells undergoing MED glucose restriction, regardless of SIRT1 manipulation. No myotubes were observed in any LOW glucose conditions at any timepoint. Formation of myotubes under NOR conditions is impaired following the addition of RES at 7D and further impaired following the addition of EX-527. Significant difference ($p < 0.05$) is denoted using a *.

5.3.2. Resveratrol increases creatine kinase activity at 7D in LOW glucose conditions despite no increase in myotube formation and reduces CK activity with SIRT1 inhibition in normal glucose conditions.

To confirm myotube number morphology as a measure of differentiation/fusion, biochemical activity of differentiation marker creatine kinase was assessed and produced a significant main effect for glucose ($F_{(2,293)} = 76.72$, $p < 0.001$) and time ($F_{(2,293)} = 4.80$, $p < 0.005$). Additionally,

a significant interaction was observed between time, glucose concentration and SIRT1 activation/inhibition ($F_{(2,293)} = 4.80, p = 0.009$). As suggested in chapter 3 and confirmed here the LOW glucose condition had significantly lower CK activity across the time points in comparison to NOR glucose conditions (LOW vs. NOR; 48 h: 26.47 ± 18.39 vs. 98.68 ± 29.56 mU.mg.ml⁻¹, $p < 0.001$ (fisher), 72 h: 38.1 ± 73.3 vs. 98.91 ± 32.39 , $p = 0.003$ (fisher), 7D: 16.82 ± 15.95 vs. 139.56 ± 22.17 mU.mg.ml⁻¹, $p < 0.001$). The same trend was also present for MED when compared to NOR glucose (MED vs. NOR; 48 h: 60.09 ± 21.36 vs. 98.68 ± 29.56 , $p = 0.056$ (fisher), 72 h : 21.71 ± 17.93 vs. 98.91 ± 32.39 , $p = 0.055$, 7D: 44.4 ± 27.14 vs. 139.56 ± 22.17 mU.mg.ml⁻¹, $p < 0.001$). There was however no significant difference between LOW and MED across time points (LOW vs. MED; 48 h: 26.47 ± 18.39 vs. 60.09 ± 21.36 , $p = 0.997$, 72 h: 38.1 ± 73.3 vs. 21.71 ± 17.93 , $p > 0.05$, 7D: 16.82 ± 15.95 vs. 44.4 ± 27.14 mU.mg.ml⁻¹, $p > 0.05$). Again this morphology and CK activity data confirms the data in chapter 3 and suggests within the present chapter these data were relevant control conditions to elucidate any additional changes in the presence of absence of SIRT1 activation/inhibition. There was however, no significant differences in CK activity in the presence of RES on a background of LOW glucose at either 48 h (LOW vs. LOW RES: 26.47 ± 18.39 vs. 16.0 ± 46.8 mU.mg.ml⁻¹, $p > 0.05$), or 72 h (LOW vs. LOW RES: 38.1 ± 73.3 vs. 14.0 ± 34.8 mU.mg.ml⁻¹, $p > 0.05$). There was however an average increase at 7D that approached significance using fisher comparisons where RES administration was responsible for an increase in CK activity under LOW glucose conditions (LOW vs. LOW RES: 16.82 ± 15.95 vs. 54.4 ± 44.7 mU.mg.ml⁻¹, $p = 0.069$). CK values were however, still significantly lower under LOW conditions with the administration of RES than values observed in the NOR glucose condition at the same time point (LOW RES vs. NOR: 54.4 ± 44.7 vs. 139.56 ± 30.08 , $p = 0.016$), therefore while SIRT1 activation was able to somewhat improve CK activity via resveratrol administration under LOW conditions these levels did not reach those observed under NOR conditions nor did we detect any

improvement in morphological differentiation via myotube number analysis, discussed above. There was also no significant difference present following the administration of EX-527 compared to LOW glucose alone conditions at 48 h (LOW EX-527 vs. LOW: 38.87 ± 25.25 vs. 26.47 ± 18.39 , $p > 0.05$) or 7D (LOW EX-527 vs. LOW: 22.1 ± 10.1 vs. 16.82 ± 15.95 , $p > 0.05$). At 72 h, however there was a significant reduction in CK under the EX-527 conditions (LOW EX-527 vs. LOW: 22.1 ± 10.1 vs. 16.82 ± 15.95 , $p = 0.019$ (fisher)). This is indicative of a complete loss of differentiation under EX-527 administration following 72 h. SIRT activation improved CK activity at 7 days. These findings confirm a role for SIRT1 in differentiation in the presence of nutrient stress, albeit SIRT1 activation was unable to return differentiation back to control levels.

We observed no significant differences when resveratrol was administered in the presence of MED glucose alone at any of the time points analysed (MED RES vs. MED; 48 h: 60.09 ± 21.36 vs. 54.65 ± 30.00 , $p > 0.05$, 72 h: 39.83 ± 22.20 vs. 21.71 ± 17.93 , $p > 0.05$, 7D: 14.4 ± 79.6 vs. 44.4 ± 27.14 , $p > 0.05$). Nor was there any significance present following EX-527 administration under MED conditions (MED vs. MED EX-527: 48 h: 60.09 ± 21.36 vs. 61.08 ± 23.85 , $p > 0.05$, 72 h: 21.71 ± 17.93 vs. 43.6 ± 42.2 , $p > 0.05$, 7D: 44.4 ± 27.14 vs. 69.3 ± 12.3 , $p > 0.05$). As with the MED glucose alone condition there was also no significant difference present under NOR conditions at any time point when supplemented with either RES (NOR vs. NOR RES; 48 h: 98.68 ± 29.56 vs. 92.8 ± 42.8 , $p > 0.05$, 72 h: 98.91 ± 32.39 vs. 88.8 ± 36.7 , $p > 0.05$, 7D: 139.56 ± 22.17 vs. 132.9 ± 30.08 , $p > 0.05$) or EX-527 (NOR vs. NOR EX-527; 48 h: 98.68 ± 29.56 vs. 99.2 ± 49.8 , $p > 0.05$, 72 h: 98.91 ± 32.39 vs. 85.2 ± 43.3 , $p > 0.05$, 7D: 139.56 ± 22.17 vs. 110.1 ± 48.8 , $p > 0.05$).

Therefore overall, while there was increased CK activity in LOW glucose conditions in the presence of RES (Fig. 5.3), there was no increase in morphological differentiation/myotube number in these conditions (Fig

5.1.). This may suggest that CK may not be a relevant marker of differentiation in this instance and may perhaps be more a marker of potential differentiation when in a larger cell population. If this is the case it would suggest that SIRT1 activation via resveratrol administration maybe increasing CK activity in an attempt to initiate differentiation in LOW glucose, without leading to successful forming myotubes observable at the morphological level. However, SIRT inhibition via EX-527 administration in low glucose conditions at 72 h did lead to a complete loss of CK activity vs. low glucose alone and RES conditions. Finally, SIRT1 activation via resveratrol seems to be unable to improve reduced differentiation observed in MED glucose conditions and surprisingly both activation and inhibition of SIRT1 via resveratrol and EX-527 administration was actually detrimental to myotube formation/number and CK activity in normal glucose conditions (albeit lowest myotube formation was observed with SIRT1 inhibition vs. RES MED glucose alone).

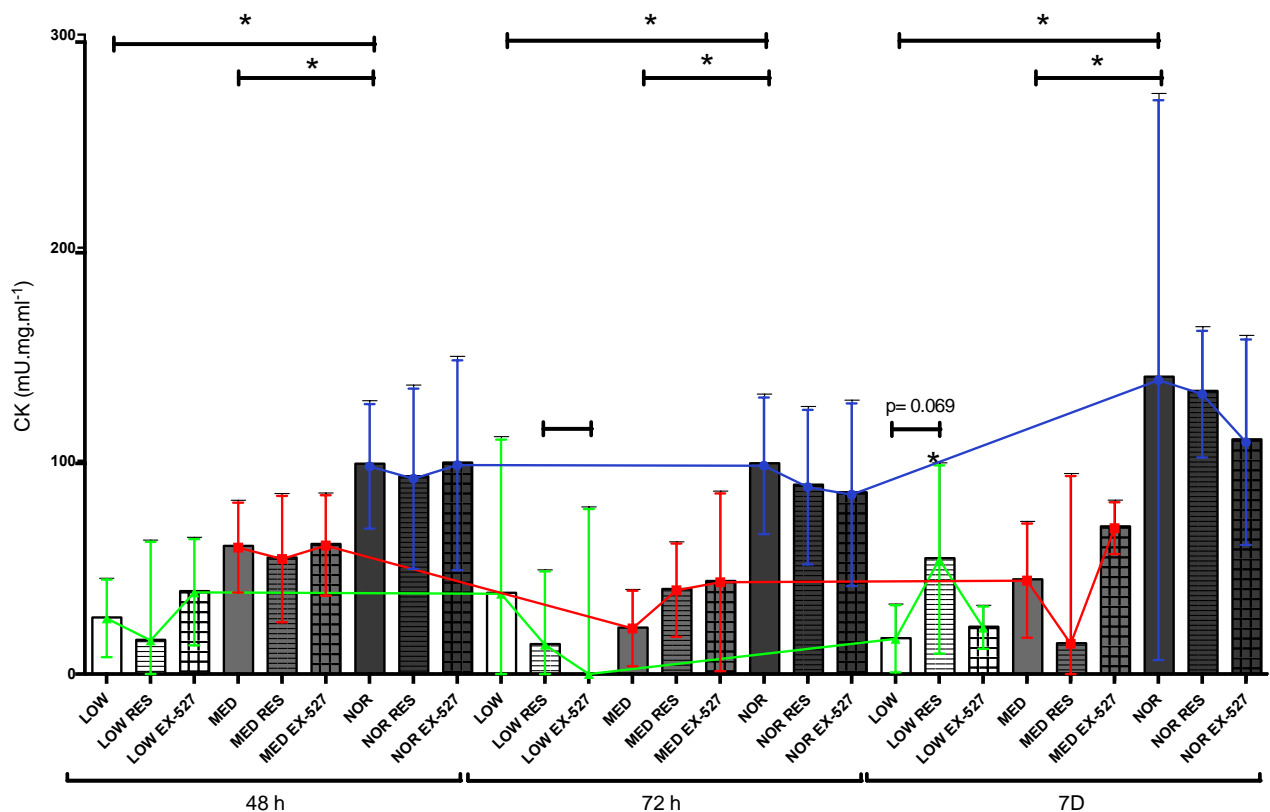


Fig 5.3. CK measurements of myoblasts undergoing differentiation under three different glucose conditions, with and without SIRT1 manipulation. As expected NOR glucose was significantly higher CK activity than the LOW and MED glucose concentrations at all time points. SIRT1 significantly increased CK activity in LOW glucose conditions at 7D, however this was without an increase in morphological myotube formation (Figure above 5.1). Means and SD displayed. $p < 0.05$ is depicted by *. If approaching significance p value is stated.

5.3.3 Myotube size increased with resveratrol administration in NOR glucose conditions.

There was no significant difference present for myotube size at 72 h for any condition within MED and NOR glucose conditions, readily observed in figure 5.4. Additionally, there was no significant difference following 7D in either MED or NOR conditions following the addition of EX-527 (All comparisons, $p > 0.05$). Myotubes were however significantly larger under NOR conditions with the addition of RES compared to the addition of EX-527 (5718.00 ± 3532.00 vs. 4142.00 ± 1873.00 , $p = 0.021$) and compared

to NOR glucose alone (NOR RES vs. NOR: 5718.00 ± 3532.00 vs. 4551.00 ± 2836.00 , $p = 0.044$, Fig 5.4.).

Myotube diameter displayed a significant main effect for glucose condition ($F_{(1, 281)} = 18.01$, $p < 0.005$), but no other main effect or interaction was present. Additionally, there was no significant change in diameter following the addition of either RES or EX-527 in either MED or NOR glucose conditions. As there were no observable myotubes in low glucose conditions as previously suggested this analysis was unavailable in these conditions.

Therefore, although there were reductions in myotube number (Fig 5.2) and CK activity (Fig. 5.3) in the presence of RES in normal glucose conditions suggesting that RES actually impaired differentiation/myotube formation in these conditions (Fig. 5.4.). Resveratrol treatment actually increased myotube hypertrophy in normal glucose conditions shown by increases in myotube size, but not diameter, suggesting that while RES reduced myotube formation it increased the size of myotubes that were still present, potentially due to an increased length of myotubes (given that diameter did not increase and overall size did increase) (Fig. 5.4.).

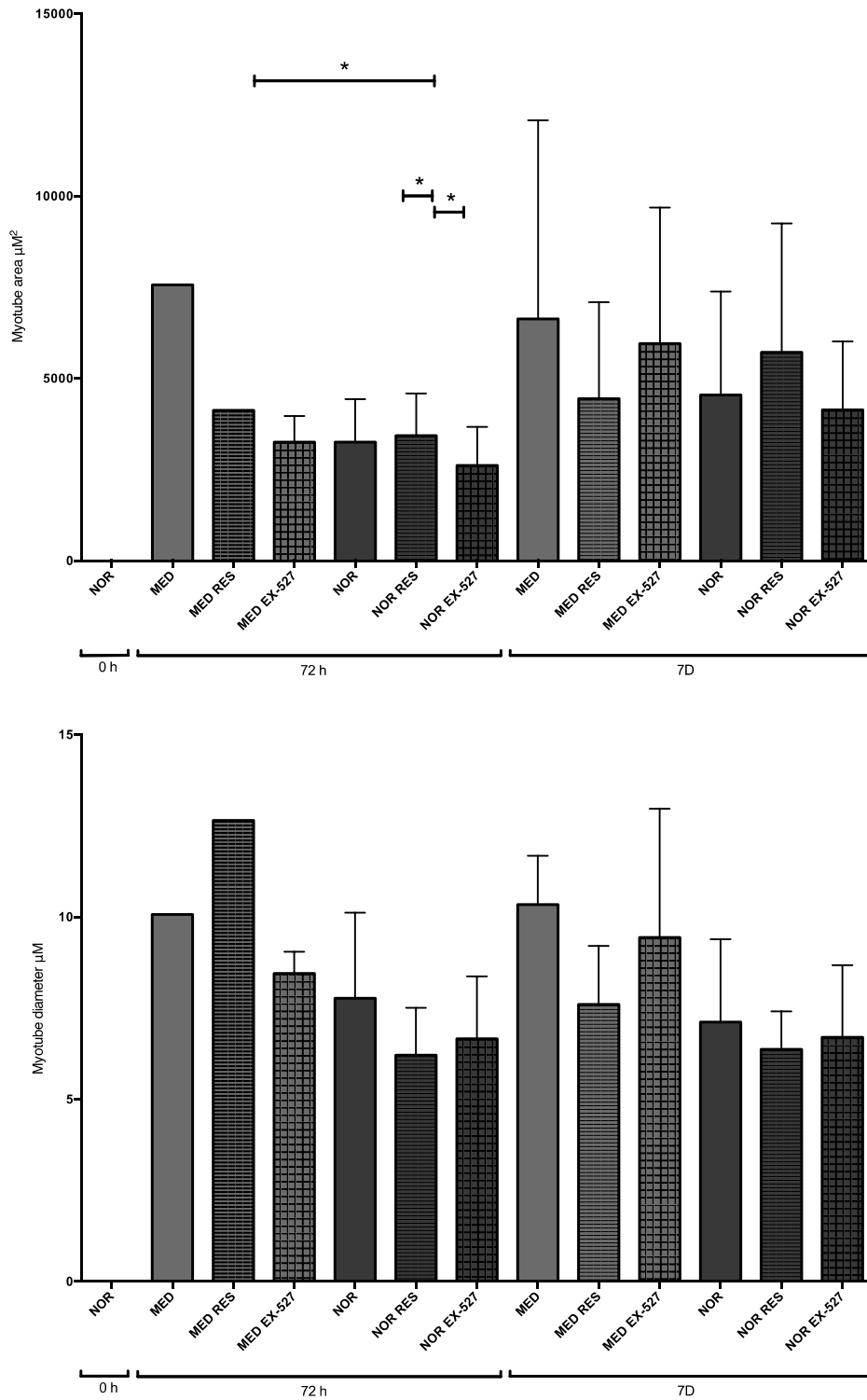


Fig. 5.4. Graph A: Myotube area was significantly increased following the administration of RES in the NOR condition compared to NOR alone and EX-527 supplementation. Additionally NOR RES also increased over time from 72 h and 7D. Graph B: No change was observed in myotube diameter. Significant difference ($p < 0.05$) is denoted using a *.

5.3.4. MRF's are unaltered following SIRT1 activation via resveratrol administration

In order to elucidate the molecular mechanisms for the increased/decreased differentiation/ CK activity we examined the role of myogenin (differentiation/myotube formation) and MRF4 (late myotube differentiation/myotube maturation). Myogenin had a significant main effect for both time ($F_{(3,54)} = 29.31$, $p < 0.001$) and glucose ($F_{(3,54)} = 36.87$, $p < 0.001$) as well as an interaction between the two ($F_{(6,54)} = 12.42$, $p = 0.004$, Figure 5.4). However, the addition of RES or EX-527 did not significantly effect myogenin expression at any time point for both the glucose restricted conditions; MED (all comparisons $p > 0.05$, Fig 5.4). In NOR glucose conditions however, the addition of both EX-527 and RES significantly decreased the expression of myogenin at 72 h (NOR vs. NOR RES: 29.68 ± 4.71 vs. 16.80 ± 20.80 , $p = 0.007$ (fisher), NOR vs. NOR EX-527: 29.68 ± 4.71 vs. 18.45 ± 6.46 , $p = 0.017$ (fisher)). This reduction in myogenin (Fig. 5.5.) corresponded with later reductions in myotube number by 7D (Fig 5.2) in these conditions. However, there was also an increase in myogenin in the presence of EX-527 at 7D, in which expression was significantly increased compared to NOR glucose alone at this time point (NOR vs. NOR EX-527: 21.60 ± 18.70 vs. 33.36 ± 0.33 , $p = 0.013$ (fisher)). RES however, induced no change in NOR conditions following 7D. Additionally NOR glucose with the addition of EX-527 also significantly increased over time, where expression was higher at 7D than at 72 h (7D vs. 72 h: 33.36 ± 0.33 vs. 18.45 ± 6.46 , $p = 0.002$ (fisher)). Overall however the myogenic regulatory factor, myogenin does not seem to be involved in the improvements in CK activity and differentiation with the addition of resveratrol in the low glucose conditions at 7D or increases in myotube size with RES in normal glucose conditions.

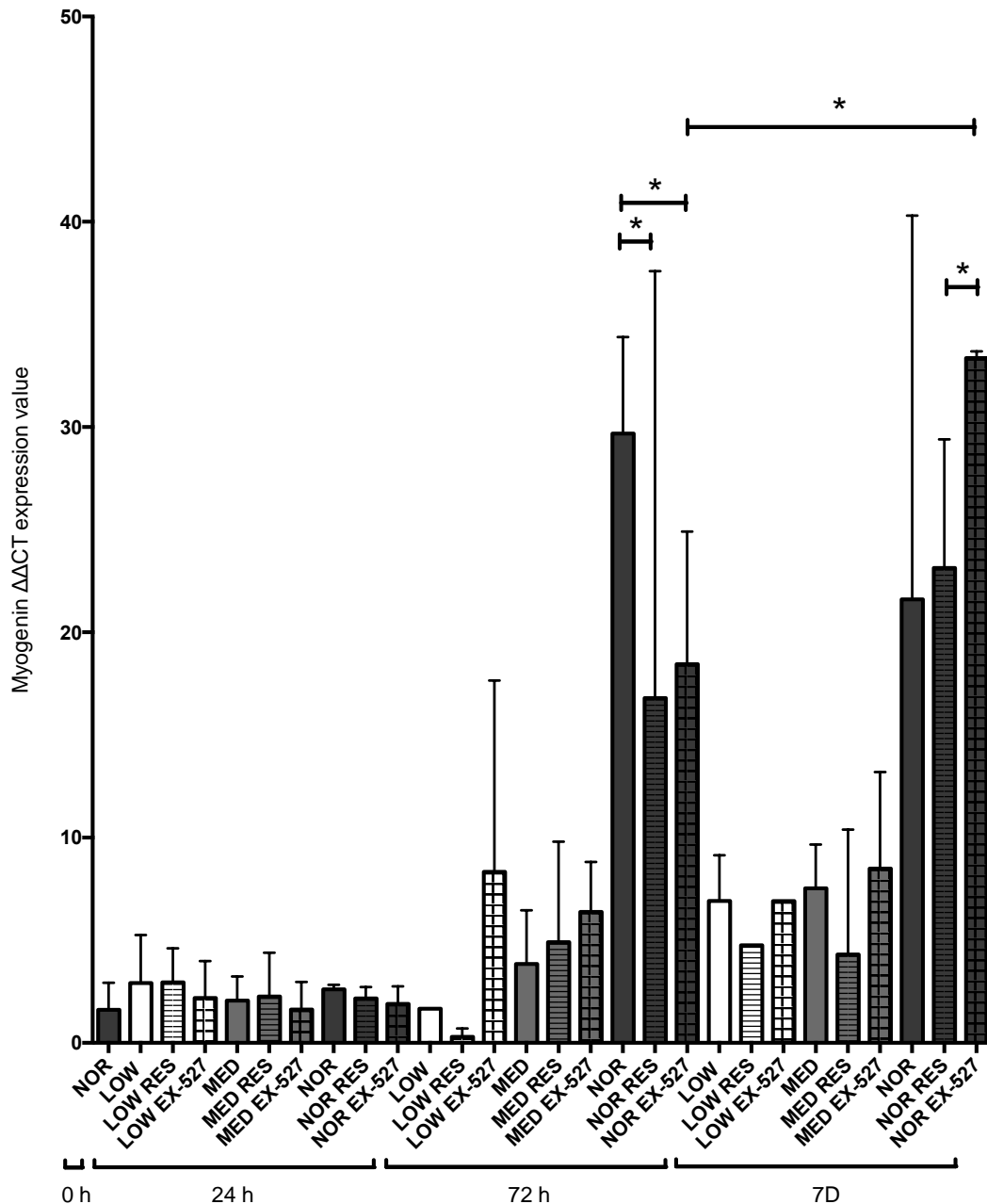


Fig. 5.5. Graph depicting means and SD's for gene expression for Myogenin. Myogenin in NOR glucose conditions in the presence of both RES and EX-527 was significantly decreased in comparison to NOR glucose alone at 72 h. Significant difference ($p < 0.05$) is denoted using a * .

There were also no significant differences in MRF4 expression with the addition of RES or EX-527 at any glucose concentration at 24 h and 72 h (all comparisons $p > 0.05$; Fig 5.6). Following 7D there was also no significant difference when SIRT1 was manipulated via resveratrol treatment in the NOR and the LOW conditions (all comparisons $p > 0.05$., Fig. 5.6.). The addition of EX-527 in MED conditions did not significantly

change MRF4 expression following 7D (MED vs. MED EX-527: 1.02 ± 1.38 vs. 5.70 ± 4.83 , $p > 0.05$). Unexpectedly, MRF4 in MED glucose conditions was however increased under RES conditions in comparison to MED glucose alone (MED vs. MED RES: 1.02 ± 1.38 vs. 58.70 ± 79.30 , $p < 0.001$ (fisher)), however, large standard deviations were observed in this condition and is therefore unlikely to be an accurate representation of expression in this condition.

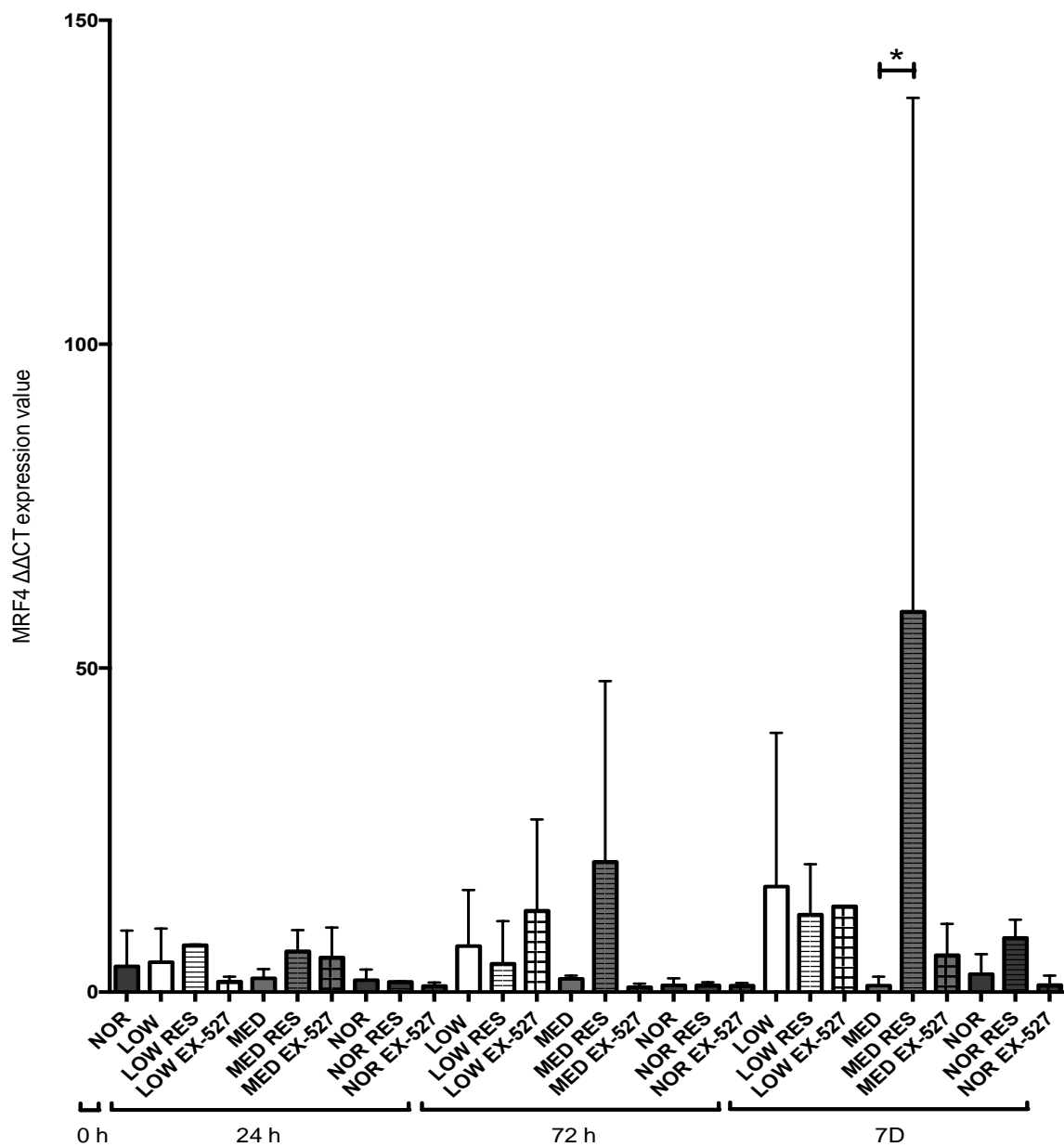


Fig. 5.6 Graph depicting means and SD's for gene expression for MRF4. Significant difference ($p < 0.05$) is denoted using a * .

5.3.5. Resveratrol administration increased MYHC7 and MYHC4 gene expression in NOR glucose conditions.

With an increase in myotube hypertrophy/size with resveratrol in normal glucose conditions and after observing a reduction in MYHCs with myotube atrophy under MED and LOW glucose concentrations in Chapter 3. The gene expression of MYHC's was assessed in order to analyse whether there was potentially increased contractile protein mRNA being transcribed in RES conditions that would subsequently lead to increased myotube protein content and hypertrophy and if there was a preference of either slow or fast MYHC's. Gene expression of the MYHC's within the muscle cells changed over time, suggested via a significant main effect for time for all MYHC measured including: MYHC7 (transcript coding for slow type I protein isoform) ($F_{(3,51)} = 8.95$, $p < 0.001$), MYHC2 (IIa) ($F_{(3,59)} = 9.32$, $p < 0.001$), MYHC4 (IIb) ($F_{(3,57)} = 23.90$, $p < 0.001$), MYHC1 (IIx) ($F_{(3,63)} = 33.83$, $p < 0.001$).

Following 72 h there was no significant difference in MYH7 (slow type I) gene expression in any glucose dose condition supplemented with either RES or EX-527 (all comparisons $p > 0.05$, Fig. 5.7). The 7D time point revealed similar results for the LOW glucose condition in which there was no significant difference with the addition of RES or EX-527 (all comparisons $p > 0.05$, Fig. 5.6). The SIRT1 inhibitor however, significantly reduced the MYHC7 gene expression within the MED glucose condition at the same time point (MED vs. MED EX-527: 58.90 ± 69.20 vs. 14.30 ± 18.40 , $p = 0.019$ (fisher)). EX-527 did not however, significantly affect the MYHC7 expression under NOR glucose conditions ($p > 0.05$). Importantly, the only significant increase in expression following RES administration was observed under the NOR glucose condition (NOR vs. NOR RES: 10.53 ± 9.84 vs. 77.50 ± 102.40 , $p = 0.002$ (fisher)) suggesting an increase in MYHC7 slow type I gene expression was present under these conditions that corresponded with an increase in myotube area/hypertrophy under these conditions at 7D. As described in chapter 3,

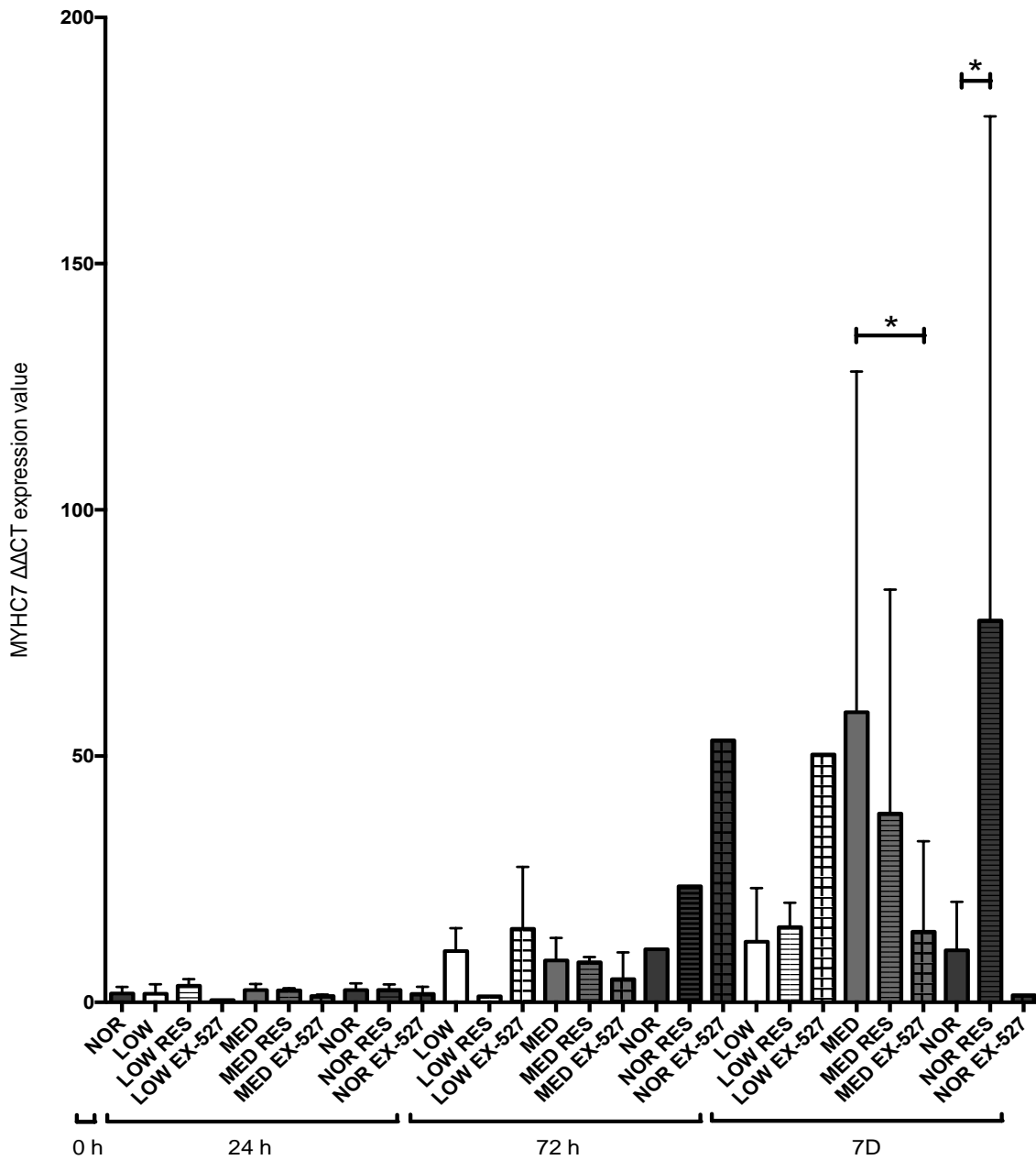


Fig. 5.7. Graph depicting means and SD's for gene expression for: MYHC7. Gene expression under NOR RES conditions was significantly increased in comparison to NOR alone at 7D. Significant difference ($p < 0.05$) is denoted using a *.

MYHC2 (type IIa) showed no significant differences in any condition (all comparisons, $p > 0.05$). (Fig. 5.8.).

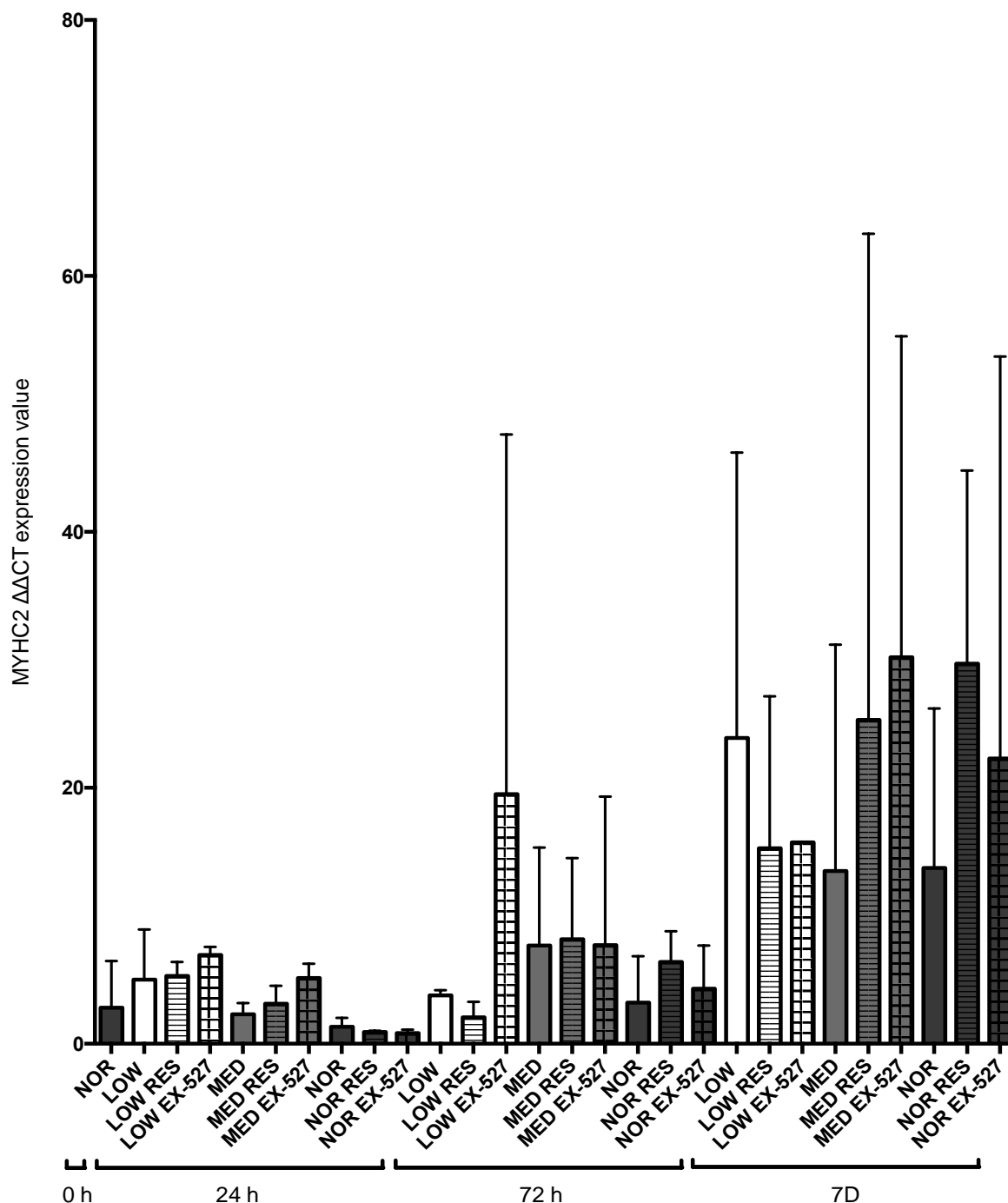


Fig. 5.8. Graph depicting means and SD's for gene expression for: MYHC2., in which no significant interactions were observed

In addition to the above reported significant main effect for time, MYHC4 (type IIb) also displayed a significant main effect for glucose ($F_{(2,57)} = 4.77$, $p = 0.012$) as well as a significant interaction between time and glucose ($F_{(6,57)} = 4.38$, $p = 0.001$). There were no significant individual differences between any of the glucose conditions and the addition of RES or EX-527 at 24 h or 72 h (all comparisons $p > 0.05$, Fig. 5.9). In LOW and MED

glucose conditions no significant differences were observed following 7D conditions following the addition of resveratrol. In LOW glucose conditions the addition of EX-527 was also non-significant (all comparisons $p > 0.05$). There was a significant increase in MYHC4 expression with EX-527 supplementation in MED conditions at 7D (MED vs. MED EX-527: 36.20 ± 42.20 vs. 79.90 ± 51.10 , $p = 0.048$ (fisher)). This confirms the morphology findings in which myotube number was increased in MED EX-527 in comparison to MED alone. Myotube number was also reduced in MED RES in comparison to MED EX-527, again MYHC4 expression mirrored these findings (29.60 ± 32.80 vs. 79.90 ± 51.10 , $p = 0.024$). Contrary to the findings observed for MED glucose the NOR condition displays no significance with the addition of EX-527 ($p > 0.05$). However, MYHC4 expression was increased in NOR RES conditions in comparison to NOR EX-527 (172.40 ± 111.80 vs. 87.70 ± 123.90 , $p = 0.002$ (fisher)), these findings complement those observed in morphological data in which area was also increased under the supplementation of RES in comparison to EX-527 supplementation. MYHC4 expression in NOR conditions supplemented with RES is also significantly increased in the presence of NOR glucose (NOR vs. NOR RES: 67.90 ± 19.20 vs. 172.40 ± 111.80 , $p < 0.001$ (fisher)). These findings corroborate the morphological findings in which myotube area was increased following RES administration in NOR glucose.

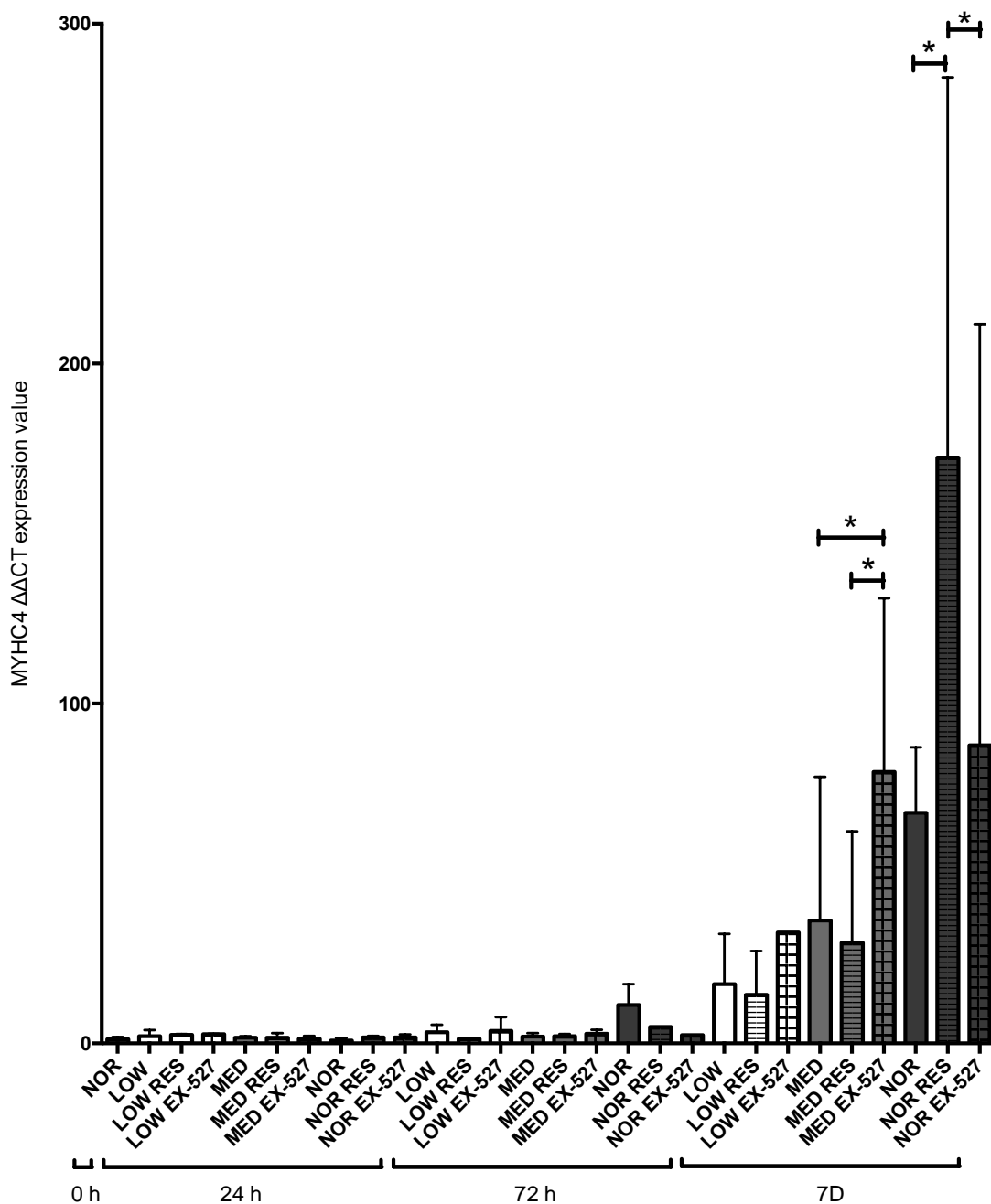


Fig. 5.9. Graph depicting means and SD's for gene expression for: MYHC4. RES in NORM glucose conditions was significantly increased compared to NOR alone and vs. NOR with the addition of EX-527 at 7D. Significant difference ($p < 0.05$) is denoted using a *.

Similarly to the MYHC4 data above there was a significant main effect for glucose dose ($F_{(2,63)} = 22.74$, $p < 0.001$) present for MYHC1 (type IIx), as well as a significant interaction between time and glucose dose ($F_{(6,63)} =$

12.24, $p < 0.001$; Fig. 5.9). Comparisons of individual experimental conditions revealed no significant differences with the addition of RES or EX-527 for 24 h and 72 h (all comparisons $p > 0.05$, Fig. 5.10.). Following 7D there was also no significant differences in MYHC1 between MED or LOW glucose conditions (all comparisons $p > 0.05$). Resveratrol increased MYHC1 on average in NOR glucose conditions however, they were not significant different to NOR alone (NOR vs. NOR RES: 212.40 ± 120.40 vs. 242.20 ± 57.00 , $p > 0.05$). There was however, a significant reduction in MYHC1 with EX-527 in NOR glucose conditions (NOR vs. NOR EX527: 212.40 ± 120.40 vs. 123.00 ± 174.00 , $p = 0.008$ (fisher)).

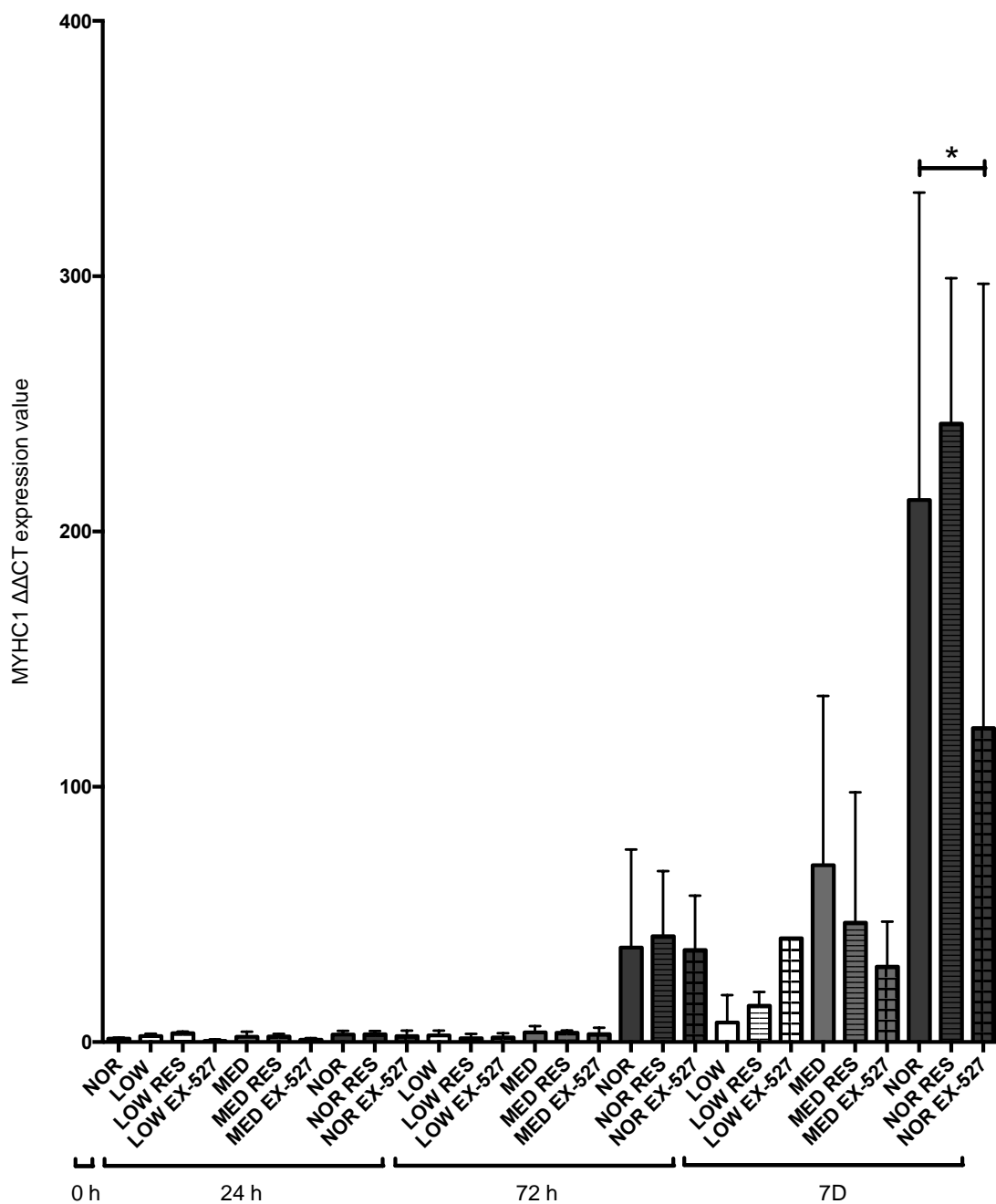


Fig. 5.10. Graph depicting means and SD's for gene expression for: MYHC1. Gene expression under NOR EX-527 conditions was significantly reduced in comparison to NOR alone and NOR RES at 7D. Significant difference ($p < 0.05$) is denoted using a *.

These data suggest that the activation of SIRT1 via RES administration in NOR glucose conditions perhaps evokes increases in both MYHC7 and MYHC4 gene transcripts coding for slow type 1 and fast IIb protein MYHC

isoforms in order to improve myotube hypertrophy as observed here by an increase in myotube size. Furthermore, SIRT inhibitor conditions suggest that MYHC1 gene transcript coding for fast IIx protein MYHC isoforms is reduced and therefore normal SIRT activity is perhaps important to maintain adequate fast IIx isoform gene expression. Having said this, MYHC changes do not seem to be involved in the improved differentiation/CK activity observed with resveratrol administration in LOW glucose conditions at 7 days.

5.3.6. SIRT1 is reduced in all conditions following 7D and GCN5 remains unchanged under most experimental conditions.

SIRT1 gene expression possessed a significant interaction for time, glucose concentration and SIRT1 manipulation ($F_{(12,50)} = 1.83$, $p = 0.069$). Additionally, a significant interaction was present between time and glucose ($F_{(6,50)} = 3.58$, $p = 0.005$) and a significant main effect for time alone ($F_{(3,50)} = 31.02$, $p < 0.001$; Fig 5.10). Interestingly, in NOR, MED and LOW conditions there was a drop in SIRT1 gene expression over the timecourse (observed by a significant main effect of time). Further, EX-527 reduced SIRT1 gene expression in NOR and MED conditions over time (NOR EX-527: 24 h vs. 72 h: 0.72 ± 0.05 vs. 0.18 ± 0.04 , $p = 0.028$ (fisher) and DM 0 h vs. MED EX-527 24 h: 1.01 ± 0.04 vs. 0.47 ± 0.31 , $p = 0.012$ (fisher). Where, MED EX-527 glucose conditions demonstrated the lowest reduction at 72hrs vs. NOR EX-527 (0.77 ± 0.09 vs. 0.21 ± 0.00). There was however no observed effect of SIRT1 activation or inhibition via resveratrol and EX-527 administration respectively in normal or MED glucose conditions within time points of 24 h, 72 h and 7d (All comparisons $p > 0.05$, Fig 5.11).

Finally, as observed in chapter 3 in LOW glucose conditions alone there was an average increase vs. NOR and MED glucose alone conditions across the timecourse (24 h: LOW: 0.56 ± 0.23 vs. MED: 0.60 ± 0.21 vs. NOR: 1.00 ± 0.53 , 72 h: LOW : 1.34 ± 1.06 vs. MED: 0.75 ± 0.38 vs. NOR: 0.39 ± 0.14 , 7D: LOW : 0.18 ± 0.00 vs. MED: 0.09 ± 0.01 vs.

NOR: 0.11 ± 0.00 , all comparisons, $p > 0.05$), however the data presented here failed to reach significance due to large standard deviations in the LOW glucose condition. Furthermore, there was no difference in SIRT1 gene expression in LOW glucose conditions with the addition of RES or EX-527 at 24 h, 72h and 7D (all comparisons, $p > 0.05$). Overall, therefore the supplementation of RES or EX-527 did not significantly change SIRT1 expression values for NOR, MED or LOW glucose.

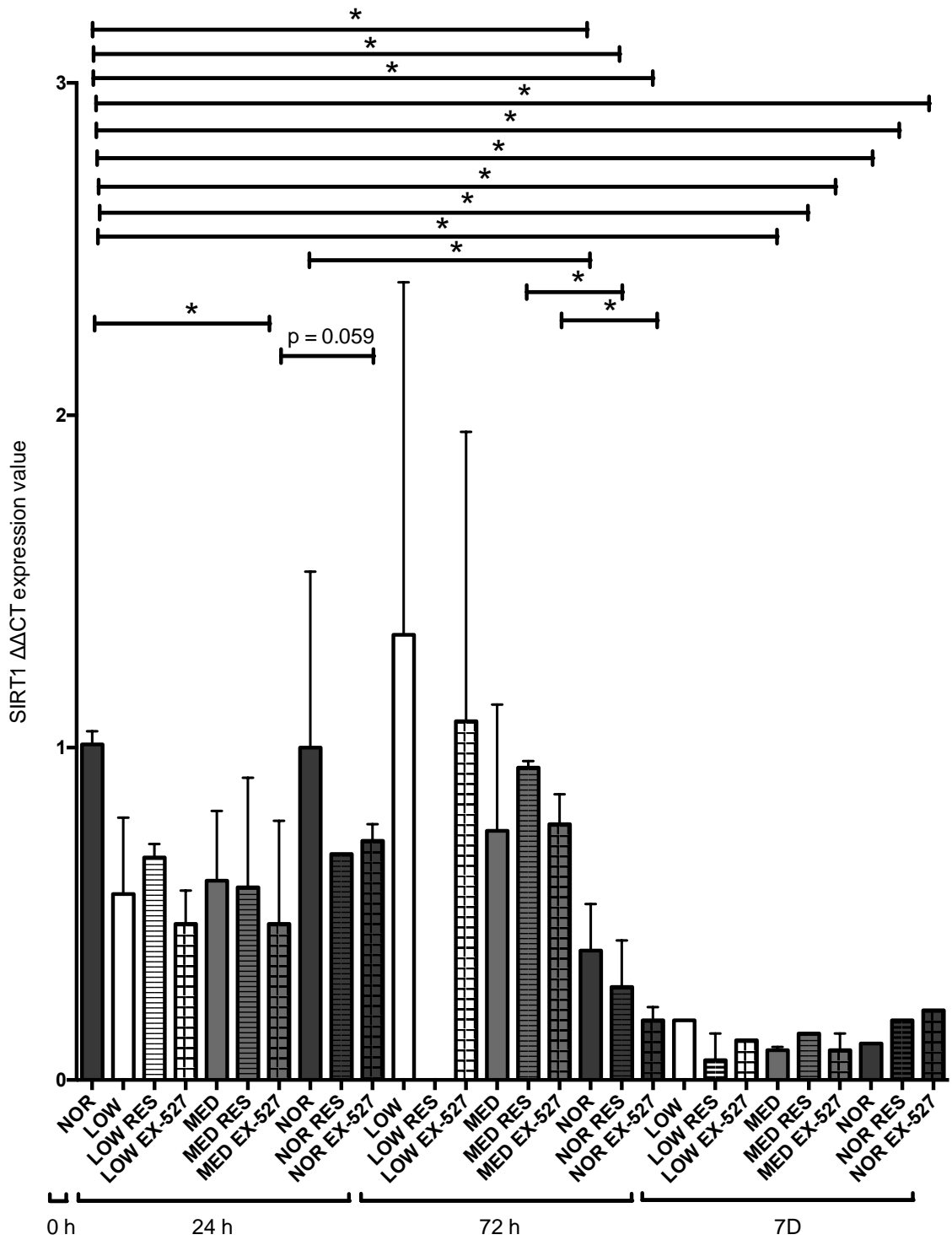


Fig. 5.11. Graph depicting means and SD's for gene expression for SIRT1. Significant difference ($p < 0.05$) is denoted using a *.

5.4. Summary

In this chapter we aimed to activate or inhibit SIRT1 activity under MED, LOW and NOR glucose conditions in differentiating myoblasts. We hypothesised that SIRT1 activation (Chapter 4) may ameliorate the blocked and reduced differentiation capacity observed under LOW and MED conditions respectively (observed in chapter 3). Overall, we partially rejected our hypothesis in that while there was increased CK activity indicative of increased differentiation in LOW glucose conditions in the presence of resveratrol, the SIRT1 activator was unable to prevent the block on morphological differentiation in low glucose conditions. This suggested that SIRT1 activation via resveratrol administration maybe increasing CK activity in an attempt to initiate differentiation in LOW glucose. Due to the small number of viable cells however, there is a lack of proximity to allow fusion to take place thus this increase in CK does not lead to the successful myotube formation observable at the morphological level.

It is worth mentioning that SIRT inhibition via EX-527 administration in low glucose conditions at 72 h did lead to a complete loss of CK activity vs. low glucose alone and RES conditions. NOR glucose conditions SIRT1 inhibition produced the lowest number of myotubes vs. resveratrol and control conditions at 7D, suggesting that normal SIRT1 activity was required to enable normal CK activity in low glucose conditions and basal myotube formation in normal glucose conditions. Furthermore, SIRT1 activation via resveratrol was unable to improve the impaired differentiation observed in MED glucose conditions (therefore rejecting the original hypothesis). Both activation and inhibition of SIRT1 via resveratrol and EX-527 respectively was detrimental to myotube formation/number, CK activity in normal glucose conditions (albeit lowest absolute myotube formation was observed with SIRT1 inhibition vs. RES/MED glucose alone). Surprisingly, inhibition of SIRT1 via EX-527 caused an increase in

myotube number, a finding that was unexpected and warrants future investigation.

The most unexpected and important finding in this study was that while the addition of both RES and EX-527 impaired CK activity, myogenin expression and formation of myotubes in NOR glucose conditions, in the myotubes that were still present resveratrol evoked an increase in myotube size/hypertrophy. This observation also corresponded with an increase in MYHC7 gene expression MYHC4 coding for the slow type I and fast IIb MYHC protein isoforms respectively. These data suggest that this adaptation following increased SIRT1 activity via resveratrol administration is perhaps responsible for the increased myotube size observed via the increased laying down of these contractile proteins. Furthermore, SIRT inhibitor conditions suggest that MYHC1 coding for the fast IIx MYHC protein isoform is reduced in normal glucose conditions and therefore suggests that normal SIRT activity is perhaps important to maintain adequate fast isoform gene expression. Having said this, MYHC changes do not seem to be involved in the improved differentiation/CK activity observed in LOW glucose conditions at 7D, which is partly expected as despite increases in CK activity this did not result in increased myotube formation.

5.4.1. Future directions for chapter 6

RES did not improve differentiation as we had previously hypothesized. There was however a beneficial increase in CK activity appears to be an indicator of differentiation potential rather than a quantifier of differentiation. As such regardless of this increase improvement in differentiation under LOW glucose conditions was present. This is potentially due to the limited cell population still present not being in close proximity to each other making fusion difficult. Therefore, in the next chapter we wished to examine the role of SIRT1 activation/inhibition in LOW and NORM glucose conditions on existing myotube cultures. The reasons for this were threefold; 1) because low glucose completely blocks myotube formation

(chapter 3), yet resveratrol does drive increases in CK activity despite no improvement in myotube formation in these conditions it is feasible that in the presence of existing myotubes, resveratrol may prevent myotube atrophy; 2) myotube cultures are perhaps more indicative of *in-vivo* tissue where myofibres already exist rather than differentiating myoblasts creating primary myotubes which more closely mimics development/regeneration; 3) and we would like to ascertain whether the increases in myotube hypertrophy are also observed in existing myotubes. In addition SIRT1 activation via resveratrol treatment in normal glucose concentrations increased myotube hypertrophy together with elevated slow type 1 MYHC (7) and type IIb MYHC4 gene expression.

Chapter 6

6. Resveratrol reduces acute myotube atrophy with glucose restriction

6.1. Introduction

In the previous chapter we determined the advantageous effects present following SIRT1 activation via resveratrol administration in LOW glucose conditions. This consisted of an increase in CK activity despite an inability to ameliorate the lack of differentiation capacity under LOW glucose observed in chapter 3. In addition to these findings we also observed an increase in myotube hypertrophy in NOR glucose conditions which was coupled with an elevation in slow type 1, MYHC7 and type IIb MYHC4 gene expression. We therefore aimed in the following chapter to ascertain the role of SIRT1 activation/ inhibition in LOW and NOR glucose conditions on mature myotubes. We hypothesised that activation of SIRT1 may reduce myotube atrophy observed in nutrient (LOW glucose) restricted conditions and that resveratrol may accentuate hypertrophy myotubes in normal glucose conditions.

6.2. Methods

6.2.1. Cell culture and treatments

6well plates were pre-treated with 0.2% porcine gelatine for 10 min at room temperature (RT) and 10 min in a humidified, 37°C with 5% CO₂. The excess gelatine was aspirated and cells were seeded at 8 x 10⁴ cells/ml in 2 ml of GM per well, these were then incubated until 80% confluence. Cells were washed in PBS and transferred into 2 ml of normal glucose DM in 37°C at 5% CO₂ for 7D in order to differentiate. Once existing myotubes had been formed over 7D in DM, cells were dosed in the below experimental conditions for a further 72 h (total 10 days in

culture) to assess the impact of the activation/inhibition of SIRT1 in nutrient restriction on existing myotubes: LOW (0.5 g/L glucose); NOR (4.5 g/L glucose); LOW + Resveratrol (RES) (0.5 g/L glucose + 10 μ M RES), MED + RES (1.125 g/L glucose + 10 μ M RES), NOR + RES (4.5 g/L glucose + 10 μ M RES); LOW + SIRT1 inhibitor (EX-527) (0.5 g/L glucose + 100 nM EX-527); MED + EX-527 (1.125 g/L glucose + 100 nM EX-527) or NOR + EX-527 (4.5 g/L glucose + 100 nM EX-527). Morphological analysis of myotube number, diameter and area were both performed at 0 and 72 h initially and then at 24 and 48 h for additional analysis (see results section). For these experiments the 0 hours baseline control condition was 30 minutes in NOR glucose (DM 0 h). Protein activity of AMPK and p70s6K were completed at 0, 15 min, 30 min, 2 h and 24 h time points after dosing in order to investigate energy sensing vs. protein synthetic/growth associated cellular signalling in myotubes. Gene expression for later differentiation and myotube maturation (MRF4, MYHC1, 2, 4, 7) and genes associated with myotube hypertrophy (IGF-I, IGF-IR, IGF-II, IGF-IIR, IGFBP2, mTOR) and myotube atrophy (TNF- α , myostatin, MuRF, MAFbx, MUSA1, FOXO1, 3, NF-kB, p53) as well as SIRT1 gene expression were completed at 0, 72hrs, with targeted gene expression based on the results from 72 h data were followed up to investigate changes at 24 h (see results below). Precise methods for morphological analysis, gene expression (RT-PCR) and cell signalling (western blotting) can be located in the methods section in chapter 2.

6.2.2. Statistical analysis

All data was performed using three separate cell populations thus performed N=3. Analysis was then carried out using Minitab® 17 (Minitab Ltd, Coventry U.K). Outliers were removed using Grubbs outlier test. All data was parametric, assessed using the Anderson-Darling test for normality. General linear models (2 x 2 x 3) for time (0, 72 h), glucose concentration (LOW, NOR) and SIRT1 activation/inhibition (DM, RES, EX-527) were carried out for morphological analysis of myotube number, area and diameter for the 72 h data. Morphological analysis for the additional

24 and 48 h data was also performed using a general linear model (2 x 3 x 3) for time (0, 24 and 48 h), glucose concentration (LOW, NORM) and SIRT1 activation/inhibition (DM, RES, EX-527). Gene expression data for both the 72 h and 24 h data was performed using a general linear model (2 x 2 x 3) for time (0, 72 h or 0, 24 h), glucose concentration (LOW, NOR) and SIRT1 activation/inhibition (DM, RES, EX-527). A general linear model for glucose (LOW , NOR) and SIRT1 activation/inhibition (DM, RES, EX-527) was performed for protein activity. Post hoc tests were performed using Bonferroni, Tukey and Fisher. The results produced through the Bonferroni tests are reported throughout results unless otherwise stated.

6.3. Results

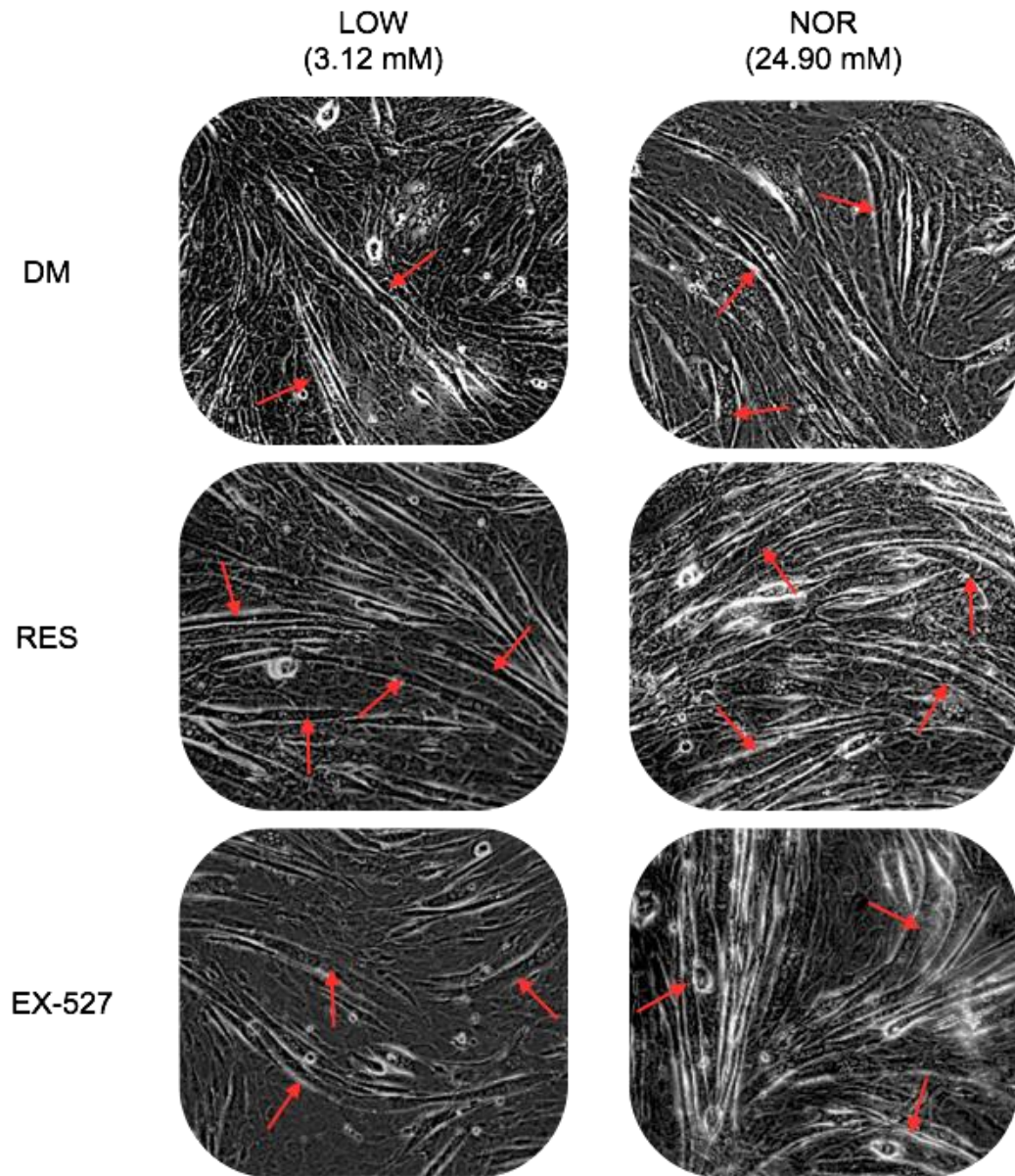


Fig. 6.1. Representative images following 24 h in LOW and NOR glucose alone and with the addition of RES or EX-527.

6.3.7. Myotube diameter and area were increased in LOW glucose conditions at 24 h after resveratrol supplementation.

Following myotube imaging (Fig 6.1.) further analysis observed reduced myotube number under EX-527 supplementation following 24 and 48 h (24 h: NOR vs. NOR EX-527: 10.69 ± 3.81 vs. 8.58 ± 3.71 , $p = 0.004$ (fisher), 48 h: NOR vs. NOR EX-527: 10.95 ± 3.15 vs. 9.48 ± 2.68 , $p = 0.046$

(fisher)). Resveratrol was unable to improve myotube number in any NOR glucose condition or timepoint, as well as any LOW glucose condition ($p > 0.005$) (Fig. 6.2.). Following 48 h in NOR conditions RES supplementation not only did not improve number but it produced a negative affect in which myotube number was reduced (NOR vs. NOR RES: 10.95 ± 3.15 vs. 9.43 ± 2.90 , $p = 0.039$ (fisher)).

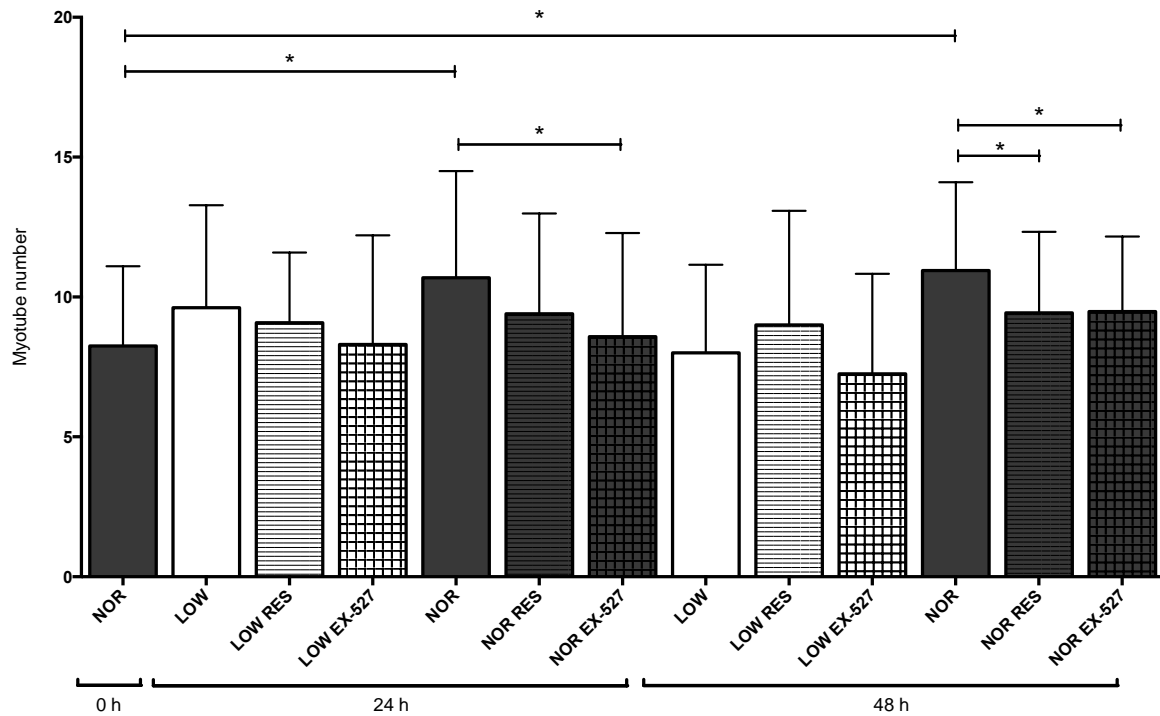


Fig. 6.2. Mean and SD of Myotube number is represented above. Myotube number declined in NOR conditions due to the supplementation of EX-527. No improvements in myotube number were observed following RES administration. Significant difference ($p < 0.05$) is denoted using *.

Myotube diameter remained unaffected at 24 h and 48 h in NOR conditions following the supplementation of both RES and EX-527. Resveratrol had no effect at the later time point on LOW glucose at 48 h (LOW vs. LOW RES: 13.48 ± 4.11 vs. 13.50 ± 4.75 μM , $p > 0.05$). EX-527 also had no significant effect on myotube diameter at 48 h and at 24 h in either NOR nor LOW glucose conditions ($p > 0.05$) (Fig 6.3.). Importantly, at 24 h RES significantly increased myotube diameter in LOW glucose condition (LOW RES vs. LOW: 13.23 ± 4.12 vs. 12.47 ± 4.05 μM , $p = 0.022$ (fisher)).

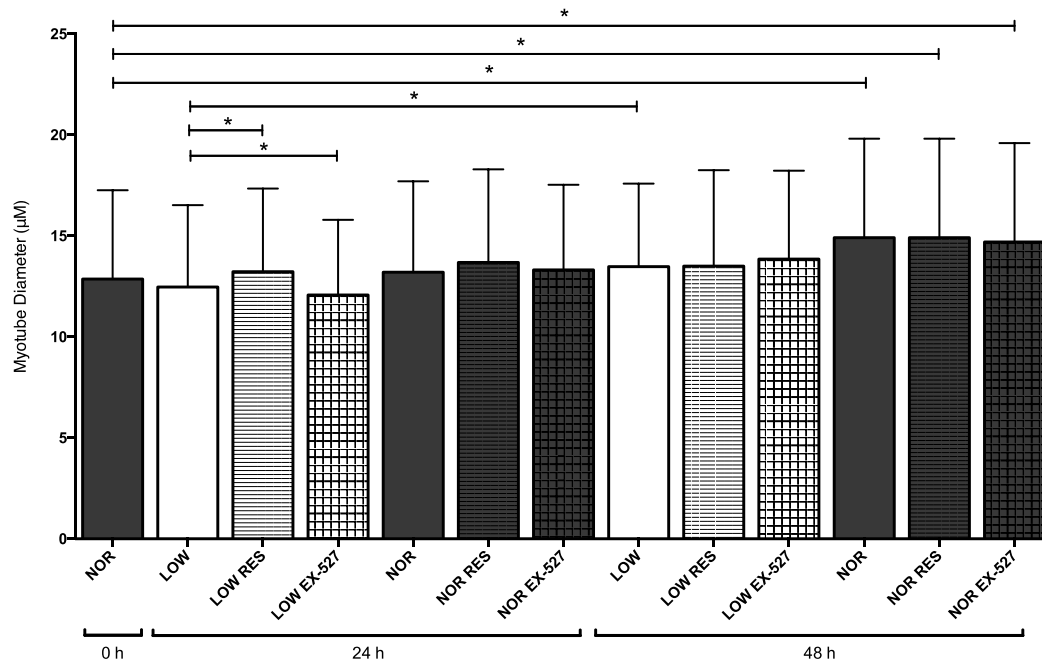


Fig. 6.3. Myotube diameter increased over time, however only RES supplementation increase diameter at 24 h whereas EX-527 decreased myotube diameter. Significant difference ($p < 0.05$) is denoted using *.

Importantly, under both LOW and NOR conditions at the 24 h timepoint the supplementation of RES significantly increased myotube area (LOW vs. LOW RES: 2635 ± 1524 vs. $3474 \pm 2235 \mu\text{M}^2$, $p < 0.001$, NOR vs. NOR RES: 2835 ± 1959 vs. $3454 \pm 2110 \mu\text{M}^2$, $p = 0.009$). As with the diameter data above, RES did not improve area at 48 h in low glucose conditions (Fig. 6.4.). Also, as with the data presented above at the 72 h timepoint, RES administration also increased myotube size in NOR glucose conditions at 48 h (NOR vs. NOR RES: 2835.20 ± 1959.40 vs. $3858.00 \pm 2800.00 \mu\text{M}^2$, $p = 0.023$ (fisher)) (Fig. 6.4.). The addition of EX-527 had no significant affect on myotube area following 24 h and 48 h for NOR nor LOW glucose conditions ($p > 0.05$).

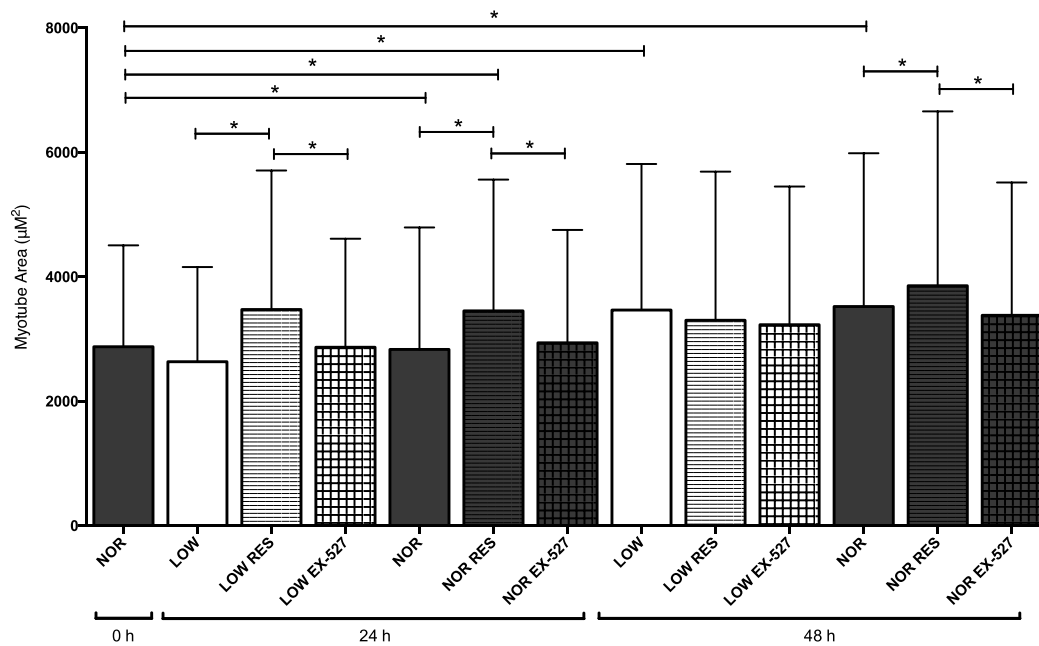


Fig. 6.4 Myotube area is increase by the supplementation of RES in NOR conditions at both 24 and 48 h whereas this increase was only observed at 24 h when in LOW glucose conditions. Supplementation of EX-527 did not differ from DM when RES increased area however it was significantly reduced in comparison to the RES condition. SD's represented as error bars. Significant difference ($p < 0.05$) is denoted using a *.

These data suggest that RES administration in LOW glucose does not improve myotube diameter or area at the later, 48 and 72 h timepoints. Following 24 h however resveratrol did ameliorate the myotube atrophy observed under LOW glucose conditions. This suggests that the low glucose conditions over a period of 3 days is driving considerable atrophy and that a single dose of RES may be sufficient to return myotubes to normal growth over the first 24 h, yet perhaps repeated doses would be required when low glucose conditions are maintained over 48-72 h.

Following RES administration in NOR glucose conditions MYHC7 gene expression increased in differentiating myoblasts, documented in chapter 5. Both MYHC7 and IGF-I gene expression were increased in mature myotubes following a 72 h incubation also following RES administration in NOR glucose conditions. As a result we next wished to assess these genes in resveratrol treated low glucose conditions at 24 h where we

observed an improvement in myotube size. Furthermore, as we found reduced gene expression of protein degradative Ub ligase MUSA1 in RES treated low glucose conditions at 72 h, without improvements in morphology at 72 h, we also sought to investigate these genes for their role in the improvements in myotube diameter and size observed in low glucose with RES at 24 hrs.

6.3.8. Resveratrol increased MYHC7 expression in NOR conditions after 24 h but not in LOW glucose conditions.

MYHC7 displayed a significant main effect for time ($F_{(1, 20)} = 19.79$, $p < 0.001$). Gene expression for MYHC7 was increased in NOR glucose conditions supplemented with RES over time vs. 0 h (NOR RES vs. 0 h: 3.85 ± 0.60 vs. 9.77 ± 1.24 , $p = 0.048$ (fisher)). However, there were no significant differences present for either glucose condition following the activation or inhibition of SIRT1 at 24 h (Fig 6.5.).

A significant main effect for time was observed for IGF-I ($F_{(1, 20)} = 174.82$, $p < 0.001$). However, there was no significant difference following SIRT1 activation/inhibition in either NOR or LOW glucose conditions at 24 h (Fig 6.5.).

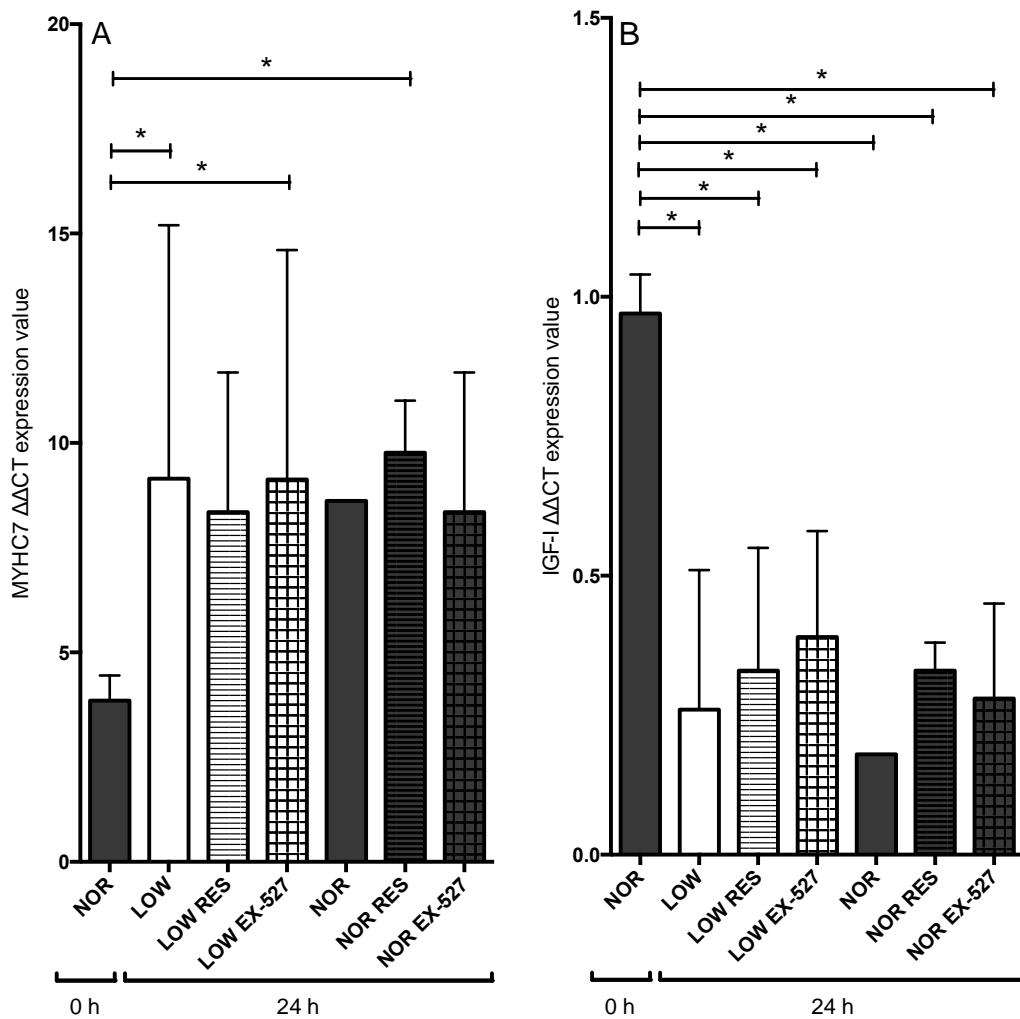


Fig. 6.5. As significant increase in MYH7 (A) expression from 0 h was observed in LOW glucose alone and following the addition of EX-527 but not in RES. NOR RES was significantly increased in 24 h compared to 0 h but not in either of the other NOR conditions. IGF-I (B) expression was significantly higher in 0 h than any other condition at 24 h. SD's represented as error bars. Significant difference ($p < 0.05$) is denoted using a *.

6.3.9. MRF4 increased after 24 h with resveratrol supplementation in LOW glucose

Without changes in MYHC's or IGF-I at 24h in low glucose with RES treatment to support the improved myotube size in the conditions at this timepoint. We therefore decided to investigate MRF4 gene expression as this is expressed temporally before adult MYHC's in the stages of myotube maturation and hypertrophy. We observed a significant increase in MRF4 gene expression with the administration of RES in LOW glucose conditions at 24 h, however, surprisingly the SIRT1 inhibitor also

increased MRF4 gene expression at this time point (LOW vs. LOW RES: 1.43 ± 0.25 vs. 21.5 ± 24.2 , $p = 0.048$ (fisher), LOW vs. LOW EX-527: 1.43 ± 0.25 vs. 25.6 ± 20.3 , $p = 0.020$ (fisher), LOW RES vs. LOW EX-527: 21.5 ± 24.2 vs. 25.60 ± 20.30 , $p = 0.638$).

6.3.10. No significant changes were present in MUSA1 gene expression following the activation/ inhibition of SIRT1.

MUSA1, a ubiquitin ligase involved in protein degradation, was reduced at 72 h in low glucose conditions in the presence of RES, yet morphological findings suggested there was no change in myotube size at this timepoint. We therefore investigated MUSA1 expression at 24 h where an improvement in myotube diameter and size were observed with RES treatment in low glucose conditions. Following 24 h MUSA1 displayed a significant main effect for time ($F_{(1,18)} = 320.00$, $p < 0.001$) (Fig 6.6.). All experimental conditions are significantly reduced in comparison to the 0 h control (0 h: 0.99 ± 0.09 vs. LOW: 0.29 ± 0.13 , $p < 0.001$ vs. LOW RES: 0.25 ± 0.00 , $p < 0.001$, 0 h vs. LOW EX-527: 0.30 ± 0.06 , $p < 0.001$ 0 h vs. NOR: 0.19 ± 0.00 , $p < 0.001$, 0 h vs. NOR RES: 0.27 ± 0.14 , $p < 0.001$, 0 h vs. NOR EX-527: 0.24 ± 0.08 , $p < 0.001$). MUSA1 however, displayed no significance was present for LOW or NOR glucose after the addition of either RES or EX-527 (Fig 6.6.).

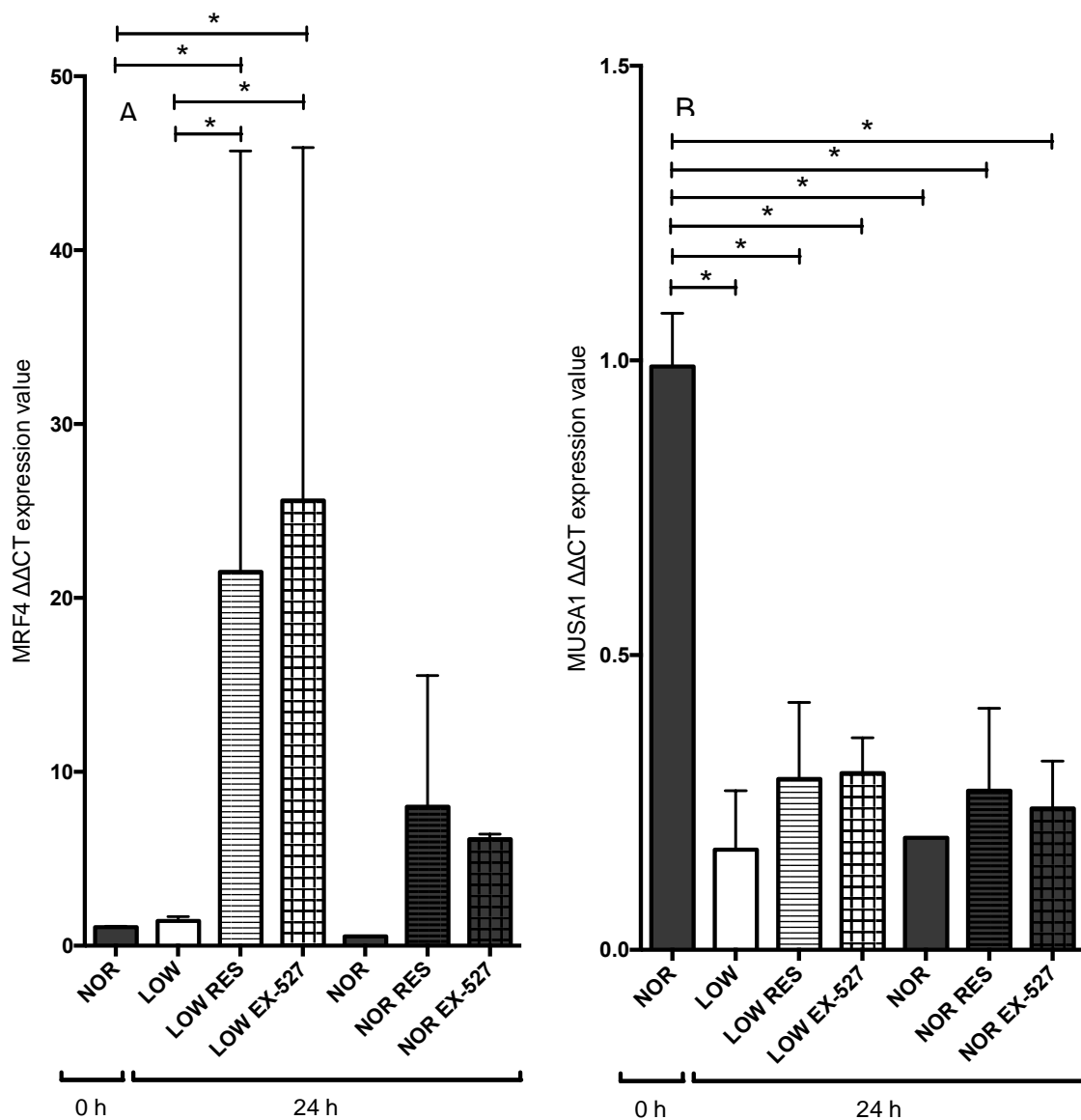


Fig. 6.6. Both graphs depict average changes using mean values and error bars represent SD's. MRF4 (A) was significantly increased in LOW glucose following both the addition of RES and EX-527. MUSA1 (B) was significantly reduced from 0 h to 24 h in all conditions, however SIRT1 manipulation did not instigate any significant changes. Significant difference ($p < 0.05$) is denoted using *.

Finally, despite no changes in gene expression at 24 h timepoint, we hypothesised that cell signalling would be temporally more immediate than gene expression changes over the first 24 h and may indicate the potential mechanisms of RES/SIRT1 activation induced improvements in myotube size vs. low alone conditions. We therefore investigated energy sensing

(AMPK) vs. protein synthetic signalling (p70S6K) across a range of timepoints over the first 24 h (0, 15, 30 min, 2 and 24 h) (Alterations in AMPK with starvation have previously been associated with reductions in mTOR/p70s6K via TSC1/2 (Inoki et al., 2003)). A significant interaction was present for AMPK protein activity between glucose and SIRT1 manipulation ($F_{(2,35)} = 3.13$, $p = 0.056$ (Fig. 6.7)). Following 15 min there was a trend toward a significant increase in AMPK activity following the administration of EX-527 in LOW glucose compared to LOW with the addition of RES (LOW RES vs. LOW EX-527: 0.95 ± 0.41 vs. 2.01 ± 1.11 , $p = 0.055$ (fisher)). Individual differences between glucose concentration or the activation/ inhibition of SIRT1 were observed.

Once incubated for 30 min the addition of EX-527 to NOR glucose increased AMPK in comparison to NOR glucose alone (Fig 6.8.) (2.63 ± 1.66 vs. 1.00 ± 0.63 , $p = 0.066$ (fisher)) and when NOR glucose was supplemented with RES (2.63 ± 1.66 vs. 1.00 ± 0.63 , $p = 0.066$ (fisher)). A trend for AMPK activity to increase was also observed in the presence of EX-527 under NOR glucose conditions in comparison to NOR glucose alone at both 2 h (NOR vs. NOR EX-527: 1.00 ± 0.36 vs. 2.24 ± 1.45 , $p = 0.086$ (fisher)) (Fig 6.9.) and 24 h (NOR vs. NOR EX-527: 1.00 ± 0.43 vs. 2.61 ± 0.75 , $p = 0.069$ (fisher)) (Fig 6.10.). Increases in AMPK with EX-527 in NOR glucose conditions also reduced protein activity for p70S6K at 15 min (Fig 6.11.) and 30 min (Fig 6.12.) vs. NOR alone, although this was not significantly different (15min, NOR vs. NOR EX-527: 1.30 ± 0.02 vs. 0.94 ± 0.20 , 30 min, NOR vs. NOR EX-527: 1.30 ± 0.02 vs. 0.94 ± 0.20 , $p > 0.05$). There were no significant difference over 2 h (Fig 6.13.) or 24 h (Fig 6.14.) for NOR glucose conditions. There were also no significant differences in AMPK or P70S6K in low glucose conditions in the absence or presence of SIRT1 activation/ inhibition (see figures 6.7- 6.14 below).

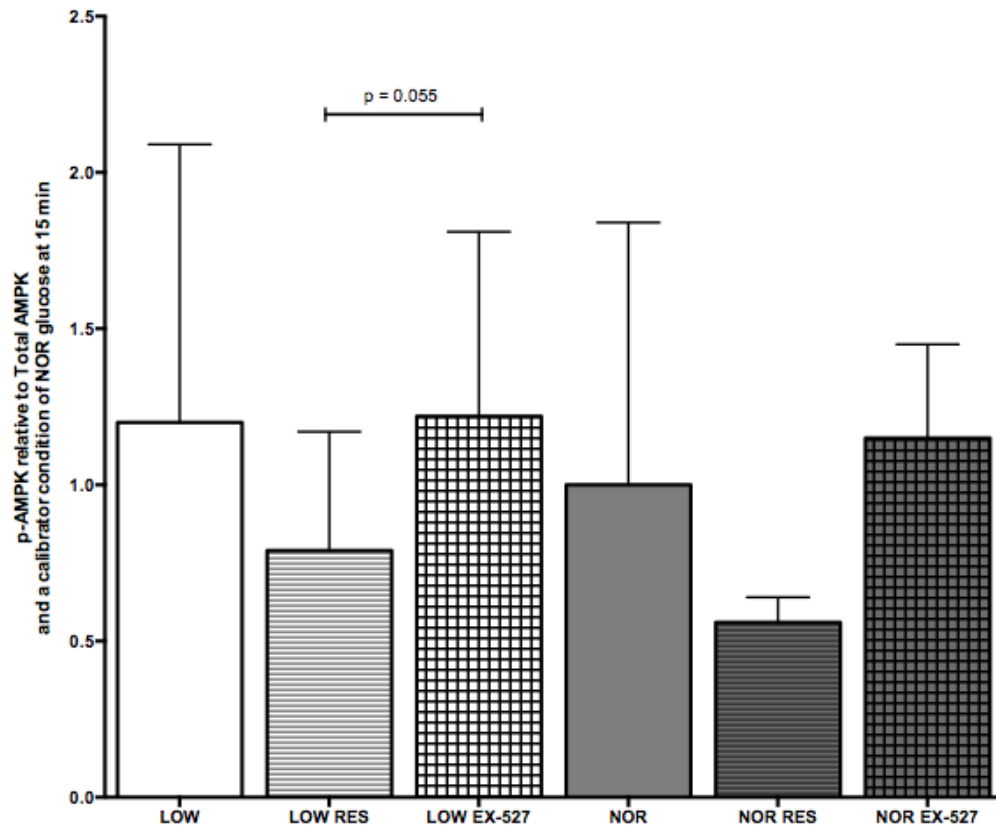
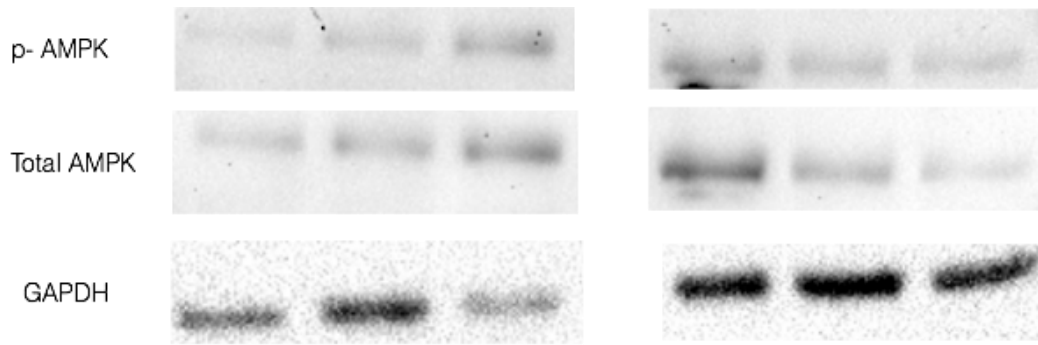


Fig. 6.7. Phosphorylated AMPK (p-AMPK) relative to Total AMPK and calibrated to NOR glucose at 15 min., this timepoint was additionally compared to GAPDH as there was a significant difference present between loading values. A trend towards significance was present for LOW RES vs. LOW EX-527. Significant difference ($p < 0.05$) is denoted using *. P values approaching significance are displayed.

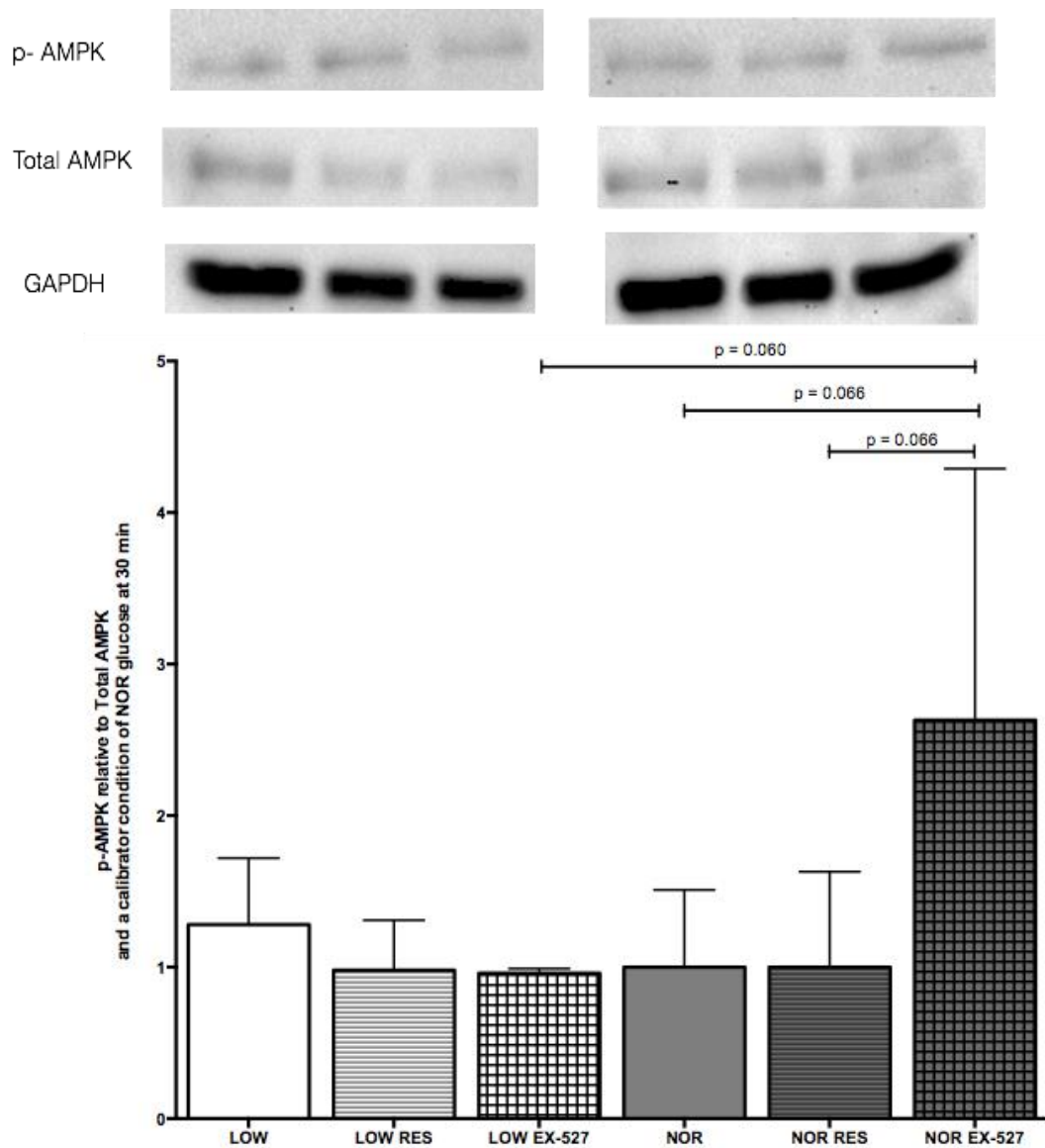


Fig. 6.8. Phosphorylated AMPK (p-AMPK) relative to Total AMPK and calibrated to NOR glucose at 30 min. 30 min incubation saw an increase in AMPK protein activity for NOR EX-527 compared to NOR, NOR RES and LOW EX-527. Significant difference ($p < 0.05$) is denoted using *. P values approaching significance are displayed.

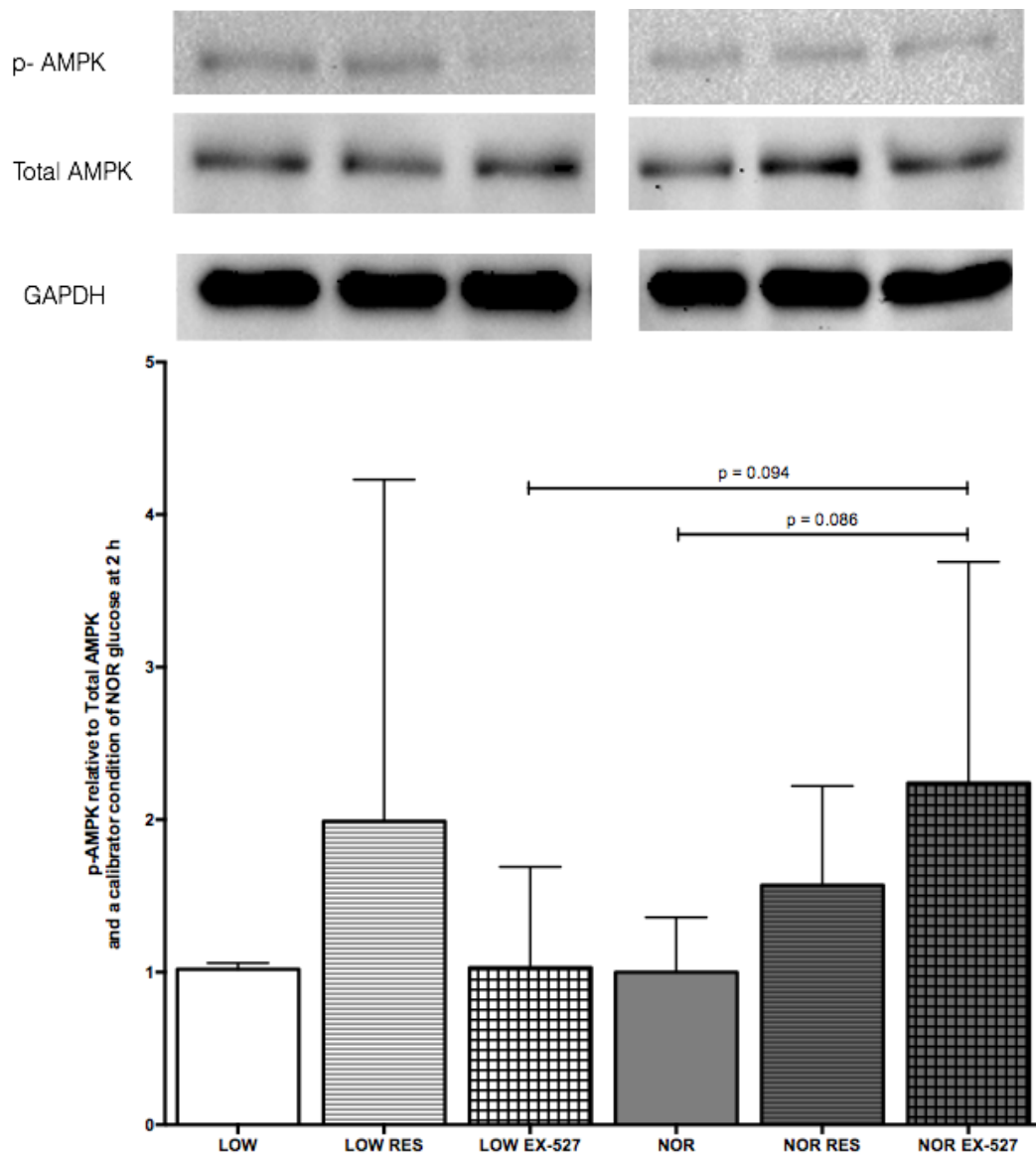


Fig. 6.9. Phosphorylated AMPK (p-AMPK) relative to Total AMPK at 2 h and calibrated to NOR glucose at 2h. A trend was present at the 2 h timepoint suggesting NOR EX-527 increased AMPK activity compared to NOR and LOW EX-527. Significant difference ($p < 0.05$) is denoted using *. P values approaching significance are displayed.

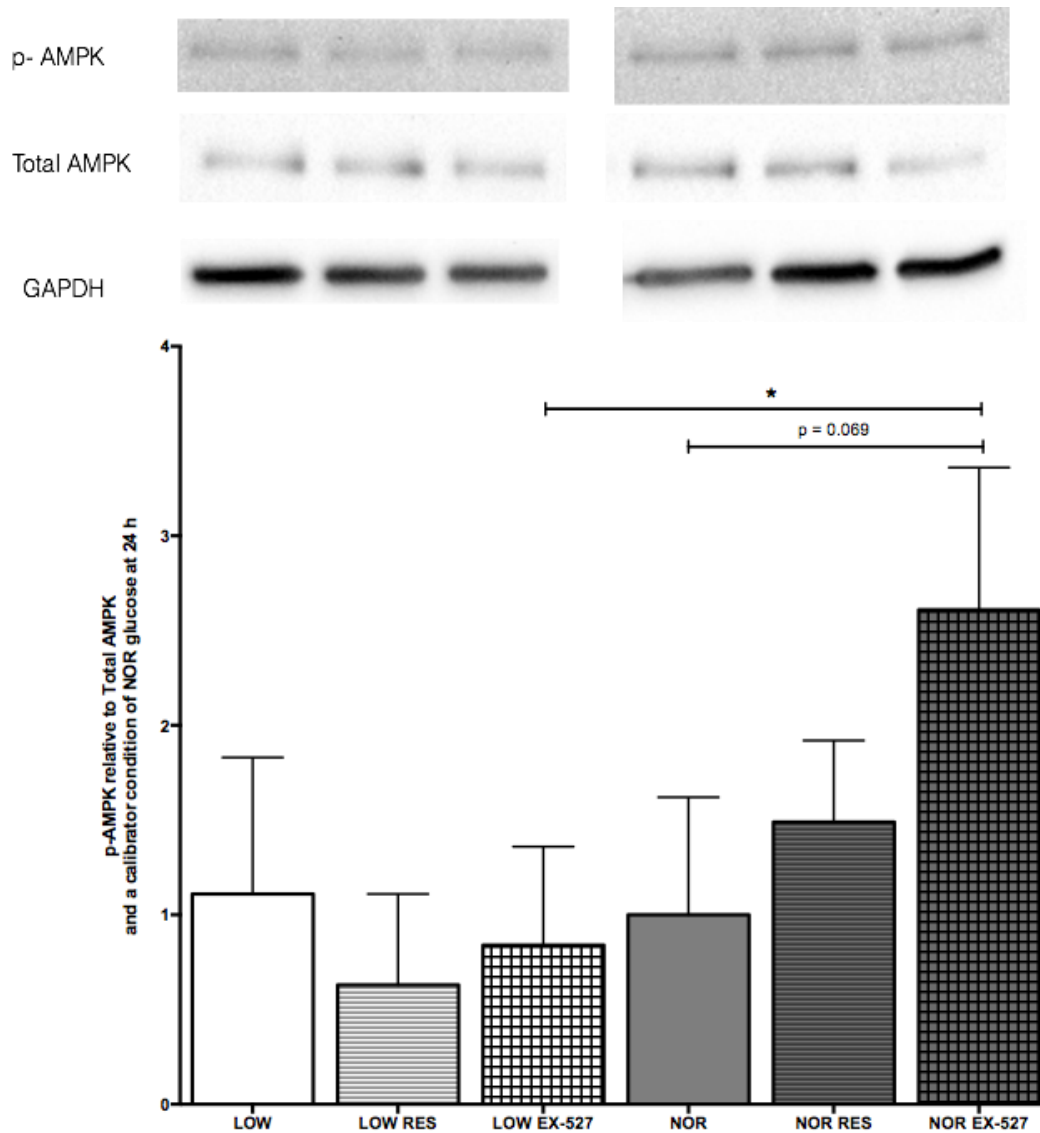


Fig. 6.10. Phosphorylated AMPK (p-AMPK) relative to Total AMPK at 24 h and calibrated to NOR glucose at 24h. The addition of EX-527 significantly increased AMPK content compared to LOW EX-527 and NOR glucose alone. Significant difference ($p < 0.05$) is denoted using a *. P values approaching significance are displayed.

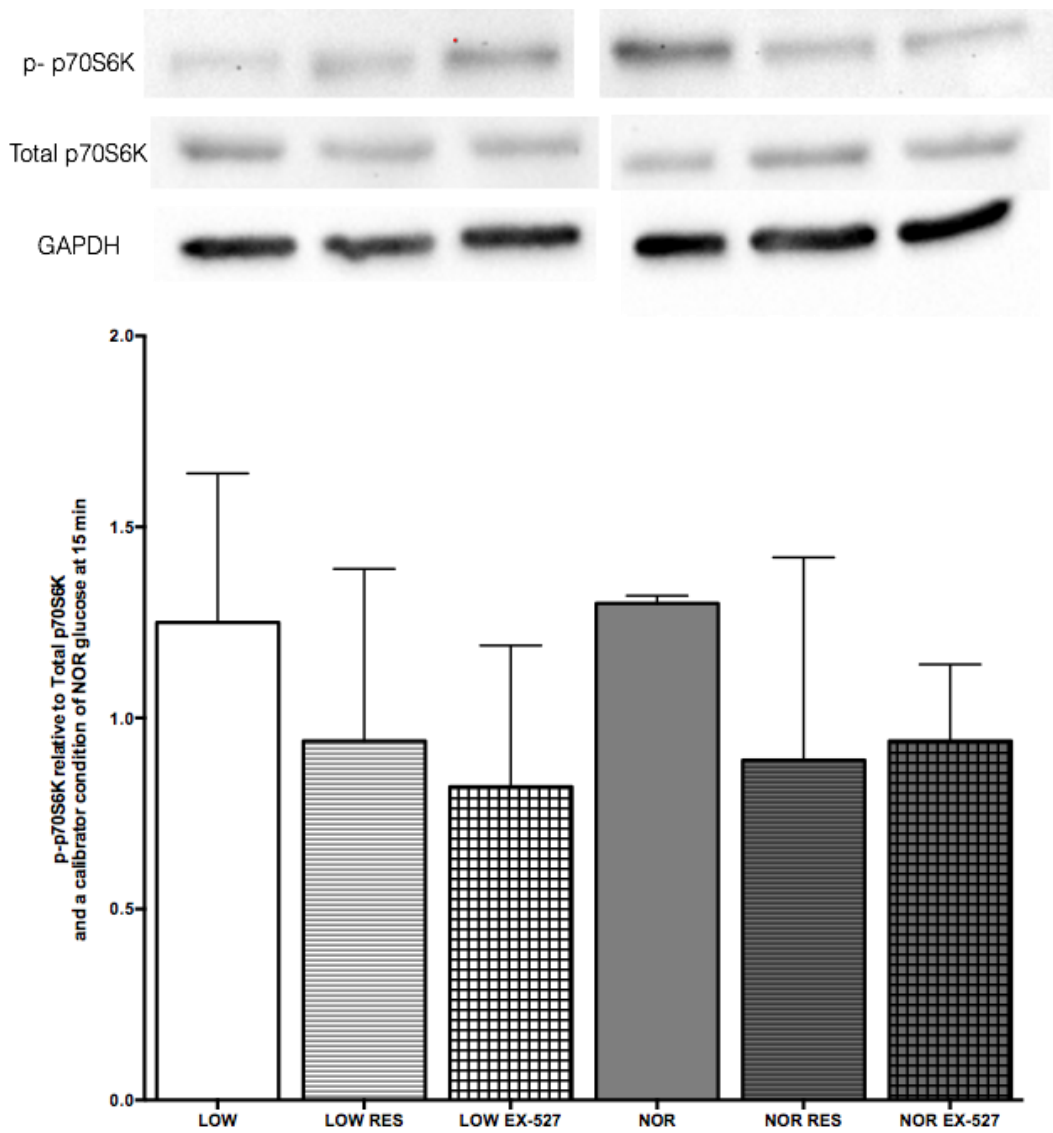


Fig. 6.11. Phosphorylated p70S6K (p-p70S6K) relative to Total p70S6K at 15 min and calibrated to NOR glucose at 15 min displayed no significant differences for any experimental conditions.

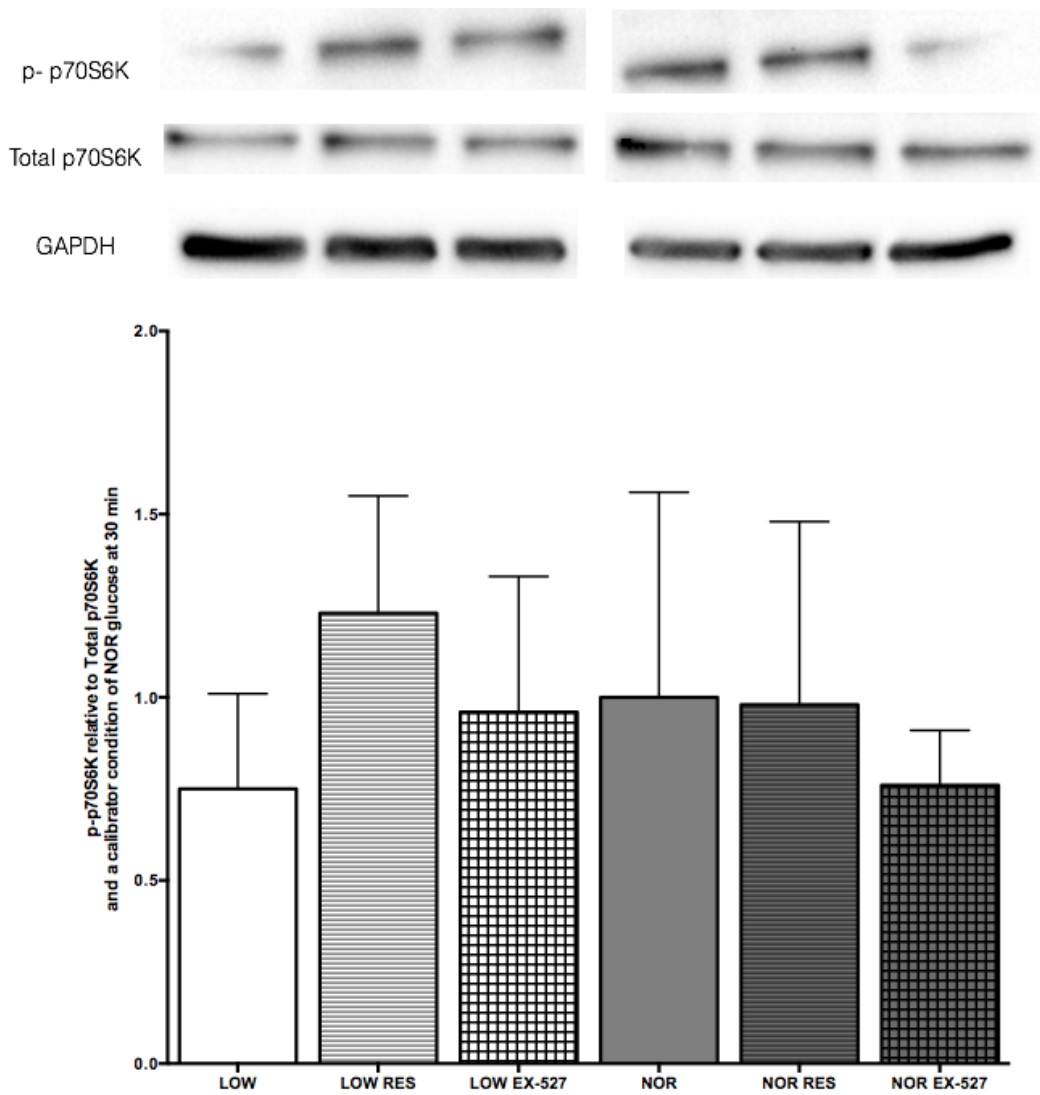


Fig. 6.12. Phosphorylated p70S6K (p-p70S6K) relative to Total p70S6K at 30 min and calibrated to NOR glucose at 30 min displayed no significant differences for any experimental conditions.

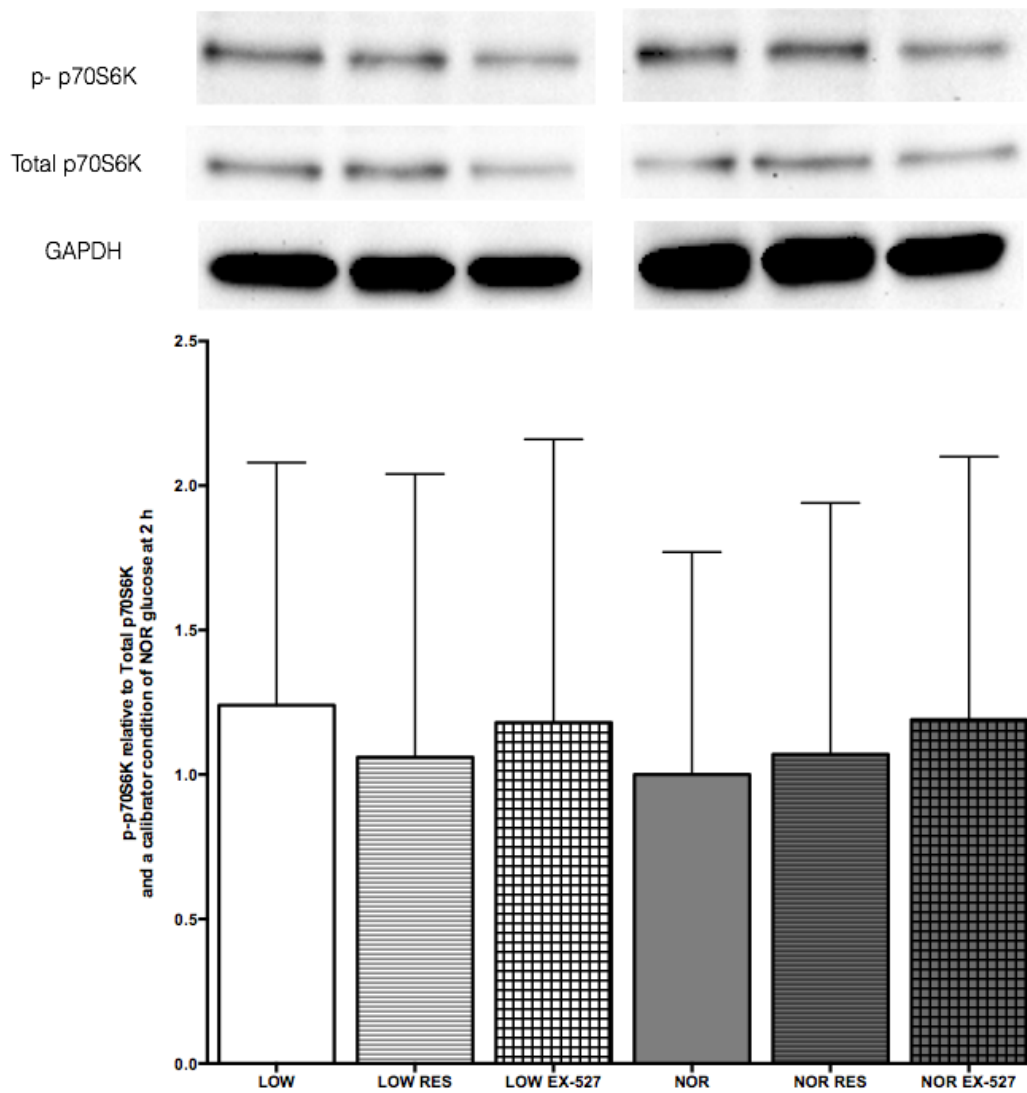


Fig. 6.13. Phosphorylated p70S6K (p-p70S6K) relative to Total p70S6K at 2 h and calibrated to NOR glucose at 2 h displayed no significant differences for any experimental conditions.

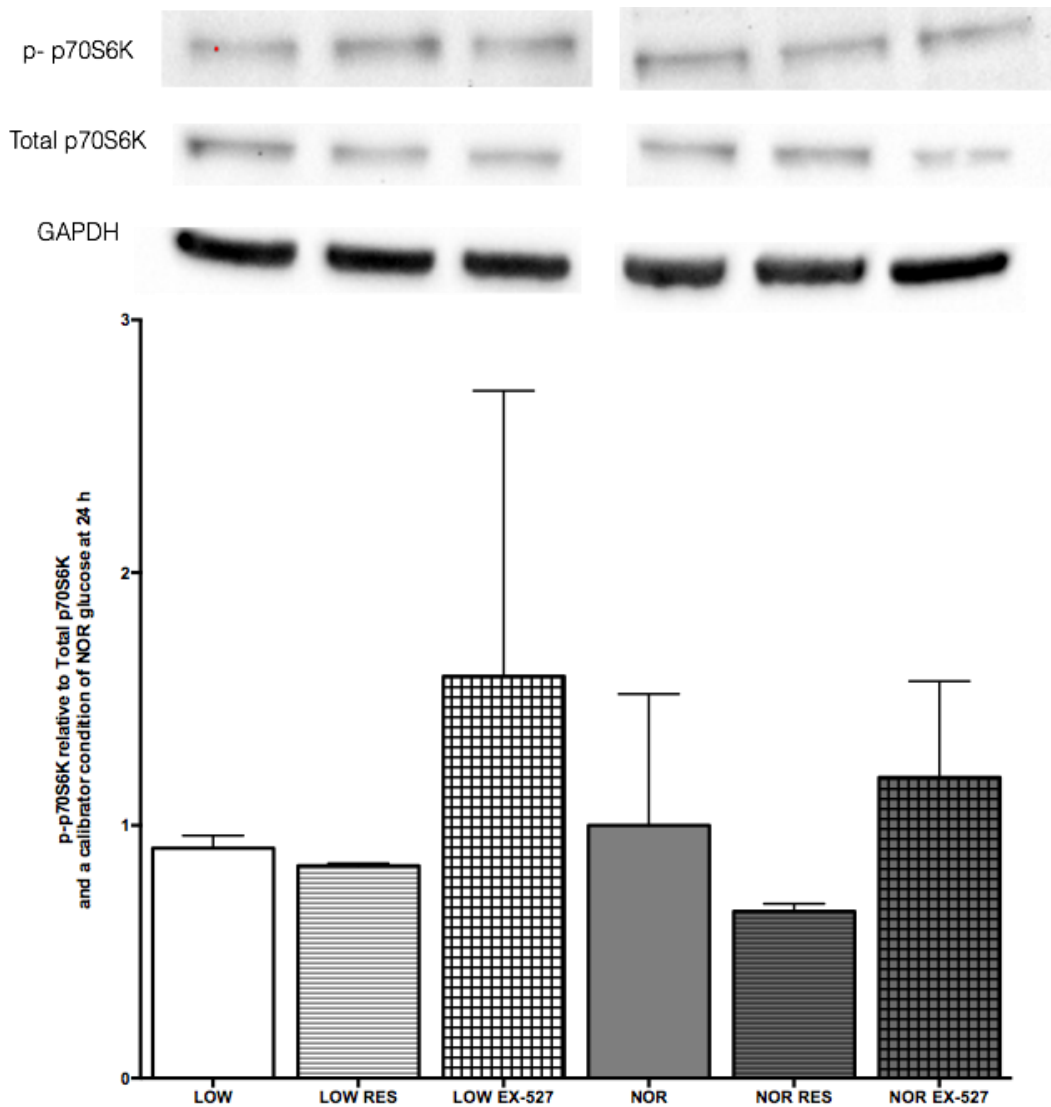


Fig. 6.14. Phosphorylated p70S6K (p-p70S6K) relative to Total p70S6K at 24 h and calibrated to NOR glucose at 24 h displayed no significant differences for any experimental conditions.

When the time points were extended to 72 h changes in myotube number and size were observed NOR glucose following manipulation of SIRT1, despite this genes associated with skeletal muscle atrophy and protein degradation appear to be unchanged. (All data presented in Appendix 1). Under LOW glucose conditions there appeared to be a reduction in atrophy/protein degradative genes such as myostatin and MUSA1, despite no increases in myotube size or number with RES treatment. This could be a continued compensatory drive to restore the atrophy observed under low glucose, although unsuccessful.

6.4. Summary

RES was able to increase both myotube area and diameter acutely over a 24 h time point. This was accompanied by increases in MRF4 (as perhaps would be expected given that MRF4 is an early driver of myotube maturation). This data suggests that the LOW glucose conditions over a period of 3 days is impairing growth and that a single dose of resveratrol may be sufficient to return myotubes to normal growth over the first 24 h. We observed that RES does not improve myotube diameter or area/ size in LOW glucose at the later time points of; 48 and 72 h (appendix 1) that repeated doses of RES when glucose conditions are restricted may maintain this increase over 48- 72h.

Area but not diameter was also increased following RES administration in NOR glucose conditions, however this was accompanied with a reduction in myotube number. These myotubes did not significantly differ from the other NOR glucose conditions, however compared to the 0 h timepoint they increased in the slow twitch myosin isoform (MYHC7). When the data was extended to the later 72 h timepoint however MYHC7 was significantly increased following RES supplementation in comparison to NOR glucose alone (appendix1). At this time point myotube number is no longer significantly reduced whereas myotube area is still increased in comparison to no RES supplementation. This is suggestive of a potential switch towards a greater number of oxidative fibres which is driving the myotubes enlarged size.

Inhibition of SIRT1 via EX-527 supplementation reduced myotube number in NOR conditions and reduced diameter within LOW conditions. As these findings do not directly oppose those observed with RES supplementation there is clearly a more complex relationship between SIRT1 and differentiation.

Despite the investigation of energy sensing pathways (AMPK) sensitive to changes in energy status have previously been shown to suppress growth signalling (p70s6k) under starvation (Inoki et al., 2003). We observed a trend towards increased AMPK with SIRT1 inhibition (EX-527 administration) approaching significance in normal glucose conditions together with non-significant reductions in p70S6K where in this condition there was a corresponding suppression of myotube hypertrophy. Furthermore, we observed increased AMPK with SIRT1 inhibition at 15 minutes in low glucose conditions in comparison with resveratrol conditions, yet the increase was not significant versus control conditions and no corresponding changes in p70S6K were observed at this timepoint. However, there were no other alterations in low glucose conditions at any other time points with the activation or inhibition of SIRT1. No changes in myotube hypertrophy were observed in normal glucose at 24 and 72h in the presence of increased SIRT1 activity via RES administration. This suggested that only SIRT1 inhibition was able to increase AMPK activity in both glucose conditions however this only resulted in non-significant reductions in p70S6k in normal glucose conditions. Despite this it is unlikely that, alterations in energy status impacted on protein synthetic signalling in the presence of RES and therefore not associated with the increased myotube hypertrophy at 24 h in low glucose and 24-72 h in normal glucose.

Chapter 7

7. Discussion

7.1. Relevant physiological model of glucose restriction

Within chapter 3 we presented two models of glucose restriction. Where under medium (MED) and low (LOW) glucose we observed a reduction and blocking (LOW glucose) in differentiation and myotube hypertrophy respectively assessed via morphological, biochemical and gene expression analysis. By using the two glucose concentrations we attempted to model physiologically similar glucose concentrations observed after dietary restriction (DR) *in vivo*. Where the MED condition possessed a glucose concentration of 1.13 g/L or 6.25 mM, similar to the average 1 g/L (5.6 mM), which has been previously observed in the circulation of rodents during DR (Cartee et al., 1994, Walford et al., 1992). Additionally, this concentration was similar to the concentration used in previous *in vitro* studies utilizing models of nutrient restriction (Elkalaf et al., 2013, Khodabukus and Baar, 2015), therefore also allowing for more accurate comparisons to be made between studies. Furthermore, based on the work of Aussedat et al. (2000) and Maggs et al. (1995) the concentration of glucose was observed to be approximately 30% lower in the interstitium than those levels found in circulating blood, as such the LOW glucose concentration was therefore in line with these levels at a concentration of 0.56 g/L or 3.12 mM, therefore making MED and LOW concentrations physiologically relevant to both circulatory and interstitial levels respectively following DR *in vivo*.

Accompanying the aforementioned morphological analysis, reductions in differentiation and myotube formation observed in these models was associated with a reduction in biochemical differentiation (reduced CK), as well as gene expression of important myogenic regulatory factors (MRF's). MyoD underpin the lineage determination of myoblasts and the onset of fusion (Buckingham et al., 2003, Cooper et al., 1999), whereas myogenin regulates formation and promotes terminal differentiation (Berkes and Tapscott, 2005). The reductions in these MRF's confirm reductions in

differentiation observed in these restricted glucose conditions. This data is in line with previous research that suggests starvation in myoblasts during differentiation reduced these MRFs and indeed that overexpression of MyoD can help restore differentiation in the presence of starvation, albeit starvation in this instance was removal of serum, amino acids and glucose (Lagirand-Cantaloube *et al.*, 2009).

Furthermore, the reduction in myotube hypertrophy at 7 days in glucose-restricted conditions resulted in a reduction in gene expression of MYHC's 1,4 and 7, which code for the myosin heavy chain protein isoforms of type IIx, IIb and slow twitch fibers respectively. With respect to LOW glucose the expression of MYHC's was almost completely abolished as a consequence of no myotubes being formed in this condition. Whereas, the MED glucose condition there was impaired yet not completely blocked myotube formation the expression of MYHC was not completely abolished, however there was a significant reduction in the expression in comparison to the control. A reduction in total MYHC protein in C2C12 cells has previously been reported under low glucose conditions, therefore suggesting again that we possess a suitable model of impaired differentiation and myotube atrophy in MED glucose and blocked differentiation in LOW glucose conditions (Fulco *et al.*, 2008).

Notably, we observed an increase in SIRT1 gene expression in the lowest glucose condition. Activation of SIRT1 (phosphorylation) has been previously observed in C2C12 muscle cells under low glucose conditions (Fulco *et al.*, 2008). Upregulation of SIRT1 gene expression has also been observed to also take place in the presence of the inflammatory cytokine, TNF- α in C2 myoblasts (Saini *et al.*, 2012). Within this model of inflammation gene silencing of SIRT1 increased cell death in the presence of TNF- α whereas activation of SIRT1 via resveratrol (RES) administration ameliorated the inflammatory induced increase in cell death and reduction in differentiation. Suggesting that resveratrol is an important in survival and differentiation in myoblasts under stress. Inferring from the previous

literature (Fulco et al., 2008), although it was demonstrated that SIRT1 increased at the gene expression level in the presence of TNF- α , that perhaps this was a precursor for increased SIRT1 protein levels available for subsequent increases in SIRT activity. We therefore suggested that this increase may not have caused the reduction in differentiation rather was a unsuccessful attempt to improve survival and perhaps enable/initiate differentiation under nutrient stress. As such we hypothesised that similarly to the findings observed under inflammation that SIRT1 activation via resveratrol treatment may improve differentiation and myotube maturation in skeletal muscle cells under reduced glucose conditions.

7.2. Dose response for SIRT1 activation and inhibition

Before the manipulation of SIRT1 activation would be possible under reduced glucose conditions, we first aimed to optimise the dosing of resveratrol and the SIRT1 inhibitor (EX-527) in chapter 4. Previously, we have administered C2C12 cells with 30 and 60 μ M of RES, however cell viability was compromised at these doses (Deane and Sharples *et al.*, 2015, unpublished). Decreased cell viability has also been observed in C2C12 at doses of 20 μ M and higher (Higashida *et al.*, 2013, Bosutti and Degens, 2015). Despite Higashida et al. (2013) observing no change in total PGC-1 α (a downstream protein modulated by SIRT1 (Rodgers *et al.*, 2005b)) following 5 and 10 μ M after a 24 h incubation, recent evidence has suggested that 10 μ M was beneficial in C2C12 myoblast remodeling under oxidative stress (Bosutti and Degens, 2015). We therefore performed a dose response of RES at 5, 10 and 15 μ M. The impact of SIRT1 activation was investigated (phosphorylation via western blotting) in which a significant increase in SIRT1 activity was observed in both 10 and 15 μ M. Activation seemed more consistently elevated over the time course of 15 min, 30 min, 2 h, and 24 h with 10 μ M RES, with the largest increase in SIRT1 phosphorylation at 15 min with a resveratrol concentration of 10 μ M. Indeed, there are limited studies characterising SIRT1 activity (phosphorylation) with RES administration in myoblasts. Studies that have

measured this previously have focused on SIRT1 mRNA (Saini et al., 2012) or SIRT1 total protein levels (Fröjdö et al., 2011). Due to SIRT1 being a histone deacetylase its function is determined both by total protein and its deacetylase activity. Phosphorylation of SIRT1 is required however to enable increases in deacetylase activity (Sasaki et al., 2008).

As mentioned above we also aimed to ascertain the optimal concentration of the commercially available SIRT1 inhibitor EX-527. Initially we observed SIRT1 activity following administration of 30 and 60 μ M of EX-527. SIRT1 activity did not significantly reduce activity under these concentrations and unexpectedly increased in some instances. EX-527 has an IC₅₀ (inhibitory concentration 50%) of 98 nM for SIRT1 inhibition (Carafa et al., 2016) and as such has been previously documented to reduce SIRT1 activation by approximately 50% at concentrations between 48 and 100 nM. However, inhibition in these studies was measured via vitro Fluor de Lys deacetylation assays in embryonic kidney cells to assess SIRT1s deacetylation activity and not phosphorylation per se (Solomon et al., 2006). We also observed average reductions in SIRT1 activity following 24 h at a concentration of 100 nM, however this was analyzed via phosphorylation and not deacetylation. From this data it could be suggested that deacetylation activity would also be reduced as a result, given that phosphorylation of SIRT1 is required however to enable deacetylase activity (Sasaki et al., 2008). However was not tested as deacetylation assays were unavailable in the labs at the time of data collection. This would be important to establish in future studies.

7.3. SIRT1 activation and inhibition in restricted and normal glucose conditions

The objective for chapter 5 was to manipulate SIRT1 activity using the concentrations characterised in chapter 4 on a background of restricted glucose previously established in chapter 3. By combining the findings from chapters 3 and 4 we were able to establish whether SIRT1 activation/inhibition could attenuate the reduction in differentiation and myotube

hypertrophy observed in the MED glucose conditions and prevent the complete depletion of myotubes observed in the LOW glucose condition. We hypothesised that SIRT1 activation via resveratrol would ameliorate the diminished and reduced differentiation observed under LOW and MED glucose conditions respectively. Despite observed improvements in creatine kinase activity in the lowest glucose condition following SIRT1 activation, we did however reject this hypothesis. Generally, RES was unable to prevent the loss of morphological differentiation in either glucose condition.

It is worth noting however that SIRT inhibition produced absolutely no CK activity in LOW conditions at 72 h and the corresponding lowest number of myotubes in comparison to the other NOR glucose conditions. This suggests that normal SIRT1 activity was required for normal CK and basal myotube formation to take place in LOW and NOR conditions respectively. The opposite was however true for MED glucose conditions in which SIRT1 inhibition implemented an increase in myotube number following SIRT inhibition. The findings in MED glucose are similar to those previously observed by Fulco et al. (2008) in which the reduction of SIRT1 via a retrovirus expressing short hairpin targeting SIRT1 mRNA (shSIRT1) was able to rescue differentiation under glucose restriction. The inference of which is that SIRT1 is required for the loss of differentiation observed under glucose-restricted conditions to take place. The glucose concentration administered in the Fulco et al. (2008) study was very similar the MED glucose condition (5.00 vs. 6.25 mM) which may be one such reason for the similarities. Although this glucose concentration was previously deemed to be physiologically similar to values available for DR *in vivo* it may also be more physiologically similar to non DR glucose concentrations than the NOR glucose control. As previously discussed NOR glucose condition is super physiological and may provide a model closer to hyperglycemia than NOR glucose *in vivo*. As such the reason that LOW and NOR observe improvements under SIRT1 increases may be due to their roles as physiological stress environments, whereas MED

glucose is not a true nutritional stress. As our findings under NOR and LOW glucose however oppose these findings in which inhibition of SIRT1 following 72 h abolished CK activity in LOW conditions. This could potentially suggest that when translated to whole organism populations that SIRT1 increases are only needed under a nutritional stress and a reduction in SIRT1 may improve muscle growth under normocaloric environments due to the lack of stress present.

Following administration of both EX-527 and RES in NOR glucose conditions there was an impairment in CK activity and myogenin expression as well as formation of myotubes. Despite this and possibly most importantly we observed an increase in myotube size in the remaining myotubes following the supplementation of resveratrol in normal glucose conditions. This observation was coupled with an increase in MYHC 7 and MYHC 4 gene expression, which code for the slow type I and fast type IIb MYHC protein isoforms respectively. These findings suggested that the adaptation observed following RES administration might be responsible for the increase in myotube size via an increase in the genes coding for contractile proteins. Indeed, these findings are in line with those previously observed by both Montesano *et al.* (2013) and Kaminski *et al.* (2012) in which total MYHC protein is increased in normal glucose conditions in the presence of RES. Montesano *et al.* (2013) did not measure myotube area, however they did observe significant increases in both myotube diameter and length following RES administration, suggesting that overall size would indeed be increased. Our measurements in myotube diameter however displayed no significant changes in any of our experimental conditions. Bosutti and Degens (2015) found that a RES concentration of 10 μ M (the same as we utilized) was the only concentration to enhance the percentage of cells in the G0-G1 phase and this was not the case in a similar concentration to that used in the Montesano *et al.* (2013) study (20 μ M). It may be proposed therefore that the increase in myotube area observed under these conditions was due to earlier cell cycle exit. It is interesting, however that an increase in

area was also observed by Montesano et al. (2013) as they observed no increase in p21 protein content (associated with cell cycle exit and early differentiation) with the administration of RES in comparison to the DM conditions alone. Despite these findings Bosutti and Degens (2015) did not observe inhibition of this cell cycle arrest until much higher concentrations (40 - 60 μ M) therefore increases in myotube size may indeed be due to early exit of the cell cycle leading to earlier initiation of differentiation and subsequently allowing more time for myotube maturation and hypertrophy. Unfortunately, Montesano et al. (2013) did not measure myotube number therefore our proposal that RES administration increases myotube size without an increase in myotube number contributes to advancing understanding in these conditions. Additionally, this previous study did not measure activation or expression of SIRT1 and as such our data extends this work by suggesting a positive role for SIRT1 activation in myotube hypertrophy in normal glucose conditions.

Although not measured within this study, resveratrol has been suggested to improve myoblast migration but not the impaired fusion induced by oxidative stress (Bosutti and Degens, 2015). The present study, albeit under the stress environment induced by low glucose, also suggested that resveratrol cannot improve fusion/ differentiation of myoblasts. Additionally, the present study also identified that the SIRT inhibitor (EX-527) evoked reductions in MYHC1 coding for the fast IIX MYHC protein in normal glucose conditions and therefore suggested that normal SIRT activity was perhaps important to maintain adequate fast isoform gene expression. A finding that to the authors knowledge has not been shown before. Moreover, future studies may wish to investigate the role of SIRT1 activation/ inhibition on Nuclear factor of activated T-cells (NFAT) activity in skeletal muscle cells. As this transcription factor, regulates activation of muscle fiber genes associated with characterization of 'slow' and 'fast' myofibres (Chin *et al.*, 1998) and is known to be transcriptionally suppressed by SIRT1 (Jia *et al.*, 2014). Future studies may wish to

investigate the role of SIRT1 activation/inhibition on NFAT activity in skeletal muscle cells. Overall, chapter 5, SIRT1 activation lead to increases in myotube hypertrophy and SIRT1 inactivation a slowing of the myotube contractile apparatus in normal glucose conditions.

Due to the interesting findings observed in chapter 5 in which RES treatment increased myotube hypertrophy in NOR glucose conditions and although resveratrol was unsuccessful in improving morphological measures, CK was increased in LOW glucose conditions following RES administration. We therefore examined the role of SIRT1 inhibition/activation in both LOW and NOR glucose conditions on existing myotube cultures. Where in the previous chapter we observed changes in differentiating myoblasts and their ability to produce myotubes this chapter involved the use of mature myotubes, which could be suggested as more indicative of *in-vivo* tissue. As resveratrol was observed to increase myotube size in NOR glucose following 7D, we chose to administer RES following 7D in culture in which myoblasts had already differentiated into myotubes. In addition, in chapter 5 RES supplementation in LOW glucose conditions following 7D did drive increases in CK, despite no improvement in myotube formation. It is therefore feasible that in the presence of existing myotubes, resveratrol may prevent myotube atrophy evoked by LOW glucose conditions. We therefore hypothesised that activation of SIRT1 may reduce myotube atrophy observed in nutrient (LOW glucose) restricted conditions and that resveratrol may further induce myotube hypertrophy in normal glucose conditions.

As observed in the myoblasts study from chapter 5, the inhibition of SIRT1 via EX-527 reduced myotube number. In addition to this myotube size was also negatively affected and the activation of SIRT1 via resveratrol increased myotube area at 72 h after dosing on to myotubes. Again MYHC expression was altered corresponding with this data, however in the myotubes studies these alterations consisted of reductions in MYHC 1, 2 and 4 following SIRT1 inhibition, coding for IIx, IIa, IIb isoforms

respectively and an increase in MYHC7 (slow twitch isoform) following SIRT1 activation. These findings suggest that increases in SIRT1 activity mediated an increase in slow fiber type isoform gene expression and a decrease in SIRT activity reduces fast fiber type isoform gene expression. A finding that consolidated observations made in chapter 5 where SIRT1 inhibition reduced fast MYHC's in differentiating myoblasts. These findings taken together with the corresponding increases in myotube size observed in normal glucose conditions following RES supplementation, suggest that the observed hypertrophy is resultant from the increase in the gene coding for increasing slow fiber type protein isoforms. As such despite possessing larger myotubes they may have a slower contractile potential. Resveratrol supplementation however little effect on myotubes in low glucose conditions at this 72 h timepoint.

In addition to the regulation of MYHC expression observed at 72 h the increase in myotube number and size observed in NOR glucose following resveratrol treatment corresponded with increases in the expression of growth related genes IGF-I but not IGF-IR, IGF-II and IGF-IIR. IGF-I has previously been associated with increased differentiation; myotube hypertrophy and increases in muscle size *in vivo* (Scimè and Rudnicki, 2006, Stewart and Rotwein, 1996, Jacquemin *et al.*, 2004, Quinn *et al.*, 2007, Sharples *et al.*, 2011, Sharples *et al.*, 2010) and as such this observation may provide insight into the mechanisms underpinning the increase in myotube hypertrophy following RES supplementation after 72 h. An increase in IGFBP2 gene expression was associated with the reduction in myotube size observed during the inhibition of SIRT1. IGFBP2 is a known inhibitor of differentiation and myotube hypertrophy when protein levels are altered in differentiating myoblasts (Sharples *et al.*, 2010, Sharples *et al.*, 2013b), however within myotube studies its role is yet to be defined. However, overexpression of IGFBP2 in mice results in a reduction in muscle size (Rehfeldt *et al.*, 2010). SIRT1 may thereby regulate IGFBP2 expression and subsequent reduction observed with EX-527 in NOR glucose conditions.

Interestingly in low glucose conditions, despite no observable increases present in myotube size following 72 h with resveratrol treatment there was a reduction in myostatin, a negative regulator of muscle mass, myostatin (Mcpheeron and Lee, 1997) and protein degradative gene MUSA1 (Milan et al., 2015). Similarly to the increase in CK, observed in LOW glucose in differentiating myoblasts (chapter 5) this may have been a compensatory mechanism attempting to restore the observed atrophy within this experimental condition. However this was unsuccessful in rescuing atrophy observed at 72 h.

Most importantly within the final data chapter (6) resveratrol improved myotube area and diameter in LOW glucose at a more acute timepoint of 24 h. This finding was observed despite no changes being observed at 48 or 72 h. These findings, however, were not driven by changes in MYHC as was the case for changes in NOR glucose in both myoblasts and mature myotubes. Improvements in myotube area and diameter were instead associated with increased MRF4 (*myf6*) which to our knowledge has not previously been associated with resveratrol in skeletal muscle. MRF4 is involved in the transition between differentiated and mature myotubes and therefore may be expected to be upregulated at the earlier timepoint of 24 h over MYHC expression (Ropka-Molik *et al.*, 2011). From these findings we can infer that the muscle atrophy experienced under LOW glucose conditions may be attenuated following a single dose of resveratrol over a 24 h time period. Unfortunately, as these positive findings were not observed at later timepoints it suggests that a repeated dose may be required to maintain myotube hypertrophy over a longer time scale in low glucose conditions and therefore this warrants further investigation.

It has previously been observed that glucose deprivation in skeletal muscle increases both AMPK and SIRT1 and that the AMPK- NAMPT- SIRT1 pathway allows the cell to respond to nutrient deprivation and adapt

accordingly in both muscle cells (Fulco et al., 2008) and animal models. Furthermore AMPK has been observed to suppress growth related signaling of p70S6K via TSC2 inhibition of mTOR (Inoki et al., 2003). Under normal glucose conditions with resveratrol treatment we observed increases in IGF-I gene expression and subsequent increases in myotube hypertrophy. Therefore, it may be expected that we would observe alterations in downstream p70S6K the translation initiator for protein synthesis from mRNA in the ribosome, thus enabling increased myotube hypertrophy (Rommel *et al.*, 2001). We observed a trend towards increased AMPK with SIRT1 inhibition (EX-527 administration) approaching significance in normal glucose conditions together with average but non-significant reductions in p70S6K where in this condition there was a corresponding suppression of myotube hypertrophy. Furthermore, we observed increased AMPK with SIRT1 inhibition at 15 minutes in LOW glucose conditions in comparison with resveratrol conditions, yet the increase was not significantly increased versus control conditions and no corresponding changes in p70S6K were observed at this timepoint. However, there were no other alterations in LOW glucose conditions at any other time points with the activation or inhibition of SIRT1. Additionally, no alterations where we observed myotube hypertrophy in normal glucose (observed at 24 and 72h) in the presence of increased SIRT1 activity via resveratrol administration. Suggesting that only SIRT1 inhibition was able to increase AMPK activity in both glucose conditions however this only resulted in reductions (albeit non-significant) in p70S6k in normal glucose conditions. Suggesting that perhaps normal SIRT1 activity was required for adequate AMPK activity to prevent the suppression of p70S6K and the corresponding reductions in myotube size observed in SIRT1 inhibitor conditions. Despite this the mechanisms responsible for the increased myotube hypertrophy following RES administration at 24 h in low glucose and 24- 72 h in normal glucose conditions are unlikely to be attributable to alterations in energy sensing signalling and/or protein synthetic signalling.

If there was significant changes present in the AMPK p70S6K pathway it would suggest that RES would be actively initiating hypertrophy, however as the morphological results following RES administration in LOW glucose condition do not significantly exceed NOR conditions it could be suggested that a reduction in atrogenes such as MuRF1 and MaFbx and not hypertrophic response per se. One such mechanism could be via modifications in FoXOs, previously suggested in skeletal muscle overload (Koltai *et al.*, 2017).

7.4. Conclusions

Despite the initial hypothesis suggesting that resveratrol would improve the loss of differentiation observed under glucose restriction we rejected this hypothesis in differentiating myoblasts as little effect was observed under these conditions. Resveratrol did however evoke increases in myotube hypertrophy under normal glucose conditions and enable improved myotube hypertrophy over an acute 24 h period when administered to existing myotubes in LOW glucose. If this finding translates to whole organisms and human populations it could provide healthspan improvements in individuals undergoing dietary restriction. Unfortunately, after the 24 h period the myotubes continued to undergo atrophy, which is suggestive of the requirement for dosing every 24 h. In the LOW glucose condition SIRT1 activation increased MRF4 gene expression and was associated with the improved myotube size at 24 h in this condition. Whereas SIRT1 activation in normal glucose conditions modulated increased gene expression coding for slow MYHC isoforms while inhibition of SIRT1 lead to reductions in gene expression coding for fast MYHCs. This finding may be particularly usefully when considering dietary interventions in fed individuals who partake in aerobic activities, potentially providing a greater number of slow twitch fibres for improvements in aerobic economy. While SIRT activation did modulate increases IGF-I gene expression, it did not appear to modulate energy sensing vs. growth related signaling pathways. However, SIRT1 inhibition (EX-527) did reduce AMPK activity in low and normal glucose conditions

with corresponding mean reductions in P70S6K in normal glucose conditions. In low glucose induced myotube atrophy resveratrol did however impair the negative regulator of muscle mass, myostatin, and protein degradative ubiquitin ligase enzyme, MUSA1. Overall, SIRT1 activation via a single dose of resveratrol appears to have a role in acutely negating the effect of myotube atrophy in low glucose conditions and promoting hypertrophy when normal levels of glucose are available.

Chapter 8

8. References

Aspnès, L., Lee, C., Weindruch, R., Chung, S., Roecker, E. & Aiken, J. 1997. Caloric restriction reduces fiber loss and mitochondrial abnormalities in aged rat muscle. *The FASEB Journal*, 11, 573-581.

Aussedat, B., Dupire-Angel, M., Gifford, R., Klein, J., Wilson, G. & Reach, G. 2000. Interstitial glucose concentration and glycemia: implications for continuous subcutaneous glucose monitoring. *American Journal of Physiology-Endocrinology and Metabolism*, 278, E716-E728.

Ballak, S. B., Jaspers, R. T., Deldicque, L., Chalil, S., Peters, E. L., De Haan, A. & Degens, H. 2015. Blunted hypertrophic response in old mouse muscle is associated with a lower satellite cell density and is not alleviated by resveratrol. *Exp Gerontol*, 62, 23-31.

Ballor, D. L., Katch, V., Becque, M. & Marks, C. 1988. Resistance weight training during caloric restriction enhances lean body weight maintenance. *The American journal of clinical nutrition*, 47, 19-25.

Barbieri, M., Bonafè, M., Franceschi, C. & Paolisso, G. 2003. Insulin/IGF-I-signaling pathway: an evolutionarily conserved mechanism of longevity from yeast to humans. *American Journal of Physiology-Endocrinology and Metabolism*, 285, E1064-E1071.

Barger, J., Kayo, T., Vann, J., Arias, E., Wang, J., Hacker, T., Wang, Y., Raederstorff, D., Morrow, J., Leeuwenburgh, C., Allison, D., Saupe, K., Gregory, C., Weindruch, R. And Prolla, T. 2008. A Low Dose of Dietary Resveratrol Partially Mimics Caloric Restriction and Retards Aging Parameters in Mice. *plos one*, 3, 1-10.

Baur, J. A., Pearson, K. J., Price, N. L., Jamieson, H. A., Lerin, C., Kalra, A., Prabhu, V. V., Allard, J. S., Lopez-Lluch, G. & Lewis, K. 2006.

Resveratrol improves health and survival of mice on a high-calorie diet. *Nature*, 444, 337-342.

Baur, J. A., Ungvari, Z., Minor, R. K., Le Couteur, D. G. & De Cabo, R. 2012. Are sirtuins viable targets for improving healthspan and lifespan? *Nature Reviews Drug Discovery*, 11, 443-461.

Benbassat, C. A., Maki, K. C. & Unterman, T. G. 1997. Circulating Levels of Insulin-Like Growth Factor (IGF) Binding Protein-1 and-3 in Aging Men: Relationships to Insulin, Glucose, IGF, and Dehydroepiandrosterone Sulfate Levels and Anthropometric Measures 1. *The Journal of Clinical Endocrinology & Metabolism*, 82, 1484-1491.

Berkes, C. A. & Tapscott, S. J. 2005. MyoD and the transcriptional control of myogenesis. *Semin Cell Dev Biol*, 16, 585-95.

Bk, L. V. K. 2006. Sirtuins in aging and age-related diseases. *Cell*, 126, 257-268.

Blau, H. M. 1993. Plasticity of the differentiated state. *Gene Expression*. Springer.

Blau, H. M., Pavlath, G. K., Hardeman, E. C., Chiu, C.-P., Silberstein, L., Webster, S. G., Miller, S. C. & Webster, C. 1985. Plasticity of the differentiated state. *Science*, 230, 758-766.

Bodine, S. C. & Baehr, L. M. 2014. Skeletal muscle atrophy and the E3 ubiquitin ligases MuRF1 and MAFbx/atrogen-1. *American Journal of Physiology - Endocrinology And Metabolism*, 307, E469-E484.

Boily, G., Seifert, E., Bevilacqua, L., Hong He, X., Sabourin, G., Estey, C., Moffat, C., Crawford, S., Saliba, S., Jardine, K., Xuan, J., Evans, M., Harper, M. And Mcburney, M. 2008. SirtT1 regulates energy metabolism and response to caloric restriction in mice. *plos one*, 3, 1-12.

Bordone, L., Cohen, D., Robinson, A., Motta, M. C., Van Veen, E., Czopik, A., Steele, A. D., Crowe, H., Marmor, S. & Luo, J. 2007. SIRT1 transgenic mice show phenotypes resembling calorie restriction. *Aging Cell*, 6, 759-767.

Bosutti, A. & Degens, H. 2015. The impact of resveratrol and hydrogen peroxide on muscle cell plasticity shows a dose-dependent interaction. *Scientific Reports*, 5.

Brenmoehl, J. & Hoeflich, A. 2013. Dual control of mitochondrial biogenesis by sirtuin 1 and sirtuin 3. *Mitochondrion*.

Brown, D. M., Parr, T. & Brameld, J. M. 2012. Myosin heavy chain mRNA isoforms are expressed in two distinct cohorts during C2C12 myogenesis. *Journal of muscle research and cell motility*, 32, 383-390.

Brown, S. & Stickland, N. 1993. Satellite cell content in muscles of large and small mice. *Journal of Anatomy*, 183, 91.

Bruunsgaard, H., Andersen-Ranberg, K., Hjelmberg, J., Pedersen, B. & Jeune, B. 2003a. Elevated levels of tumor necrosis factor alpha and mortality in centenarians. *American Journal of Medicine*, 115, 278-283.

Bruunsgaard, H., Ladelund, S., Pedersen, A. N., Schroll, M., Jørgensen, T. & Pedersen, B. 2003b. Predicting death from tumour necrosis factor-alpha and interleukin - 6 in 80 - year - old people. *Clinical & Experimental Immunology*, 132, 24-31.

Bruunsgaard, H., Ladelund, S., Pedersen, A. N., Schroll, M., Jørgensen, T. & Pedersen, B. K. 2003c. Predicting death from tumour necrosis factor-alpha and interleukin-6 in 80-year-old people. *Clin Exp Immunol*, 132, 24-31.

Bruunsgaard, H. & Pedersen, B. K. 2003. Age-related inflammatory cytokines and disease. *Immunol Allergy Clin North Am*, 23, 15-39.

Brüünsgaard, H. & Pedersen, B. K. 2003. Age-related inflammatory cytokines and disease. *Immunology and allergy clinics of North America*, 23, 15-39.

Buckingham, M., Bajard, L., Chang, T., Daubas, P., Hadchouel, J., Meilhac, S., Montarras, D., Rocancourt, D. & Relaix, F. 2003. The formation of skeletal muscle: from somite to limb. *Journal of Anatomy*, 202, 59-68.

Bustin, S. A., Benes, V., Garson, J. A., Hellems, J., Huggett, J., Kubista, M., Mueller, R., Nolan, T., Pfaffl, M. W., Shipley, G. L., Vandesompele, J. & Wittwer, C. T. 2009. The MIQE guidelines: minimum information for publication of quantitative real-time PCR experiments. *Clin Chem*, 55, 611-22.

Canto, C. & Auwerx, J. 2008. Glucose restriction: Longevity SIRTainly, but without building muscle? *Developmental Cell*, 14, 642-644.

Carafa, V., Rotili, D., Forgione, M., Cuomo, F., Serretiello, E., Hailu, G. S., Jarho, E., Lahtela-Kakkonen, M., Mai, A. & Altucci, L. 2016. Sirtuin functions and modulation: from chemistry to the clinic. *Clinical epigenetics*, 8, 61.

Cartee, G., Kietzke, E. & Briggs-Tung, C. 1994. Adaptation of muscle glucose transport with caloric restriction in adult, middle-aged, and old rats. *American Journal of Physiology-Regulatory, Integrative and Comparative Physiology*, 266, R1443-R1447.

Carter, C. S., Hofer, T., Seo, A. Y. & Leeuwenburgh, C. 2007. Molecular mechanisms of life- and health-span extension: role of calorie restriction and exercise intervention. *Applied Physiology, Nutrition & Metabolism*, 32, 954-966.

Carter, C. S., Leeuwenburgh, C., Daniels, M. & Foster, T. C. 2009. Influence of Calorie Restriction on Measures of Age-Related Cognitive Decline: Role of Increased Physical Activity. *Journals of Gerontology Series A: Biological Sciences & Medical Sciences*, 64A, 850-859.

Cerletti, M., Jang, Y. C., Finley, L. W., Haigis, M. C. & Wagers, A. J. 2012. Short-term calorie restriction enhances skeletal muscle stem cell function. *Cell stem cell*, 10, 515-519.

Chamberlain, J. S., Jaynes, J. B. & Hauschka, S. D. 1985. Regulation of creatine kinase induction in differentiating mouse myoblasts. *Molecular and Cellular Biology*, 5, 484-492.

Charge, S. B. P. & Rudnicki, M. A. 2004. Cellular and molecular regulation of muscle regeneration. *Physiological Reviews*, 84, 209-238.

Chen, B., Han, B. H., Sun, X. H. & Lim, R. W. 1997. Inhibition of muscle-specific gene expression by Id3: requirement of the C-terminal region of the protein for stable expression and function. *Nucleic Acids Research*, 25, 423-430.

Chen, D., Bruno, J., Easlson, E., Lin, S.-J., Cheng, H.-L., Alt, F. W. & Guarente, L. 2008. Tissue-specific regulation of SIRT1 by calorie restriction. *Genes & Development*, 22, 1753-1757.

Chin, E. R., Olson, E. N., Richardson, J. A., Yang, Q., Humphries, C., Shelton, J. M., Wu, H., Zhu, W., Bassel-Duby, R. & Williams, R. S. 1998. A

calcineurin-dependent transcriptional pathway controls skeletal muscle fiber type. *Genes & Development*, 12, 2499-2509.

Clancy, D. J., Gems, D., Harshman, L. G., Oldham, S., Stocker, H., Hafen, E., Leivers, S. J. & Partridge, L. 2001. Extension of life-span by loss of CHICO, a *Drosophila* insulin receptor substrate protein. *Science*, 292, 104-106.

Clempus, R. E., Sorescu, D., Dikalova, A. E., Pounkova, L., Jo, P., Sorescu, G. P., Lassègue, B. & Griendling, K. K. 2007. Nox4 is required for maintenance of the differentiated vascular smooth muscle cell phenotype. *Arteriosclerosis, thrombosis, and vascular biology*, 27, 42-48.

Cohen, H., Miller, C., Bitterman, K., Wall, N., Hekking, B., Kessler, B., Howitz, K., Gorospe, M., Cabo, R. And Sinclair, D. 2004. Calorie restriction promotes mammalian cell survival by inducing the SIRT1 deacetylase. *Science (Washington)*, 305, 390-392.

Colman, R. J., Anderson, R. M., Johnson, S. C., Kastman, E. K., Kosmatka, K. J., Beasley, T. M., Allison, D. B., Cruzen, C., Simmons, H. A. & Kemnitz, J. W. 2009. Caloric restriction delays disease onset and mortality in rhesus monkeys. *Science*, 325, 201-204.

Colman, R. J., Beasley, T. M., Allison, D. B. & Weindruch, R. 2008. Attenuation of sarcopenia by dietary restriction in rhesus monkeys. *The Journals of Gerontology Series A: Biological Sciences and Medical Sciences*, 63, 556-559.

Cooper, R. N., Tajbakhsh, S., Mouly, V., Cossu, G., Buckingham, M. & Butler-Browne, G. S. 1999. In vivo satellite cell activation via Myf5 and MyoD in regenerating mouse skeletal muscle. *J Cell Sci*, 112 (Pt 17), 2895-901.

Deane, C. S., Hughes, D. C., Sculthorpe, N., Lewis, M. P., Stewart, C. E. & Sharples, A. P. 2013. Impaired hypertrophy in myoblasts is improved with testosterone administration. *J Steroid Biochem Mol Biol*, 138, 152-61.

Dimchev, G. A., Al-Shanti, N. & Stewart, C. E. 2013. Phospho-tyrosine phosphatase inhibitor Bpv (Hopic) enhances C2C12 myoblast migration in vitro. Requirement of PI3K/AKT and MAPK/ERK pathways. *Journal of muscle research and cell motility*, 34, 125-136.

Edström, E., Altun, M., Hägglund, M. & Ulfhake, B. 2006. Atrogin-1/MAFbx and MuRF1 are downregulated in aging-related loss of skeletal muscle. *The Journals of Gerontology Series A: Biological Sciences and Medical Sciences*, 61, 663-674.

Elkalaf, M., Anděl, M. & Trnka, J. 2013. Low Glucose but Not Galactose Enhances Oxidative Mitochondrial Metabolism in C2C12 Myoblasts and Myotubes. *plos one*, 8, e70772.

Fontana, L. & Klein, S. 2007. Aging, adiposity, and calorie restriction. *Jama*, 297, 986-994.

Fontana, L., Klein, S. & Holloszy, J. O. 2006. Long-term low-protein, low-calorie diet and endurance exercise modulate metabolic factors associated with cancer risk. *The American journal of clinical nutrition*, 84, 1456-1462.

Fontana, L., Partridge, L. & Longo, V. D. 2010. Extending healthy life span—from yeast to humans. *Science*, 328, 321-326.

Fröjdö, S., Durand, C., Molin, L., Carey, A. L., El-Osta, A., Kingwell, B. A., Febbraio, M. A., Solari, F., Vidal, H. & Pirola, L. 2011. Phosphoinositide 3-kinase as a novel functional target for the regulation of the insulin signaling pathway by SIRT1. *Molecular and Cellular Endocrinology*, 335, 166-176.

Fulco, M., Cen, Y., Zhao, P., Hoffman, E. P., Mcburney, M. W., Sauve, A. A. & Sartorelli, V. 2008. Glucose restriction inhibits skeletal myoblast differentiation by activating SIRT1 through AMPK-mediated regulation of Nampt. *Developmental Cell*, 14, 661-673.

Gertz, M., Nguyen, G. T. T., Fischer, F., Suenkel, B., Schlicker, C., Fränzel, B., Tomaschewski, J., Aladini, F., Becker, C. & Wolters, D. 2012. A molecular mechanism for direct sirtuin activation by resveratrol. *plos one*, 7, e49761.

Giannakou, M. E. & Partridge, L. 2007. Role of insulin-like signalling in *Drosophila* lifespan. *Trends in Biochemical Sciences*, 32, 180-188.

Greiwe, J. S., Cheng, B., Rubin, D. C., Yarasheski, K. E. & Semenkovich, C. F. 2001. Resistance exercise decreases skeletal muscle tumor necrosis factor α in frail elderly humans. *The FASEB Journal*, 15, 475-482.

Gurd, B. J., Yoshida, Y., Mcfarlan, J. T., Holloway, G. P., Moyes, C. D., Heigenhauser, G. J., Spriet, L. & Bonen, A. 2011. Nuclear SIRT1 activity, but not protein content, regulates mitochondrial biogenesis in rat and human skeletal muscle. *American Journal of Physiology-Regulatory, Integrative and Comparative Physiology*, 301, R67-R75.

Hao, C., Hao, J., Wang, W., Han, Z., Li, G., Zhang, L., Zhao, X. & Yu, G. 2011. Insulin sensitizing effects of oligomannuronate-chromium (III) complexes in C2C12 skeletal muscle cells. *plos one*, 6, e24598.

Hao, E., Yim, S. V., Chung, J. H., Yoon, K. S., Kang, I., Cho, Y. H. & Baik, H. H. 2006. Melatonin stimulates glucose transport via insulin receptor substrate - 1/phosphatidylinositol 3 - kinase pathway in C2C12 murine skeletal muscle cells. *Journal of pineal research*, 41, 67-72.

Harper, J. M., Leathers, C. W. & Austad, S. N. 2006. Does caloric restriction extend life in wild mice? *Aging Cell*, 5, 441-449.

Hekimi, S. & Guarente, L. 2003. Genetics and the Specificity of the Aging Process. *Science*, 299, 1351-1354.

Hepple, R. T., Qin, M., Nakamoto, H. & Goto, S. 2008. Caloric restriction optimizes the proteasome pathway with aging in rat plantaris muscle: implications for sarcopenia. *American Journal of Physiology-Regulatory, Integrative and Comparative Physiology*, 295, R1231-R1237.

Herranz, D., Munoz-Martin, M., Canamero, M., Mulero, F., Martinez-Pastor, B., Fernandez-Capetillo, O. & Serrano, M. 2010. Sirt1 improves healthy ageing and protects from metabolic syndrome-associated cancer. *Nat Commun*, 1, 3.

Higashida, K., Kim, S. H., Jung, S. R., Asaka, M., Holloszy, J. O. & Han, D.-H. 2013. Effects of resveratrol and SIRT1 on PGC-1 α activity and mitochondrial biogenesis: a reevaluation. *PLoS Biol*, 11, e1001603.

Holloszy, J. O. & Fontana, L. 2007. Caloric restriction in humans. *Experimental gerontology*, 42, 709-712.

Holzenberger, M., Dupont, J., Ducos, B., Leneuve, P., G elo en, A., Even, P. C., Cervera, P. & Le Bouc, Y. 2003. IGF-1 receptor regulates lifespan and resistance to oxidative stress in mice. *Nature*, 421, 182-187.

Howitz, K. T., Bitterman, K. J., Cohen, H. Y., Lamming, D. W., Lavu, S., Wood, J. G., Zipkin, R. E., Chung, P., Kisielewski, A. & Zhang, L.-L. 2003. Small molecule activators of sirtuins extend *Saccharomyces cerevisiae* lifespan. *Nature*, 425, 191-196.

Hughes, D. C., Stewart, C. E., Sculthorpe, N., Dugdale, H. F., Yousefian, F., Lewis, M. P. & Sharples, A. P. 2016. Testosterone enables growth and hypertrophy in fusion impaired myoblasts that display myotube atrophy: deciphering the role of androgen and IGF-I receptors. *Biogerontology*, 17, 619-39.

Inoki, K., Zhu, T. & Guan, K.-L. 2003. TSC2 Mediates Cellular Energy Response to Control Cell Growth and Survival. *Cell*, 115, 577-590.

Inoue, T., Hiratsuka, M., Osaki, M. & Oshimura, M. 2007. The molecular biology of mammalian SIRT proteins - SIRT2 in cell cycle regulation. *Cell Cycle*, 6, 1011-1018.

Jacquemin, V., Furling, D., Bigot, A., Butler-Browne, G. & Mouly, V. 2004. IGF-1 induces human myotube hypertrophy by increasing cell recruitment. *Experimental Cell Research*, 299, 148-158.

Janssen, I. & Ross, R. 1999. Effects of sex on the change in visceral, subcutaneous adipose tissue and skeletal muscle in response to weight loss. *International journal of obesity and related metabolic disorders: journal of the International Association for the Study of Obesity*, 23, 1035-1046.

Jen, Y., Weintraub, H. & Benezra, R. 1992. Overexpression of Id protein inhibits the muscle differentiation program: in vivo association of Id with E2A proteins. *Genes & Development*, 6, 1466-1479.

Jia, Y.-Y., Lu, J., Huang, Y., Liu, G., Gao, P., Wan, Y.-Z., Zhang, R., Zhang, Z.-Q., Yang, R.-F. & Tang, X. 2014. The involvement of NFAT transcriptional activity suppression in SIRT1-mediated inhibition of COX-2 expression induced by PMA/Ionomycin. *plos one*, 9, e97999.

Kaeberlein, M., Mcvey, M. & Guarente, L. 1999. The SIR2/3/4 complex and SIR2 alone promote longevity in *Saccharomyces cerevisiae* by two different mechanisms. *Genes & Development*, 13, 2570-2580.

Kaeberlein, T. L., Smith, E. D., Tsuchiya, M., Welton, K. L., Thomas, J. H., Fields, S., Kennedy, B. K. & Kaeberlein, M. 2006. Lifespan extension in *Caenorhabditis elegans* by complete removal of food. *Aging Cell*, 5, 487-494.

Kaminski, J., Lançon, A., Aires, V., Limagne, E., Tili, E., Michaille, J.-J. & Latruffe, N. 2012. Resveratrol initiates differentiation of mouse skeletal muscle-derived C2C12 myoblasts. *Biochemical Pharmacology*, 84, 1251-1259.

Kauppinen, T. M., Gan, L. & Swanson, R. A. 2013. Poly(ADP-ribose) polymerase-1-induced NAD⁺ depletion promotes nuclear factor-κB transcriptional activity by preventing p65 de-acetylation. *Biochimica et Biophysica Acta (BBA) - Molecular Cell Research*, 1833, 1985-1991.

Kenyon, C. 2011. The first long-lived mutants: discovery of the insulin/IGF-1 pathway for ageing. *Philosophical Transactions of the Royal Society of London B: Biological Sciences*, 366, 9-16.

Khodabukus, A. & Baar, K. 2014. Glucose concentration and streptomycin alter in vitro muscle function and metabolism. *Journal of Cellular Physiology*.

Khodabukus, A. & Baar, K. 2015. Glucose concentration and streptomycin alter in vitro muscle function and metabolism. *Journal of Cellular Physiology*, 230, 1226-1234.

Koltai, E., Bori, Z., Chabert, C., Dubouchaud, H., Naito, H., Machida, S., Davies, K. J., Murlasits, Z., Fry, A. C., Boldogh, I. & Radak, Z. 2017.

SIRT1 may play a crucial role in overload induced hypertrophy of skeletal muscle. *J Physiol*.

Lagirand-Cantaloube, J., Cornille, K., Csibi, A., Batonnet-Pichon, S., Leibovitch, M. P. & Leibovitch, S. A. 2009. Inhibition of atrogen-1/MAFbx mediated MyoD proteolysis prevents skeletal muscle atrophy in vivo. *plos one*, 4, e4973.

Lam, Y. Y., Peterson, C. M. & Ravussin, E. 2013. Resveratrol vs. Calorie Restriction: Data from Rodents to Humans. *Experimental gerontology*.

Larson-Meyer, D. E., Heilbronn, L. K., Redman, L. M., Newcomer, B. R., Frisard, M. I., Anton, S., Smith, S. R., Alfonso, A. & Ravussin, E. 2006. Effect of calorie restriction with or without exercise on insulin sensitivity, β -cell function, fat cell size, and ectopic lipid in overweight subjects. *Diabetes care*, 29, 1337-1344.

Lassar, A. B., Buskin, J. N., Lockshon, D., Davis, R. L., Apone, S., Hauschka, S. D. & Weintraub, H. 1989. MyoD is a sequence-specific DNA binding protein requiring a region of myc homology to bind to the muscle creatine kinase enhancer. *Cell*, 58, 823-831.

Léger, B., Derave, W., De Bock, K., Hespel, P. & Russell, A. P. 2008. Human sarcopenia reveals an increase in SOCS-3 and myostatin and a reduced efficiency of Akt phosphorylation. *Rejuvenation research*, 11, 163-175B.

Lightfoot, A. P., McCormick, R., Nye, G. A. & Mcardle, A. 2014. Mechanisms of skeletal muscle ageing; avenues for therapeutic intervention. *Current Opinion in Pharmacology*, 16, 116-121.

Longo, V. D. & Mattson, M. P. 2014. Fasting: Molecular Mechanisms and Clinical Applications. *Cell metabolism*, 19, 181-192.

Maggs, D., Jacob, R., Rife, F., Lange, R., Leone, P., During, M., Tamborlane, W. & Sherwin, R. 1995. Interstitial fluid concentrations of glycerol, glucose, and amino acids in human quadriceps muscle and adipose tissue. Evidence for significant lipolysis in skeletal muscle. *Journal of Clinical Investigation*, 96, 370.

Mahoney, L. B., Denny, C. A. & Seyfried, T. N. 2006. Caloric restriction in C57BL/6J mice mimics therapeutic fasting in humans. *Lipids in Health and Disease*, 5, 13-13.

Masoro, E. J. 2005. Overview of caloric restriction and ageing. *Mechanisms of Ageing and Development*, 126, 913-922.

Mattison, J. A., Roth, G. S., Beasley, T. M., Tilmont, E. M., Handy, A. M., Herbert, R. L., Longo, D. L., Allison, D. B., Young, J. E. & Bryant, M. 2012. Impact of caloric restriction on health and survival in rhesus monkeys from the NIA study. *Nature*.

Mccay, C., Crowell, M. F. & Maynard, L. 1935. The effect of retarded growth upon the length of life span and upon the ultimate body size. *J Nutr*, 10, 63-79.

Mccay, C. M., Maynard, L., Sperling, G. & Barnes, L. L. 1939. Retarded Growth, Life Span, Ultimate Body Size and Age Changes in the Albino Rat after Feeding Diets Restricted in Calories Four Figures. *The Journal of Nutrition*, 18, 1-13.

Mckiernan, S. H., Bua, E., Mcgorray, J. & Aiken, J. 2004. Early-onset calorie restriction conserves fiber number in aging rat skeletal muscle. *The FASEB Journal*, 18, 580-581.

Mckiernan, S. H., Colman, R. J., Lopez, M., Beasley, T. M., Aiken, J. M., Anderson, R. M. & Weindruch, R. 2011. Caloric restriction delays aging-induced cellular phenotypes in rhesus monkey skeletal muscle. *Experimental gerontology*, 46, 23-29.

Mcpheeron, A. C. & Lee, S.-J. 1997. Double muscling in cattle due to mutations in the myostatin gene. *Proceedings of the National Academy of Sciences*, 94, 12457-12461.

Mercken, E. M., Crosby, S. D., Lamming, D. W., Jebrailey, L., Krzysik-Walker, S., Villareal, D. T., Capri, M., Franceschi, C., Zhang, Y. & Becker, K. 2013. Calorie restriction in humans inhibits the PI3K/AKT pathway and induces a younger transcription profile. *Aging Cell*, 12, 645-651.

Mercken, E. M., Hu, J., Krzysik-Walker, S., Wei, M., Li, Y., Mcburney, M. W., Cabo, R. & Longo, V. D. 2014a. SIRT1 but not its increased expression is essential for lifespan extension in caloric-restricted mice. *Aging Cell*, 13, 193-196.

Mercken, E. M., Mitchell, S. J., Martin-Montalvo, A., Minor, R. K., Almeida, M., Gomes, A. P., Scheibye-Knudsen, M., Palacios, H. H., Licata, J. J. & Zhang, Y. 2014b. SRT2104 extends survival of male mice on a standard diet and preserves bone and muscle mass. *Aging Cell*, 13, 787-796.

Milan, G., Romanello, V., Pescatore, F., Armani, A., Paik, J.-H., Frasson, L., Seydel, A., Zhao, J., Abraham, R. & Goldberg, A. L. 2015. Regulation of autophagy and the ubiquitin-proteasome system by the FoxO transcriptional network during muscle atrophy. *Nature communications*, 6.

Montesano, A., Luzi, L., Senesi, P., Mazzocchi, N. & Terruzzi, I. 2013. Resveratrol promotes myogenesis and hypertrophy in murine myoblasts. *Journal of translational medicine*, 11, 310.

Nakashima, K. & Yakabe, Y. 2007. AMPK activation stimulates myofibrillar protein degradation and expression of atrophy-related ubiquitin ligases by increasing FOXO transcription factors in C2C12 myotubes. *Bioscience, biotechnology, and biochemistry*, 71, 1650-1656.

Napper, A. D., Hixon, J., Mcdonagh, T., Keavey, K., Pons, J.-F., Barker, J., Yau, W. T., Amouzegh, P., Flegg, A. & Hamelin, E. 2005. Discovery of indoles as potent and selective inhibitors of the deacetylase SIRT1. *Journal of medicinal chemistry*, 48, 8045-8054.

Pearson, K. J., Baur, J. A., Lewis, K. N., Peshkin, L., Price, N. L., Labinskyy, N., Swindell, W. R., Kamara, D., Minor, R. K. & Perez, E. 2008. Resveratrol delays age-related deterioration and mimics transcriptional aspects of dietary restriction without extending life span. *Cell metabolism*, 8, 157-168.

Pete, G., Fuller, C. R., Oldham, J. M., Smith, D. R., D'ercole, A. J., Kahn, C. R. & Lund, P. K. 1999. Postnatal Growth Responses to Insulin-Like Growth Factor I in Insulin Receptor Substrate-1-Deficient Mice 1. *Endocrinology*, 140, 5478-5487.

Phillips, T. & Leeuwenburgh, C. 2005. Muscle fiber specific apoptosis and TNF- α signaling in sarcopenia are attenuated by life-long calorie restriction. *The FASEB Journal*, 19, 668-670.

Piper, M., Selman, C., Mcelwee, J. & Partridge, L. 2008. Separating cause from effect: how does insulin/IGF signalling control lifespan in worms, flies and mice? *Journal of internal medicine*, 263, 179-191.

Price, N. L., Gomes, A. P., Ling, A. J., Duarte, F. V., Martin-Montalvo, A., North, B. J., Agarwal, B., Ye, L., Ramadori, G. & Teodoro, J. S. 2012. SIRT1 is required for AMPK activation and the beneficial effects of resveratrol on mitochondrial function. *Cell metabolism*, 15, 675-690.

Quinn, L. S., Anderson, B. G. & Plymate, S. R. 2007. Muscle-specific overexpression of the type 1 IGF receptor results in myoblast-independent muscle hypertrophy via PI3K, and not calcineurin, signaling. *American Journal of Physiology-Endocrinology and Metabolism*, 293, E1538-E1551.

Rehfeldt, C., Renne, U., Sawitzky, M., Binder, G. & Hoeflich, A. 2010. Increased fat mass, decreased myofiber size, and a shift to glycolytic muscle metabolism in adolescent male transgenic mice overexpressing IGFBP-2. *American Journal of Physiology-Endocrinology and Metabolism*, 299, E287-E298.

Rodgers, J. T., Lerin, C., Haas, W., Gygi, S. P., Spiegelman, B. M. & Puigserver, P. 2005a. Nutrient control of glucose homeostasis through a complex of PGC-1 α and SIRT1. *Nature*, 434, 113-118.

Rodgers, J. T., Lerin, C., Haas, W., Gygi, S. P., Spiegelman, B. M. & Puigserver, P. 2005b. Nutrient control of glucose homeostasis through a complex of PGC-1 α and SIRT1. *Nature*, 434, 113-118.

Rommel, C., Bodine, S. C., Clarke, B. A., Rossman, R., Nunez, L., Stitt, T. N., Yancopoulos, G. D. & Glass, D. J. 2001. Mediation of IGF-1-induced skeletal myotube hypertrophy by PI(3)K/Akt/mTOR and PI(3)K/Akt/GSK3 pathways. *Nat Cell Biol*, 3, 1009-1013.

Ropka-Molik, K., Eckert, R. & Piorkowska, K. 2011. The expression pattern of myogenic regulatory factors MyoD, Myf6 and Pax7 in postnatal porcine skeletal muscles. *Gene Expression Patterns*, 11, 79-83.

Ross, R., Dagnone, D., Jones, P. J., Smith, H., Paddags, A., Hudson, R. & Janssen, I. 2000. Reduction in obesity and related comorbid conditions after diet-induced weight loss or exercise-induced weight loss in men: A randomized, controlled trial. *Annals of Internal Medicine*, 133, 92-103.

Roth, G. S., Lane, M. A., Ingram, D. K., Mattison, J. A., Elahi, D., Tobin, J. D., Muller, D. & Metter, E. J. 2002. Biomarkers of caloric restriction may predict longevity in humans. *Science*, 297, 811-811.

Rudnicki, M. A., Le Grand, F., Mckinnell, L. & Kuang, S. 2008. The Molecular Regulation of Muscle Stem Cell Function. *In: Stillman, B., Stewart, S. & Grodzicker, T. (eds.) Control and Regulation of Stem Cells.*

Saini, A., Al-Shanti, N., Sharples, A. & Stewart, C. 2012. Sirtuin 1 regulates skeletal myoblast survival and enhances differentiation in the presence of resveratrol. *Experimental Physiology*, 1-19.

Sandri, M., Sandri, C., Gilbert, A., Skurk, C., Calabria, E., Picard, A., Walsh, K., Schiaffino, S., Lecker, S. H. & Goldberg, A. L. 2004. Foxo transcription factors induce the atrophy-related ubiquitin ligase atrogin-1 and cause skeletal muscle atrophy. *Cell*, 117, 399-412.

Sasaki, T., Maier, B., Koclega, K. D., Chruszcz, M., Gluba, W., Stukenberg, P. T., Minor, W. & Scoble, H. 2008. Phosphorylation regulates SIRT1 function. *plos one*, 3, e4020.

Schmittgen, T. D. & Livak, K. J. 2008. Analyzing real-time PCR data by the comparative CT method. *Nature protocols*, 3, 1101-1108.

Scimè, A. & Rudnicki, M. A. 2006. Anabolic potential and regulation of the skeletal muscle satellite cell populations. *Current Opinion in Clinical Nutrition & Metabolic Care*, 9, 214-219.

Selman, C. 2014. Dietary restriction and the pursuit of effective mimetics. *Proceedings of the Nutrition Society*, 73, 260-270.

Selman, C., Lingard, S., Choudhury, A. I., Batterham, R. L., Claret, M., Clements, M., Ramadani, F., Okkenhaug, K., Schuster, E. & Blanc, E.

2008. Evidence for lifespan extension and delayed age-related biomarkers in insulin receptor substrate 1 null mice. *The FASEB Journal*, 22, 807-818.

Selman, C., Partridge, L. & Withers, D. J. 2011. Replication of extended lifespan phenotype in mice with deletion of insulin receptor substrate 1. *plos one*, 6, e16144.

Sharples, A., Al-Shanti, N. & And Stewart, C. 2010. C2 and C2C12 Murine Skeletal Myoblast models of Atrophic and Hypertrophic potential: Relevance to disease and ageing?

Sharples, A., Al-Shanti, N., Lewis, M. & Stewart, C. 2011. Reduction of Myoblast Differentiation following multiple population doubling in mouse C2C12 Cells: A model to investigate ageing? *Journal of Cellular Biochemistry*, 112, 3773-3785.

Sharples, A. P., Al-Shanti, N., Hughes, D. C., Lewis, M. P. & Stewart, C. E. 2013a. The role of insulin-like-growth factor binding protein 2 (IGFBP2) and phosphatase and tensin homologue (PTEN) in the regulation of myoblast differentiation and hypertrophy. *Growth Horm IGF Res*, 23, 53-61.

Sharples, A. P., Al-Shanti, N., Hughes, D. C., Lewis, M. P. & Stewart, C. E. 2013b. The role of insulin-like-growth factor binding protein 2 (IGFBP2) and phosphatase and tensin homologue (PTEN) in the regulation of myoblast differentiation and hypertrophy. *Growth Hormone & IGF Research*, 23, 53-61.

Sharples, A. P., Hughes, D. C., Deane, C. S., Saini, A., Selman, C. & Stewart, C. E. 2015. Longevity and skeletal muscle mass: the role of IGF signalling, the sirtuins, dietary restriction and protein intake. *Aging Cell*, 14, 511-523.

Simms, D., Cizdziel, P. E. & Chomczynski, P. 1993. TRIzol: A new reagent for optimal single-step isolation of RNA. *Focus*, 15, 532-535.

Smith, P., Krohn, R. I., Hermanson, G., Mallia, A., Gartner, F., Provenzano, M., Fujimoto, E., Goeke, N., Olson, B. & Klenk, D. 1985. Measurement of protein using bicinchoninic acid. *Analytical biochemistry*, 150, 76-85.

Solomon, J. M., Pasupuleti, R., Xu, L., Mcdonagh, T., Curtis, R., Distefano, P. S. & Huber, L. J. 2006. Inhibition of SIRT1 catalytic activity increases p53 acetylation but does not alter cell survival following DNA damage. *Molecular and Cellular Biology*, 26, 28-38.

Spaulding, C. C., Walford, R. L. & Effros, R. B. 1997a. Calorie restriction inhibits the age-related dysregulation of the cytokines TNF- α and IL-6 in C3B10RF1 mice. *Mechanisms of Ageing and Development*, 93, 87-94.

Spaulding, C. C., Walford, R. L. & Effros, R. B. 1997b. Calorie restriction inhibits the age-related dysregulation of the cytokines TNF- α and IL-6 in C3B10RF1 mice. *Mechanisms of Ageing and Development*, 93, 87-94.

Staiger, H., Kaltenbach, S., Staiger, K., Stefan, N., Fritsche, A., Guirguis, A., Péterfi, C., Weisser, M., Machicao, F. & Stumvoll, M. 2004. Expression of adiponectin receptor mRNA in human skeletal muscle cells is related to in vivo parameters of glucose and lipid metabolism. *Diabetes*, 53, 2195-2201.

Steitz, S. A., Speer, M. Y., Curinga, G., Yang, H.-Y., Haynes, P., Aebbersold, R., Schinke, T., Karsenty, G. & Giachelli, C. M. 2001. Smooth muscle cell phenotypic transition associated with calcification upregulation of cbfa1 and downregulation of smooth muscle lineage markers. *Circulation Research*, 89, 1147-1154.

Stewart, C. & Rotwein, P. 1996. Growth, differentiation, and survival: multiple physiological functions for insulin-like growth factors. *Physiological Reviews*, 76, 1005-1026.

Stitt, T. N., Drujan, D., Clarke, B. A., Panaro, F., Timofeyeva, Y., Kline, W. O., Gonzalez, M., Yancopoulos, G. D. & Glass, D. J. 2004. The IGF-1/PI3K/Akt pathway prevents expression of muscle atrophy-induced ubiquitin ligases by inhibiting FOXO transcription factors. *Molecular Cell*, 14, 395-403.

Tatar, M., Bartke, A. & Antebi, A. 2003. The endocrine regulation of aging by insulin-like signals. *Science*, 299, 1346-1351.

Timmers, S., Konings, E., Bilet, L., Houtkooper, R. H., Van De Weijer, T., Goossens, G. H., Hoeks, J., Van Der Krieken, S., Ryu, D., Kersten, S., Moonen-Kornips, E., Hesselink, M. K. C., Kunz, I., Schrauwen-Hinderling, V. B., Blaak, E. E., Auwerx, J. & Schrauwen, P. 2011. Calorie Restriction-like Effects of 30 Days of Resveratrol Supplementation on Energy Metabolism and Metabolic Profile in Obese Humans. *Cell metabolism*, 14, 612-622.

Tollefsen, S. E., Sadow, J. L. & Rotwein, P. 1989. Coordinate expression of insulin-like growth factor II and its receptor during muscle differentiation. *Proceedings of the National Academy of Sciences*, 86, 1543-1547.

Towbin, H., Staehelin, T. & Gordon, J. 1979. Electrophoretic transfer of proteins from polyacrylamide gels to nitrocellulose sheets: procedure and some applications. *Proceedings of the National Academy of Sciences*, 76, 4350-4354.

Trendelenburg, A. U., Meyer, A., Rohner, D., Boyle, J., Hatakeyama, S. & Glass, D. J. 2009. Myostatin reduces Akt/TORC1/p70S6K signaling,

inhibiting myoblast differentiation and myotube size. *American Journal of Physiology-Cell Physiology*, 296, C1258-C1270.

Vallejo, A. N., Michel, J. J., Bale, L. K., Lemster, B. H., Borghesi, L. & Conover, C. A. 2009. Resistance to age-dependent thymic atrophy in long-lived mice that are deficient in pregnancy-associated plasma protein A. *Proceedings of the National Academy of Sciences*, 106, 11252-11257.

Vinciguerra, M., Fulco, M., Ladurner, A., Sartorelli, V. & Rosenthal, N. 2010. SirT1 in muscle physiology and disease: lessons from mouse models. *Disease Models & Mechanisms*, 3, 298-303.

Walford, R. L., Harris, S. B. & Gunion, M. W. 1992. The calorically restricted low-fat nutrient-dense diet in Biosphere 2 significantly lowers blood glucose, total leukocyte count, cholesterol, and blood pressure in humans. *Proceedings of the National Academy of Sciences*, 89, 11533-11537.

Walle, T., Hsieh, F., DeLegge, M. H., Oatis, J. E. & Walle, U. K. 2004. High absorption but very low bioavailability of oral resveratrol in humans. *Drug metabolism and disposition*, 32, 1377-1382.

Wang, D.-T., Yin, Y., Yang, Y.-J., Lv, P.-J., Shi, Y., Lu, L. & Wei, L.-B. 2014. Resveratrol prevents TNF- α -induced muscle atrophy via regulation of Akt/mTOR/FoxO1 signaling in C2C12 myotubes. *International immunopharmacology*, 19, 206-213.

Weindruch, R., Walford, R. L., Fligiel, S. & Guthrie, D. 1986. The retardation of aging in mice by dietary restriction: longevity, cancer, immunity and lifetime energy intake. *J Nutr*, 116, 641-54.

Weiss, E. P., Racette, S. B., Villareal, D. T., Fontana, L., Steger-May, K., Schechtman, K. B., Klein, S., Ehsani, A. A., Holloszy, J. O. & Group, W. U.

S. O. M. C. 2007. Lower extremity muscle size and strength and aerobic capacity decrease with caloric restriction but not with exercise-induced weight loss. *Journal of Applied Physiology*, 102, 634-640.

Yang, H., Yang, T., Baur, J. A., Perez, E., Matsui, T., Carmona, J. J., Lamming, Dudley w., Souza-Pinto, N. C., Bohr, V. A., Rosenzweig, A., De Cabo, R., Sauve, Anthony a. & Sinclair, D. A. 2007. Nutrient-Sensitive Mitochondrial NAD⁺ Levels Dictate Cell Survival. *Cell*, 130, 1095-1107.

Yang, S., Alnaqeeb, M., Simpson, H. & Goldspink, G. 1996. Cloning and characterization of an IGF-1 isoform expressed in skeletal muscle subjected to stretch. *Journal of Muscle Research & Cell Motility*, 17, 487-495.

Zhao, X., Allison, D., Condon, B., Zhang, F., Gheyi, T., Zhang, A., Ashok, S., Russell, M., Macewan, I. & Qian, Y. 2013. The 2.5 Å crystal structure of the SIRT1 catalytic domain bound to nicotinamide adenine dinucleotide (NAD⁺) and an indole (EX527 analogue) reveals a novel mechanism of histone deacetylase inhibition. *Journal of medicinal chemistry*, 56, 963-969.

Zu, Y., Liu, L., Lee, M. Y. K., Xu, C., Liang, Y., Man, R. Y., Vanhoutte, P. M. & Wang, Y. 2010. SIRT1 Promotes Proliferation and Prevents Senescence Through Targeting LKB1 in Primary Porcine Aortic Endothelial Cells. *Circulation Research*, 106, 1384-U184.

9. Appendices

9. Appendix 1

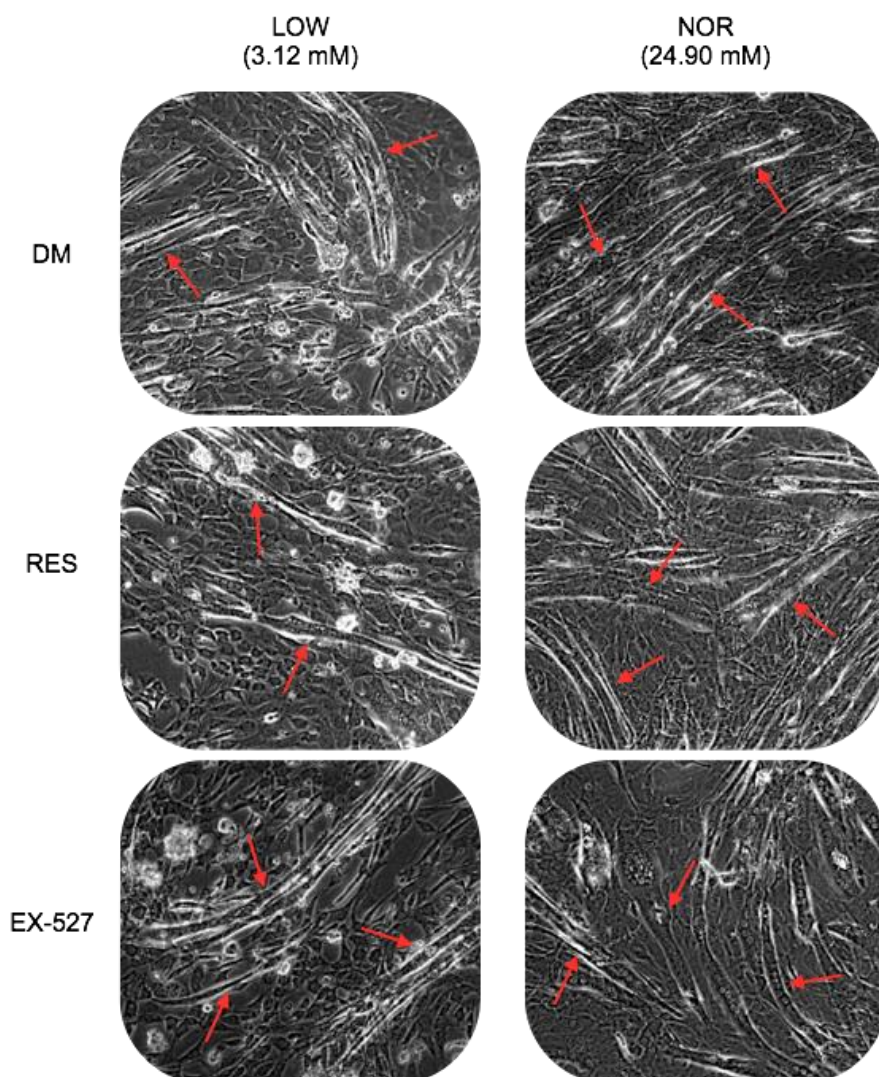


Fig. A1.1. Representative images following 72 h in LOW and NOR glucose alone and with the addition of RES or EX-527.

6.3.1. Low glucose reduces myotube number and promotes myotube atrophy

Following image collection (Fig A1.1) myotube number was analysed at 72 h over time in comparison to a 0 h control, following this incubation a significant interaction between timepoint, glucose concentration and SIRT1 manipulation was observed ($F_{(2, 466)} = 6.55$, $p = 0.002$) as well as between timepoint and glucose concentration ($F_{(1, 466)} = 16.89$, $p < 0.001$). Additionally, all variables: glucose ($F_{(1, 466)} = 9.20$, $p = 0.003$), time ($F_{(1, 466)}$

= 36.81, $p < 0.001$) and SIRT1 manipulation ($F_{(1, 466)} = 7.89$, $p < 0.001$) displayed a significant main effect. No change in myotube area was observed from the 0 h control to 72 h in NOR glucose conditions. There was no change in myotubes grown in NOR conditions with the administration of RES compared with 0 h baseline control myotubes (0 h: 8.25 ± 2.85 vs. NOR: 9.00 ± 2.59 , $p > 0.05$, vs. NOR RES: 8.33 ± 2.74 , $p > 0.05$). By supplementing NOR glucose conditions with SIRT1 inhibitor (EX-527) a reduction in myotube number was observed from 0 h to 72 h (0h vs. NOR EX-527: 9.00 ± 2.59 vs. 5.62 ± 2.94 , $p < 0.001$, Fig 6.2.). All LOW glucose conditions had a significantly reduced number of myotubes following 72 h versus the 0 h control (0 h: 8.25 ± 2.85 vs. LOW: vs. 5.38 ± 2.28 , $p < 0.001$, vs. LOW RES: 5.73 ± 2.97 , $p < 0.001$, vs. LOW EX-527: 5.62 ± 2.94 , $p < 0.001$). However, there was no significant difference observed for this glucose concentration when SIRT1 activity was manipulated (LOW vs. LOW RES: 5.38 ± 2.28 vs. 5.73 ± 2.97 , $p > 0.05$, LOW vs. LOW EX-527: 5.38 ± 2.28 vs. 5.62 ± 2.94 , $p > 0.05$, LOW RES vs. LOW EX-527: 5.38 ± 2.28 vs. 5.62 ± 2.94 , $p > 0.05$).

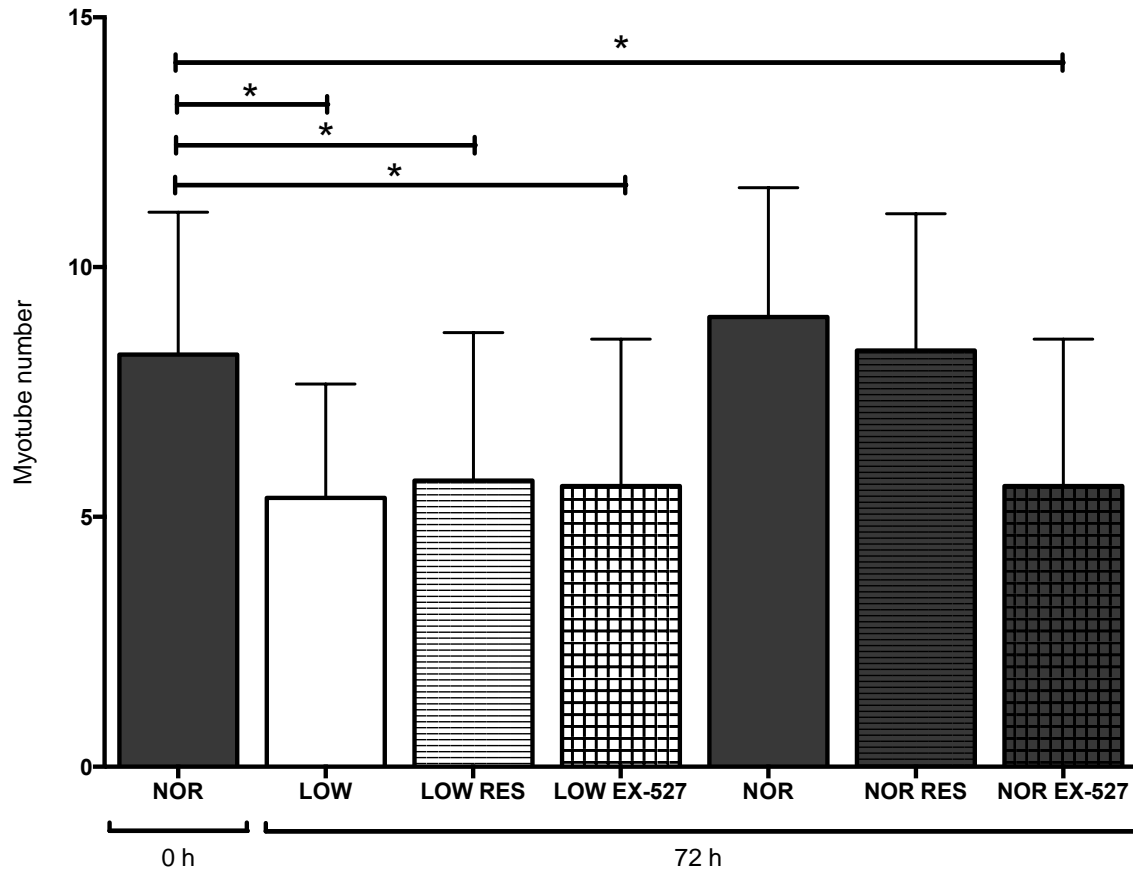


Fig. A1.2. Myotube number following the addition of EX-527 in NOR conditions in comparison to the 0 h control. All LOW glucose conditions were also reduced in comparison to the 0 h control. Significant difference ($p < 0.05$) is denoted using *.

Myotube diameter displayed a significant main effect for time following comparisons between 0 h control and 72 h incubation ($F_{(1, 3661)} = 13.68$, $p < 0.001$) and glucose concentration ($F_{(1, 3661)} = 138.24$, $p < 0.001$) as well as a significant interaction for time x glucose concentration ($F_{(1, 3661)} = 116.42$, $p < 0.001$). There was also a significant increase in diameter for all NOR glucose conditions in comparison to the 0 h control (0 h: 12.86 ± 4.40 vs. NOR: 15.53 ± 5.37 μm , $p < 0.001$, vs. NOR RES: 15.08 ± 5.32 μm , $p < 0.001$, vs. NOR EX-527: 15.23 ± 5.30 μm , $p < 0.001$). Whereas, in LOW glucose there was a significant decrease in diameter from the 0 h control across all conditions (0 h: 12.86 ± 4.40 vs. LOW: 12.01 ± 4.25 μm , $p = 0.033$ (fisher), vs. LOW RES: 11.79 ± 4.32 μm , $p = 0.007$ (fisher), vs. LOW EX-527: 11.71 ± 4.20 μm , $p = 0.004$ (fisher)). There were no significant differences observed at 72 h in low glucose conditions with

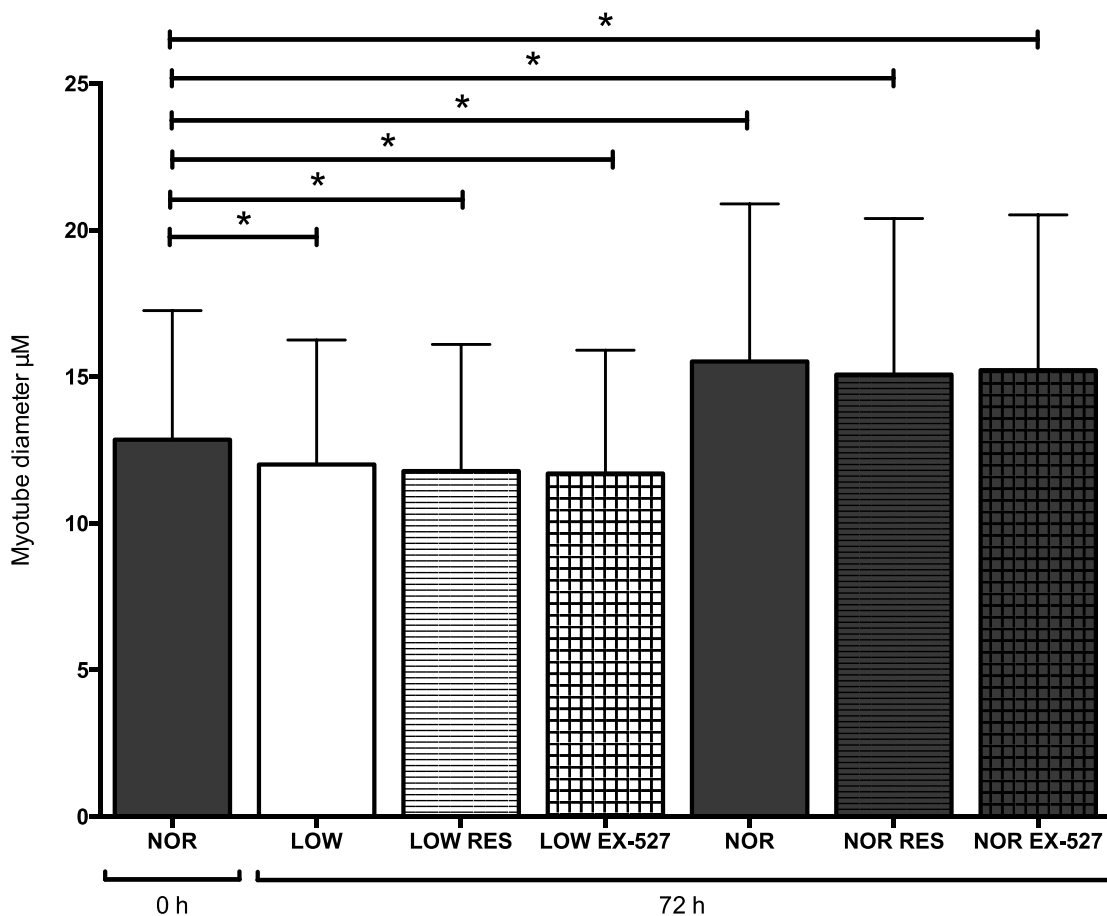


Fig. A1.3. Myotube diameter is reduced in all LOW glucose conditions in comparison to the 0 h control whereas All NOR glucose conditions are significantly increased in comparison o the 0 h control. Repeated measures analysis carried out using 36 images per experimental condition provided significant values between the small changes observed between NOR and LOW glucose. Significant difference ($p < 0.05$) is denoted using *.

activation or inhibition of SIRT1 (All comparisons $p > 0.05$, Fig 6.3.).

Significant interactions were present for myotube area again following a 72 h incubation in comparison to a 0 h control: Timepoint x glucose concentration ($F_{(1, 3723)} = 51.43$, $p < 0.001$), timepoint x SIRT1 manipulation ($F_{(2, 3723)} = 4.28$, $p = 0.014$), and SIRT1 manipulation x glucose ($F_{(2, 3723)} = 3.31$, $p = 0.037$). Significant main effects were also observed for time ($F_{(1, 3723)} = 14.07$, $p < 0.001$), glucose ($F_{(1, 3723)} = 55.86$, $p < 0.001$) and SIRT1 manipulation ($F_{(2, 3723)} = 12.36$, $p < 0.001$). Myotube area increased from 0 h in all NOR conditions (0 h: 2876 ± 1628 vs. NOR: $3785 \pm 2542 \mu\text{m}^2$, $p < 0.001$, vs. NOR RES: $4088 \pm 2728 \mu\text{m}^2$, $p < 0.001$, vs. NOR EX-527: $3433 \pm 2394 \mu\text{m}^2$, $p < 0.001$). However, there was no change from 0 h to 72 h in LOW glucose conditions (0 h: 2876 ± 1628 vs. LOW: $2862 \pm 1947 \mu\text{m}^2$, $p > 0.05$ vs. LOW RES: $2816 \pm 2207 \mu\text{m}^2$, $p = 0.442$, vs. LOW EX-527: $2643 \pm 1743 \mu\text{m}^2$, $p = 0.250$). At 72 h, although there were no increases in myotube size following RES administration in the LOW glucose condition, there was an increase with RES in NOR glucose (LOW vs. LOW RES: vs. $2816 \pm 2207 \mu\text{m}^2$, $p > 0.05$, NOR vs. NOR RES: 3785 ± 2542 vs. $4088 \pm 2728 \mu\text{m}^2$, $p = 0.052$ (fisher)). Additionally, there was a reduction in myotube size with the addition of the SIRT1 inhibitor (EX-527) in NOR conditions; however this reduction was not observed in LOW glucose conditions at 72 h (NOR vs. NOR EX-527: 3785 ± 2542 vs. $3433 \pm 2394 \mu\text{m}^2$, $p = 0.026$ (fisher), LOW vs. LOW EX-527: 2862 ± 1947 vs. $2643 \pm 1743 \mu\text{m}^2$, $p > 0.05$, Fig. 6.4.).

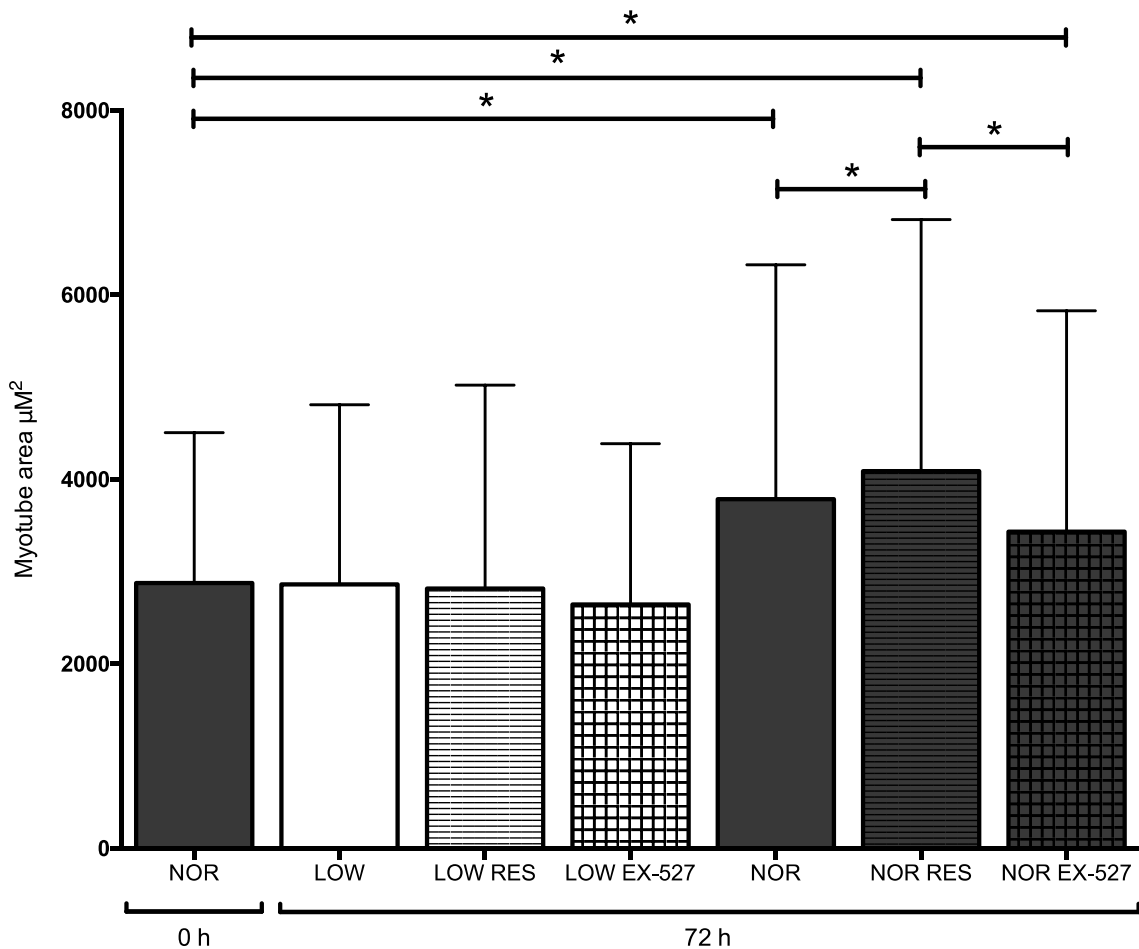


Fig. A1.4. Myotube area is increased in all NOR glucose conditions in comparison to the 0 h control. In NOR glucose RES increases whereas EX-527 decreased area. Significant difference ($p < 0.05$) is denoted using *.

Unlike SIRT1 activation via resveratrol administration improving differentiation at 7D in differentiating myoblasts, altering SIRT1 activity with resveratrol was unable to improve myotube survival/loss or myotube atrophy in low glucose conditions when administered to existing myotube cultures. Importantly however, SIRT1 inhibition (EX-527) reduced myotube number and myotube size and, SIRT1 activation via resveratrol increased myotube area in normal glucose conditions. As such we next wished to assess the impact on important regulators of late differentiation/ myotube maturation such as MRF4 and adult myosin heavy chains (MYHC) 1, 2, 4 and 7 gene expression that would be involved laying contractile proteins for myotube maturation/hypertrophy.

6.3.2. MRF4 was unchanged with resveratrol or SIRT1 inhibitor

As with the morphological data the following gene expression analysis was carried out following a 72 h incubation. Following this 72 h incubation on existing myotubes there were no significant interactions for MRF4 in either of the previous myoblast studies in chapters 3 and 5. MRF4 is involved in late differentiation/early myotube maturation, as such in mature myotubes a significant interaction between glucose and time was observed ($F_{(1, 36)} = 4.86$, $p = 0.034$). There was also a significant main effect for glucose dosing ($F_{(1, 36)} = 4.86$, $p = 0.034$), and time ($F_{(1, 36)} = 64.35$, $p < 0.001$). All conditions were significantly reduced following 72 h compared to the 0 h control (0 h: 1.01 ± 0.19 vs. NOR: 0.48 ± 0.09 , $p = 0.006$, vs. NOR RES: 0.52 ± 0.10 , $p = 0.015$, vs. NOR EX-527: 0.53 ± 0.09 , $p = 0.039$, vs. LOW RES: 0.68 ± 0.20 , $p = 0.008$ (fisher), vs. LOW EX-527: 0.68 ± 0.14 , $p = 0.005$ (fisher)). This was perhaps because myotubes were already formed for 7 days in the 0h control and the peak MRF4 expression occurred earlier in myotube formation vs. 72hrs (total 10 days in differentiation). This reduction in MRF4 at 72 h in all conditions was with the exception of LOW glucose alone, where this did not significantly drop vs. 0h (0 h vs. LOW: 1.01 ± 0.19 vs. 0.83 ± 0.22 , $p > 0.05$). These data suggest a prolonged MRF4 expression in low glucose alone. There were no significant differences with the addition of either of the SIRT1 activation/inhibition within LOW conditions at 72 h (LOW vs. LOW RES: 0.83 ± 0.22 vs. 0.68 ± 0.20 , $p > 0.05$, LOW vs. LOW EX-527: 0.83 ± 0.22 vs. 0.68 ± 0.14 , $p > 0.05$). No significance was observed under SIRT1 manipulations in NOR glucose conditions either. This data reflected the previous observations in myoblast studies (NOR vs. NOR RES: 0.48 ± 0.09 vs. 0.52 ± 0.10 , $p > 0.05$, NOR vs. NOR EX-527: 0.48 ± 0.09 vs. 0.53 ± 0.09 , $p > 0.05$). There was however, significantly delayed reductions in MRF4 in LOW vs. NOR conditions without the supplementation of RES or EX-527 in which no significance was observed (LOW vs. NOR: 0.83 ± 0.22 vs. 0.48 ± 0.09 , $p = 0.007$ (fisher), LOW RES vs. NOR RES: 0.68 ± 0.20 vs. 0.52 ± 0.10 , $p > 0.05$, LOW EX-527 vs. NOR EX-527: 0.68 ± 0.14 vs. 0.53 ± 0.09 , $p > 0.05$), again suggesting that perhaps LOW may be

attempting to improve their delayed impaired differentiation by keeping MRF4 expression higher than NOR conditions. However, RES/SIRT1 inhibitor did not significantly improve MRF4 in low glucose conditions.

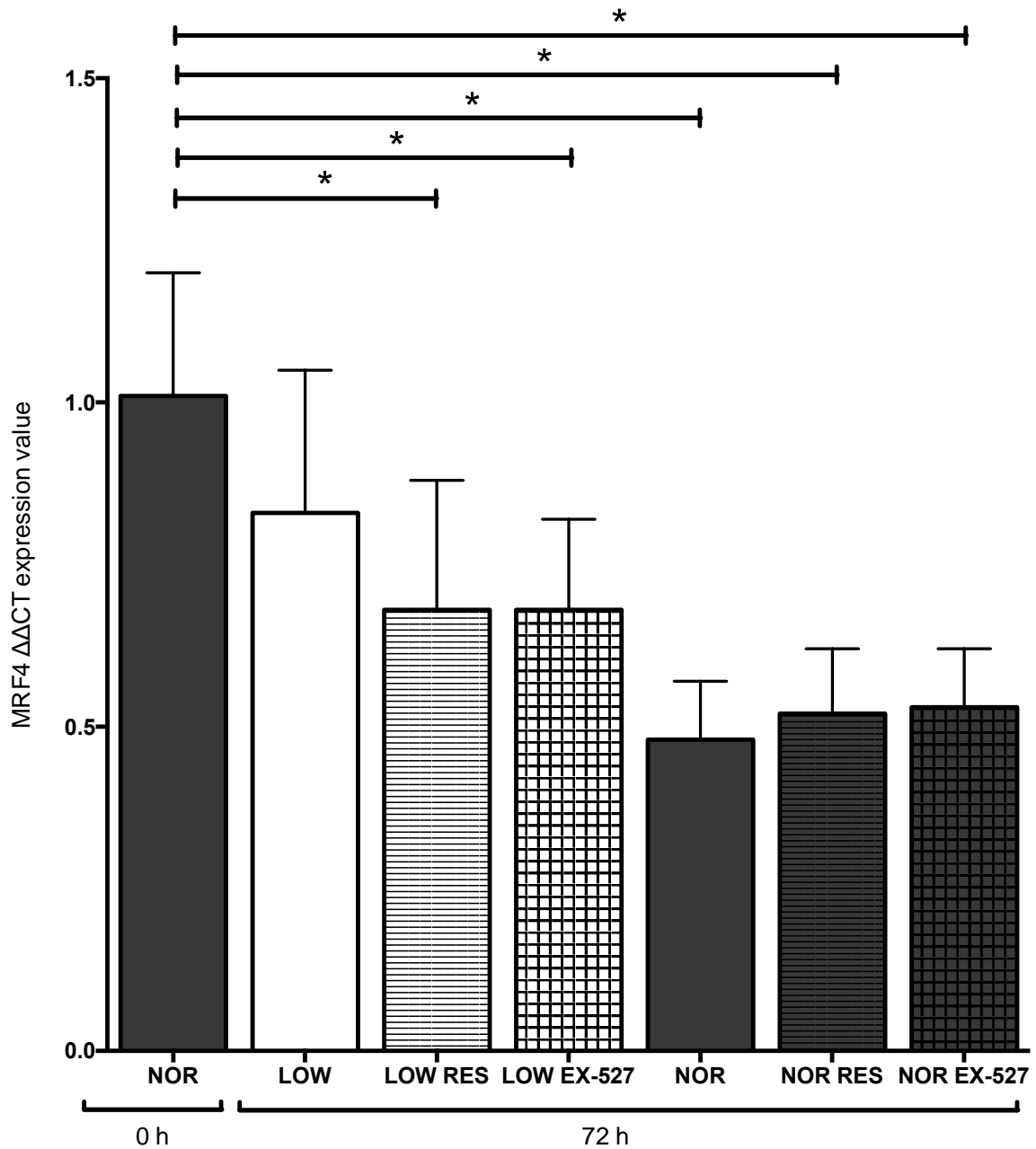


Fig. A1.5. Graph depicting means and SD's for gene expression for MRF4 at 72 h compared to the 0 h control. All experimental conditions were significantly reduced in comparison to the 0 h control except LOW glucose alone. Significant difference ($p < 0.05$) is denoted using *.

6.3.3. MYHC 7 expression is increased with SIRT1 activator resveratrol and MYHC 1,2,4 reduced with SIRT1 inhibitor EX-527 in normal glucose conditions.

Significant main effects were observed for glucose dosing ($F_{(1, 35)} = 60.28$, $p < 0.001$), SIRT1 manipulation ($F_{(2, 35)} = 4.39$, $p = 0.020$) and time ($F_{(1, 35)} = 69.24$, $p < 0.001$) for MYHC7 gene expression. Significant interactions were also present between time and both glucose ($F_{(1, 35)} = 60.28$, $p < 0.001$) and SIRT1 manipulation ($F_{(2, 35)} = 4.39$, $p = 0.020$). The manipulation of SIRT1 did not significantly affect the LOW glucose conditions (LOW vs. LOW RES: 1.04 ± 0.22 vs. 1.29 ± 0.49 , $p > 0.05$, LOW vs. LOW EX-527: 1.04 ± 0.22 vs. 1.39 ± 0.84 , $p > 0.05$). Although there was an average reduction, there was no significant effect on MYHC7 expression in the NOR condition upon the administration of EX-527 (3.08 ± 0.81 vs. 2.52 ± 0.66 , $p > 0.05$). There was however, a significant increase in MYHC7 expression following the addition of SIRT1 activator, RES in NOR conditions (3.08 ± 0.81 vs. 4.20 ± 0.82 , $p = 0.002$ (fisher)).

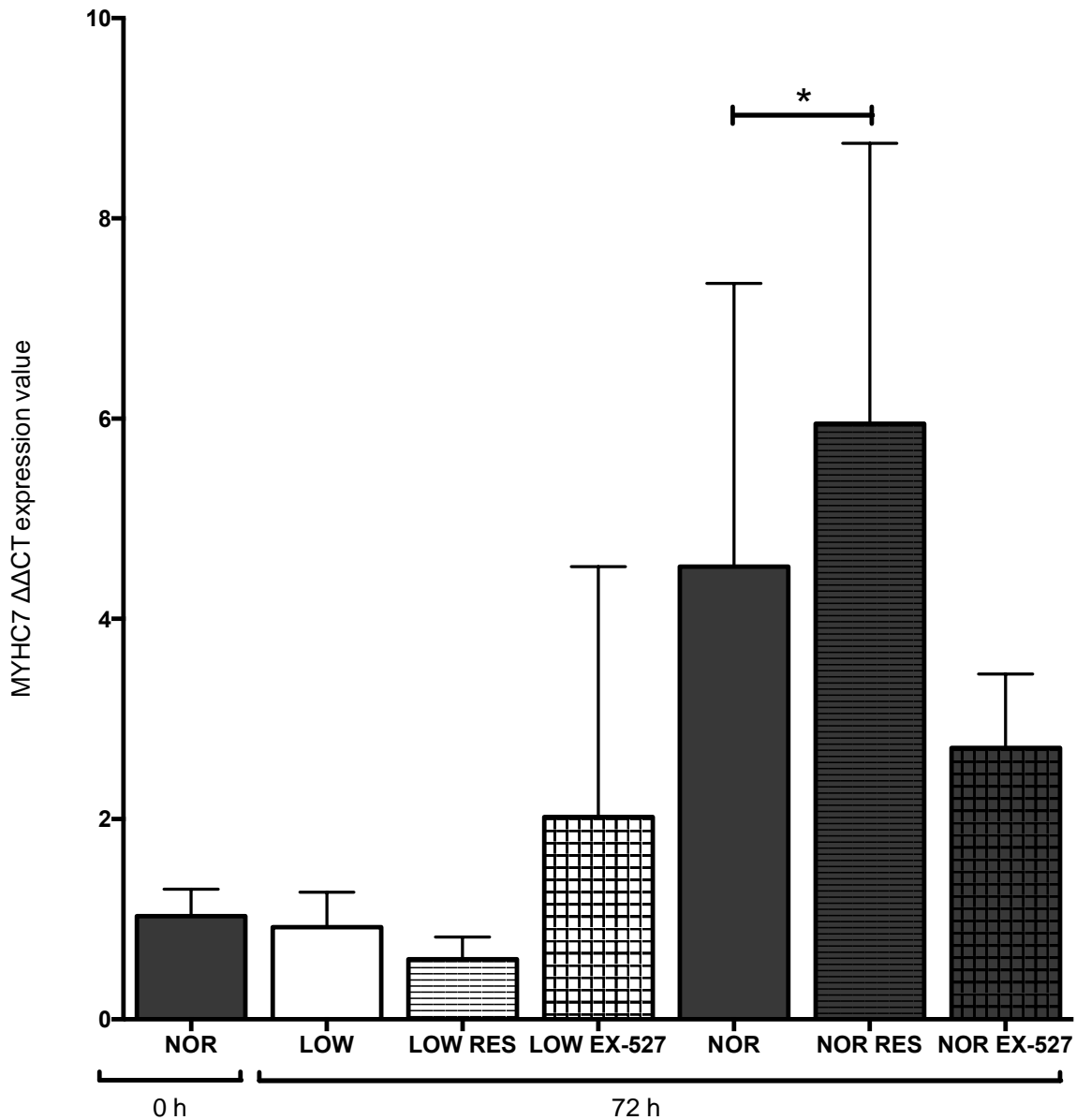


Fig. A1.6. Graph depicting means and SD's for gene expression for MYHC7 at 72 h compared to the 0 h control. RES significantly increased MYHC7 expression in NOR conditions. Significant difference ($p < 0.05$) is denoted using *.

For MYHC2 gene expression, a significant main effect was present for time ($F_{(1, 29)} = 10.32$, $p = 0.003$) and glucose concentration ($F_{(1, 29)} = 156.49$, $p < 0.001$). There was also a significant interaction between time x glucose concentration ($F_{(1, 29)} = 156.49$, $p < 0.001$). As with MYHC1 there was no significant difference found following SIRT1 manipulation in the LOW glucose conditions (LOW vs. LOW RES: 0.37 ± 0.05 vs. 0.32 ± 0.11 , $p > 0.05$, LOW vs. LOW EX-527: 0.37 ± 0.05 vs. 0.71 ± 0.83 , $p > 0.05$). In the NOR condition RES did not affect MYHC2 expression (NOR vs. NOR

RES: 1.86 ± 0.41 vs. 1.89 ± 0.34 , $p > 0.05$). In the NOR glucose conditions, the SIRT1 inhibitor EX-527 significantly reduced MYHC2 expression (NOR vs. NOR EX-527: 1.86 ± 0.41 vs. 1.55 ± 0.08 , $p = 0.034$ (fisher)).

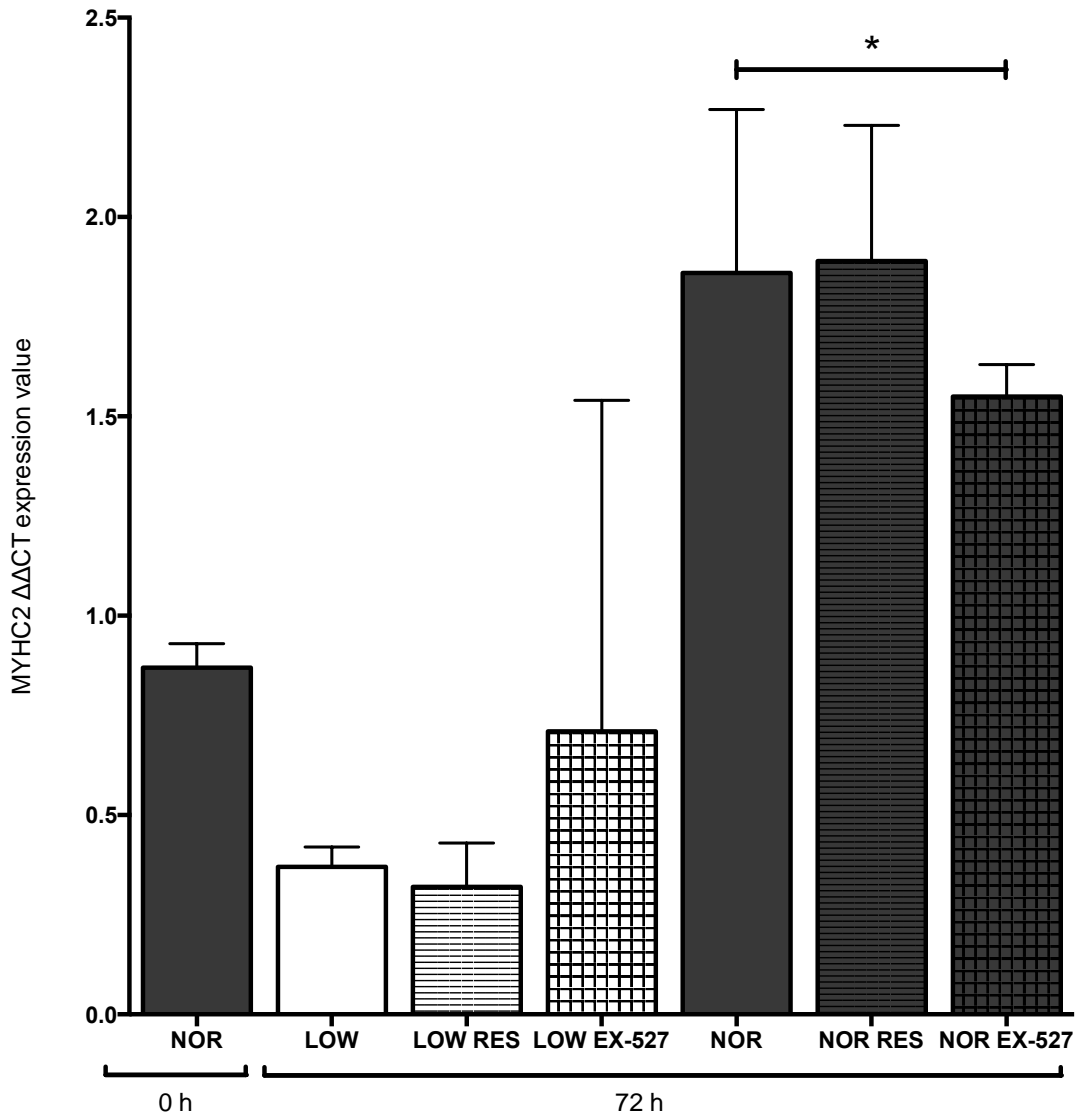
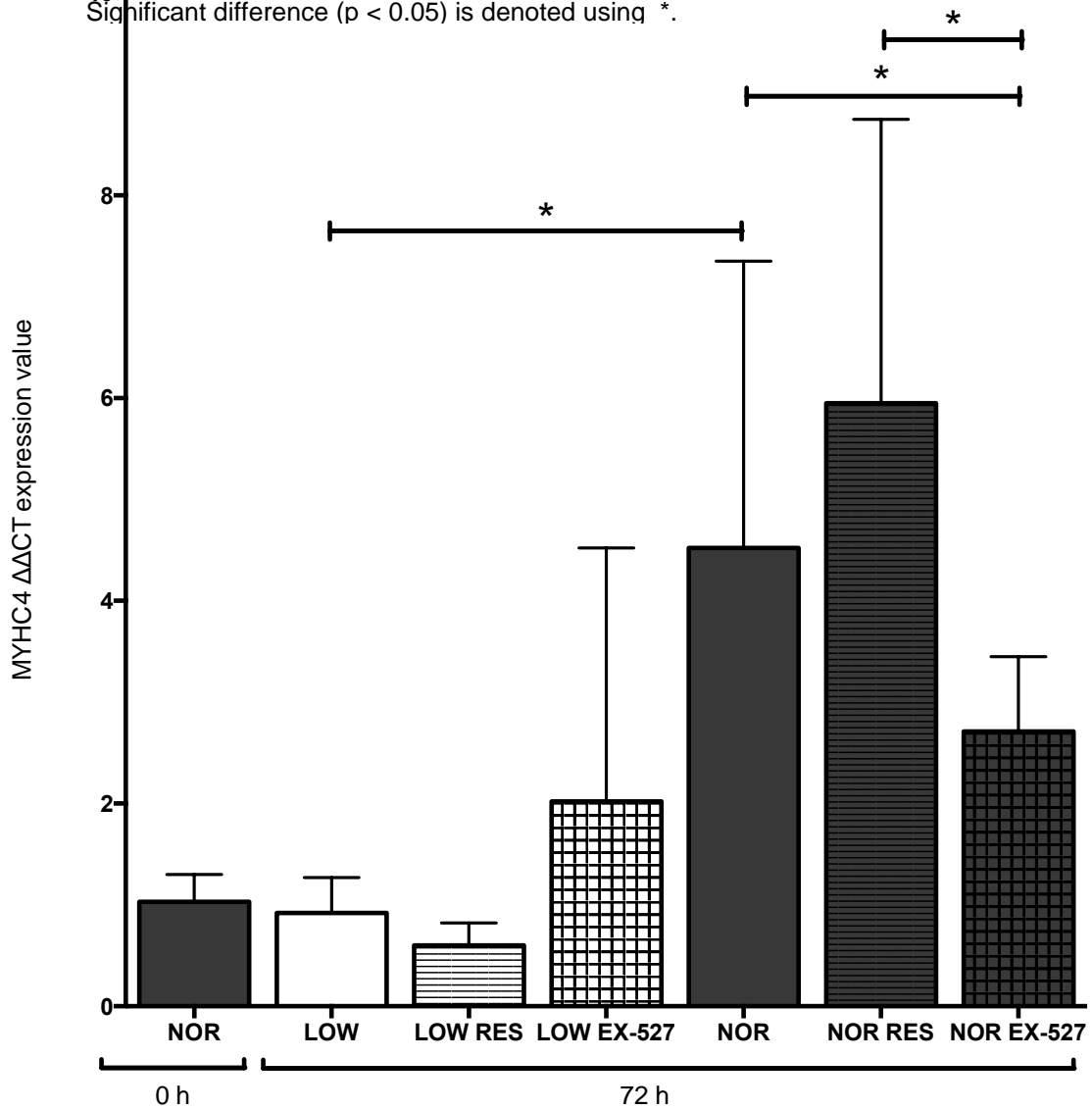


Fig. A1.7. Graph depicting means and SD's for gene expression for MYHC2 at 72 h compared to the 0 h control. NOR glucose was significantly increased in comparison to NOR EX-527. Significant difference ($p < 0.05$) is denoted using *.

MYHC4 displayed a significant main effect for glucose concentration ($F_{(1, 35)} = 25.91$, $p < 0.001$), time ($F_{(1, 35)} = 19.98$, $p < 0.001$) as well as a significant interaction between glucose concentration and time ($F_{(1, 35)} = 25.91$, $p < 0.001$). In NOR glucose conditions, expression of MYHC4 was

significantly increased following 72 h in comparison to LOW glucose conditions (4.52 ± 2.83 vs. 0.92 ± 0.35 , $p = 0.011$). SIRT1 activation/inhibition had no effect on MYHC4 expression in LOW glucose conditions (LOW vs. LOW RES: 0.92 ± 0.35 vs. 0.60 ± 0.22 , $p > 0.05$, LOW vs. LOW EX-527: 0.92 ± 0.35 vs. 2.02 ± 2.50 , $p > 0.05$). There were also no significant differences following RES administration in NOR glucose conditions (NOR vs. NOR RES: 4.52 ± 2.83 vs. 5.95 ± 2.80 , $p > 0.05$). Again, as with MYHC2, there was a reduction in MYHC4 expression following SIRT1 inhibition via EX-527 administration (NOR vs. NOR EX-527: 4.52 ± 2.83 vs. 2.72 ± 0.74 , $p = 0.058$ (fisher)).

Fig. A1.8. Graph depicting means and SD's for gene expression for MYHC4 at 72 h compared to the 0 h control. EX-527 reduced MYHC4 expression in NOR conditions. Significant difference ($p < 0.05$) is denoted using *.



Similar to myoblast studies, MYHC1 displayed significant interactions between glucose concentration and time ($F_{(1, 35)} = 23.83$, $p < 0.001$). There was also an individual main effects for glucose ($F_{(1, 35)} = 23.83$, $p < 0.001$) and time ($F_{(1, 35)} = 23.09$, $p < 0.001$). MYHC1 expression was significantly increased in NOR in comparison to LOW glucose conditions (3.39 ± 1.38 vs. 1.20 ± 0.30 , $p = 0.007$). There was however, no significant difference following the administration of RES in either NOR (NOR vs. NOR RES: 3.39 ± 1.38 vs. 3.61 ± 1.61 , $p = 1.000$) or LOW glucose conditions (LOW vs. LOW RES: 1.20 ± 0.30 vs. 1.05 ± 0.35 , $p > 0.05$). There was also no significant difference following EX-527 administration in LOW glucose (LOW vs. LOW EX-527: 1.20 ± 0.30 vs. 1.63 ± 0.14 , $p > 0.05$) or NOR

glucose, (NOR vs. NOR EX-527: 3.39 ± 1.38 vs. 2.26 ± 0.69 , $p = 0.094$ (fisher)), however there was a trend that was approaching significance.

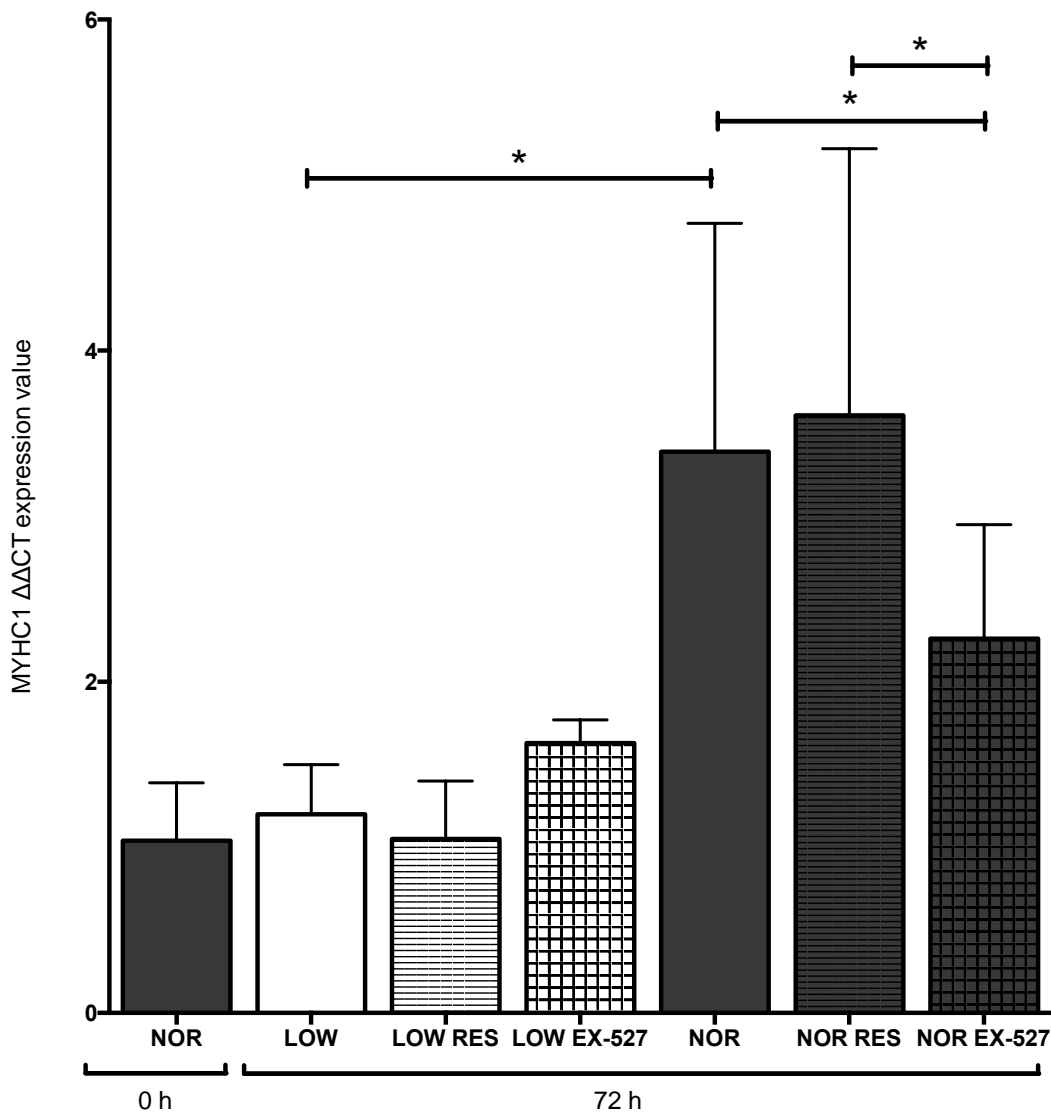


Fig. A1.9. Graph depicting means and SD's for gene expression for MYHC1 at 72 h compared to the 0 h control. EX-527 significantly reduced MYHC1 expression in NOR conditions even when RES was supplemented. Significant difference ($p < 0.05$) is denoted using *.

Overall, the inhibition (EX-527) of SIRT1 reduced myotube number and myotube size, The activation of SIRT1 via RES increased myotube area in normal glucose conditions. These findings corresponded with reductions in IIX, IIA, IIB coding MYHC isoforms (1,2,4 respectively) following SIRT1

inhibition and increases in slow isoform coding MYH7 gene expression with SIRT1 activation. Suggesting that changes in SIRT1 activity mediates gene expression of these important genes coding for increasing contractile protein isoforms. There are also associated with increased myotube maturation and hypertrophy observed in normal glucose conditions in the presence of SIRT1 activator, RES. However, SIRT1 activation had little effect on myotubes in low glucose conditions at this timepoint (72 h).

Because of this interesting finding, we then wished to investigate some of the other important gene regulatory targets of altered SIRT1 activity following the same 72 h timepoint. Including genes associated with myotube growth/hypertrophy (IGF-I, IGF-IR, IGF-II, IGF-IIR, IGFBP2, mTOR) and myotube atrophy (TNF- α , MuRF, MAFbx, MUSA1, p53, GADD45a and b, FOXO1 and 3, NF-kB), as well as SIRT1 gene expression.

6.3.4. Myotube growth/hypertrophy

Increased IGF-I has previously been observed with advancing differentiation and myotube hypertrophy in-vitro (Sharples et al., 2010, Sharples et al., 2011). This group has shown that a reduction in calories has been shown to reduce IGF-I expression (Sharples *et al.*, 2015). The manipulation of SIRT1 during glucose restriction in mature myotubes displayed a significant interaction for glucose x time ($F_{(2, 29)} = 233.98$, $p < 0.001$) as well as a significant main effect for glucose alone ($F_{(2, 29)} = 233.98$, $p < 0.001$). Under all NOR glucose conditions there was an increase in IGF-I expression over time from 0 h to 72 h (0 h: 1.03 ± 0.01 vs. NOR: 1.61 ± 0.40 , $p = 0.024$, vs. NOR RES: 2.12 ± 0.20 , $p < 0.001$, vs. NOR EX-527: 1.79 ± 0.45 , $p = 0.002$), whereas from 0 to 72 h LOW glucose decreased IGF-I expression in all conditions (0 h: 1.03 ± 0.01 vs. LOW: 0.05 ± 0.01 , $p < 0.001$, vs. LOW RES: 0.05 ± 0.01 , $p < 0.001$, 0 h vs. LOW EX-527: 0.46 ± 0.01 $p < 0.001$). This resulted in gene expression for IGF-I being significantly lower in LOW versus NOR glucose conditions (LOW vs. NOR: 0.05 ± 0.01 vs. 1.61 ± 0.40 , $p < 0.001$). SIRT1 inhibitor

EX-527 did not affect IGF-I under NOR (NOR vs. NOR EX-527: 1.61 ± 0.40 vs. 1.79 ± 0.45 , $p > 0.05$) or LOW conditions (LOW vs. LOW EX-527: 0.05 ± 0.01 vs. 0.46 ± 0.01 , $p > 0.05$). RES conditions significantly increase IGF-I expression in NOR (NOR vs. NOR RES: 1.61 ± 0.40 vs. 2.12 ± 0.20 , $p < 0.033$) conditions but not in LOW (LOW vs. LOW RES: 0.05 ± 0.01 vs. 0.05 ± 0.01 , $p > 0.05$ (Fig 5.9.)).

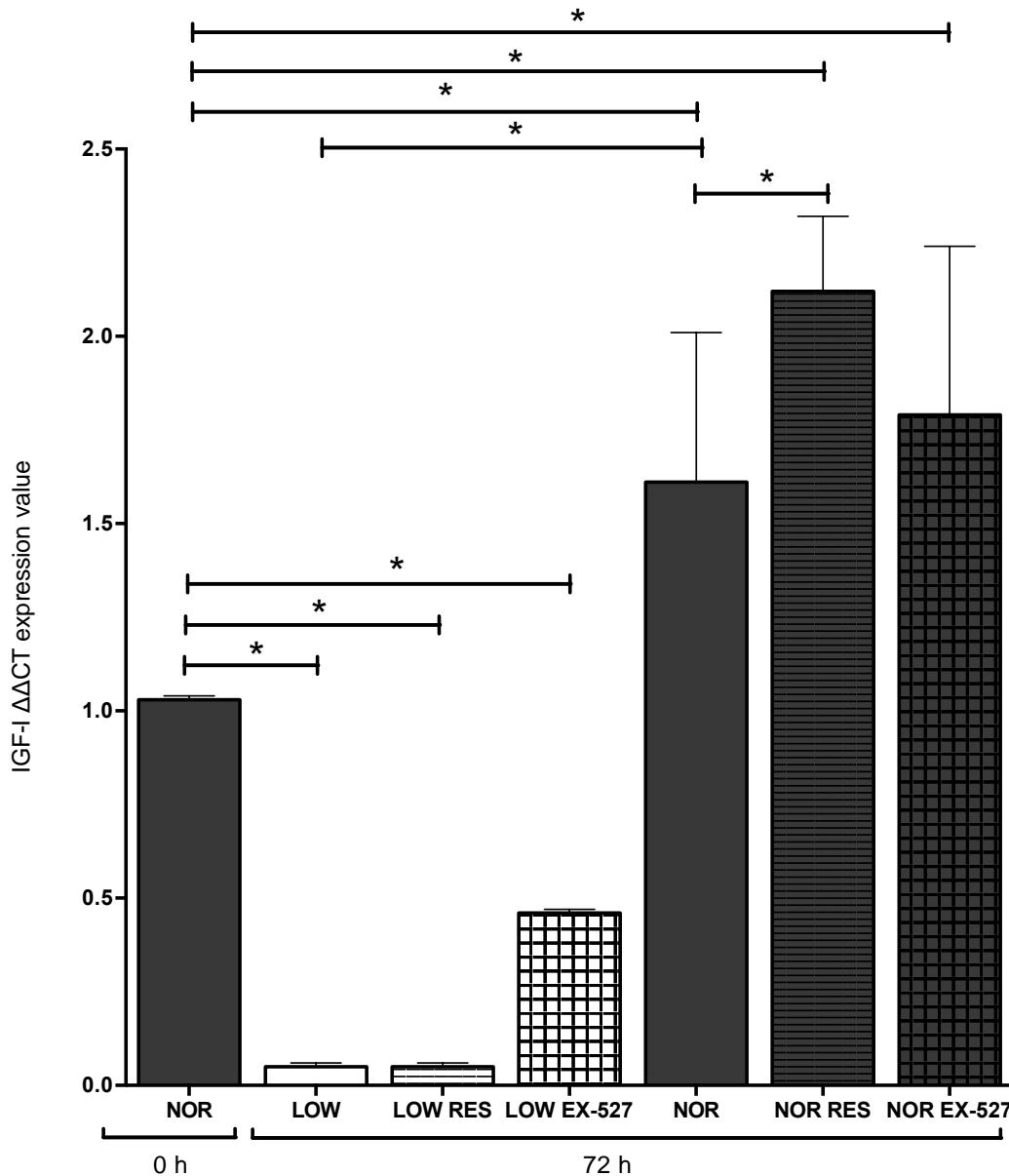


Fig. A1.10. Graph depicting means and SD's for gene expression for IGF-I at 72 h compared to the 0 h control. RES significantly increased IGF-I expression in NOR conditions following RES administration. Significant difference ($p < 0.05$) is denoted using a *.

A significant interaction was present for IGF-IR gene expression between time, SIRT1 manipulation ($F_{(2, 36)} = 4.79$, $p = 0.014$) and glucose concentration ($F_{(1, 36)} = 76.60$, $p < 0.001$). Time ($F_{(1, 36)} = 73.40$, $p < 0.001$), SIRT1 manipulation ($F_{(2, 36)} = 4.79$, $p = 0.014$) and glucose concentration ($F_{(1, 36)} = 76.60$, $p < 0.001$) were also significant main effects. All LOW glucose conditions at 72 h were significantly reduced IGF-IR expression in comparison to 0 h (0 h: 1.15 ± 0.04 vs. LOW: 0.74 ± 0.05 , $p < 0.001$, vs. LOW RES: 0.66 ± 0.05 , $p < 0.001$, vs. LOW EX-527: 0.79 ± 0.16 , $p < 0.001$ (Fig. 6.11)). NOR glucose remained unchanged overtime from 0 h to 72 hrs (0 h vs. NOR: 1.15 ± 0.04 vs. 1.11 ± 0.13 , $p > 0.05$), as did NOR RES (0 h vs. NOR RES: 1.15 ± 0.04 vs. 1.05 ± 0.05 , $p > 0.05$). At 72 h In NOR glucose conditions supplemented with SIRT1 inhibitor, EX-527 significantly increased IGF-IR expression in comparison to 0 h (0 h vs. NOR EX-527: 1.15 ± 0.04 vs. 1.29 ± 0.11 , $p = 0.034$ (fisher)). NOR EX-527 was also increased in comparison to NOR alone at 72 h (NOR vs. NOR EX-527: 1.11 ± 0.13 vs. 1.29 ± 0.11 , $p = 0.010$ (fisher)). No other significant differences were detected in either glucose condition following the activation/inhibition of SIRT1 at 72 h (LOW vs. LOW RES: 0.74 ± 0.05 vs. 0.66 ± 0.05 , $p > 0.05$, LOW vs. LOW EX-527: 0.74 ± 0.05 vs. 0.79 ± 0.16 , $p > 0.05$, NOR vs. NOR EX-527: 1.11 ± 0.13 vs. 1.29 ± 0.11 , $p = 0.667$).

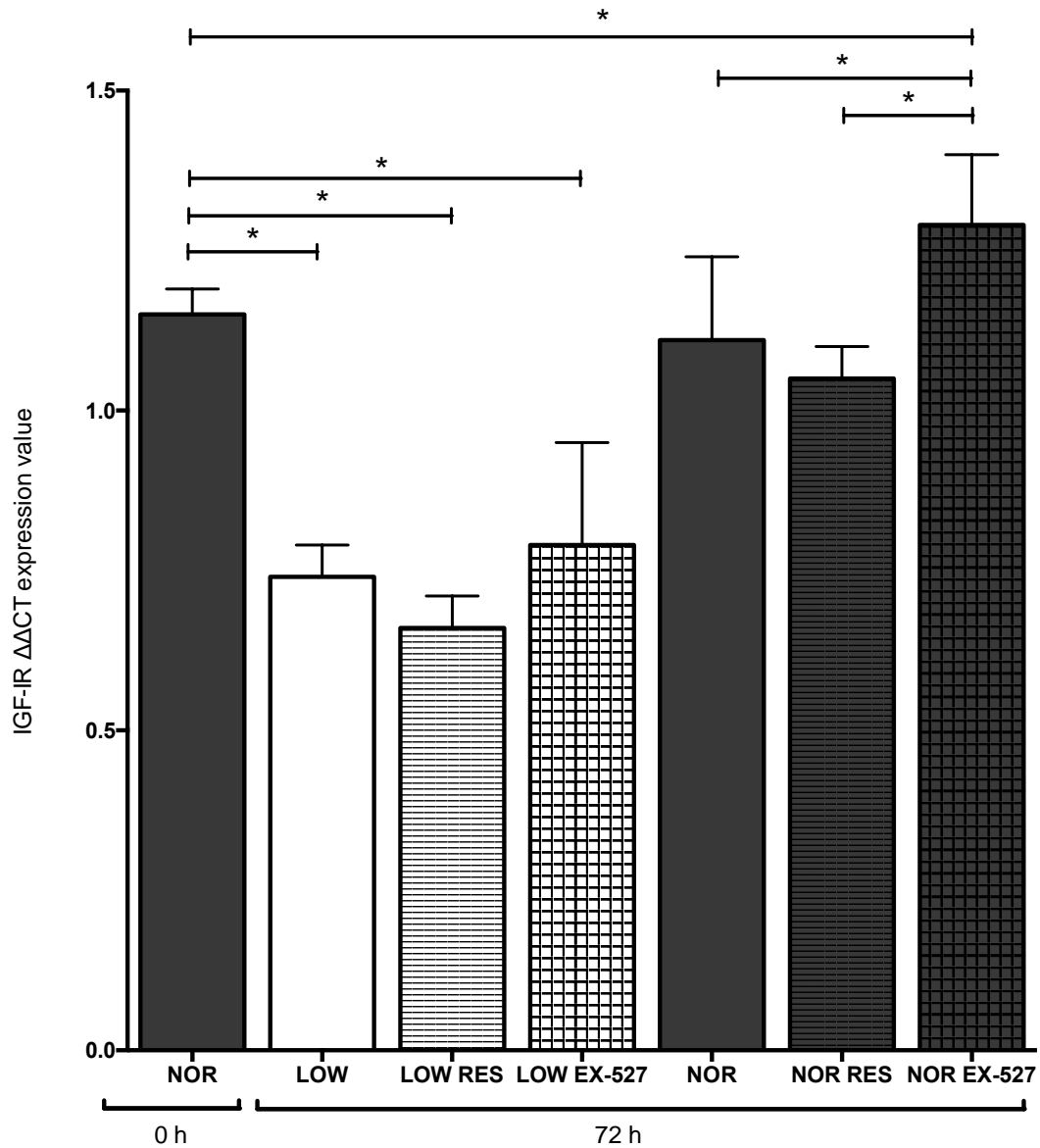


Fig. A1.11. Graph depicting means and SD's for gene expression for IGF-IR at 72 h compared to the 0 h control. LOW conditions all displayed a reduced expression of IGF-IR following 72 h. No significant difference was observed from the control condition in NOR glucose until EX-527 was supplemented. Significant difference ($p < 0.05$) is denoted using a *.

There was no significant interaction or main effect present for IGF-II expression. There was also no significant differences observed following post hoc tests (Fig. 6.12).

Fig. A1.12. Graph depicting means and SD's for gene expression for IGF-II at 72 h compared to the 0 h control, in which no significant differences were observed. Significant difference ($p < 0.05$) is denoted using *.

IGF-IIR had a significant main effect for glucose ($F_{(1, 35)} = 8.22, p = 0.007$) and time point ($F_{(1, 35)} = 87.10, p < 0.001$) and a significant interaction between the two ($F_{(1, 35)} = 8.22, p = 0.007$). The two glucose conditions did not express significantly different IGF-IIR expression values at 72 h (LOW vs. NOR: 0.86 ± 0.09 vs. $0.79 \pm 0.04, p = 1.000$). All experimental conditions significantly reduced IGF-IIR expression compared to the 0 h control (0 h: 1.00 ± 0.05 vs. NOR: $0.79 \pm 0.04, p = 0.005$, vs. NOR RES: $0.78 \pm 0.09, p = 0.003$, vs. NOR EX-527: $0.72 \pm 0.10, p < 0.001$, vs. LOW: $0.86 \pm 0.09, p = 0.004$ (fisher), vs. LOW EX-527: $0.86 \pm 0.11, p < 0.001$) except LOW glucose with RES supplementation at 72 h that was maintained at a similar level to 0 h control (0 h vs. LOW RES: 1.00 ± 0.05

vs. 0.95 ± 0.11 , $p = 1.000$). As a result, at 72 h gene expression of IGF-IIR with RES administration under LOW conditions was higher than LOW alone (LOW vs. LOW RES: 0.86 ± 0.09 vs. 0.95 ± 0.11 , $p = 0.054$ (fisher)).

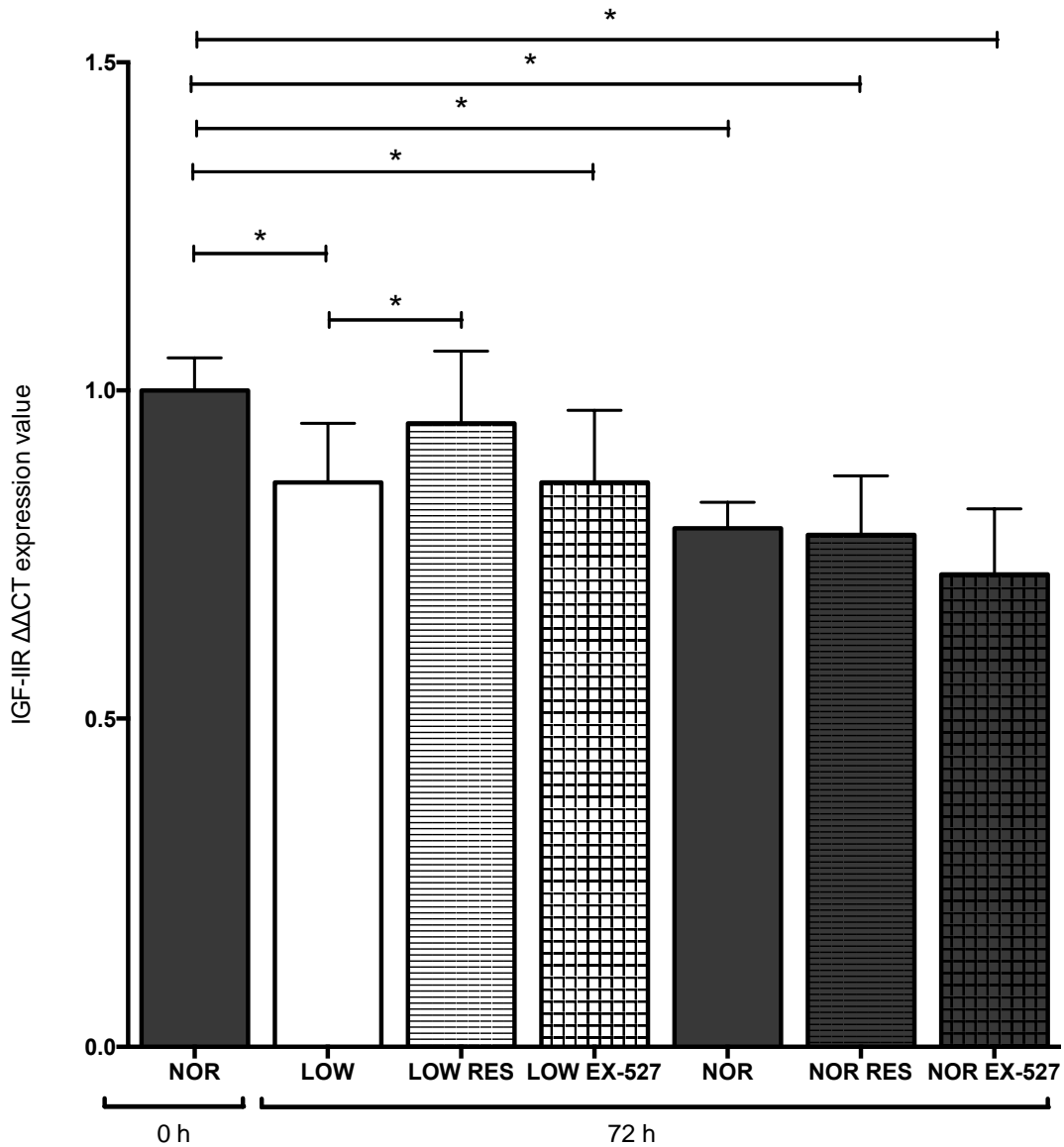


Fig. A1.13. Graph depicting means and SD's for gene expression for IGF-IIR at 72 h compared to the 0 h control. RES significantly increased IGF-IIR in LOW conditions. Significant difference ($p < 0.05$) is denoted using *.

A significant interaction between glucose concentration and time was present for IGFBP2 gene expression ($F_{(1, 24)} = 2.12$, $p < 0.001$) in addition to significant main effects for time and glucose concentration respectively ($F_{(1, 24)} = 2.12$, $p < 0.001$), ($F_{(1, 24)} = 11.01$, $p = 0.003$). IGFBP2 gene

expression in all NOR glucose conditions with or without supplementation or SIRT1 activator or inhibitor at 72 h is similar to 0 h control (0 h: 1.21 ± 0.00 vs. NOR: 1.20 ± 0.55 , $p = 1.000$, vs. NOR RES: 1.37 ± 0.27 , $p = 1.000$, vs. NOR EX-527: 1.65 ± 0.45 , $p = 1.000$). LOW glucose on the other hand, significantly reduced IGFBP2 expression at 72 h in comparison to 0 h (0 h: 1.21 ± 0.00 vs. LOW: 0.44 ± 0.12 , $p = 0.003$ (fisher), vs. LOW RES: 0.22 ± 0.03 , $p = 0.022$, vs. LOW EX-527: 0.46 ± 0.25 , $p = 0.003$ (fisher)). As such there was a significant difference between NOR and LOW glucose at 72 h (NOR vs. LOW: 1.20 ± 0.55 vs. 0.44 ± 0.12 , $p = 0.042$), as previously observed in myoblast studies in chapter 5. SIRT1 activation via RES supplementation did not affect either glucose concentration significantly at 72 h (NOR vs. NOR RES: 1.20 ± 0.55 vs. 1.37 ± 0.27 , $p = 1.000$, LOW vs. LOW RES: 0.44 ± 0.12 vs. 0.22 ± 0.03 , $p = 1.000$). SIRT1 inhibition via EX-527 administration increased IGFBP2 expression in NOR (NOR vs. NOR EX-527: 1.20 ± 0.55 vs. 1.65 ± 0.45 , $p = 0.043$ (fisher)) but not LOW glucose concentrations at 72 h (LOW vs. LOW EX-527: 0.44 ± 0.12 vs. 0.46 ± 0.25 , $p = 1.000$).

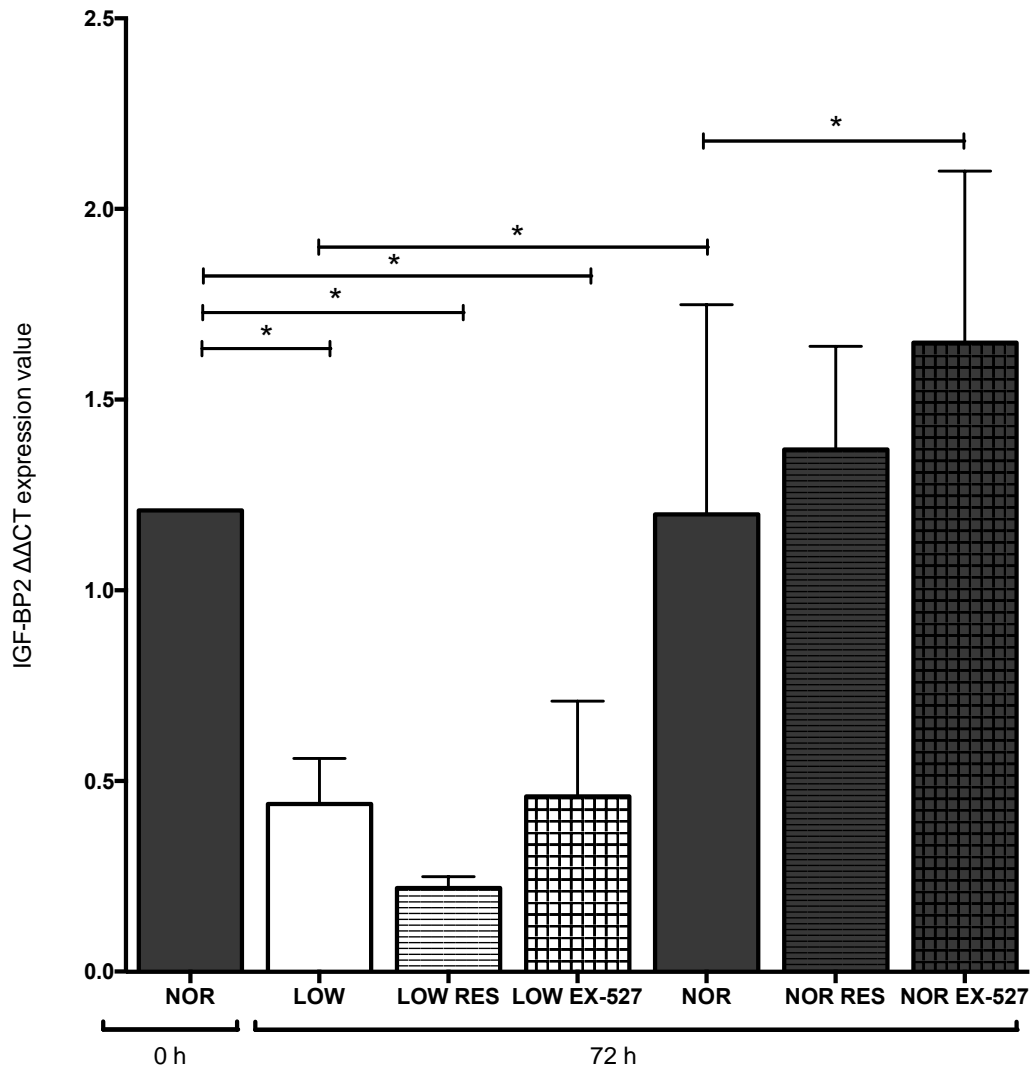


Fig. A1.14. Graph depicting means and SD's for gene expression for IGF-BP2 at 72 h compared to the 0 h control. LOW glucose conditions displayed a reduced expression of IGFBP2 after 72 h whereas NOR conditions did not in fact EX-527 further increased IGFBP2 levels from the 0h control. Significant difference ($p < 0.05$) is

There was no significant interaction or main effect for any of the variables analysed for mTOR expression. Additionally, there were no significant individual differences present between any experimental conditions following pairwise comparison analysis.

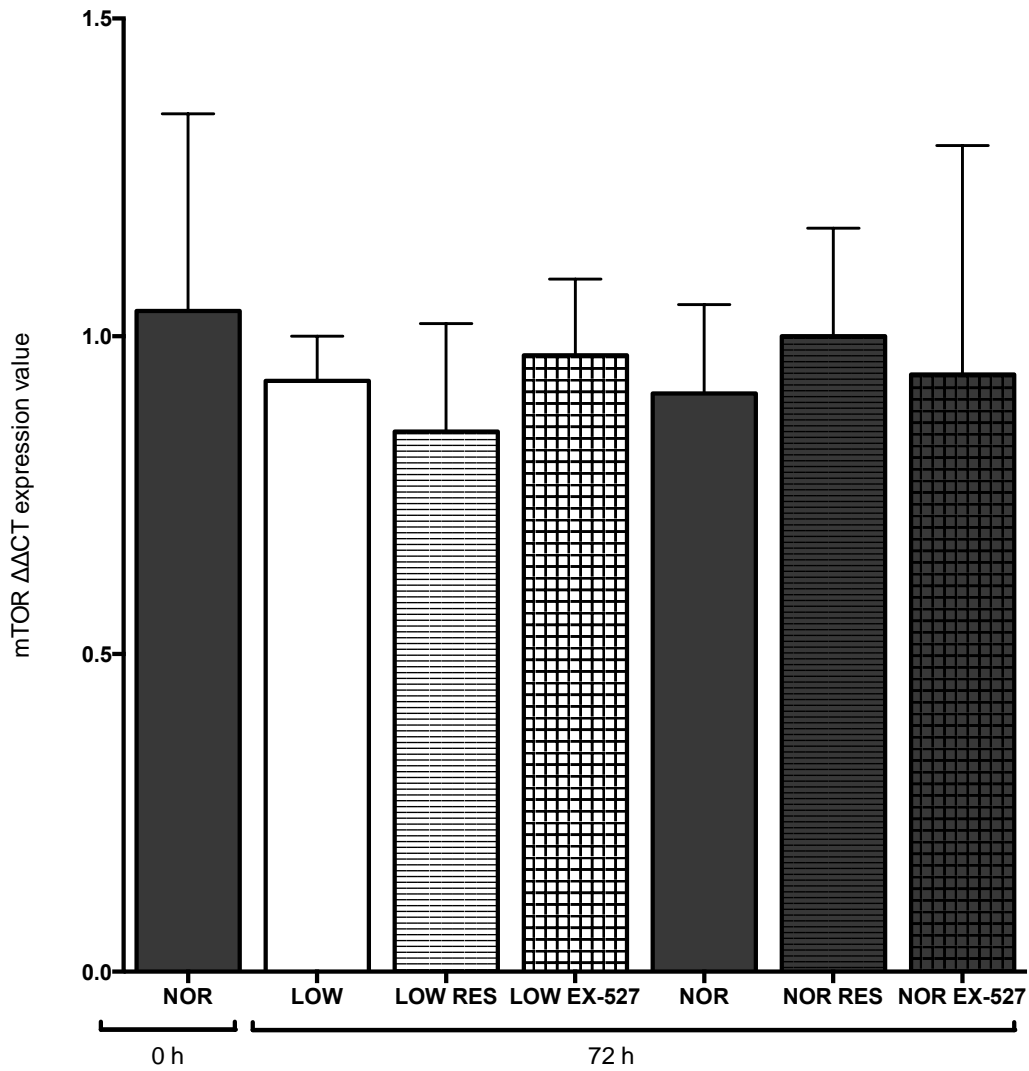


Fig. A1.15. Graph depicting means and SD's for gene expression for mTOR at 72 h compared to the 0 h control. mTOR remained unchanged following 72 h

With respect to genes associated with myotube growth, where there were increased number of myotubes and myotube hypertrophy with RES administration in normal glucose conditions there were corresponding increases in IGF-I but not IGF-IR, IGF-II, IGF-IIR. There were reductions in IGFBP2 (a known inhibitor of differentiation when at high levels (Sharples et al., 2013)) with RES in LOW glucose conditions and increases with SIRT1 inhibitor EX-527 in normal glucose conditions. The reductions in myotube size associated with SIRT1 inhibition corresponded with increased in IGFBP2 expression in normal glucose a known inhibitor of differentiation in myoblasts. Therefore, these changes in IGFBP2 may

have been important in the myotube atrophy seen in normal glucose with SIRT1 inhibition, however, as yet there is an undefined role for IGFBP2 in myotubes. Somewhat, paradoxically SIRT1 inhibition increased IGF-IR expression perhaps as a compensatory drive, albeit unsuccessful in rescuing growth observed morphologically. In low glucose conditions, although no improvements in myotube growth were observed at 72 h with RES administration, RES was able to somewhat maintain normal IGF-IIR expression at 72 h.

6.3.5. Genes associated with myotube atrophy and protein degradation:

TNF- α displayed a significant main effect for time ($F_{(1, 36)} = 5.81, p = 0.021$). There were however, no significant differences in TNF- α expression with SIRT1 manipulation.

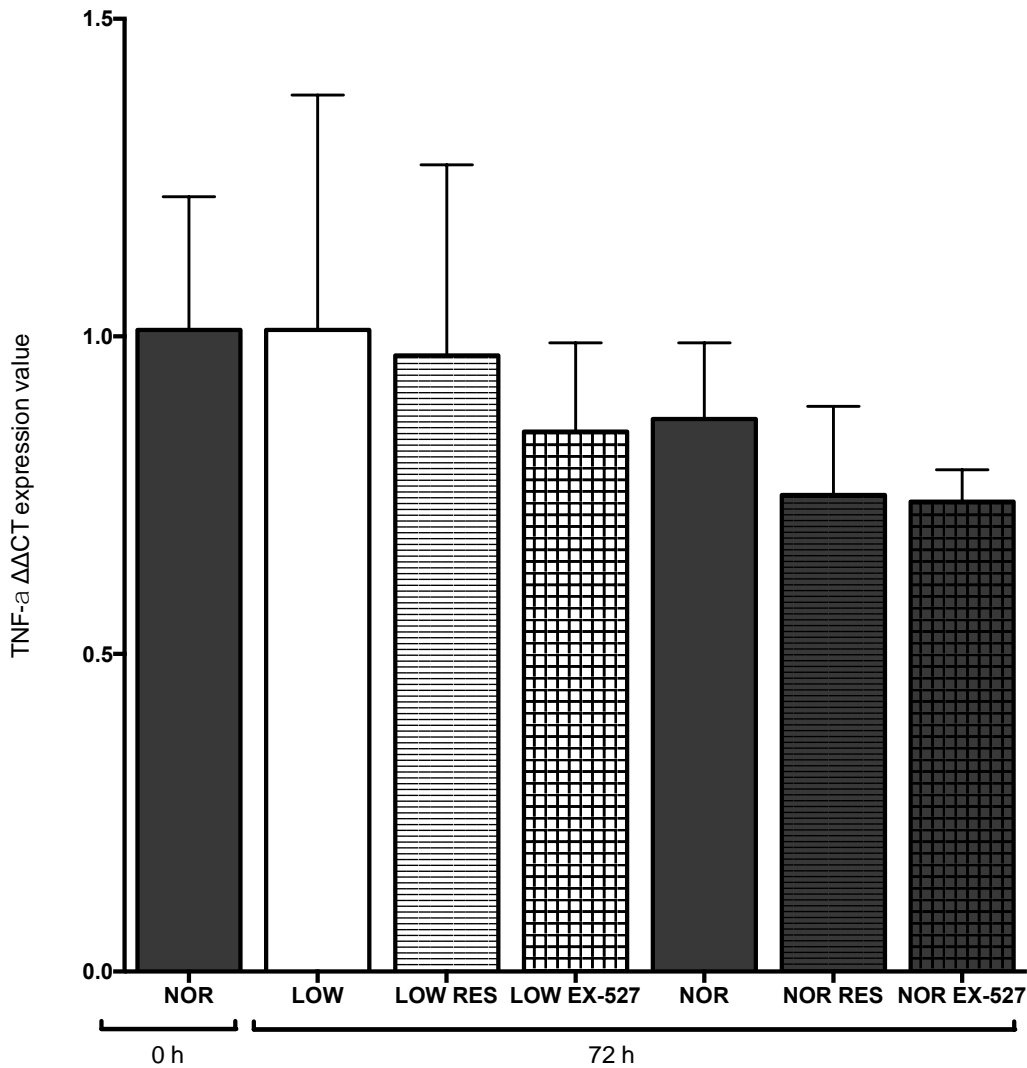


Fig. A1.16. Graph depicting means and SD's for gene expression for TNF- α at 72 h compared to the 0 h control. No experimental control elicited a change in TNF- α . Significant difference ($p < 0.05$) is denoted using *.

TNFRSF1 β (TNF-alpha soluble receptor) gene expression analysis revealed both a significant interaction ($F_{(1, 35)} = 92.48$, $p < 0.001$) and significant main effects were for glucose concentration ($F_{(1, 35)} = 92.48$, $p < 0.001$) and time ($F_{(1, 35)} = 4.30$, $p = 0.046$). All LOW glucose conditions at 72 h were significantly increased in comparison to the 0 h control (0 h: 1.00 ± 0.13 vs. LOW: 0.56 ± 0.08 , $p < 0.001$, vs. LOW RES: 0.65 ± 0.08 , $p = 0.009$, vs. LOW EX-527: 0.73 ± 0.30 , $p = 0.001$). Both NOR alone and NOR RES were significantly lower than the 0 h control (0 h: 1.00 ± 0.13 vs. NOR: 1.32 ± 0.04 , $p = 0.039$, vs. NOR RES: 1.33 ± 0.16 , $p = 0.023$). The only condition that was not significant in comparison to the 0 h control was

NOR glucose supplemented with SIRT1 inhibitor, EX-527 at 72 h (0 h vs. NOR EX-527: 1.00 ± 0.13 vs. 1.14 ± 0.16 , $p = 1.000$). As a result, NOR glucose conditions with SIRT 1 inhibitor, EX-527 had a significantly lower expression than NOR RES at 72 h (NOR EX-527 vs. NOR RES: 1.14 ± 0.16 vs. 1.33 ± 0.16 , $p = 0.039$ (fisher)) and versus NOR glucose alone at 72 h (NOR vs. NOR EX-527: 1.32 ± 0.04 vs. 1.14 ± 0.16 , $p = 0.055$ (fisher)). No significance was present between the three LOW conditions at 72 h (LOW vs. LOW RES: 0.56 ± 0.08 vs. 0.65 ± 0.08 , $p = 1.000$, LOW vs. LOW EX-527: 0.56 ± 0.08 vs. 0.73 ± 0.30 , $p = 1.000$).

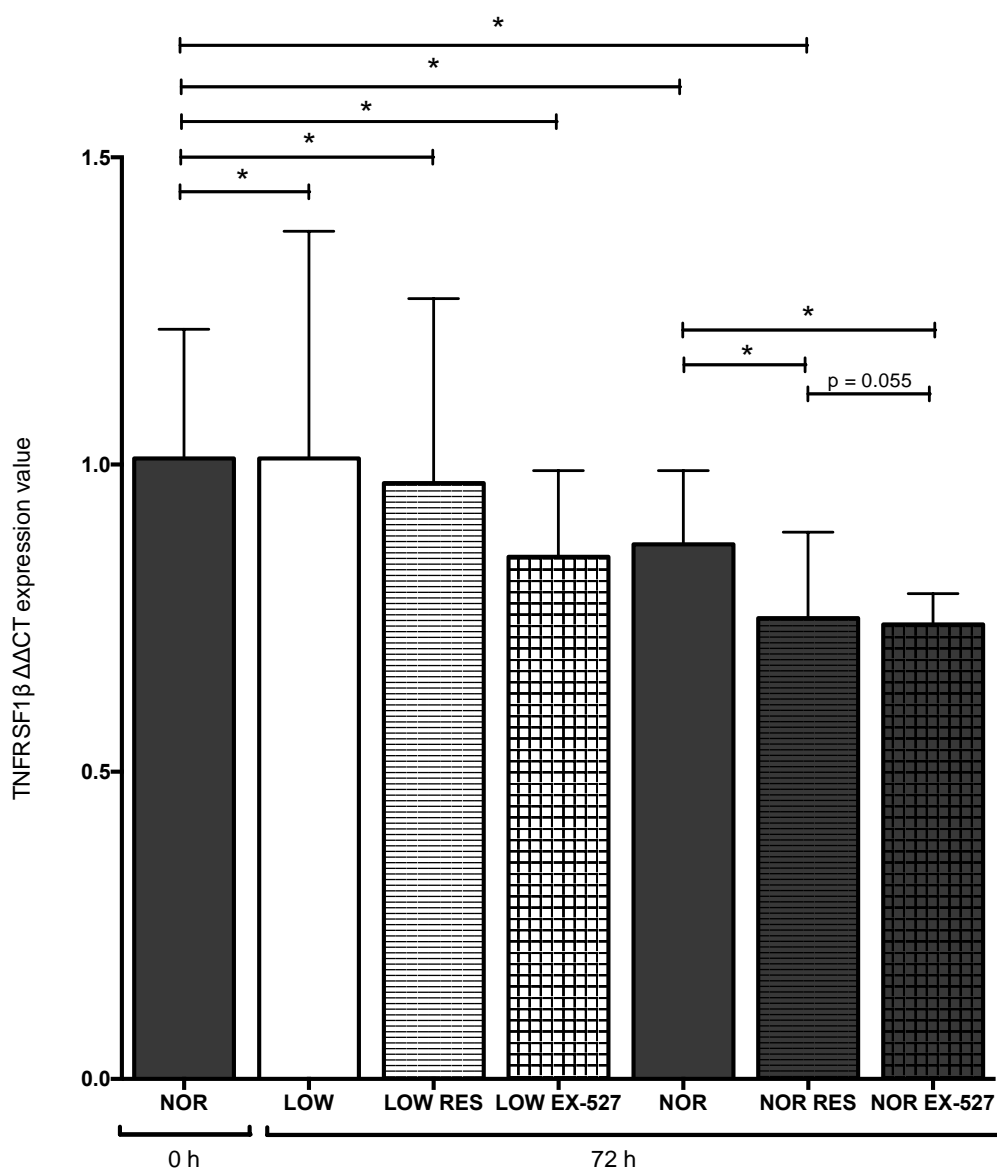


Fig. A1.17. Graph depicting means and SD's for gene expression for TNFRSF1 β at 72 h compared to the 0 h control. A change over time was observed for TNFRSF1 β , in addition to decreases in NOR following both RES and EX-527 supplementation. Significant difference ($p < 0.05$) is denoted using *. p values approaching significance are displayed.

There was a significant main effect for time for myostatin gene expression ($F_{(1,28)} = 19.43$, $p < 0.001$). NOR glucose alone and with the addition of EX-527 at 72 h were not significantly changed in comparison to the 0 h baseline control (0 h: 0.71 ± 0.17 vs. NOR: 1.27 ± 0.65 , $p = 1.000$, vs. NOR EX-527: 1.58 ± 0.49 , $p = 1.000$). Myostatin expression under NOR conditions with the addition of RES was significantly increased in comparison the 0 h control (0 h vs. NOR RES: 0.71 ± 0.17 vs. 1.99 ± 0.81 , $p = 0.007$ (fisher)). This condition was also significantly increased in comparison to NOR glucose alone at 72 h alone (NOR vs. NOR RES: 1.27 ± 0.65 vs. 1.99 ± 0.81 , $p = 0.027$ (fisher)). Under LOW conditions alone there was a significant increase in myostatin expression over time (0 h vs. LOW: 0.71 ± 0.17 vs. 2.12 ± 1.33 , $p = 0.004$ (fisher)). Despite no improvement in myotube number or size with RES addition in LOW glucose conditions, at 72 h in the addition of RES to LOW glucose significantly reduced the gene expression of the negative muscle mass regulator, myostatin (LOW vs. LOW RES: 2.12 ± 1.33 vs. 1.41 ± 0.70 , $p = 0.024$ (fisher)).

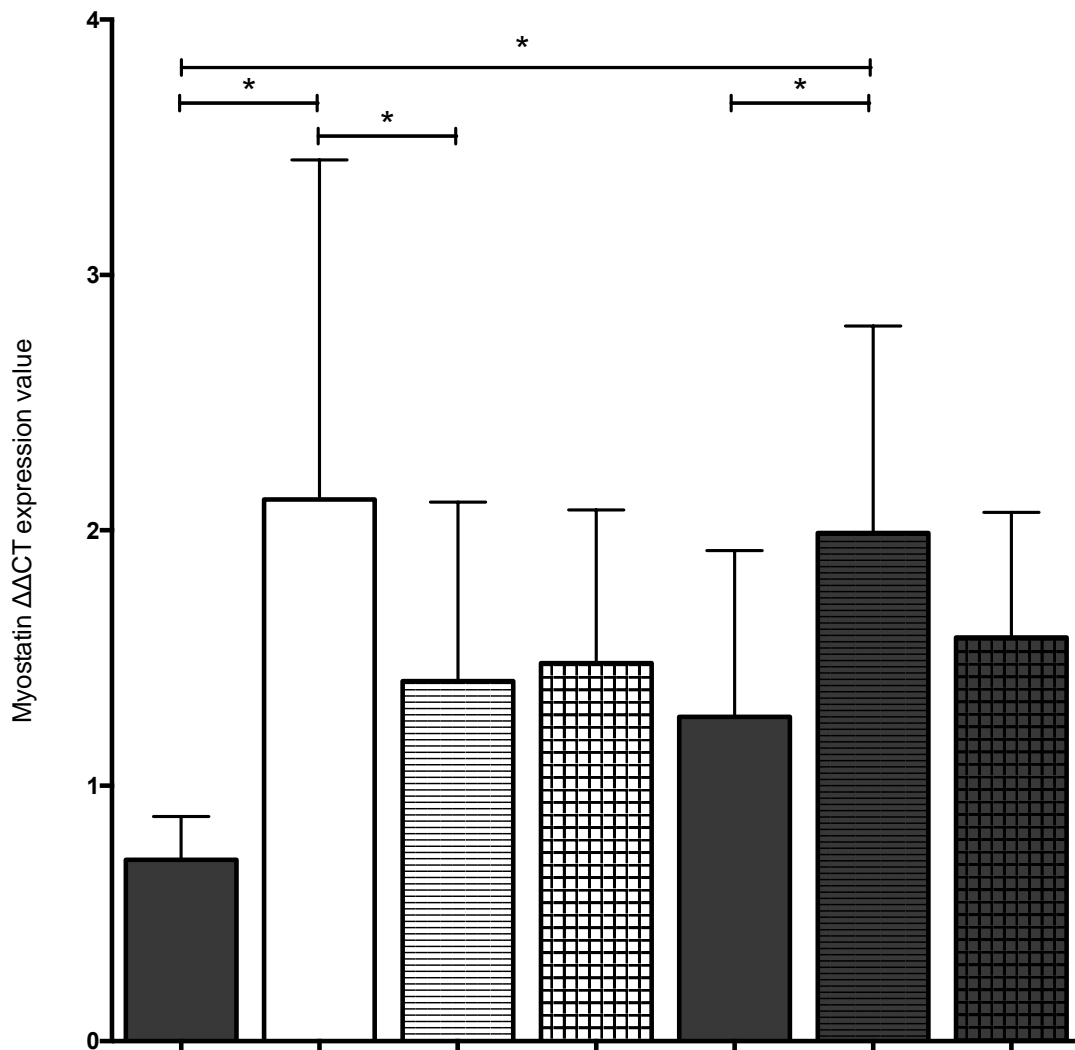


Fig. A1.10. Graph depicting means and SD's for gene expression for myostatin at 0 h compared to the 0 h control. RES decreased myostatin in LOW and increased in NOR. Significant difference ($p < 0.05$) is denoted using *.

6.3.6. Ubiquitin Ligases: MAFbx, MuRF1 and MUSA1

As discussed in the previous chapter (5) both muscle ring finger1 (MuRF1) and muscle atrophy F-box (MAFbx) and muscle ubiquitin ligase of SCF complex in atrophy 1 (MUSA1) have been identified as important regulators of skeletal muscle atrophy (Bodine and Baehr, 2014). There was a main significant effect for time for MuRF1 ($F_{(1, 36)} = 39.60, p < 0.001$). There was a decrease over time in MuRF1 from 0 to 72 h in both the NOR and LOW glucose conditions (0 h: 1.03 ± 0.30 vs. NOR: $0.63 \pm 0.20, p = 0.011$, vs. NOR RES: $0.72 \pm 0.17, p = 0.070$ vs. NOR EX-527: $0.57 \pm 0.01, p = 0.016$ vs. LOW: $0.58 \pm 0.11, p = 0.022$, vs. LOW RES: $0.47 \pm 0.10, p = 0.002$, vs. LOW EX-527: $0.61 \pm 0.17, p = 0.012$ (all significance was

observed following fisher comparisons, Fig 6.10.). However, there was no significant difference between these two conditions at 72 h (LOW vs. NOR: 0.58 ± 0.11 vs. 0.63 ± 0.20 , $p = 1.000$). Additionally, there were no significance differences present at 72 h when SIRT1 was activated or inhibited in either of the two glucose conditions investigated.

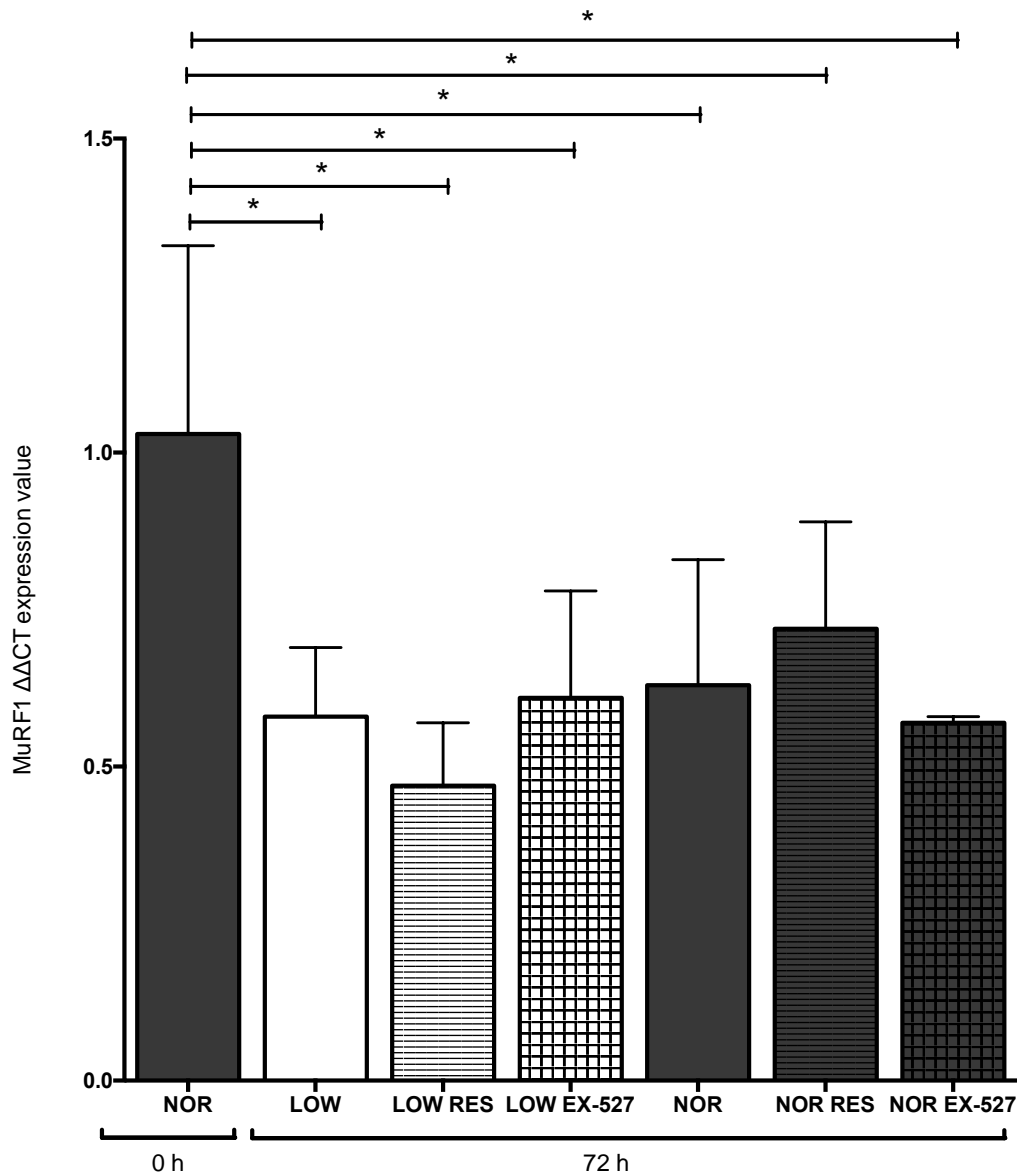


Fig. A1.19. Graph depicting means and SD's for gene expression for MuRF1 at 72 h compared to the 0 h control, in which the 0 h control possessed a higher gene expression than all other experimental conditions. Significant difference ($p < 0.05$) is denoted using *.

Similarly to MuRF1, MAFbx also displayed a significant main effect for time ($F_{(1, 35)} = 34.05$, $p < 0.001$). Compared to 0 h there was no significant reduction present when the glucose concentration was reduced at the 72 h

(LOW vs. 0 h: 0.92 ± 0.20 vs. 1.01 ± 0.19 , $p = 1.000$, Fig. 6.20). Under NOR conditions there was a significant reduction in MAFbx compared to 0 h (0 h vs. NOR: 1.01 ± 0.19 vs. 0.69 ± 0.06 , $p = 0.006$ (fisher)). Additionally, at 72 h there was a significant increase present in LOW vs. NOR glucose conditions (NOR vs. LOW: 0.69 ± 0.06 vs. 0.92 ± 0.20 , $p = 0.044$ (fisher)). The addition of RES or EX-527 had no effect on the NOR glucose conditions (NOR vs. NOR RES: 0.69 ± 0.06 vs. 0.72 ± 0.07 , $p = 1.000$, NOR vs. NOR EX-527: 0.69 ± 0.06 vs. 0.70 ± 0.02 , $p = 1.000$). EX-527 also had no effect on MAFbx gene expression in the LOW glucose conditions at 72 h (LOW vs. LOW EX-527: 0.92 ± 0.20 vs. 0.81 ± 0.13 , $p = 1.000$). There was however an average reduction in MuRF1 when RES was administered to LOW glucose condition (LOW vs. LOW RES: 0.92 ± 0.20 vs. 0.71 ± 0.08 , $p = 0.064$ (fisher)), despite no increase in myotube number or area in this condition.

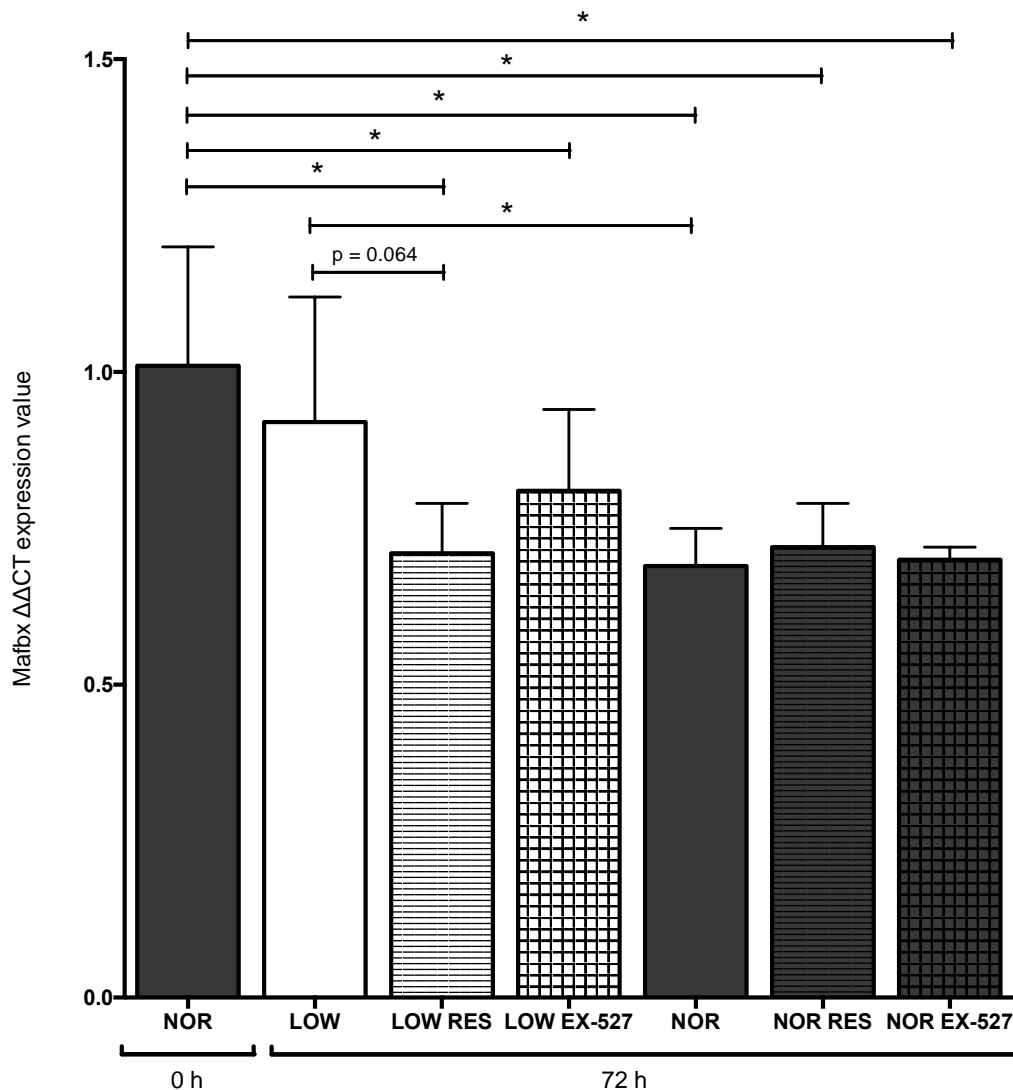


Fig. A1.20. Graph depicting means and SD's for gene expression for Mafbx at 72 h compared to the 0 h control. LOW glucose produced significantly higher expression of Mafbx in comparison to NOR, this was reduced following RES supplementation. Significant difference ($p < 0.05$) is denoted using a *. p values approaching significance are displayed.

MUSA1 increases in expression following denervation induced muscle atrophy where knockdown can attenuate the loss of muscle mass (Milan et al., 2015). A significant main effect was present for glucose ($F_{(2, 35)} = 9.13$, $p = 0.005$) and time ($F_{(1, 35)} = 21.79$, $p < 0.001$), as well as a significant interaction between these factors ($F_{(2, 35)} = 9.13$, $p = 0.005$). In low glucose conditions LOW glucose expression of MUSA1 was significantly higher than the NOR glucose condition (LOW vs. NOR: 1.09 ± 0.16 vs. 0.74 ± 0.05 , $p = 0.013$). NOR glucose remains unchanged when SIRT1 was activated or inhibited (NOR vs. NOR RES: 0.74 ± 0.05 vs. 0.71 ± 0.10 , $p = 1.000$, NOR vs. NOR EX-527: 0.74 ± 0.05 vs. 0.74 ± 0.03 , $p = 1.000$). The

increase in MUSA1 expression experienced under LOW glucose conditions alone was reduced following treatment with RES (LOW vs. LOW RES: 1.09 ± 0.16 vs. 0.77 ± 0.21 , $p = 0.023$ (fisher)). However, these reductions were also observed with the SIRT1 Inhibitor, EX-527 (LOW vs. LOW EX-527: 1.09 ± 0.16 vs. 0.86 ± 0.28 , $p = 0.006$ (fisher)).

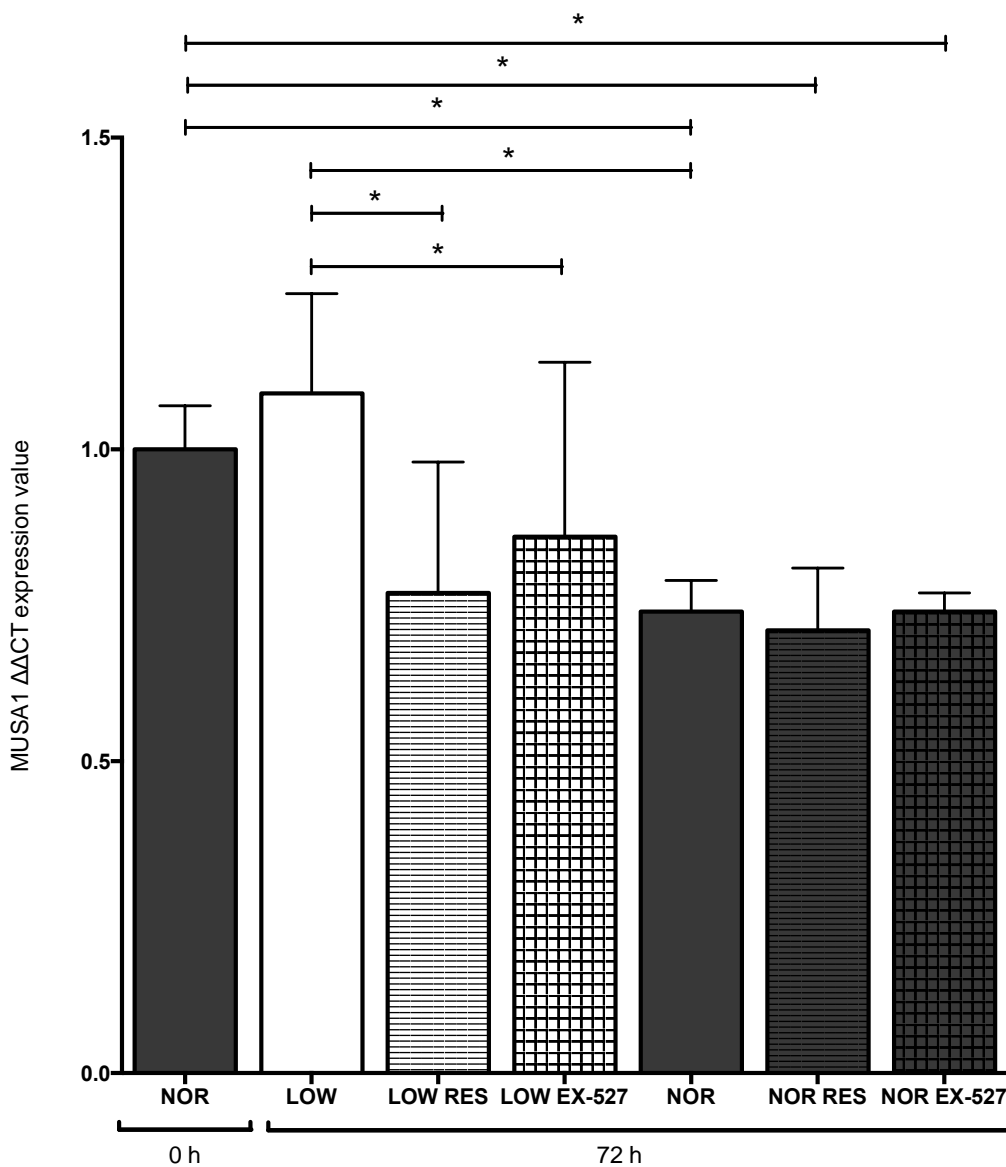


Fig. A1.21. Graph depicting means and SD's for gene expression for MUSA1 at 72 h compared to the 0 h control. Decreases in LOW glucose following both RES and EX-527 supplementation. Significant difference ($p < 0.05$) is denoted using *.

SIRT1 expression did not possess any significant main or interactional effects. Unlike myoblasts studies (where there were increases in SIRT1 in low glucose conditions) but there were no significant pairwise comparisons between any experimental conditions for SIRT1 gene expression (Figure 6.22).

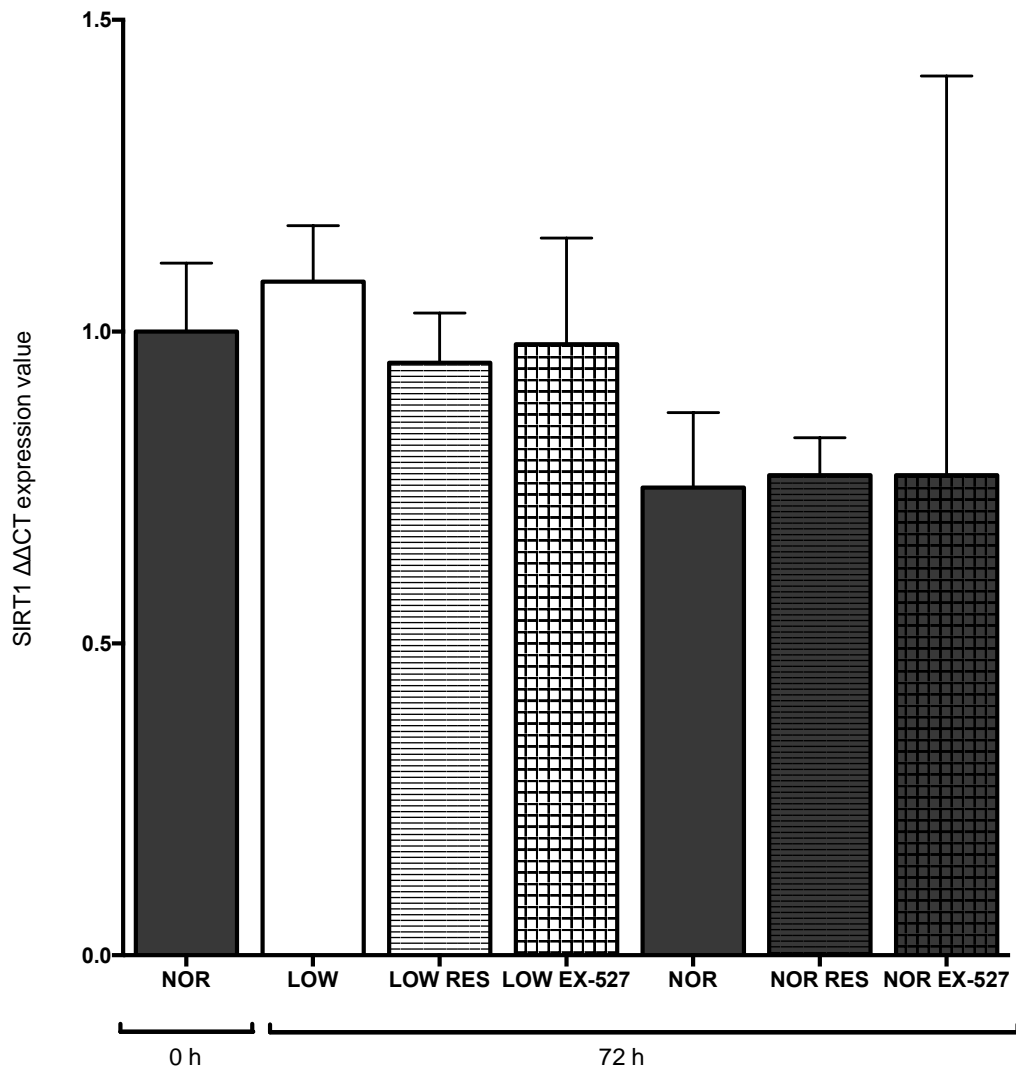


Fig. A1.22. Graph depicting means and SD's for gene expression for SIRT1 at 72 h compared to the 0 h control, in which no significant difference was observed.